การจำแนกแหล่งกำเนิดไนเทรตโดยใช้ข้อมูลอุทกธรณีเคมีและไอโซโทปเสถียรในชั้นน้ำ
บาดาล อำเภอแก่งคอย จังหวัดสระบุรี

นางสาววัลลภา วิศิษฏ์ธรรมศรี

วิทยานิพนธ์นี้เป็นส่วนหนึ่งของการศึกษาตามหลักสูตรปริญญาวิทยาศาสตรมหาบัณฑิต
สาขาวิชาธรณีวิทยา ภาควิชาธรณีวิทยา
คณะวิทยาศาสตร์ จุฬาลงกรณ์มหาวิทยาลัย
ปีการศึกษา 2559
ลิขสิทธิ์ของจุฬาลงกรณ์มหาวิทยาลัย

IDENTIFICATION OF NITRATE SOURCES USING HYDROGEOCHEMICAL A
ND STABLE ISOTOPE IN THE AQUIFER, AMPHOE KAENG KHOI, CHANGW
AT SARABURI

Miss Wanlapa Wisittammasri

A Thesis Submitted in Partial Fulfillment of the Requirements

for the Degree of Master of Science Program in Geology

Department of Geology

Faculty of Science

Chulalongkorn University

Academic Year 2016

Thesis Title	IDENTIFICATION OF NITRATE SOURCES USING HYDROGEOCHEMICAL AND STABLE ISOTOPE IN THE AQUIFER, AMPHOE KAENG KHOI, CHANGWAT SARABURI
By	Miss Wanlapa Wisittammasri
Field of Study	Geology
Thesis Advisor	Associate Professor Srilert Chotpantarat, Ph.D.
Thesis Co-Advisor	Assistant Professor Thanop Thitimakorn, Ph.D.

Accepted by the Faculty of Science, Chulalongkorn University in Partial Fulfillment of the Requirements for the Master's Degree

                                                                Dean of the Faculty of Science
(Associate Professor Polkit Sangvanich, Ph.D.)

THESIS COMMITTEE
                                                                Chairman
(Professor Montri Choowong, Ph.D.)
                                                                Thesis Advisor
(Associate Professor Srilert Chotpantarat, Ph.D.)
                                                                Thesis Co-Advisor
(Assistant Professor Thanop Thitimakorn, Ph.D.)
                                                                Examiner
(Associate Professor Chakkaphan Sutthirat, Ph.D.)
                                                                External Examiner
(Chulalak Changul, Ph.D.)

วัลลภา วิศิษฏ์ธรรมศรี : การจำแนกแหล่งกำเนิดไนเทรตโดยใช้ข้อมูลอุทกธรณีเคมีและ
ไอโซโทปเสถียรในชั้นน้ำบาดาล อำเภอแก่งคอย จังหวัดสระบุรี (IDENTIFICATION
OF NITRATE SOURCES USING HYDROGEOCHEMICAL AND STABLE
ISOTOPE IN THE AQUIFER, AMPHOE KAENG KHOI, CHANGWAT
SARABURI) อ.ที่ปรึกษาวิทยานิพนธ์หลัก: รศ. ดร. ศรีเลิศ โชติพันธรัตน์, อ.ที่ปรึกษา
วิทยานิพนธ์ร่วม: ผศ. ดร.ฐานบ ธิติมากร, 193 หน้า.

การทำเกษตรกรรมเป็นระยะเวลานานส่งผลให้เกิดการปนเปื้อนของไนเทรตในแหล่งน้ำ
บาดาล วัตถุประสงค์ของงานวิจัยคือ สังเกตข้อมูลอุทกธรณีเคมี และลักษณะอุทกธรณีวิทยาเพื่อ
ประเมินความเข้มข้นของสารละลายไนเทรตในน้ำบาดาล และใช้คุณสมบัติทางอุทกธรณีเคมี และ
ข้อมูลไอโซโทปเสถียร เพื่อจำแนกแหล่งกำเนิดของไนเทรต และกระบวนการที่ส่งผลกระทบกับ
การปนเปื้อนของสารละลายไนเทรตในน้ำบาดาล น้ำบาดาลทั้งหมด 44 ตัวอย่าง ถูกเก็บจากอำเภอ
แก่งคอย จังหวัดสระบุรี ในเดือนพฤศจิกายน พ.ศ. 2557 (ฤดูฝน) และเดือนพฤษภาคม พ.ศ. 2558
(ฤดูร้อน) เพื่อวิเคราะห์ Fe, Ca^{2+}, Mg^{2+}, Na^+, K^+, NH_4^+, Cl^-, F^-, Br^-, NO_2^-, NO_3^-, SO_4^{2-},
PO_4^{3-}, ความกระด้าง และ ^{18}O และ ^2H

ผลการศึกษาพบว่าทิศทางการไหลของน้ำบาดาลจะไหลจากด้านทิศตะวันออกไปทางทิศ
ตะวันตก สอดคล้องกับลักษณะภูมิประเทศ และระดับน้ำในช่วงฤดูร้อนต่ำกว่าช่วงฤดูฝนประมาณ
0.64 เมตร พื้นที่เติมน้ำบาดาลถูกพบทางด้านทิศตะวันออก และชนิดของน้ำบาดาลส่วนใหญ่ใน
พื้นที่ คือ $Ca-Na-HCO_3$ ผลการวิเคราะห์ความเข้มข้นของไนเทรตค่อนข้างมีค่าสูงในช่วงฤดู
ร้อน เนื่องจากผลของอุณหภูมิ ความเข้มข้นของไนเทรตสูงที่ถูกพบบริเวณจุดที่ 2 ในทั้งสองฤดูกาล
ซึ่งแหล่งกำเนิดของไนเทรตมาจากการละลายของแร่ไนโตรเจนที่อยู่ในดิน และการใช้ปุ๋ยสำหรับทำ
นา จากข้อมูลไอโซโทปเสถียรมี 11 จุดที่อยู่ในแนวโน้มของการระเหย (D = 4.2485^{18}O –
15.935) กระบวนการเจือจาง และกระบวนการดีไนตริฟิเคชัน เป็นกระบวนการสำคัญที่ทำให้ความ
เข้มข้นของไนเทรตในพื้นที่ลดลง นอกจากนี้ ยังพบกระบวนการไนตริฟิเคชันซึ่งเป็นกระบวนการที่
ทำให้ความเข้มข้นของไนเทรตเพิ่มสูงขึ้น ดังนั้น ข้อมูลอุทกธรณีเคมี และข้อมูลไอโซโทปเสถียร
จึงเป็นเครื่องมือที่ช่วยให้เข้าใจแหล่งที่มา และกระบวนการที่ส่งผลกระทบต่อการเปลี่ยนแปลง
ความเข้มข้นของไนเทรต

ภาควิชา   ธรณีวิทยา   ลายมือชื่อนิสิต ....
สาขาวิชา   ธรณีวิทยา   ลายมือชื่อ อ.ที่ปรึกษาหลัก ....
ปีการศึกษา 2559   ลายมือชื่อ อ.ที่ปรึกษาร่วม ....

5572234223 : MAJOR GEOLOGY

KEYWORDS: NITRATE / SOURCES / CONTAMINATION

WANLAPA WISITTAMMASRI: IDENTIFICATION OF NITRATE SOURCES USING HYDROGEOCHEMICAL AND STABLE ISOTOPE IN THE AQUIFER, AMPHOE KAENG KHOI, CHANGWAT SARABURI. ADVISOR: ASSOC. PROF. SRILERT CHOTPANTARAT, Ph.D., CO-ADVISOR: ASST. PROF. THANOP THITIMAKORN, Ph.D., 193 pp.

A long time agricultural activities result in the NO_3^- contamination in groundwater in Thailand. The objectives of this research were: to investigate hydrogeochemical and hydrogeological characteristics, to assess nitrate concentration in groundwater and finally to further use hydrogeochemical properties and stable isotopes for identifying the sources of nitrate, including their processes affecting nitrate contamination in groundwater.

Total 44 groundwater samples were collected from Amphoe Kaeng Khoi, Saraburi in November, 2014 (rainy season) and May, 2015 (summer season) to analyze Fe, Ca^{2+}, Mg^{2+}, Na^+, K^+, NH_4^+, Cl^-, F^-, Br^-, NO_2^-, NO_3^-, SO_4^{2-}, PO_4^{3-}, alkalinity, and ^{18}O and ^2H. The mainly groundwater flow direction is from east to west, which conforms to the topography. Average groundwater level in the summer season was lower than that in the rainy season average 0.64m. The recharge area is located in the eastern part of the study area. Groundwater type mainly is $Ca-Na-HCO_3$. NO_3^- concentration is relatively higher in the summer season due to temperature effect. The highest NO_3^- concentration was found at station No. 2 in both seasons. The sources of NO_3^- are from mineral in soils and fertilizer. According to the stable isotope analysis, 11 stations deviate along an evaporation trend ($D = 4.2485^{18}O - 15.935$). Dilution process and denitrification plays an important role in nitrate attenuation. On the other hand, the nitrification process is a key process affecting the increase of NO_3^- concentration. Thus, the hydrogeochemical and stable isotope analysis are an essential tool for understanding the sources and processes, influencing on nitrate concentration.

Department:	Geology	Student's Signature	....
Field of Study:	Geology	Advisor's Signature	....
Academic Year:	2016	Co-Advisor's Signature	....

ACKNOWLEDGEMENTS

CONTENTS

จุฬาลงกรณ์มหาวิทยาลัย
CHULALONGKORN UNIVERSITY

LIST OF TABLES

LIST OF FIGURES

จุฬาลงกรณ์มหาวิทยาลัย
CHULALONGKORN UNIVERSITY

CHAPTER I

INTRODUCTION

1.1 Background

Groundwater is an important water resource in Thailand that has been developed to use widely in plants growth, animals and human living such as household consumption, agricultural and industrial activities. In the last few decades, due to the growing of population and expanding of economic and society have experienced the water shortage problem and the groundwater contamination, especially in unconfined aquifers. The contaminants such as industrial chemicals, herbicide, insecticide, chemical fertilizers and various wastes polluted on the ground and eventually reach into the subsurface system directly by rain, degrading the quality of groundwater.

Thailand has a risk of NO_3^- contamination of groundwater due to the various agricultural activities scattered throughout the country, covering the area approx. 54.36% of the whole country (*The types of land use Thailand map 2010-2013*, 2014). addition, the farmers have intensively used chemical fertilizer to increase agricultural production, but the quantity of fertilizer is relatively high over the needs of the plant, leading to the groundwater contamination of NO_3^-, which is the main component of chemical fertilizers. The western areas of Thailand was found to be groundwater contamination with NO_3^- such as Kanchanaburi and Suphanburi, which are the area of asparagus cultivation with the usage of high doses of nitrogen fertilizers. That causes the quantity of NO_3^- higher than the safety standards of drinking groundwater (Tirado, 2007). Furthermore, the United States Environmental Protection Agency (USEPA) determined the maximum contamination level of drinking groundwater at 45 mg/l NO_3^- or 11.3 mg/l NO_3^--N (Macler, 2007). If the NO_3^- concentration is higher than the criterion for human drinking water, it will adversely affect to people's health. For example, especially in the pregnant woman, it will affect to the abortion or miscarriage (Beaudet, Otter, Karr, Sathyanarayana, & Perkins, 2014). In addition, the infant with less than 6 months age is diseased, namely, "blue–baby syndrome" or "Methemoglobinemia". The disease causes the acidity in the digestive system of children to be at a low level and makes the bacteria, which help in the digestion

changing NO_3^- to toxic NO_2^-. This NO_2^- will go to the blood system of the infant and react to hemoglobin, i.e. oxygen carrier in the blood system. Then hemoglobin will transform to methemoglobin and interfere with oxygen carrying in blood. Level of oxygen decreasing makes the babies to be asphyxiated, causes the skin become blue that clearly visible around the eyes and mouth, and the babies will die later (Mahler, colter, & Hirnyck, 2007; Pietro, 2006). Some studies indicated that drinking contaminated water for a long time period may cause the cancer (Ward et al., 2005). In addition, it also found that if the large quantities of NO_3^- leach into the surface water, it will happen the "red tide" or "Eutrophication" phenomenon that finally affect to the ecosystem. High quantity of nitrogen and phosphorus cause quick growth of algae. Then, they cover in wide areas that block sunlight to pass into the surface water, so the amount of oxygen in the water decreases. The photosynthetic of water plant will deadly affect to the aquatic animals and the other creatures (BoQiang et al., 2012; Duncan, Kleinman, & Sharpley, 2012; Kaff, 2012; Minaudo, Meybeck, Moatar, Gassama, & Curie, 2015; Sahanawin, 2012; Vonlathen, Bittner, & Hudson, 2012).

Many research used the stable isotope approach to indicate the sources and mechanism of NO_3^- contaminated in groundwater because it shows a special fingerprint of the different sources of NO_3^-. So, the stable isotope is an efficient tool for tracing source of NO_3^- and helps to explain the mechanism or the process of changing in concentration of NO_3^- (Chen, Tang, & Yu, 2006; Chen et al., 2007; Fenech, Rock, Nolan, Tobin, & Morrissey, 2012; Kellman & Hillaire-Marcel, 2003; Mcquillan, 2004; Min, Yun, Kim, Kim, & Kim, 2003; Munster, 2008; Stewart, Stevens, Thomas, Raaij, & Trompetter, 2011; Townsend & Whittemore, 2005; Wieben, Baker, & Nicholson, 2013). However, this technique dose not widely use to identify the sources of NO_3^- contamination in Thailand.

To tackle these problems, the sources of NO_3^- contamination from nature and anthropogenic activities should be addressed (Gu, Ge, Chang, Luo, & Chang, 2013; Gu et al., 2011; Willian E. Motzer, 2006). Nitrate may come from many sources, for example, the usage of inorganic and organic fertilizers in the agricultural area, wastewater from the industrial areas, sewage from household and livestock, the KNO_3 using in glass industry (Polishchuk, Fakeev, Krasil'shchik, & Vendilo, 2012), the

$NaNO_3$ using for preserving foods (Sindelar & Milkowski, 2012) and a variety of the process in soils by microorganism. These factors are associated causes of NO_3^- concentration in the groundwater. As mentioned, this study used the stable isotope technique combined with hydrogeochemical and hydrogeological characteristics to identify sources and describe the processes, affecting NO_3^- concentration in the groundwater system underneath the intense agricultural areas. This information can be beneficially used as a database in planning of groundwater quality conservation and the appropriate remediation plan for the safely consumption and household usage in the future.

1.2 Objectives

As mentioned earlier, this research aimed to address the sources of NO_3^- contaminated in groundwater, which are important for assessing the current situation of groundwater quality and providing the suitable remediation technique and sustainable groundwater management plan in the future. The main objectives in this research were;

1. To investigate the hydrogeochemical and hydrogeological characteristics and assess NO_3^- concentration in groundwater

2. To identify the sources of NO_3^- in groundwater

1.3 Scope of study

In this research, the hydrogeochemical and stable isotopes in groundwater were analyzed. The positions of groundwater sampling distributed around the study area cover a total area approx. 262 km^2, and is located between latitude 14°25′ N to 14°33′ N and longitude 100°55′ E to 101°08′ E.

1.4 Study Area

The study area covers in Huay Haeng, Tan Diao, Cham Phak Phaeo, Tha Maprang, Cha-Om, Amphoe Kaeng Khoi, and Taling Chan, Kut Nok Plao, Pak Khao San, Nong Pla Lai, Amphoe Muang, Changwat Saraburi (Figure 1.1). The reason why selecting this study area is that Saraburi has the agricultural areas over 57% (*The map of land use, Changwat Saraburi* 2011), contributing the main cause of NO_3^-

contamination in the groundwater moreover the wastewater that come from farming landfill and household, These will lead to NO_3^- contamination in the groundwater too. The quality of the surface water, which had been analyzed since the year 2011 to 2014 in regions of the upstream of Huay Wa, Ban Khok Cheuak Tai, Tan Dio, the upstream of Huay Na Dee, Ban Wang Phae, the upstream of Khong Phriao, Ban Pa Pai, Cham Phak Phaeo and zone of Huay Na Dee, Ban Na Dee, Huay Haeng, revealed that the quantity of NO_3^- was more than the standard (not exceeding 5.0 mg/l NO_3^-) during 2012 to 2013 (Environmental Research Institute, 2014; "The quality standard of the surface water," 1994). Although the quantities of NO_3^- tended to decreased in 2014 until less than the standard, it does not mean that the NO_3^- cannot continually leach into the groundwater. Thus, it is very important to study the distribution of NO_3^- levels, contributing to the people who live in the area with insufficient and contaminate groundwater issues. The detail of the study area is described in Chapter 3.
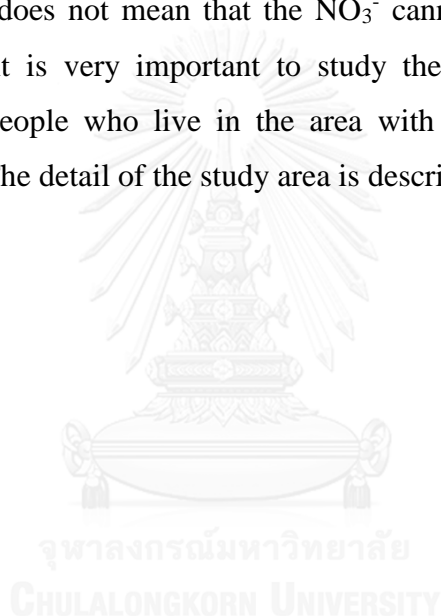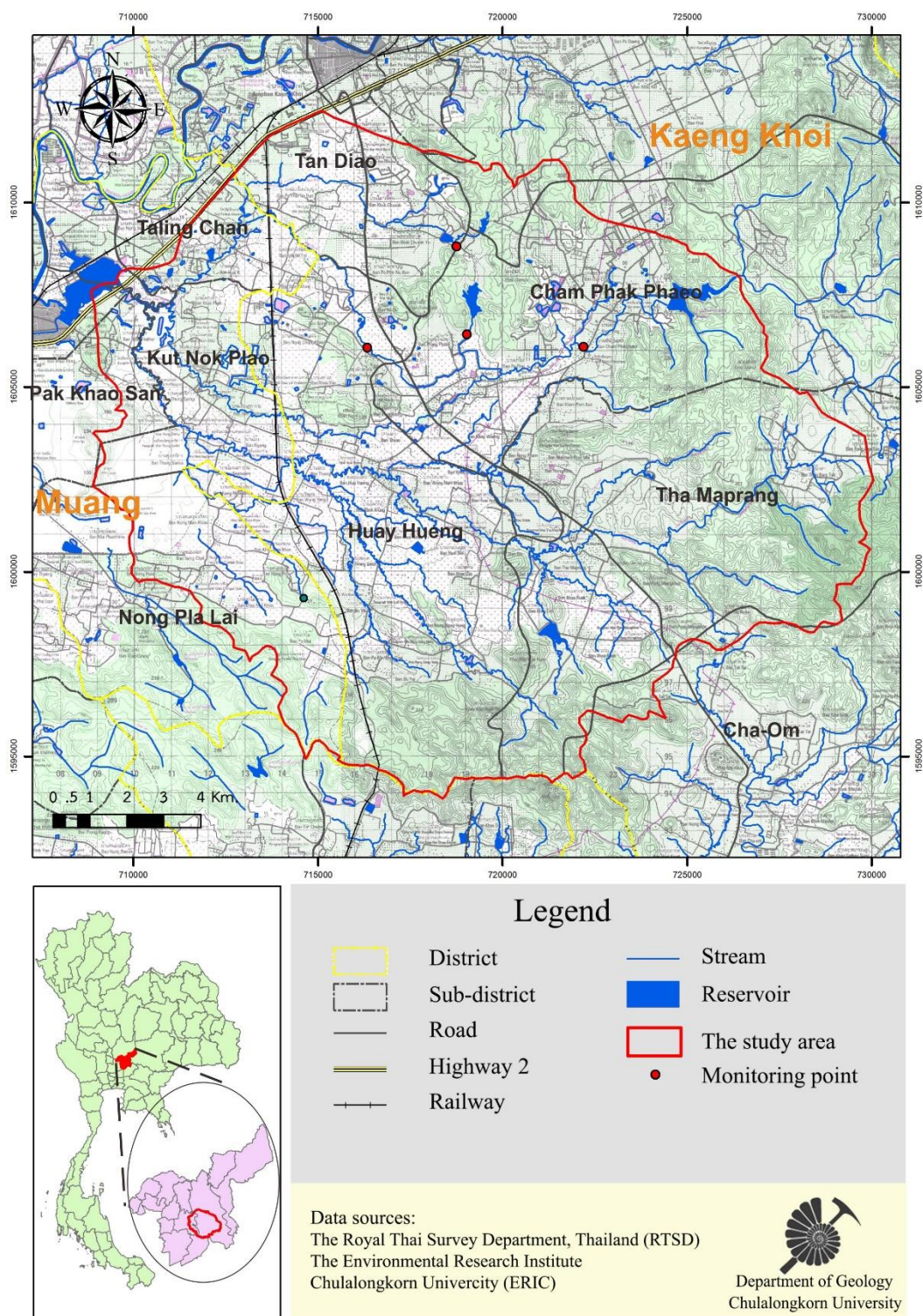
Figure 1.1 The study area map sheet 5138II, 5238III, 5137I and 5237IV series L7018 (modified from map of Royal Thai Survey Department, 1997)

1.5 The framework of the research

        Methodology in this research can be seperated into 4 part, including 1) in the office work: literature reviewing, collecting secondary data and planning for the water sampling. 2) fieldwork: in situ physiochemical and groundwater level measurements, land use checking and water sampling. 3) laboratory work: cations, anions, deuterium and oxygen isotope. And 4) data analysis to interprete the sources of NO_3^- contamination and process in groundwater as shown in Figure 1.2.

Methodology

Literature reviewing and collecting secondary data in the study area

Planning for the water sampling

Field work

In situ physiochemical measurements/ground-water level measurement

Land use checking

Water sampling

Laboratory analysis

Cation;
Ca^{2+}, Mg^{2+}, Na^+, K^+, Fe and NH_4^+

Anion;
Alkalinity, Cl^-, SO_4^{2-}, NO_3^-, NO_2^-, PO_4^{3-}, Br^- and F^-

Deuterium and Oxygen isotope

Data analysis

Microsoft Excel;
Relationship graphs

ArcGIS;
Various maps

GW Chart;
Piper diagrams

The sources and processes of nitrate contamination in groundwater

Figure 1.2 Methodology and data analysis in this research

1.6 Expected Outcome

   The understanding of processes occurred throughout the area and the sources of NO_3^- in the groundwater expects to be addressed in this area.

CHAPTER II
LITERATURE REVIEWS

2.1 Nitrogen

Nitrogen is an important nutrient for plants to synthesize and form protein, amino acid and hormones (Damrongsri & Pruksanan, 2007). Nitrogen is an element found the most in the atmosphere in a form of nitrogen gas (N_2) and on the ground in a form of ammonium (NH_4^+), nitrite (NO_2^-) and nitrate (NO_3^-) (Tantanasarit, 2006). In the organic matter, nitrogen is a main compound that is called an organic nitrogen, which plants can not available (except legumes). The organic is transformed into inorganic nitrogen by mineralization process. Plants can use nitrogen compound in a form of NO_3^- because high concentration of ammonium is high will toxic to the plants. However, the quantities of both are limited through the processes such as leaching into the groundwater, biological reduction, erosion or runoff on the soil surface, so it will limit the growth of plants (Vityakorn, 2014). Nitrogen is an indicator of water quality. If an amount of ammonia in the water is high, it indicates recently dirty water, but if NO_3^- is high, indicating the contamination of water for a long time. In addition, it can indicate oxidation in the water. If nitrogen compound is high, the nitrification is occurred and a quantity of oxygen decreases.

2.1.1 Nitrogen Cycle

The beginning of nitrogen cycle is a fixation of nitrogen in the atmosphere by nitrogen-fixing bacteria for creating amino acid and protein. This process is called aminization according to the equation below.

$$N_2 + \text{Nitrogen fixing bacteria or algae} \longrightarrow \text{Protein}$$
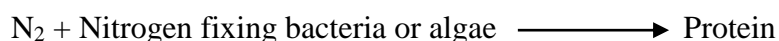
After the organisms are dead, bacteria and fungus digest protein to become amino acid. Subsequently, the heterotrophs, i.e. a genus of the microorganism which cannot create the food by itself, transform amino acid into NH_4^+ by ammonification process. This process is easily happen in the place that has ventilation.

$$\text{Proteins} \longrightarrow R\text{-}NH_2 + CO_2 + \text{Energy} + \text{Other products}$$
$$\text{(Amines or amino acids)}$$

$$R\text{-}NH_2 \xrightarrow[\text{hydrolysis}]{\text{Enzymatic}} R\text{-}OH + NH_3 + Energy$$

$$2NH_3 + H_2CO_3 \longrightarrow (NH_4)_2CO_3 \rightleftharpoons 2NH_4^+ + CO_3^-$$
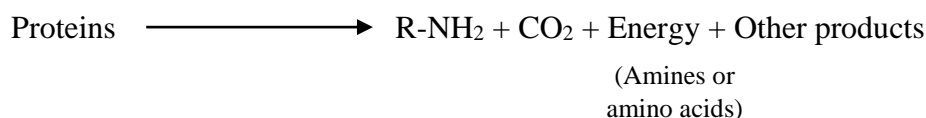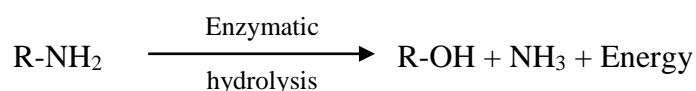
Furthermore, the NH_4^+ may come from urine, which is a waste of the animal and human. Nitrogen in a form of urea is hydrolyzed by urease enzyme for changing ifinto ammonium carbonate in the hydrolysis process according to the equation.

$$NH_2 - \overset{\overset{\displaystyle O}{\displaystyle \|}}{C} - NH_2 + 2H_2O \xrightarrow[\text{Urease}]{} (NH_4)_2CO_3$$
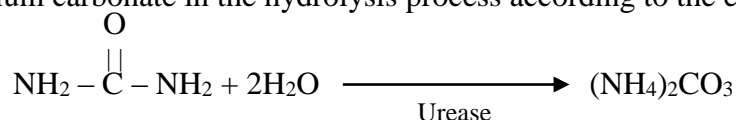
The concentration of NH_4^+ can decrease by the assimilation of the plants, restrict in the space between particles of clay or oxidize into NO_3^- or NO_2^- in the nitrification process. This process is the oxidation process which happens in the oxygen conditions by nitrifying bacteria. The first step of this process is to change NH_4^+ into NO_2^- by the nitrosomonas and the nitrosococcus. Then the nitrobacter oxidizes NO_2^- again to change into NO_3^-.

$$2NH_4^+ + 3O_2 \xrightarrow{\text{Enzymatic}} 2NO_2^- + 2H_2O + 4H^+ + Energy$$

$$2NO_2^- + O_2 \xrightarrow{\text{Enzymatic}} 2NO_3^- + Energy$$
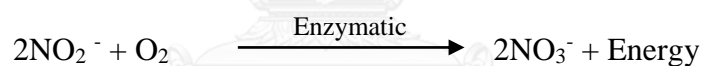
Nitrogen can return into the atmosphere when NO_3^- is reduced by denitrifying bacteria in the denitrification process, i.e. in anaerobic condition (Boonkaewwan, 2013) (Figure 2.1).

$$2NO_3^- \longrightarrow NO_2^- \longrightarrow N_2 + NO + N_2O$$
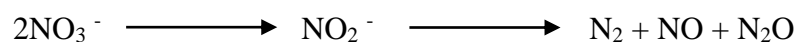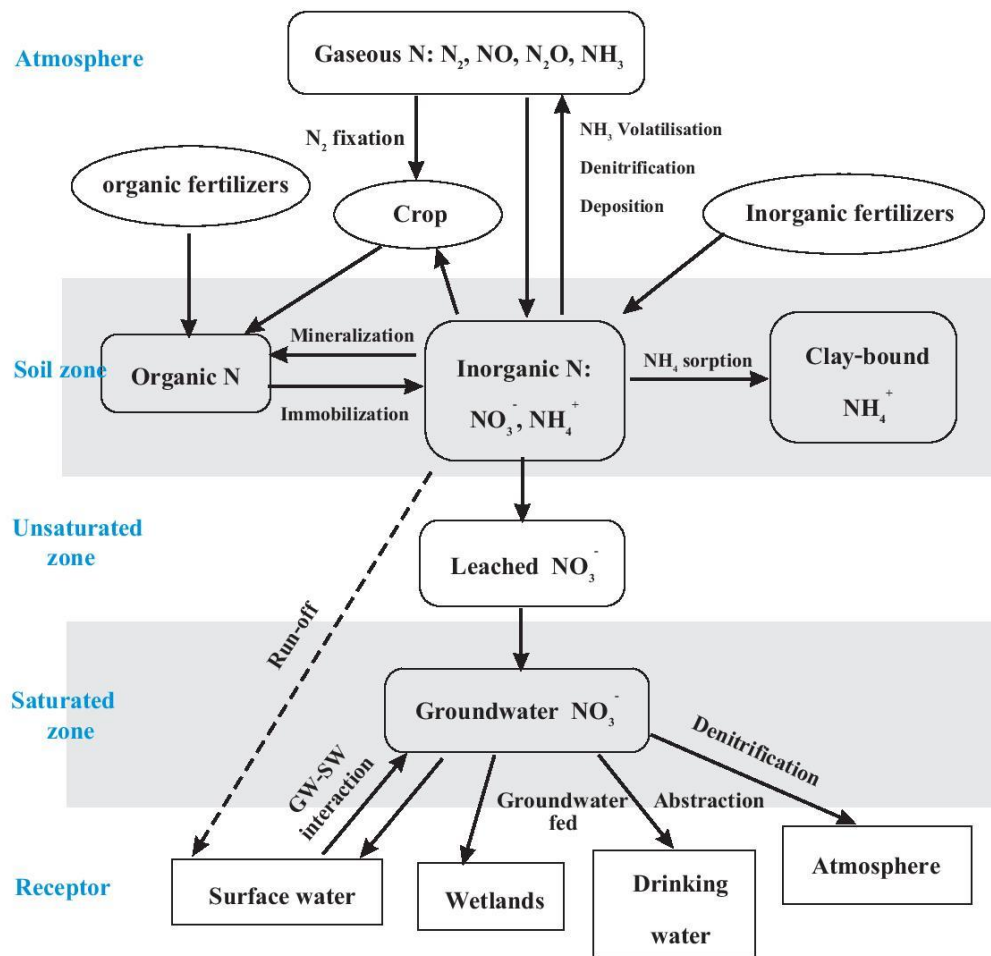
Figure 2.1 Diagram of nitrogen cycle

(modified from Stuart, Gooddy, Bloomfield, & Williams, 2011)

2.1.2 Nitrate

Nitrate (NO_3^-) is one of the nitrogen compound that is relatively stable than NO_2^-. The NO_2^- can transform to NO_3^- from microbial and chemical process, as mentioned above.

A major natural source of NO_3^- comes from the remains of animal and plants (humus). The quantity of NO_3^- depends on the characteristics and thickness of soil, topography and climate. In addition, it may come from the human activity such as the usage of synthetic fertilizer, which has the ingredient of nitrogen, manure and organic nitrogen fertilizer for agriculture, sewage from human and animal, or wastewater from

factory and residential area. The quantities of NO_3^- from these sources are based on the land use (Wongcharlie, 1991). In a form of inorganic nitrogen, not only NO_3^- and NO_2^- is found, but it is also found the NH_4^+ that can be directly absorbed by plants. Generally, the NH_4^+ is quickly absorbed by the matrix in soil because it has a positive charge. But the NO_3^- has a negative charge, so the NO_3^- does not bond with the particle of soil and move along water or runoff on the surface and finally, it reaches into the groundwater. The factors affected to convection of NO_3^- in the nature are rainfall, the physical feature of the soil, slope, degree of weathering and conservation of the top soil such as cropping for covering soil. These affect to the infiltration of NO_3^- into the soil (Hensler & Attoe, 1970). In this area, if the concentration of NO_3^- is lower than 5 mg/l NO_3^--N, it indicates that this area is not affected from the human (Meybeck & Helmer, 1996).

2.2 Isotope

This section explains about the definition of the isotope, the processes that effect to isotope ratio, isotope of nitrogen and principle analysis on mass to charge by the isotope-ratio mass spectrometry.

2.2.1 Definition

The element is a pure substance that consists of the same kind of atom. Atom is a smallest unit of the element and shows specific properties of the each element. The center of atom has a nucleus. The nucleus composes of the basic particle that is proton and neutron (except hydrogen has only the particle of proton), which they both have a nearby mass size. Proton shows the positive charge while neutron is a neutral. By outside of the nucleus has electron that is negative charge moving around. The same element should have the proton equal. But neutron may be equal or unequal. If the neutron is difference, it was called the isotope. So the isotope is the same element but it has a dissimilar of neutron. The mass is difference because it is the sum total of proton and neutron. The isotope is divided to 2 types including the stable isotope, which is not decay and stable. And the radioactive isotope that is unstable isotope and can decay to the other element by releasing alpha and beta particles and gamma ray during the decay. In the same element may be found in the both types. So the chemical properties of the element are alike but the physical properties are different according to the characteristic

of mass. The analysis of isotope cannot evaluate from the chemical reaction, but can measure from the mass. Which mass of the same element is very little different. The instrument with a high resolution should be used for evaluation by using the principles of mass per charge proportion.

2.2.2 Isotope fraction

The difference of physical and chemical properties of the isotope depends on the mass. Variation of mass will greatly impact to chemical, physical and biological processes. Processes of changing in the isotope ratio are called isotope fractionation. And it is divided to 2 types, i.e. equilibrium and kinetic isotope fractionation.

2.2.2.1 Equilibrium Isotope Fractionation

Equilibrium isotope fractionation is a reaction happens between compounds and it changes ratio of the isotope in equilibrium state. It makes the rate of forward reaction equal to the rate of backward reaction, but it does not mean that each isotope from the two compounds is equal. Similarly, the ratio of each isotope in the different compounds is constant. During the equilibrium reaction, the substance with high energy has tendency to enrich with the heavy isotope. In addition, if substance is changed the state, the ratio between the heavy and light isotope will change along the changing of state. For example, in the liquid state, water rather has a heavy isotope (^{18}O, ^{2}H) while a vapor of water rather has a light isotope (^{16}O, ^{1}H).

2.2.2.2 Kinetic Isotope Fractionation

Kinetic isotope fractionation is a reaction happens in the imbalance. It makes the rate of forward reaction and the rate of backward reaction to be unequal. When the product of reaction is separated, then the reaction will occur in the one direction. The rate of reaction depends on ratio of mass and vibration energy. In general, the bond of the light isotope is looser than the heavy isotope, so the light isotope will be easy to react than the heavy isotope. The light isotope is rather in the product while the heavy isotope remains in the substrate. For example, biological processes are the process happens in one direction and has a tendency to use the light isotope because split energy between the light and heavy isotope is low. Degree of split depends on the path way of

reaction and energy to use for reaction. The slowly reaction will be better to split the isotope. So, this process involves with the kinetic and will split the isotope more than the equilibrium conditions (Kendall & Caldwell, 1998).

2.2.3 Oxygen Isotope

Oxygen in the nature has three isotopes consist of the light isotope, ^{16}O, with atomic mass about 15.9949. The quantity of the light isotope found in nature is 99.76 percent. The heavy isotope, ^{18}O, has atomic mass approximately 17.9991. The quantity of the heavy isotope is 0.2 percent. The last is ^{17}O with atomic mass about 16.9991. The quantity of this isotope is only 0.04 percent. The combination of oxygen isotope and the hydrogen isotope is mostly used for tracing the source of precipitation and hydrological system because hydrogen and oxygen are in a molecular of the water. The heavy isotope in molecular of water is depleting. So, in the nature is found the molecular of the water in three forms; $^{1}H_2^{16}O$, $^{2}H_2^{16}O$, $^{1}H_2^{18}O$. The factors that affect to the variation of isotope compositions are vapor pressure, humidity, temperature, altitude, rainfall and evaporation. In addition, there are a many types of the water such as vapor in the atmosphere, seawater, polar ice and precipitation, which cause the changing in component of the isotope too.

2.2.4 Hydrogen Isotope

Hydrogen consists of two stable isotopes, i.e. the light isotope ^{1}H or protium with atomic mass about 1.00794, and the heavy isotope ^{2}H or deuterium with atomic mass about 2.0141. The quantity of the light isotope found in nature is 99.985 percent while the quantity of the heavy isotope is only 0.015 percent. In addition, the hydrogen isotope has one radioactive isotope, i.e. ^{3}H or tritium with the half-life period about 12.43 years. The stable hydrogen isotope form together with oxygen isotope in water molecules is mostly used for studying hydrological system both global and local scales. The radioactive isotope is used for dating young groundwater (less than 50 years) and helps for determining the flow rates and flow direction. In the hydrological cycle, the fractionation of hydrogen and oxygen isotope in between transformation of water vapor to liquid precipitation depends on two major processes, i.e. evaporation and condensation. The lighter isotopes (^{16}O, ^{1}H) preferentially evaporate or enter the vapor

phase, whereas the heavy isotopes (^{18}O, ^{2}H) preferentially condense or enter the liquid phase. Thus the water vapor is enriched in ^{16}O and ^{1}H, whereas the remaining liquid water is enriched in ^{18}O and ^{2}H. The mostly form is ^{1}H$_2$^{18}O in liquid water (SAHRA, 2005).

2.2.5 Hydrologic cycle

During the water molecules travel in hydrologic cycle, the water will be changed to a different status pass the processes are both condensation and evaporation. These contribute to changeable of isotope ratio in the body of water, such as oxygen is split into oxygen 16 or light isotope (^{16}O) and oxygen 18 or heavy isotope (^{18}O) isotopes. Which isotopes have a great mass number are distinguished from isotopes that has a low mass number. The difference of isotope ratio was called isotope fingerprints. This method used to tracer location of groundwater from the relationship between ^{18}O and ^{2}H isotopes of the rainwater which it means to the global meteoric water line (GMWL) and worldwide monitored by IAEA (International Atomic Energy Agency).

The isotope composition are reported as delta values (δ) due to the difference of isotope ratio is a small (units of parts per thousand), it will express in terms of per mill (‰). However, isotope ratio of samples are compare to international reference standard which known composition The standard used to calculate is VSMOW (Vienna-Standard Mean Ocean Water) and calculated according to the equation below:

$$\delta(in\text{‰}0) = \left(\frac{Rx}{R_s} - 1 \right) x1\,000$$

Where R_x is the ratio of heavy and light isotope in the sample.

        R_s is the ratio of heavy and light isotope in the standard.

A factors that affect to isotope fractionation, including 1) rainout effect: when ocean water evaporates, the light isotope is easily evaporated and enriched in water vapor. So isotope values in cloud are low when compare with the ocean water. After that, this cloud move into the continental and condense as precipitation, the heavier isotopes are fall together and resulted in the depleted in heavier isotope in the cloud.

Thus the rain that furthest from the coastal will be depleted with heavier isotopes. 2) an increment of temperature affect to evaporation and in the precipitation is enriched heavier isotopes. It shows isotope values in the same way with the precipitation at the equator, low altitude and near the coastal. Which these are result from the latitude and altitude, so the polar regions and high altitude show a low isotope values because enriched lighter isotopes. Moreover the vapor sources that affect to precipitation is enriched heavier isotopes as compared to the humid area. (Figure 2.2-2.3)
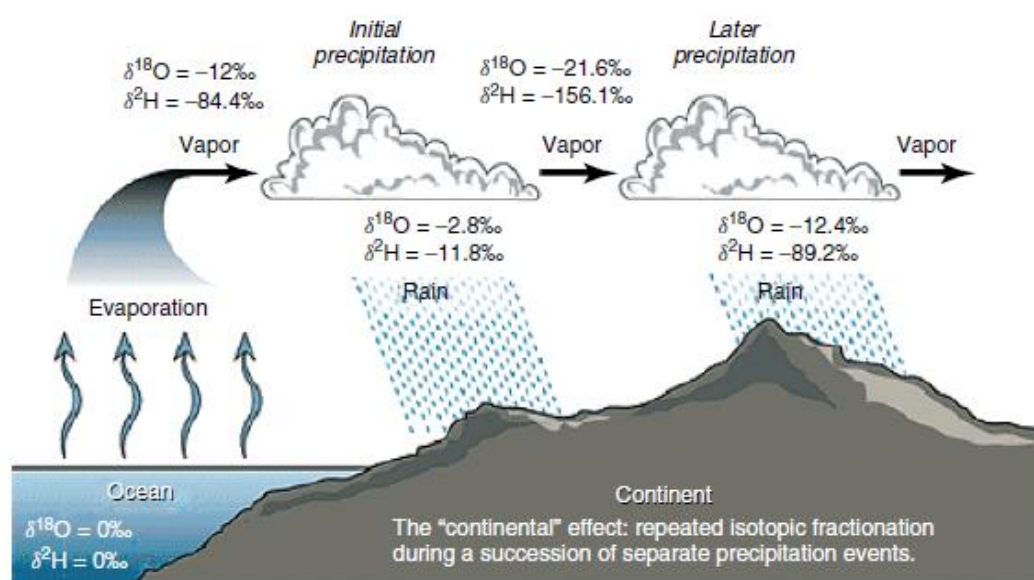
Figure 2.2 Rainout effect on isotope fractionation (Hoefs, 1997)
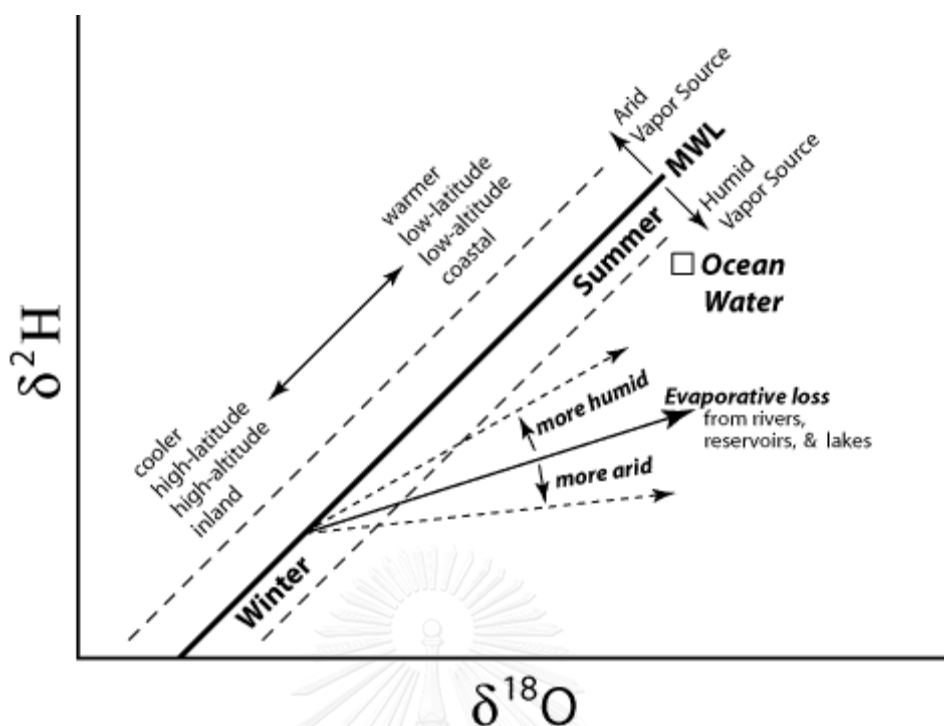
Figure 2.3 Temperature effect on isotope fractionation (SAHRA, 2005)

2.2.6 The Principle of Cavity Ring-Down Spectroscopy

Cavity ring-down spectroscopy (CRDS) is known as cavity ring-down laser absorption spectroscopy (CRLAS). This technique has a potential for trace-gas or small gas-phase molecule analysis because it provides the high precision, accuracy, sensitivity and extraordinary low drift. Its measurement is a fast, continuous and real-time speed. The instrument requires minimal or no sample preparation and low operating costs. It is used for environmental monitoring, emissions monitoring, greener automotive engine development, cleanroom technology and biopharmaceutical process monitoring.

The CRDS is an optical absorption analysis of atoms, molecules and optical components of gas species that has a unique near-infrared and mid-infrared absorption spectrum. It consists of a series of narrow, well resolved and sharp lines with a well-known characteristic of wavelength (Figure 2.4). So the concentration of gas can determine from measuring the strength of absorption. The laser source of spectroscopy creates a single-frequency laser to enter a cavity which quickly fills with laser light. These lasers circulate continuously and create effective path lengths of many kilometers

by two or three high reflectivity mirrors in cavity that enables gases to be monitored in seconds or less at the level of parts per billion. This research used Picarro Inc. water isotope analyzer model L2130-i that its cavity has 25 cm length and effective path length over 20 km. It has three mirror cavities and provides superior signal to noise when compared with a two mirror cavities model. When a laser is on, the photo detector signal reaches a threshold level and then the laser abruptly turned off. The laser light in cavity continues to travel between the mirrors about 100,000 times. But the mirrors have a slightly 99.999% reflectivity, so the light intensity leaks out and decays to zero. That result to the signal will decay exponentially with time. The decay is also known as ring down monitored in real-time by photo detector. The most decay time depends on the reflectivity of mirrors and distances between two or three mirrors (length of cavity) by follow to Beer- Lambert Law, i.e. a relationship between the attenuation of light and the properties of the material which the light is traveling. Another is from the speed of light and the absorption coefficient of any gas species.
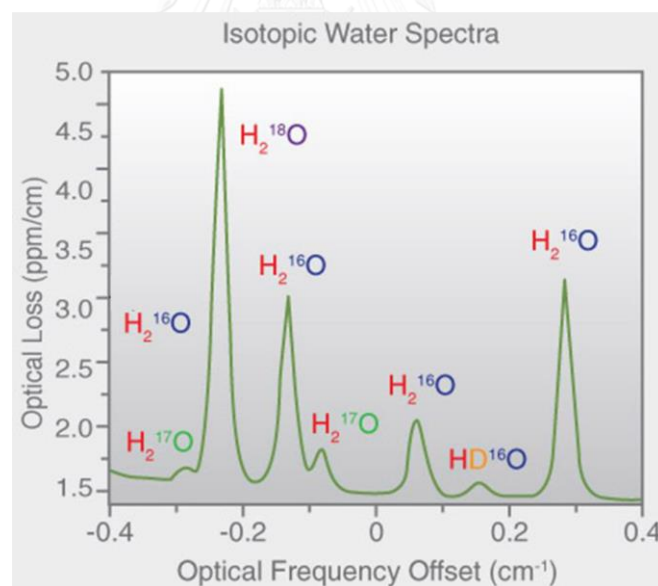
Figure 2.4 The absorption spectrum for water isotopologues

(Winkler & Peters, 2013)

When the gas species are in cavity, the ring down time accelerate compared to the empty cavity because additional optical is lost. The gas concentration derives from

the difference between these ring-down times that is measured at all locations across the target gas's spectral absorption line (Figure 2.5-2.6).

(A)

(B)
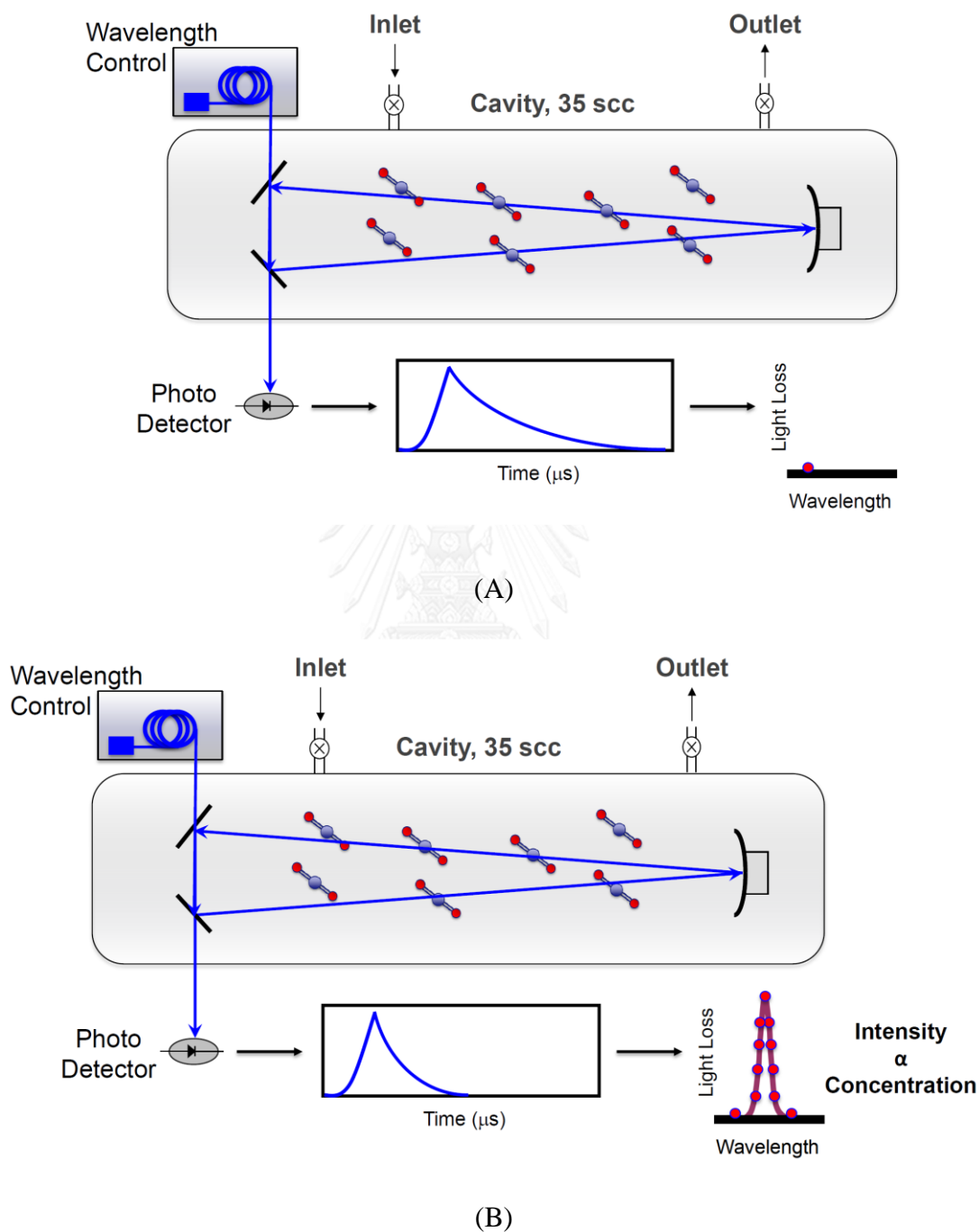
Figure 2.5 Inner diagram of the CRDS. (A) The molecule that light is not absorbed. (B) The molecule that light is absorbed (Winkler & Peters, 2013)
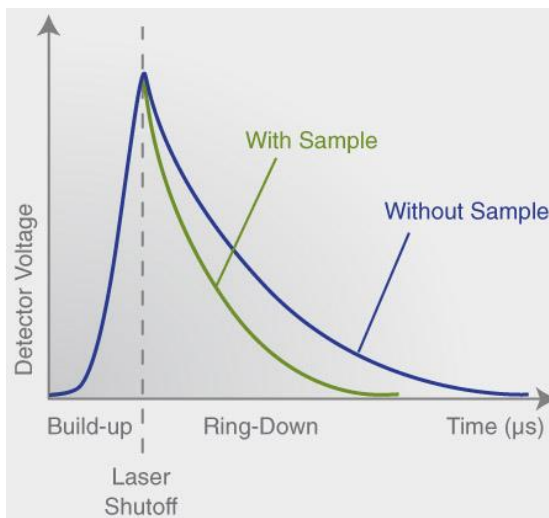
Figure 2.6 Graph of comparing between the ring down time of the cavity without any

absorbing gas and detector voltage when a target gas is absorbing light

(Winkler & Peters, 2013)

From mentioned above, the absorption spectroscopy is generated by the Beer-Lambert Law that is given by Sprague (2012);

$$A = ln\left(\frac{I_0}{I}\right) = \sigma L_{abs} N$$

Where A is the absorbance.

I_0 is the initial light intensity.

I is the transmitted light intensity.

σ is the absorption cross section.

L_{abs} is the path length of light through the absorber.

N is the number density of absorber molecules (per unit volume).

The intensity of light within the cavity is determined as an exponential function of time. The transmitted light through the mirrors is proportional to the intensity of light in the cavity. If the cavity loss process of light is only leakage due to transmission of the cavity mirrors, the ring-down time constant is characterized by;

$$I = I_0 \, exp\left(\frac{-t}{T_0}\right), \text{ with } T_0 = \frac{t_r}{2(1-R)} = \frac{L_{opt}}{c(1-R)}$$

When an absorber is presented in the cavity. Then the ring-down time constant can be calculated from a modification equation above, which according to the below equation.

$$I = I_0 \, exp\left(\frac{-t}{T}\right), \text{ with } \frac{1}{T} = \frac{1}{T_0} + (\sigma L_{abs} N)\left(\frac{c}{L_{opt}}\right)$$

Finally, the absorbance concentration can be calculated from below equation (Osthoff et al., 2006).

$$N = \frac{L_{opt}}{c\sigma L_{abs}}\left(\frac{1}{T} - \frac{1}{T_0}\right) = \frac{R_L}{\sigma}\alpha$$

Where N is the number density of absorber molecules (per unit volume).

L_{opt} is the distance between the mirrors or the total cavity length.

c is the speed of light.

σ is the absorption cross section.

L_{abs} is the path length of light through the absorber.

T is the 1/e decay time of the light in the presence of the absorber.

T_0 is the 1/e decay time of the light (the empty ring-down lifetime).

R_L is the ratio of the total cavity length and the sample length.

α is the absorption coefficient (also referred to as extinction).

2.3 Literature Reviews

This section shows the previously studies, which help to understand about how to interpret the result. In addition, these data connect to this research for identifying the source and mechanism of NO_3^- in the study area.

S.V. Panno, Hackley, Hwang, and Kelly (2001) evaluated the source of NO_3^- in the sinkhole plain at the western of Illinois. The geology of the area was limestone in Mississippian perios. The position of sinkhole in the area had estimate 10,000 sinkholes. The 10 samples came from the area discharged from the groundwater basin which showed the chemistry of the groundwater. The sampling was conducted during

autumn in 1998 through winter, spring and summer in 1999. Many parameters were analyzed such as pH, temperature, redox potential, conductivity, cation, anion, dissolved organic carbon , atrazine and the dual isotope of NO_3^-. The type of groundwater was Ca^{2+}-HCO_3^-. The concentration of NO_3^- was higher than in the nature. Quantity of NO_3^- in the early spring came from nitrogen fertilizer usage, which was different from the winter and summer. In addition, there was the evidence showed the denitrification process in the epikarst and the shallow karst aquifer.

Mohamed et al. (2003) analyzed the nitrogen isotope and hydrogeochemical analysis of 57 groundwater samples distributed throughout the area. The time of sampling was 17 and 21 May 1999. The purpose of study was to observe the concentrations of NO_3^- in the present and to check the denitrification process in the Kakamigahara aquifer located at the central of china. The results found that the quantity of $Ca2^+$, Mg^{2+}, NO_3^- and SO_4^{2-} were high in the eastern area which is an agricultural area using chemical fertilizer. In addition, the concentration of NO_3^- was decreased from the eastern to the western area that conforms to the direction flow of the groundwater. Some sample had high concentration of NO_3^- at the western area which possibility came from the other source. The denitrification process occurred in the area because the quantities of HCO_3^-, pH and nitrogen isotope were increased.

The contamination of the NO_3^- came from the various sources, both the nature and relatively complex anthropogenic which could be explained from the fingerprint of NO_3^- source. William E. Motzer (2006) said that the original method for analyzing the concentration of NO_3^- shows only a quantity of NO_3^- and cannot identify the different sources. So the isotope of NO_3^- analysis can classify the sources of NO_3^- in the groundwater and surface water including the mechanism in unsaturated zone. For a clear understanding, it should be interpreted with the land use and hydro chemical of the groundwater.

Choi et al. (2007b) studied the concentration of NO_3^- in unconfined aquifer at Kyonggi, Korea. The water samples came from 12 wells with different land use. For example, 4 wells were in agricultural area, 4 wells were in complex farming area, 2 wells were in the residence and 2 wells were in the uncontaminated area. All of 279

water samples were collected every month since 1997-1999 for analyzing the concentration of NO_3^- and nitrogen isotope ratio. Results of the study showed that the concentration of NO_3^- was high in April to September and the unconfined aquifer was sensitive to the land use. The nitrogen isotope in uncontaminated area was in a range from $+1.4\permil$ to $+4.5\permil$, in cropping area was $+8.7\permil$ to $+14.4\permil$ and $+4.5\permil$ to $+8.5\permil$ for the area using inorganic fertilizer mixed with manure, in the complex area was in range from $+1.0\permil$ to $+17.7\permil$, the area near cattle was $+8.7\permil$ to $+17.6\permil$, and in the residence had value over $+10\permil$.

The study of Tirado (2007) kept 49 the groundwater samples, 14 from surface water samples from agricultural area in the Philippines and Thailand to study the concentration of NO_3^- in drinking water. The results showed that the deep groundwater was contaminated by NO_3^- related to a large quantity of fertilizer usage. In Thailand, the contamination was found in the central of country (Kanchanaburi and Suphanburi), especially in the asparagus cultivation area that was a cause of blue baby syndrome or called methemoglobinemia.

K. S. Lee, Bong, Lee, Kim, and Kim (2008) studied the Han River basin in Korea. They kept samples from the northern and southern of Branch River and Main River during four seasons. The analyzed parameters consisted of Cl^-, NO_3^-, SO_4^{2-}, HCO_3^- and stable isotope of NO_3^-. The concentration of NO_3^- in the southern of Branch River were higher than these in the northern that possibly occurred from manure or wastewater. That was opposite to the NO_3^- in the northern of Branch River that came from atmosphere or soil organic nitrogen. While NO_3^- in the main river was relatively distributed and came from mixing process from the other river. In addition, the nitrogen isotope in the summer was diluted by rainfall and it was lower than the other seasons.

Kaown, Koh, Mayer, and Lee (2009) identified the source of NO_3^- and SO_4^{2-} in the groundwater at agricultural area of Chuncheoun, Korea. By using the dual stable isotope of NO_3^- cooperated with hydrochemistry, total of samples from the shallow and deep aquifer were collected about 35 samples during April 2006, and December 2007. The NO_3^- and SO_4^{2-} were high at the western area because of the chemical fertilizer

usage. Moreover, the evidence of denitrification was found in the area that the quantity of NO_3^- conformed to topography.

Kamdee et al. (2011) modified the modeling by using isotope techniques with hydrological and chemical data. The study area was in Chiang Mai basin where the size of area was about 5,000 km^2. The basin had two main attributes, Mae Ping and Kuang River. The main aquifer was Chao Phraya Aquifer, Chiang Mai Aquifer and Chiang Rai Aquifer. The water samples included 36 samples from groundwater, 6 samples from river and 3 samples from Mae Kuang Dam. Local precipitation was collected on March 2007 (dry season) and August 2008 (rainy season). The analysis results showed 2 groundwater types including $Ca-Mg-HCO_3^-$ and $Na-K-HCO_3^-$. The age of groundwater was 2,300 ±240 to +30,000 years (ancient water). In addition, the evidence showed mixture of young water (less than 1,500 years) and ancient water too. From the comparing between local meteoric water line (LMWL) and Bangkok local meteoric water line (BKK LMWL), climatic condition and altitude affected to the slope that the local line was slightly higher than the Bangkok line. The distribution of isotope in groundwater showed cool or high altitude characteristic that in the shallow wells affected from evaporation conformed to the surface water. In summary, the origin of groundwater came from the local rainfall at the difference altitude and the deeper aquifer directly recharged from younger water in the upper layer.

Jin et al. (2012) studied the source of NO_3^- in Huzhou, the eastern China. The groundwater was collected in April and July 2010 at the paddy field and cultivated vegetable area. The depth of sampling was different from 60 to 300 cm. The analysis mainly showed a weakly alkalinity in groundwater. The dissolved oxygen of both was decreased along the depth, while conductivity in paddy area increased along the depth corresponding to the vegetable area. The concentration of NO_3^- and SO_4^{2-} were high, which was caused by the manure, chemical fertilizer and soil organic. The NO_3^- was controlled by nitrification process.

The study of Hosono et al. (2013) used the nitrogen isotope and oxygen isotope for understanding the flow direction of groundwater in Kumamoto that is important to trace the source and mechanism of NO_3^-. These samples came from the unconfined and

confined aquifer. The analysis results showed that the NO_3^- tends to increase. The sources of NO_3^- were chemical fertilizer and effluent from the factory and dwelling. They found the evidence of denitrification process that nitrogen and oxygen isotope increased, while dissolved oxygen (DO) decreased along the flow direction. If the dissolved oxygen were over 8 mg/l, the isotope had little change. This process was diluted by irrigation water. In addition, the denitrification affected to the reduction of NO_3^- was more than the dilution.

Kamdee et al. (2013) studied the origin, movement, age of groundwater and interaction with surface water. They analyzed the stable isotope ratios of hydrogen and oxygen, carbon-14, tritium, chemical and physico-chemical parameters in precipitation. The samples were collected from 53 wells of groundwater at depth from 10 to 70 m and 97 samples from the surface water (rivers and reservoir) during June and August 2008. The study area was in Upper Chi river basin, Chaiyaphum province, northeastern Thailand. The size of area was about 13,550 km^2. The results showed that the groundwater types are $Ca-HCO_3$, $Ca-Na-HCO_3$, $Na-Mg-HCO_3$, $Ca-HCO_3-Cl$, $Ca-Mg-HCO_3$, $Na-HCO_3$, $Na-Cl$ and $Na-Ca-SO_4$. LMWL of precipitation in the area had a slope lower than Bangkok because it was affected from evaporation during the rainy season, and the hydrogen and oxygen isotopes of groundwater scattered along this line. Some samples deviated from LMWL and distributed along the evaporation line that created from the data of surface water. These showed that some groundwater might be affected from surface water. From the tritium and carbon data, more groundwater samples were modern (5-10 years) and sub-modern ages. It showed recharge prior to 1952. In addition, some groundwater showed old ages and the flow direction of groundwater moved from the west to east.

Pasten-Zapata, Ledesma-Ruiz, Harter, Ramirez, and Mahlknecht (2014) studied a contamination of NO_3^- in the shallow aquifer below agricultural area by using the multi-tracer for tracing source and mechanism that control the concentration of NO_3^-. The study area was in Zona Citricola, Nuevo Leon state, Mexico with size about 8,000 km^2. The types of plant consisted of grass, sorghum, wheat, avocado, corn and walnuts. The first sampling was in December 2009, the next was June 2010 and a number of samples analyzed were 39. The analysis result showed an age of the groundwater was

after 1960 that is the modern groundwater. The kinds of groundwater were $Ca\text{-}HCO_3$ and $Ca\text{-}SO_4$. The relationship between NO_3^- and Cl^- helped to indicate the source that came from the manure and wastewater. The concentration of NO_3^- in the cropping and orchard were higher than the grassland. The source of NO_3^- in the farming came from animal or human sewage while the other came from soil nitrogen and animal waste. In addition, the nitrogen isotope in June was enricher than in December.

Li, Li, Liu, and Suzuki (2014) observed the moving and distribution of NO_3^- in the surface water and groundwater and evaluated the factors that have an effect to the distribution. The area was in Yellow River that is southern of Taihang Piedmont and a part of north china plain. The agriculture in the area was the wheat, rice and corn cultivation. They kept the surface water and groundwater about 190 samples during July to December 2007. The parameters of analysis were EC, pH, Ca^{2+}, Mg^{2+}, K^+, Na^+, Cl^-, SO_4^{2-}, HCO_3^-, NO_3^-, deuterium and oxygen isotope. The conclusion was that the concentration of Ca^{2+} was higher than Na^+, Mg^{2+} and K^+ respectively. While the concentration of HCO_3^- was higher than SO_4^{2-}, Cl^- and NO_3^- respectively. The types of water were $Ca\text{-}HCO_3$, $Ca\text{-}Na\text{-}HCO_3$, $Ca\text{-}HCO_3.SO_4$, $Ca\text{-}HCO_3.Cl$, $Mg.Ca\text{-}SO_4.HCO_3$ and $Ca\text{-}Na\text{-}SO_4$. The concentration of NO_3^- in groundwater was higher than the surface water so the variance of distribution was high as well. This would conform to the flow direction. And it was affected from a migration of wastewater. The data of isotope presented interaction between groundwater and surface water. Contamination from the wastewater in irrigation area might occur by infiltration into the soil profile and changed to NO_3^- concentration.

Noipow (2015) used the stable isotope (deuterium and oxygen ratios) for studying water cycle. The samples were daily collected during April 2013 to March 2015 from 2 rain stations in Nakorn Phanom (NPM-RW) and Nong Khai (NKI-RW), and were weekly collected water from Mekong River and the distributaries that locates near the rain stations. The total samples were analyzed by Cavity Ring-Down Spectroscopy (CRDS). When they plotted the relationship between deuterium and oxygen isotope, the LMWL of Nakorm Phanom and Nong khai showed slightly high slope when comparing to Luang Phrabang in 1961-1967. The average values of local rainwater depleted heavy isotopes which indicate continental effect and altitude effects.

In January-April (pre-monsoon period), the relative humidity (RH) in air was low and evaporation was high. They were controlled by seasonal and affected to the delta values of oxygen to be high. In April- May (late monsoon period), the low delta value was caused by amount effect. On late May, the delta value started high again because of the high relative humidity. The isotope feature of run-off samples in pre-monsoon period was high independently to the average rainfall. Whereas in monsoon and late monsoon period, the isotope features conformed to the local precipitation.

Y. Zhang, Li, Zhang, Li, and Liu (2014) studied the nitrogen isotope and oxygen isotope of NO_3^- as well as oxygen isotope and deuterium in the surface water and groundwater. Each type of the water samples were kept from 5 positions during May to October 2012. The study area was at the North China plain where geology was clay and limestone. Agricultures in the area were wheat, corn and vegetable. The concentration of NO_3^- in surface water ranged from 0.2 to 29.6 mg/l. The high value was in the dry season (May) over against the concentration of NO_3^- in groundwater that ranged from 0.1 to 19.4 mg/l. The value was also high in the wet season (June) because the rainfall in June took concentrate NO_3^- in surface water to infiltrate to groundwater system. The sources of NO_3^- in this month were fertilizer and effluent from the industrial areas. In addition, in May and October, NO_3^- in the groundwater came from mineralization of soil organic nitrogen and sewage. The data of isotope indicated that the groundwater did not directly recharge from the precipitation, but from the seepage of surface water.

Yanpeng Zhang et al. (2015) studied the feature of nitrogen and oxygen isotope of NO_3^- and carbon isotope of dissolve organic carbon (DOC) at Shijiazhuang, China. Furthermore, they also analyzed the other parameters such as cations, anions and DOC. The samples were kept from the groundwater of the Huangbizhuang reservoir, Hutuo River and Shijin canal in November 2011. The type of water in surface water was SO_4-HCO_3-Ca-Mg, except for Shijin canal was HCO_3-SO_4-Ca-Mg, and the groundwater was mainly HCO_3-Cl-Ca type. From the isotope data, surface water and shallow groundwater were similar. There were indicators came from the modern rainfall. But in the deep groundwater, with lower data, its indicator came from the ancient rainfall. The processes affected to chemistry of groundwater were the dissolution of gypsum and carbonate and the denitrification process that control the isotope fractionation of NO_3^-.

These processes were important to the deep groundwater more than the shallow groundwater. The sources of NO_3^- in shallow groundwater were ammonium fertilizer and wastewater while NO_3^- in the deep groundwater came from rainfall and soil organic nitrogen.

CHAPTER III

METHODOLOGY

Methodology in this research for evaluating sources and explaining mechanisms of NO_3^- are divided into 3 parts as following: 1) all secondary data used in the study area such as topography, geology, hydrogeology, location of wells and land use were collected and compiled. In this step, the previous studies related to this research were reviewed and then the groundwater sampling plan was established. 2) groundwater sampling, land use investigation and several parameters measurements were conducted in the field and 3) Laboratory work for analyzing cation, anion and stable isotope was carried out and finally all laboratory results and field investigation would be interpreted together to satisfy all objectives.

3.1 Data Collection

3.1.1 General Topography

The study area is located between latitude 14°25′ N to 14°33′ N and longitude 100°56′ E to 101°07′ E, covering area of approx. 262 km² (see Figure 3.1). It appears in the topographic map of series L7018 number 5138II (Changwat Saraburi), 5238III (Amphoe Muak Lek), 5137I (Amphoe Nong Khae) and 5237IV (Amphoe Ban Na) at scale of 1:50,000. The central and eastern areas covering area of approx. 209.726 km² or 27.23 percent of the total area locates at the southwest of Amphoe Kaeng Khoi. The western area covering area of approx. 52.181 km² or 28.88 percent of the total area locates at the east of Amphoe Muang.

The topography of the western and central area are alluvial plains as a part of Lower Chao Phraya plains, which consist of alluvial plain, flood plain, terrace plain and river terrace. The elevation varies from less than 50 m to 50 - 100 m (amsl.). The mountainous areas mainly appear in the southern and eastern part of the study area which has an approximately 12-13 km long and the elevation of 150 - 400 m (amsl) (see Figure 3.1).
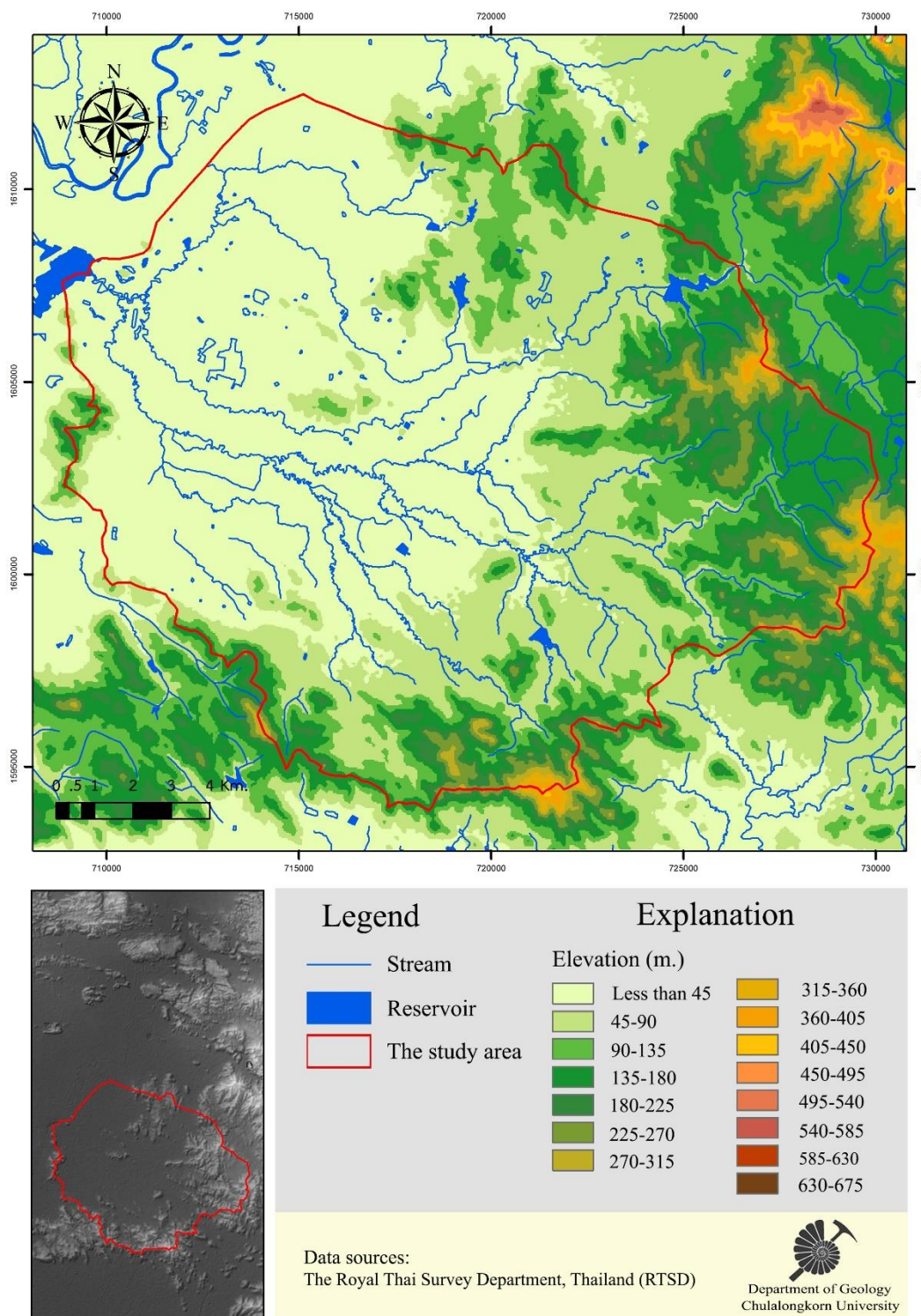
Figure 3.1 Topographic map of the study area

3.1.2 Geology

The geology of study area consists of igneous rocks and quaternary sediments. The area of igneous rock is about 172.406 km^2 or 65.80 percent of the whole area. The area covering with quaternary sediments is about 89.604 km^2 or 34.20 percent of the whole area (see Figure 3.2).

3.1.2.1 Permo-Triassic

The mainly extrusive igneous rock is Permo-Triassic rock of Khao Yai group (260-220 Ma). It is divided into 2 types as following:

Khao Yai group 1 (PTrku) is volcanic rocks widely spread in the central and eastern of the study area. A total area is 161.646 km^2 or 61.69 percent of the whole area. It consists of rhyolite, andesite, rhyolitic tuff, andesitic tuff, volcanic conglomerate and volcanic breccia.

Khao Yai group 2 (PTrkr) spreads over a small area of central and western of the study area. It covers an area of 10.76 km^2 or 4.11 percent of the whole area. It consists of rhyolite and rhyolitic tuff.

3.1.2.2 Quaternary

The unconsolidated sediments spread over the central and western parts of the study area about 89.604 km^2 or 34.20 percent of the whole area. Unconsolidated sediments are mainly alluvial sediments consisting of clays, sands and silts. Moreover, these sediments come up with river and deposit along channels and floodplains.
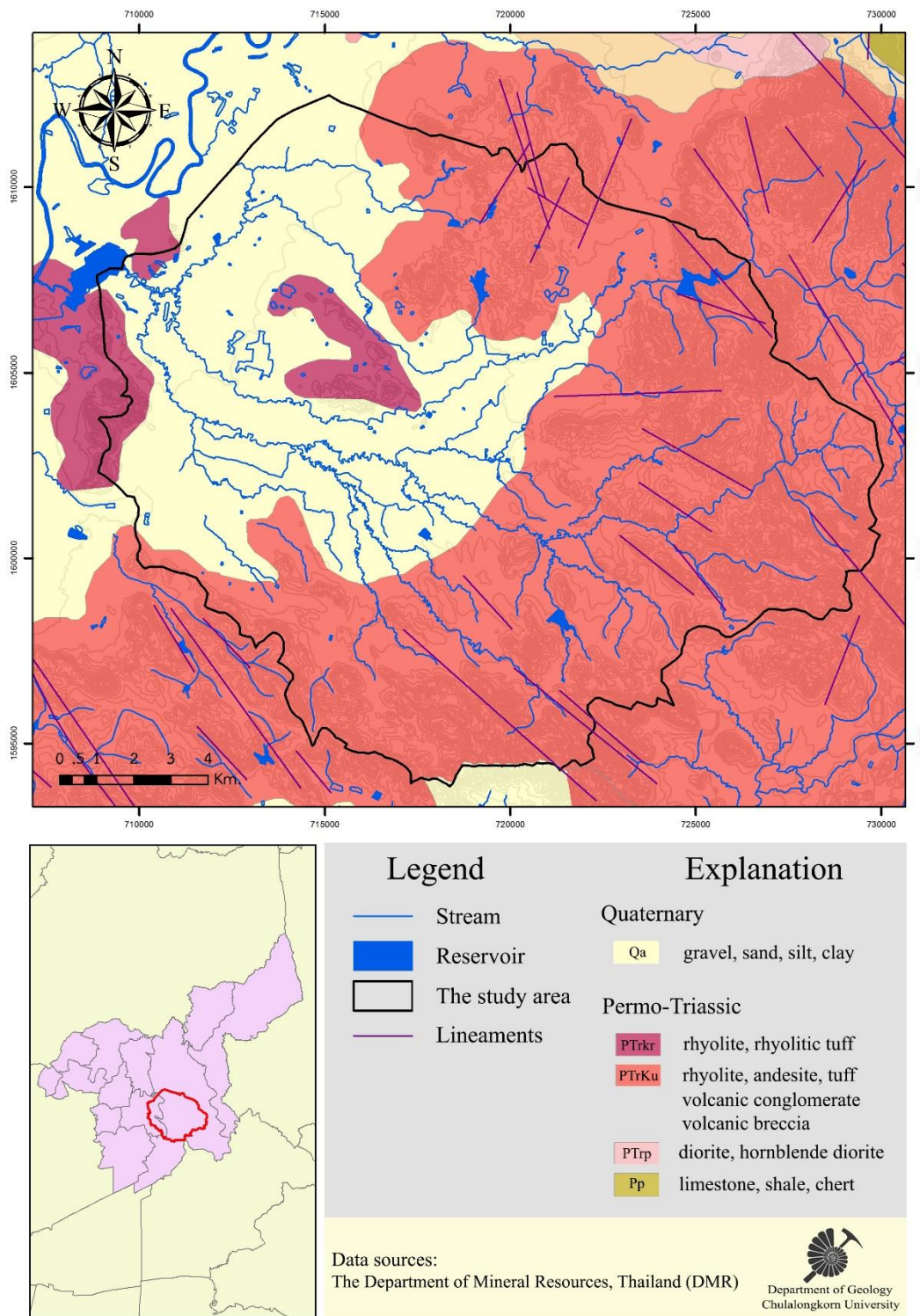
Figure 3.2 Geological map of the study area

3.1.3 Hydrogeology

The study area is in a part of the Lower Chao Phraya Basin which is floodplain basins. This sediment is originated from 4 main watersheds, including Ping River, Wang River, Yom River and Nan River. On top of Tertiary deposits, it is called the Chao Phraya aquifer. This aquifer has a thickness not exceeding 50 m and the sediment is relatively thick in the middle of the basin. The eastern of basin is younger terrace deposits (Qyt) with more than 50 m thick. The old terrace deposits (Qot) or Chiang Mai aquifer are placed on the top. The aquifers are divided into two types according to the hydrogeological appearance of study area, which consists of both unconsolidated and consolidated aquifers (Figure 3.3).

3.1.3.1 Unconsolidated Aquifer

This aquifer has a potential for generating water by stored them in the pore or space between particles of gravels, sands, silts and clays. Ability of retaining water depends on thickness, sorting and texture of sediment. Unconsolidated aquifer in the study area is floodplain deposit aquifer (Qfd) consisting of sand, gravel and clay deposits. This aquifer occurs from Pasak River and floodplain and alluvial deposits appears in the central and western parts of the area. The thickness of sediment ranges from 20 to 150 m, which is continuous in the western part with a narrow valley in between the mountainous areas, mainly consisting of sediments in the central part of the area.

3.1.3.2 Consolidated Aquifer

Groundwater in the consolidated aquifer is stored in the space or stratum structure such as fracture, joint, fault, cleavage, bedding plane, underground cavity and limestone zone. The quantity of water depends on rock type and a structure size. The consolidated aquifer in the study area is mainly the volcanic aquifer (Vc), underlined at the bottom of floodplain deposits aquifer (Qfd), consisting of rhyolite, andesite, tuff and volcanic breccia. The depth of stratum varies differently in each area in a range of 13 - 110 m. This aquifer is generally found in a shallow level at the valley and foothill in the central and eastern areas, and in the deep level at the western area. Generally, this

aquifer yields little groundwater, depending on geological structures such as joints and fractures of volcanic rocks.
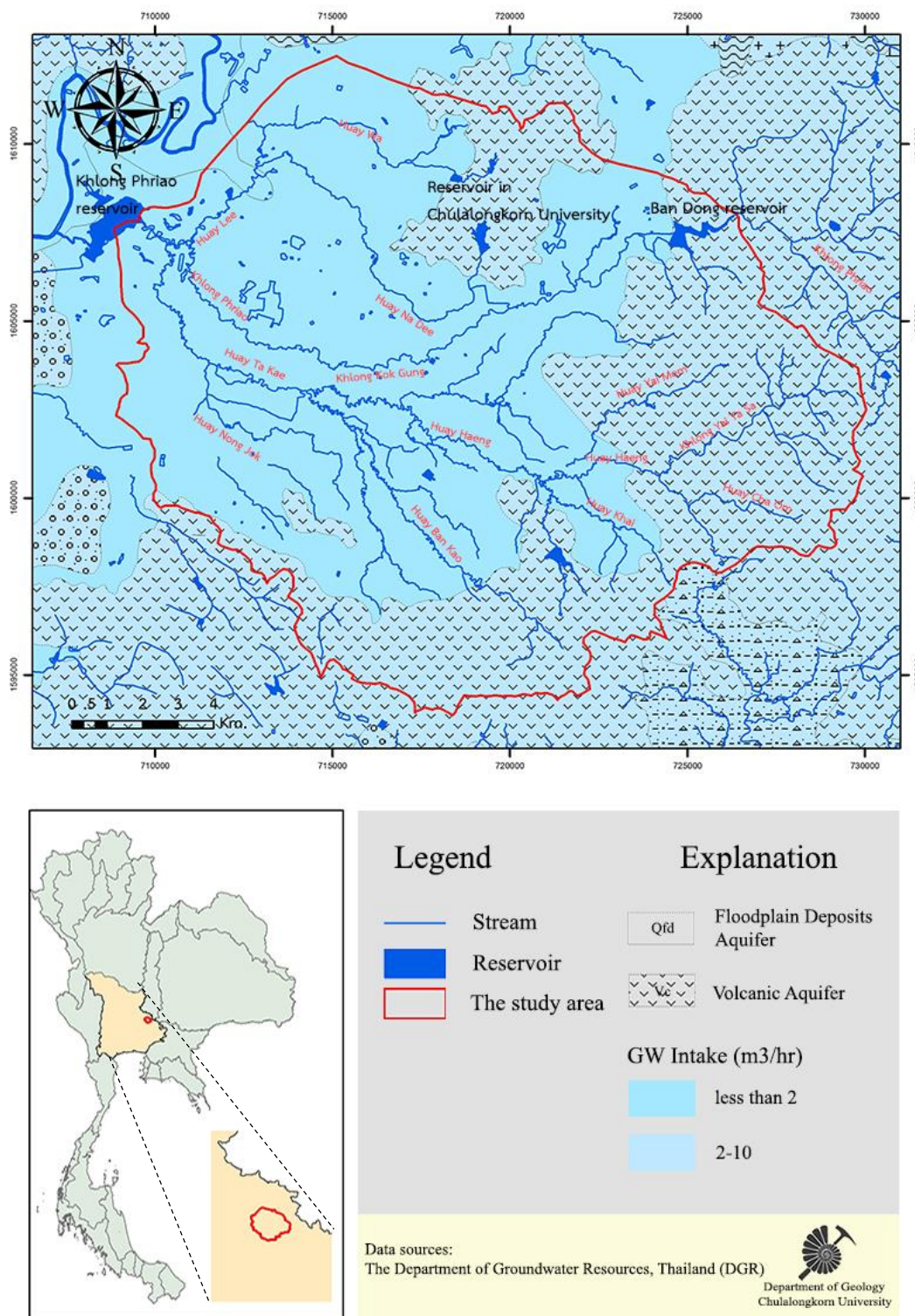
Figure 3.3 Hydrogeological map of the study area

3.1.4 Water resources

The rivers in study area are mainly small and ephemeral channels, including Huay Wa, Khlong Phriao, Huay Haeng, Huay Yai Mom, Huay Cha Om, Huay Khai, Huay Ban Kao, Huay Nong Jok, Huay Lee and Huay Ta Kae. The sources of creek are in the eastern area, so the rivers flow from the east to west along the slope down to small reservoirs and floodplains. The major reservoirs in the area are the Khlong Phriao reservoir, Ban Dong reservoir and a reservoir in the Campus areaof Chulalongkorn University.

3.1.5 Climate

The climate of study area is similar to that found in Saraburi province. There are 3 seasons with the weather is under influence of 2 types of monsoon. The northeast monsoon causes the weather to be cool and dry. The southwest monsoon causes moist air and precipitation. The summer is during February to May and the rainy season is during May to October. The winter is during October to February. The study area locates deep inland far from coastal areas, so the temperature of summer is high while the weather of winter is rarely cold. Average annual temperature is approx. 25.9 - 28.8°C. Minimum temperature is on December and maximum temperature is on April. The average annual rainfall is approx. 1,140 mm.

3.1.6 Soil Resource

According to characteristics of soil, there are 12 different soil types in this area. The slope complex is an area of mountain and massif with a slope greater than 35 percent. The characteristics of soil texture and their abundance are different, depending upon rock sources. In the eastern part, rock fragments are scattered with an area of approx. 84.716 km^2. In addition, Kaeng Khoi series is found in the eastern part with an area of approx. 62.878 km^2. The central and western areas are found Hin Kong series with an area of 52.422 km^2. The remaining soil textures are Tha Muang series, Monorom series, On series, Korat series, Sakon series, Tha Li series, Chong Kae series and Phimai series.

The textures of the two layers of soil are loam, clay loam, sandy loam, loamy sand, silt loam and clay, but in the lower soil may found iron, manganese, laterite, pebbles and mottle. If there is more oxygen, it appears to be oxidized, causing the iron compounds to be changed and color of soil texture to be red. The soil pH varies from 4.5 to 7. The thickness of the upper soil is about 50 cm from the ground surface. The weathering rock is found at depth greater than 80 cm. In the plains area, undifferentiated alluvium is found and consists of various units of soils and their features (i.e, texture, color and depth of soil) are uncertainty (see Figure 3.4).
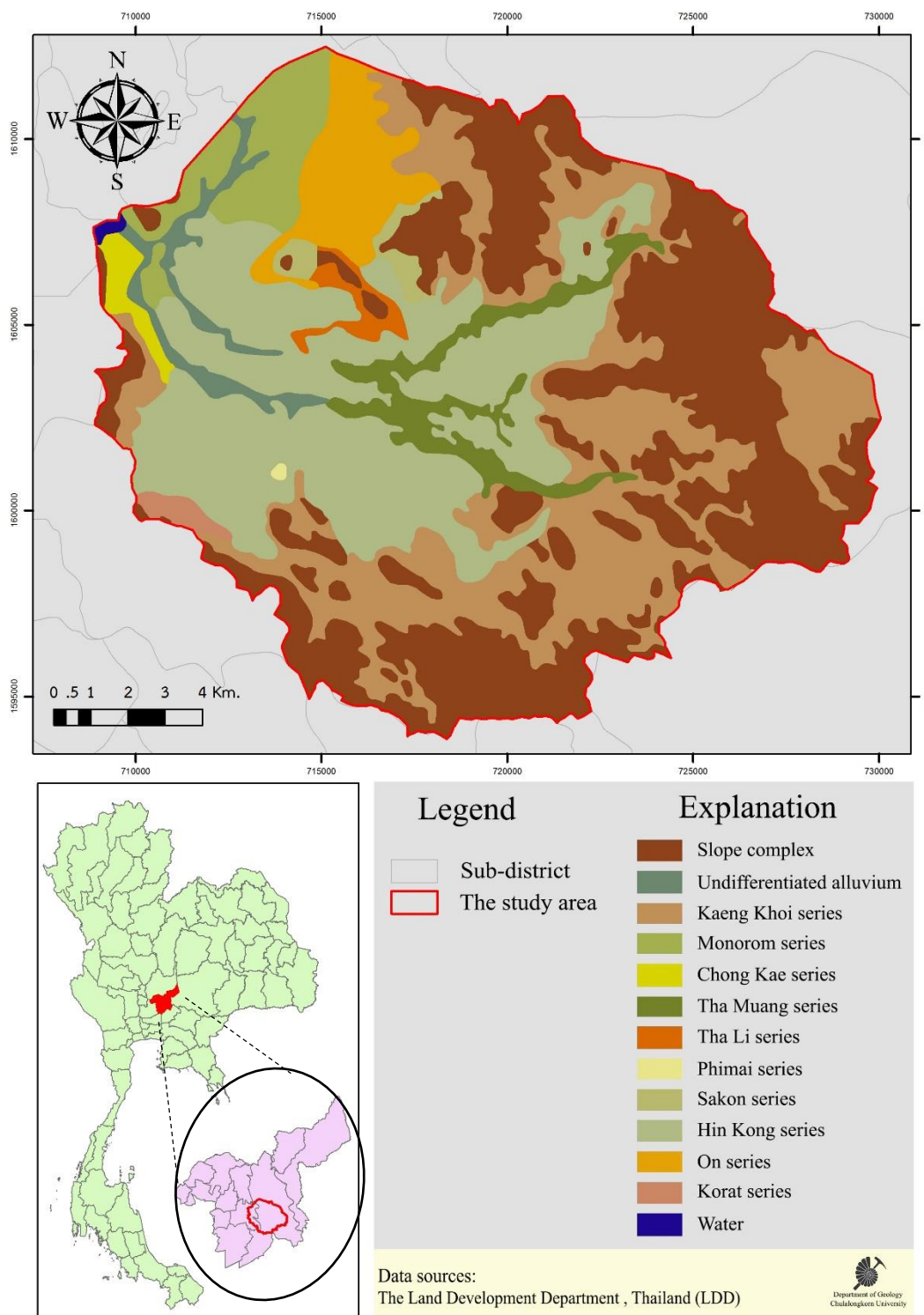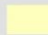
Figure 3.4 Soil resource map of the study area

3.1.7 Land Use

From the land use map of the Land Development Department (LDD) in 2009, the study area were divided to 5 types along the land use characteristic as following. The agricultural area is approximately 131.420 km^2 (50.16 percent of the whole area) consisted of approx. 84.94 km^2 of rice paddy, 24.78 km^2 of sugarcane, 8.79 km^2 of corn and 4.11 km^2 of swidden cultivation. In addition, there is a small area for mango, mixed orchard, mixed perennial, eucalyptus, teak, casuarina, banana, vine, truck crop, mixed horticulture and mixed field crop. The forest area is approx. 110.42 km^2 (42.15 percent of the whole area). The area of urban is approx. 12.15 km^2 (4.64 percent of the whole area), consisting of approx. 9.03 km^2 of village, 2.53 km^2 of cemetery and the remaining are road and institutional land. The area of factory is approximately 2.89 km^2 (1.10 percent of the whole area). The areas of poultry farm and fish farm are approx. 1.48 km^2 (0.56 percent of the whole area). The area of water resources are about 4.01 km^2 (1.53 percent of the whole area). Map of land use in the study area is shown as Figure 3.5.

Figure 3.5 Land use map of the study area

3.2 Fieldwork

3.2.1 Sampling location

In this research, water samples were collected during 2 seasons. The first field sampling during 10 to 13 November 2014, had 68 samples consisting of 44 groundwater samples, 14 surface water samples and 10 rain water samples. Details of sampling locations are shown in Table 3.1 and locations of the first field sampling are shown in Figure 3.6. For the second field sampling during 11 to 14 May 2015, only groundwater was collected at the same groundwater wells as collected in the previous field. There are 2 groundwater samples which were failed since groundwater pumps were unavailable. So, only 42 samples were completely collected in the second field (see Figure 3.7).
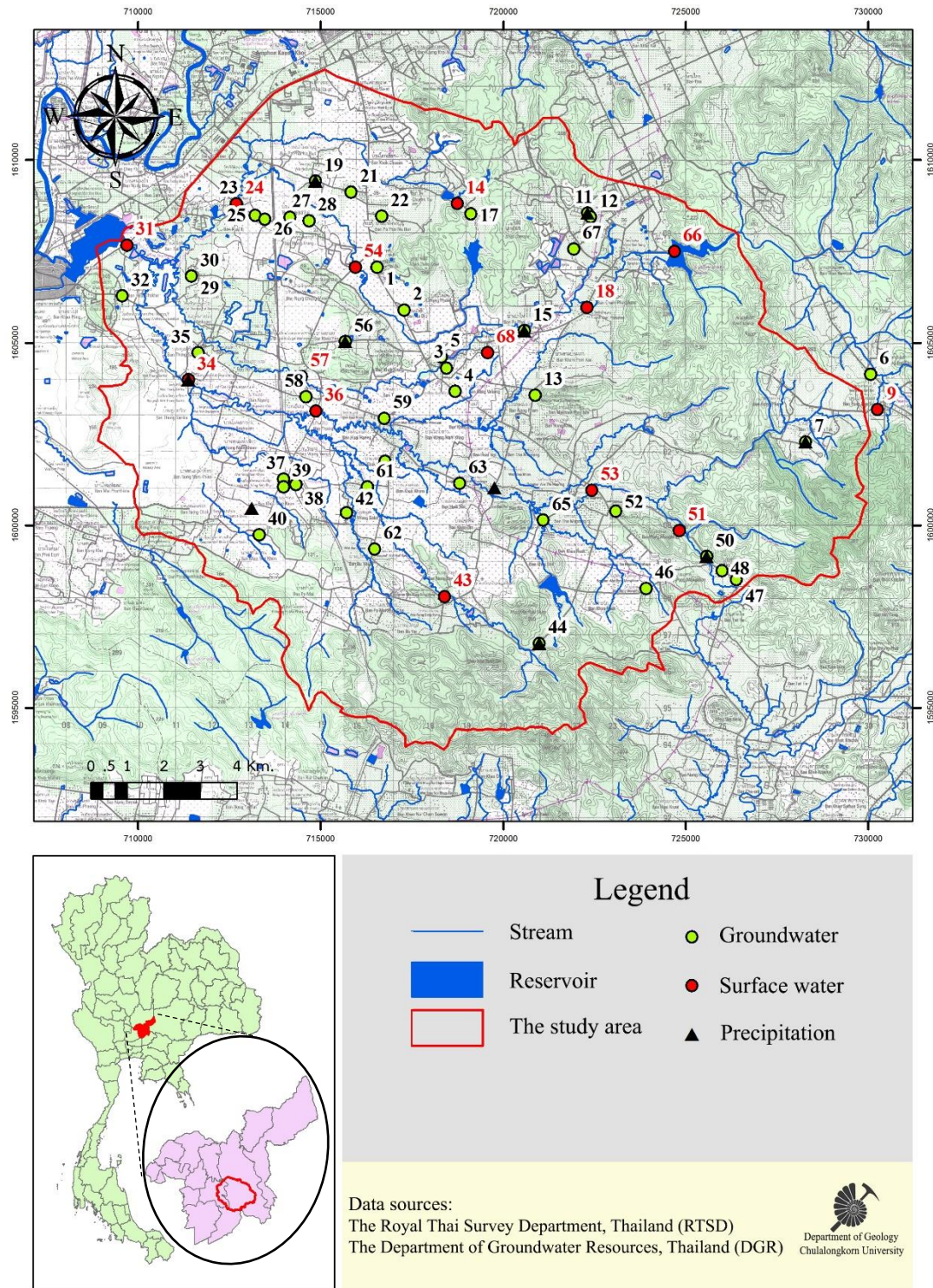
Figure 3.6 Map showing sampling locations of the first field sampling
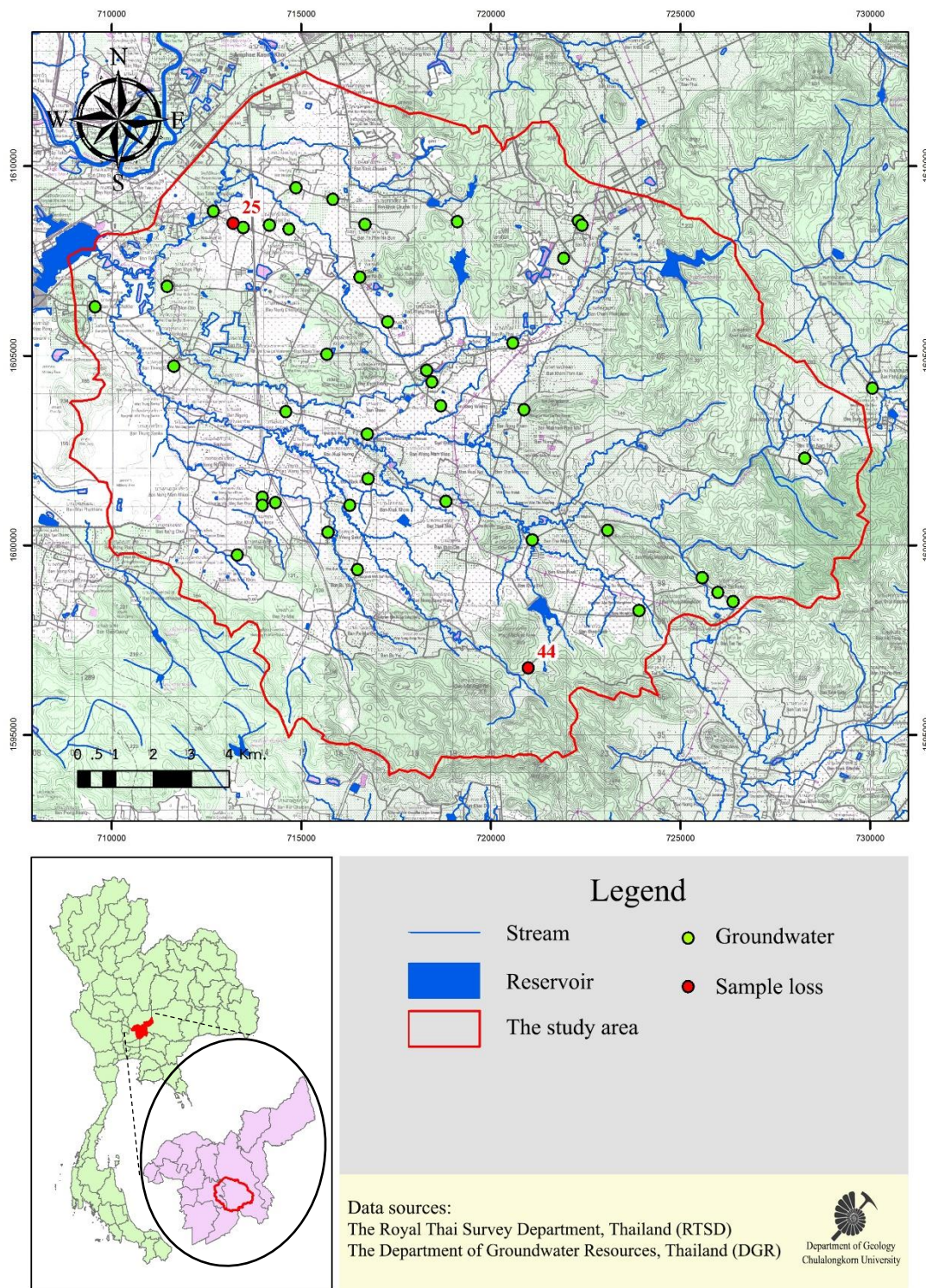
Figure 3.7 Map showing sampling locations of the second field sampling

Table 3.1 Details of sampling locations of precipitation, surface water and groundwater

Station	East	North	Elevation (m)	Water Types	Aquifer Types
ST01	716539	1607076	33	Groundwater	Qfd
ST02	717275	1605897	35	Groundwater	Qfd
ST03	718440	1604309	41	Groundwater	Qfd
ST04	719867	1602920	45	Groundwater	Qfd
ST05	718300	1604615	52	Groundwater	Qfd
ST06	730059	1604144	145	Groundwater	Vc
ST07	728277	1602291	163	Groundwater	Vc
ST08	728277	1602291	-	Precipitation	-
ST09	730253	1603172	159	Surface water	-
ST10	722311	1608558	-	Precipitation	-
ST11	722311	1608558	77	Groundwater	Vc
ST12	722399	1608447	72	Groundwater	Vc
ST13	720870	1603571	38	Groundwater	Qfd
ST14	718745	1608815	54	Surface water	-
ST15	720578	1605334	42	Groundwater	Qfd
ST16	720578	1605334	-	Precipitation	-
ST17	719117	1608537	66	Groundwater	Qfd
ST18	722288	1605971	38	Surface water	-
ST19	714853	1609432	28	Groundwater	Vc
ST20	714853	1609432	-	Precipitation	-
ST21	715830	1609126	45	Groundwater	Vc
ST22	716671	1608466	34	Groundwater	Vc
ST23	712684	1608809	27	Groundwater	Qfd
ST24	712684	1608809	27	Surface water	-
ST25	713202	1608493	27	Groundwater	Vc
ST26	713464	1608383	24	Groundwater	Vc
ST27	714156	1608442	24	Groundwater	Vc
ST28	714671	1608348	27	Groundwater	Vc
ST29	711461	1606825	22	Groundwater	Vc
ST30	711461	1606825	22	Groundwater	Vc
ST31	709687	1607677	16	Surface water	-
ST32	709563	1606287	34	Groundwater	Vc
ST33	711368	1603989	-	Precipitation	-
ST34	711368	1603989	15	Surface water	-
ST35	711636	1604727	34	Groundwater	Vc
ST36	714868	1603135	32	Surface water	-

Qfd = Quaternary Floodplain Aquifer

Vc = Volcanic Aquifer

Station	East	North	Elevation (m)	Water Types	Aquifer Types
ST37	713973	1601267	32	Groundwater	Vc
ST38	714315	1601126	36	Groundwater	Vc
ST39	713975	1601057	34	Groundwater	Vc
ST40	713311	1599740	45	Groundwater	Vc
ST41	713110	1600480	-	Precipitation	-
ST42	715703	1600345	46	Groundwater	Vc
ST43	718397	1598054	56	Surface water	-
ST44	720988	1596769	82	Groundwater	Vc
ST45	720988	1596769	-	Precipitation	-
ST46	723906	1598275	68	Groundwater	Vc
ST47	726386	1598514	109	Groundwater	Qfd
ST48	725990	1598761	96	Groundwater	Qfd
ST49	725570	1599148	-	Precipitation	-
ST50	725570	1599148	84	Groundwater	Qfd
ST51	724824	1599866	70	Surface water	-
ST52	723083	1600389	74	Groundwater	Vc
ST53	722422	1600966	54	Surface water	-
ST54	715946	1607073	17	Surface water	-
ST55	715669	1605038	-	Precipitation	-
ST56	715669	1605038	26	Groundwater	Vc
ST57	714471	1604079	22	Surface water	-
ST58	714592	1603520	25	Groundwater	Vc
ST59	716739	1602934	32	Groundwater	Vc
ST60	716759	1601752	31	Groundwater	Vc
ST61	716278	1601055	33	Groundwater	Vc
ST62	716478	1599358	41	Groundwater	Vc
ST63	718808	1601157	51	Groundwater	Vc
ST64	719755	1601038	-	Precipitation	-
ST65	721091	1600142	57	Groundwater	Vc
ST66	724687	1607510	98	Surface water	-
ST67	721925	1607575	72	Groundwater	Vc
ST68	719564	1604736	52	Surface water	-

Qfd = Quaternary Floodplain Aquifer

Vc = Volcanic Aquifer

3.2.2 Sampling Method

The sampling was conducted according to the measurement parameters that divided into 2 types as follows.

3.2.2.1 Details of the first field sampling

Samples were collected in 210 ml polyethylene bottles and 120 ml. amber bottle (120 ml.). In each station, 3 bottles of polyethylene were collected, consisting of 2 bottles with no any acid adding for using in cations and anions analysis, and 1 bottle with nitric acid (HCO_3^- concentration 1:1) adding for iron analysis. An amber bottle was collected by no acid adding for the oxygen and deuterium isotope analysis. All samples should be carefully stored with no air bubbles appeared in the bottle.

3.2.2.2 Details of the second field sampling

For this period, only the groundwater samples were collected with the same procedures and equipment as described in the first field sampling but no amber bottle for water sampling.

If groundwater well had a pump installed, pumping approx. 5 - 10 minutes was required before collecting a groundwater sample. But in a case of open well, a bailer was used for collecting a groundwater sample by draining water out 2 - 3 times before collecting a groundwater sample. All of equipment was rinsed by the groundwater itself to prevent cross-contamination from the other wells. Then all of bottles were closed with parafilm, labeled on a side of bottle and refrigerated at temperature 4°C prior to analysis in the laboratory (see Figure 3.8).

Figure 3.8 Groundwater well and equipment used in samples collecting (A) The open well, (B) The installed pump well, (C) Equipment for groundwater sampling and (D) Water samples in polyethylene bottles

3.2.3 Measurement of Parameters

Several parameters of the sample were measured during the field work by portable meters because they are sensitive and may change easily. These parameters were: potential of hydrogen ion (pH, no unit) showing acidity of solution. Temperature (T, °C) indicates a rate of oxidation by the biological process because it is directly proportional to temperature and impacts to dissolution of oxygen. Electric conductivity (EC, µS/cm or mS/cm) is used to assess the concentration of minerals or chemical compound which dissolves in the water. Generally, conductivity of pure water is zero. If the conductivity is high, it indicates that water has high dissociation substances. Total

dissolved solids (TDS, mg/l) is an amount of small solid particles dissolved in the water. TDS is an indicator of minerals, both organic and inorganic substances, being accumulated in water. Oxidation reduction potential (ORP, mV) is an index showing the ability of oxidation and reduction occurrence. ORP is measured from the concentration of electron in the water that occurs from oxidation process (adding oxygen) and reduction process (reducing oxygen). If this value is negative, it shows that oxidizing agents are high when it receives electron, then negative charge will increase. So reducing oxygen or reduction process is occurred. Every sample would be measured the same parameters except in the second time. Dissolved Oxygen (DO, mg/l) is oxygen dissolved in water which is an indicator of water source conditions and changing occurrence (in aerobic and anaerobic) in the water. During the day, oxygen will fluctuate along period of time. The Oxygen gas dissolves a little in the water and not chemically reaction with water. So, the quantity of oxygen depends on physical process, chemical and biological process of creature, pressure, T and TDS. In addition, water level is also measured to indicate groundwater flow direction of groundwater in area (see Figure 3.9).

Figure 3.9 Equipment for parameters measurement in the field. (A) pH 3210 WTW meter for measuring pH and ORP. (B) 341350A-P Oyster Series meter for measuring EC, T and TDS. (C) Equipment for measuring water level. (D) Procedure of water level measurement.

3.2.4 Exploring in the Study Area

The types of mainly crops grown are rice, corn, tapioca, and eucalyptus and mango in some area. The cultivation of palm trees is at station no. 48 (Figure 3.10). These plants mainly use rainfall for growth. The fertilizer used in area consists of minerals necessary for growth of plants such as nitrogen, phosphorus and potassium. The formulas of fertilizer by ratio of minerals are 16-8-8, 16-20-0, 15-15-15, 16-16-16, 46-0-0 and 14-5-22. The remaining areas are grassland, housing, water resource and the cattle at station nos. 12 and 65. The conditions of surface water in the first period are different from the other period. In the summer, water sources were dry and could not collect samples for chemical analysis. The type of rocks in the area mainly is andesite (Figure 3.11).

Figure 3.10 The agriculture in the study area: (A) Paddy, (B) Tapioca cultivation, (C) Corn cultivation, (D) Palm cultivation, (E) Eucalyptus cultivation

Figure 3.11 The other land use types in the study area: (A) The cattle (cow) farms, (B) The poultry (chicken) farms, (C) Grassland, (D) The character of andesite in the area, (E) The condition of surface water in the first period (early winter) and (F) The condition of surface water in the second period (late summer).

3.3 Laboratory Analysis

After sampling, these samples were sent to analyze in a laboratory. Many parameters were analyzed including cations: sodium (Na^+), potassium (K^+), calcium (Ca^{2+}), magnesium (Mg^{2+}), iron (Fe) and ammonium (NH_4^+) and anions: chloride (Cl^-), fluoride (F^-), bromide (Br^-), nitrite (NO_2^-), nitrate (NO_3^-), sulfate (SO_4^{2-}), phosphate

(PO_4^{3-}) and alkalinity, oxygen and deuterium isotopes. For cations and anions, Na^+, K^+, Ca^{2+}, Mg^{2+}, NH_4^+, Cl^-, F^-, Br^-, NO_2^-, NO_3^-, SO_4^{2-}, and PO_4^{3-} would be analyzed by the ion chromatography. The oxygen isotope, deuterium isotope and nitrogen isotope would be analyzed by the liquid water isotope analyzer. These tools locate at the Thailand Institute of Nuclear Technology (TINT). Only iron and alkalinity were analyzed by atomic absorption spectrometer (AAS) and titration method at Department of Geology, Faculty of Science, Chulalongkorn University.

3.3.1 Ion Chromatography

Ion chromatography can determine both cations and anions with different systems. The principle of measurement by ion chromatography is the separation of substances relied on different charges. These substances were converted into a form of ions by exchanging of charge within the column. System of ion chromatography consists of 4 parts as following;

1) Column acts like an ion exchange with charge in the column different from the samples

2) Eluent is buffer solution that takes the sample to the column and brings it into a detector.

3) Suppressor acts like an amplifier and reduces a noise signal.

4) Detector measures the substances released from the column.

A different of period of output signal in each substance depends on strength of bound between the sample and the column. This signal was compared with the duration of standard graph that can indicate types of substance in sample. The quantity of substances were obtained from calculation of the area under graph and compared with a calibration curve. Ion chromatography and other equipment used in this procedure are shown in Figure 3.12.
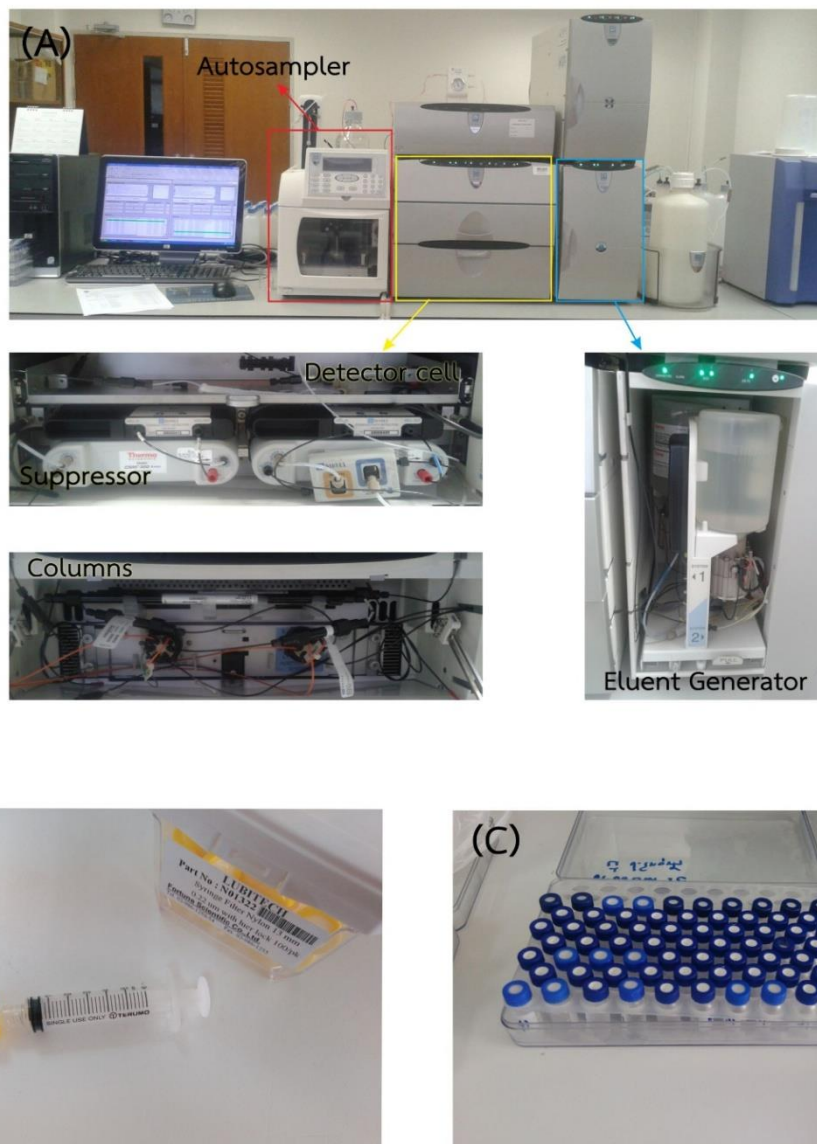
Figure 3.12 Dionex ICS-3000 ion chromatography. (A) The components of ion chromatography, (B) The syringe with 0.22 μm nylon filter for filtration, (C) The samples are put in 1.5 ml glass bottles for analyzing in ion chromatography

3.3.2 Liquid Water Isotope Analyzer

This research used the Cavity Ring-Down Spectroscopy (CRDS) to analyze the oxygen and deuterium isotopes in water samples. The principle of measurement is the state changing of water from liquid phase to become gas phase by boiling water at temperature 110°C. Then, this gas passes into the cavity that has 3 mirrors for reflecting the laser, which is closed when the signal reaches to a threshold level. Because the mirrors have a 99.999% reflection, a light in cavity will leak and decay until zero. This decay called ring down and are measured by the photo detector in real-time. If the gas absorbs light of laser, its decay will be fast. The different of the ring down time, with and without absorption due to the gas, is used to calculate the gas concentration (see Figure 3.13).
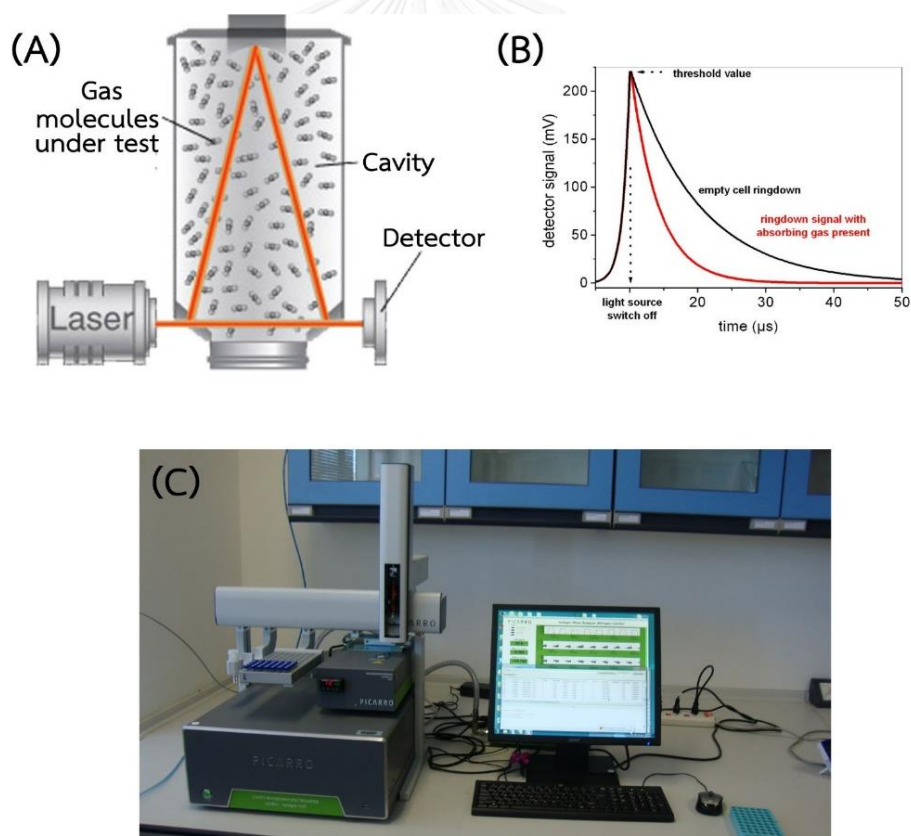
Figure 3.13 Liquid water isotope analyzing by CRDS. (A) The laser pulse within the cavity, (B) The graph shows a characteristic of ring down time, (C) Picarro L2130i Isotopic H_2O Analyzer.

3.3.3 Atomic Absorption Spectrometer

The atomic absorption spectrometer (AAS) is used to analyze amount of iron. The samples for analysis must be liquid to be absorbed into the air-acetylene flame of atomic absorption spectrometer. The heat makes dissociation of solution and results to the vaporization process and atomization process at ground state. Then, these atoms absorb the light at different wavelengths for changing from a ground state to an excited state. Light emits from the Hollow Cathode lamp. The appropriate wavelength for iron analysis is 248.33 nm. The absorbance is measured by the detector. In addition, it is directly proportional to the concentration of element by Beer-Lambert law. Figure 3.14 shows equipment used in this procedure.
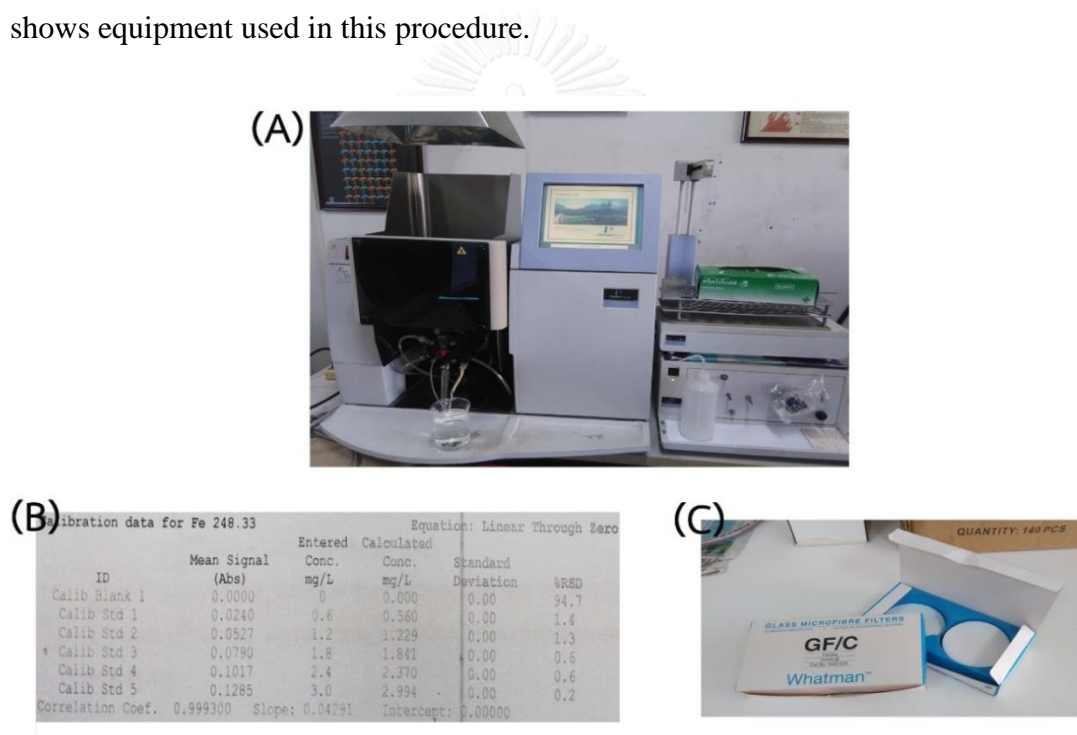
Figure 3.14 The calibration data and graph from AAS. (A) PerkinElmer AAnalyst 200 AAS, (B) The calibration data were prepared from iron standard solution with various concentrations (0.6, 1.2, 1.8, 2.4 and 3.0 mg/l) and were brought them into spectrometer again to measure a mean signal in each concentration, (C) Whatman ™1822-070 Grade GF/C glass microfiber filters for filtration samples before analysis in AAS.

3.3.4 Alkalinity Analysis

The compounds which result to the alkalinity in the water are hydroxide (OH^-), carbonate (CO_3^{2-}), bicarbonate (HCO_3^-), a combination of OH^- and CO_3^{2-} or a combination of CO_3^{2-} and HCO_3^-. In this research, indicator method was used for alkalinity analysis. By this method, color appearance is measured from the change of indicator. Therefore, this is an appropriate method for the water that is colorless and no turbidity. Quantity of alkalinity can be found by titrating with strong acids, i.e. sulfuric acid. Then the equilibrium point was observed from the changing of color of indicator. The chemicals used for titration consist of phenolphthalein, mixed indicator between methyl red and bromocresol green, and 0.02 N sulfuric acid. The procedure of chemicals preparation is shown as following.

3.3.4.1 Indicator Solution

Phenolphthalein ($C_{20}H_{14}O_4$) with 200 ml volume was prepared from weighting 1 g of phenolphthalein powder and then dissolved into 100 ml of ethanol 95% (C_2H_5OH). Final volume was adjusted to 200 ml by the deionized water.

Mixed indicator between methyl red and bromocresol green ($C_{15}H_{15}N_3O_2$ + $C_{21}H_{14}Br_4O_5S$) with volume of 100 ml was prepared from weighting 20 mg of methyl red powder and 100 mg of bromocresol green powder. Then these substances were dissolved in 100 ml of 95% ethanol.

3.3.4.2 Acid Solution

The acid solution is 0.02 N sulfuric acid (H_2SO_4) which is made from 0.1 N sulfuric acid. To prepare 0.1 N sulfuric acid, concentrated sulfuric acid of 3 ml volume was adjusted by the deionized water until its volume increased to 1000 ml (note that only the acid should be added into the water). When the preparation complete, the concentration of sulfuric acid cannot be determined that it is equal to 0.1 N. So, the concentration must be checked by sodium carbonate (Na_2CO_3).

To prepare the 0.05 N Na_2CO_3 solution of 1000 ml volume, the substance of 35 g was baked at 250°C for 4 hours, and then made them cool by the desiccator. The substance weighed 2.5 g was dissolved in the deionized water, and then adjusted the

volume of water to 1000 ml (a lifetime about 1 week). After that, about 40 ml of Na_2CO_3 solution was poured into the 100 ml beaker and acid was in the burette. The probe was dipped into the solution and began the titration until reach to pH of 5. The volume of acid used in the first time had to be recorded. The beaker was closed by a wash glass and boiled the solution for 3-5 minutes and let it cool down to a room temperature. The solution was poured onto the wash glass in beaker. Phenolphthalein was dropped about 4 drops to mix with 2 drops of the solution. Then, titration was performed again until the blue color changed to orange-red color. The volume of acid used in the second time was recorded. This recorded value was calculated according to the formula below.

$$N = \frac{A \times B}{53 \times C}$$

Where N is the concentration of sulfuric acid that is prepared from the concentrated acid. A is the weight of sodium carbonate in 1000 ml of solution (2.5 g). B is the volume of sodium carbonate (Na_2CO_3) that is used for titration (40 ml). C is the volume of sulfuric acid that is used for titration in both times. The concentration calculated from the above formula was used to calculate the volume for preparing the 0.02 N sulfuric acid in formula;

$$C_1V_1 = C_2V_2$$

Where C_1 is the concentration calculated from the above formula. V_1 is the volume retrieved from 0.1 N acid to prepare the 0.02 N acid. C_2 is the desired concentration. V_2 is the desired volume. The acid solution was used to titrate 50 ml of water samples. Then phenolphthalein was dropped about 2 drops. Titration with 0.02 N sulfuric acid was needed until the color of water change from pink to colorless (no color indicates none of hydroxide and carbonate). The volume of acid used was called P-alkalinity (see Figure 3.15). About 3 drops of the mixed solution were put into the water. The water would appear a blue color. Then titration was performed until the water become pink-orange color. The volume of acid used was called M.O.-alkalinity (see Figure 3.16). The volume of acid used can be calculated in the formula below.

$$\text{P-alkalinity or M.O.-alkalinity} = \frac{A \times N \times 50,000}{\text{Volume of Samples}}$$

Where P-alkalinity is the alkalinity which is measured by phenolphthalein indicator. M.O.-alkalinity is the alkalinity which is measured by mixed indicator. A is the volume of sulfuric acid used for titration. N is the concentration of sulfuric acid. Total alkalinity can be calculated by a formula;

Total alkalinity (T-alkalinity) = P-alkalinity + M.O.-alkalinity

Finally, only two values is needed, i.e. P-alkalinity and total alkalinity. These values are compared in the Table 3.2 for indicating the hydroxide, carbonate and bicarbonate in the water.

Table 3.2 The relationship between P-alkalinity and Total alkalinity

Alkalinity	OH^-	CO_3^{2-}	HCO_3^-
P-alkalinity = 0	0	0	T
P-alkalinity = T-alkalinity	T	0	0
P-alkalinity < 0.5 (T-alkalinity)	0	2P	T - (2P)
P-alkalinity = 0.5 (T-alkalinity)	0	T	0
P-alkalinity > 0.5 (T-alkalinity)	(2P) - T	2(T - P)	0
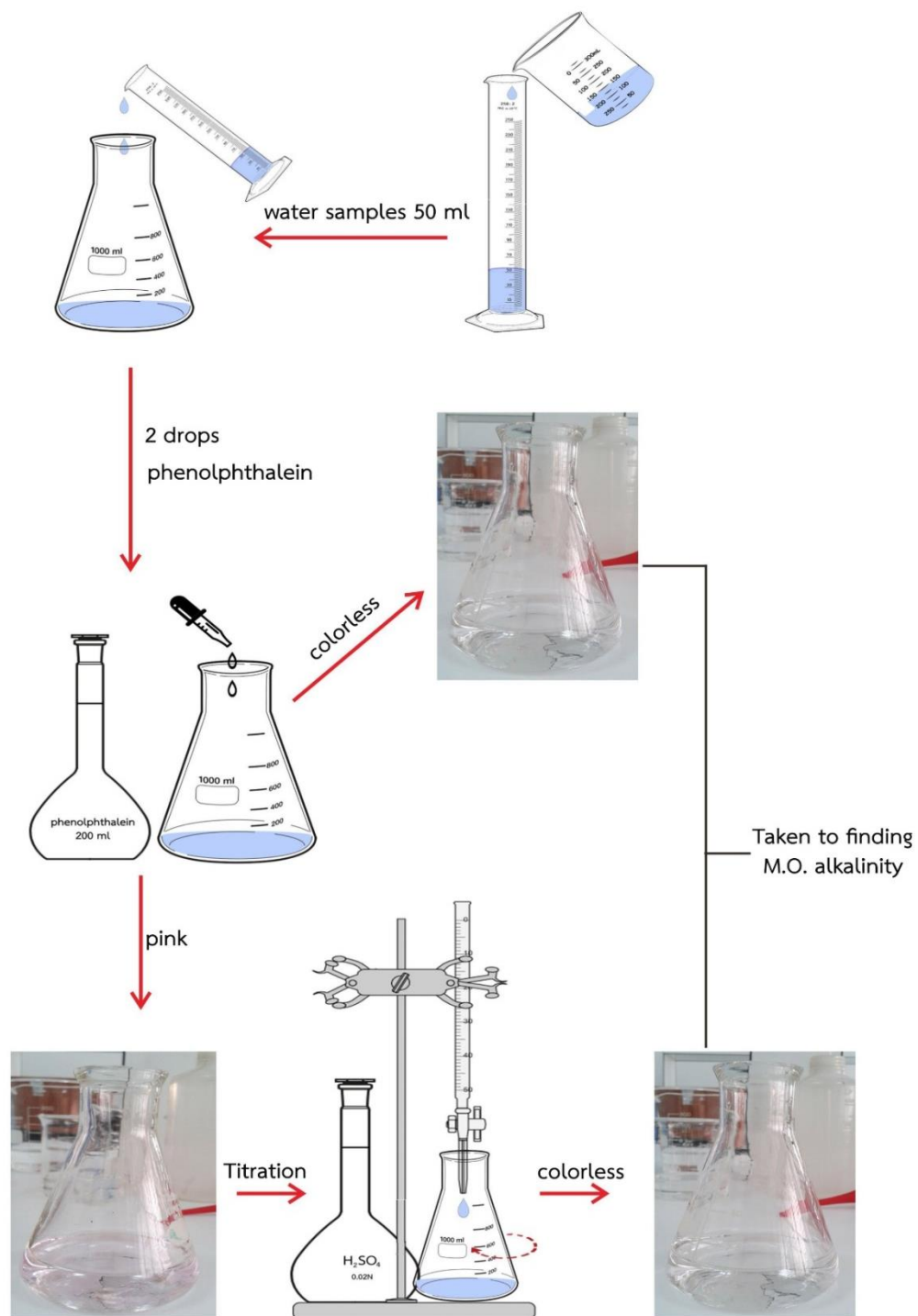
Figure 3.15 Procedure of the P-alkalinity estimation
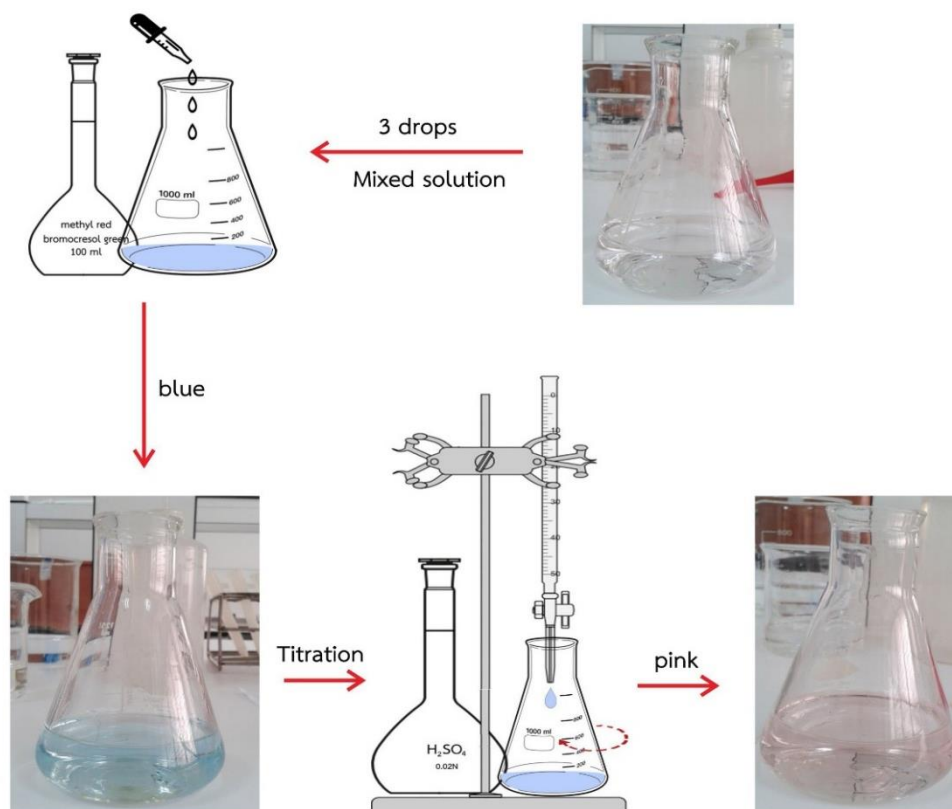
Figure 3.16 Procedure of the M.O.-alkalinity estimation

3.4 The Data Processing

Before the data was used to interpret, the reliability of the data must be checked by calculating the balance between cations and anions. This method is called ion balance. Ideally, the sum of the cations is equal to the sum of the anions, but if the value from the calculation does not exceed 15 percent, it would be acceptable. After assessing the quality of the data, the available positions of groundwater well data were then considered. These wells were separated along the characteristic of aquifer so the data is split into two groups. Then, the relationship between the ions in the water, NO_3^- and the other ions as well as the effects of the seasons on the quantity of ions could be created. Types of groundwater could be assessed by creating a piper diagram, creating a distribution map of NO_3^- that interpret together with the land use map, data from the field survey and the relationship between the other ions such as data of stable isotope for identifying the sources of NO_3^-. In addition, groundwater level map was also generated for observing the groundwater flow direction that may affect to the concentration of NO_3^-.

CHAPTER IV
RESULTS AND DISCUSSIONS

4.1 The Flow Direction

This chapter shows the results of the study about the groundwater flow direction that was created from the data of groundwater level measured in the field. It may help us to understand the distribution of NO_3^- in groundwater. Furthermore, the stable isotope data was used to explain the interaction between surface water and groundwater that may result to changing of NO_3^- concentrations in this area. In the section of chemical analysis results, the concentration of major cations and anions was used for constructing the piper diagram to identify groundwater facies. The relationship of these ions is indirectly used to explain the sources of NO_3^- contamination.

During the field, groundwater levels of total 58 wells was measured in and nearby of the study area and then groundwater level contour map was created. The flow direction of groundwater can be created by dragging an arrow perpendicular to a contour line. The mainly wells distribute in the central area, but at the western of area cannot be measured because the wells were tightly closed and cannot drop a groundwater measurement device. So, no data was measured in these areas. But that is not quite a problem because the groundwater flow direction could be estimated on the map. The main flow direction flows from the east to the west that conforms to topography and the flow direction of surface water. The direction of groundwater flow into the wells is shown as Figure 4.1. The groundwater level was measured in two seasons, which were in November, the end of rainy season, and in May, the end of summer. The result of groundwater level contour map in rainy seasons shows that the flow direction conforms to that in the summer (see Figures 4.2 and 4.3). But the groundwater level in the summer season appeared to be decreased more than in the rainy season because of an arid and no rain conditions. So a demand of water for household consumption and agriculture increased.
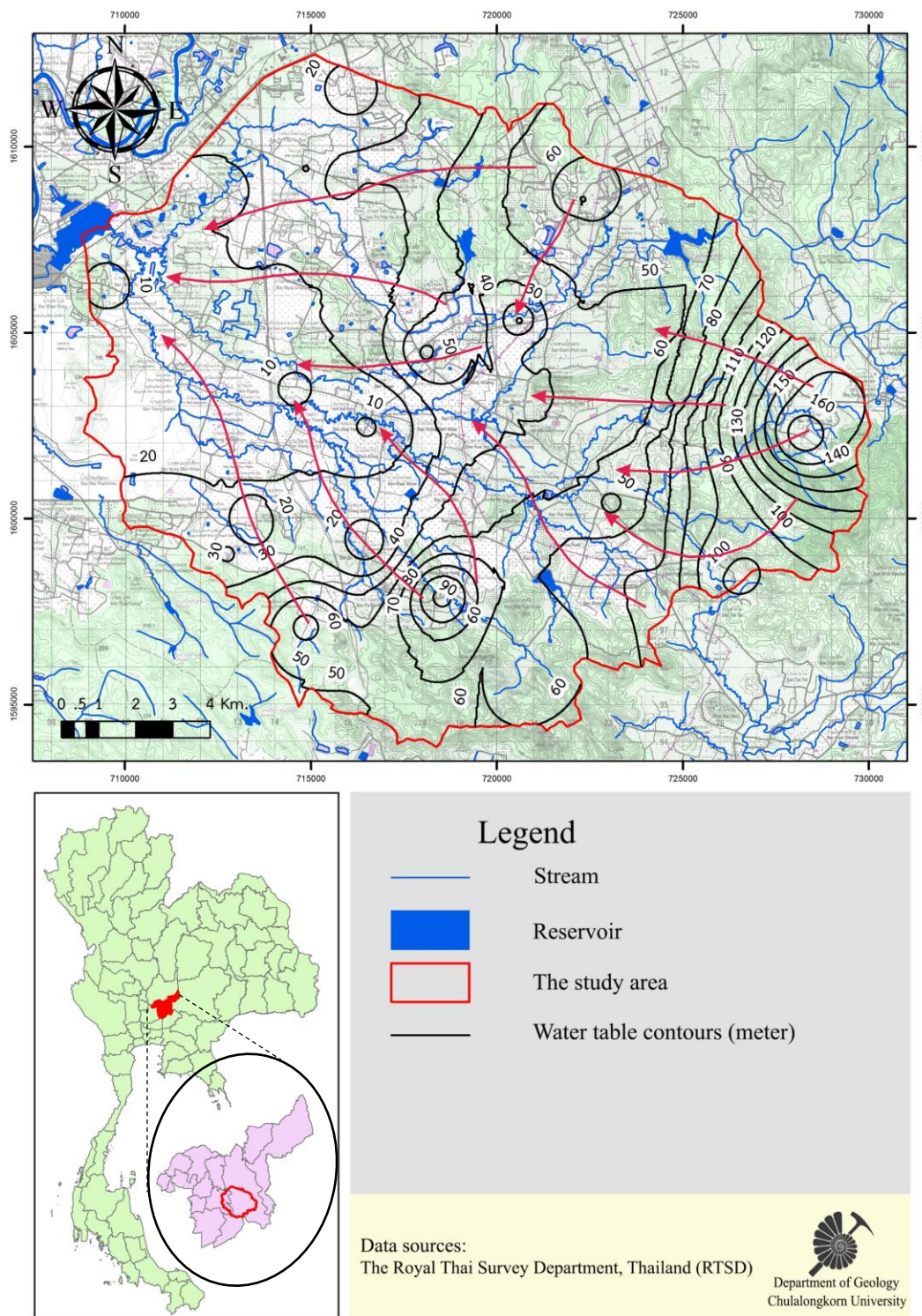
Figure 4.1 The map showing groundwater level contour map with groundwater flow directions in the study area
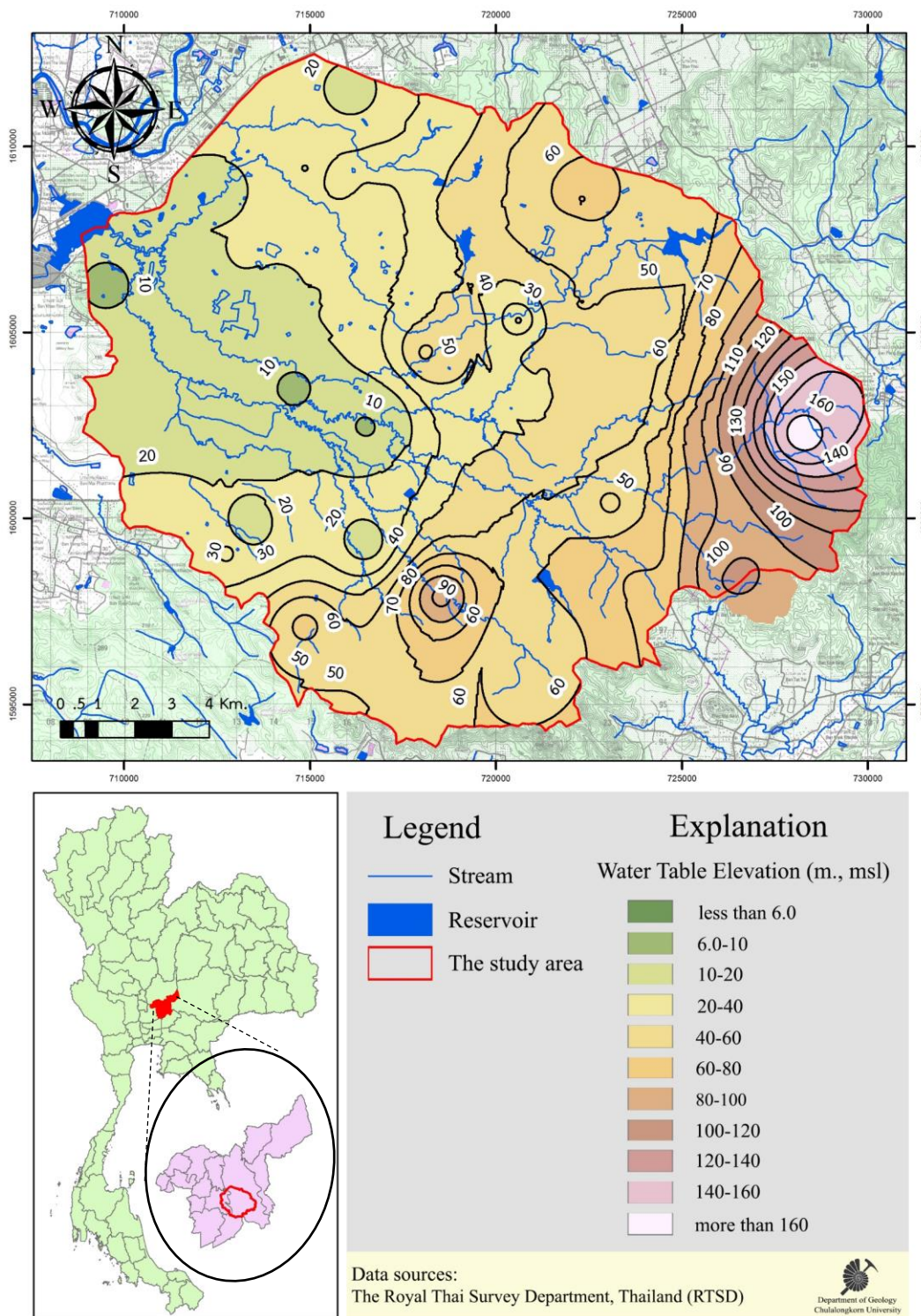
Figure 4.2 The map showing groundwater level in the rainy season.
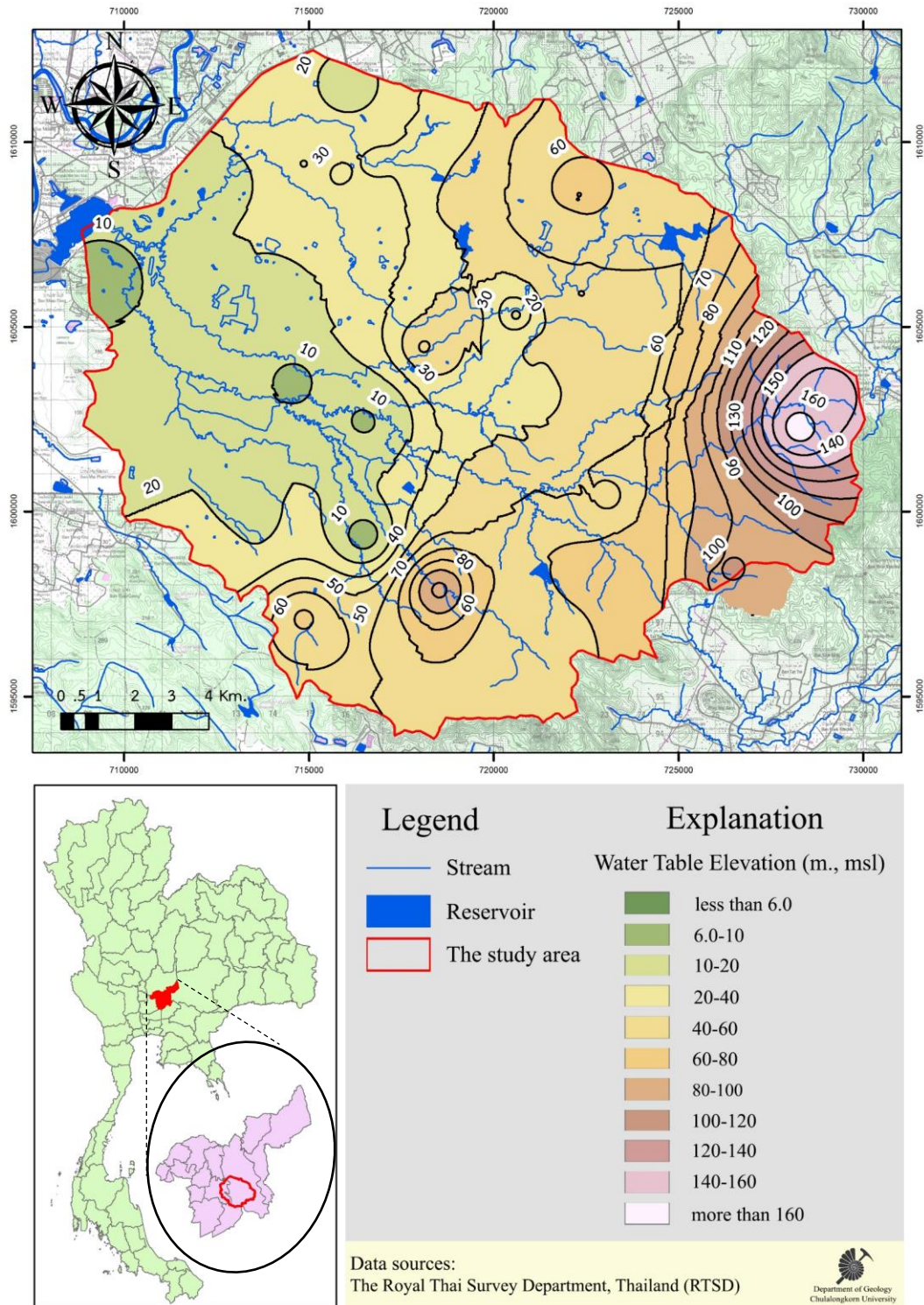
Figure 4.3 The map showing groundwater level in the summer season.

4.2 Ion Charge Balance

The first step, prior data analysis, ion charge balance of data must be calculated. The analysis results have units of milligram per liter (mg/l) and were converted to the units of milliequivalents per liter (meq/l). Then an error of ion charge balance was calculated by the following equation.

$$Error\, of\, ion\, balance = \frac{\Sigma cations - \Sigma anions}{\Sigma cations + \Sigma anions} \times 100$$

In this research, cations used consist of sodium (Na^+), calcium (Ca^{2+}), magnesium (Mg^{2+}) and potassium (K^+). Anions consist of chloride (Cl^-), sulfate (SO_4^{2-}), fluoride (F^-) and alkalinity ($CO_3^{2-} + HCO_3^-$). Ideally, the sum of cations must be equal to the sum of anions. But in fact, the acceptable criteria of difference should not exceed $\pm 10\%$ (Boyd, 2002; HYDRAULICS & HALCROW, 1999; *Ionic Balance Calculations*, 2014). The calculation found in rainy season, there were five stations having error higher than $\pm 10\%$, which were station nos. 03, 05, 37, 39, 58, 60 and 63. Therefore, these stations would not be used for further interpretation. In addition, the error of ion balance of surface water samples in two seasons is less than $\pm 10\%$.

4.3 Geochemistry of surface water and groundwater

4.3.1 The pH

In the rainy season, the pH of groundwater samples was in a range from 6.32 to 9.89 with an average pH of 7.65. Some groundwater samples showed high alkaline, especially at station nos.1 and 3, which were of 8.92 and 9.89, respectively. The groundwater in these stations were hardness. In summer, the pH was in a range from 6.28 to 7.83 with an average of 7.0. The maximum pH was 7.83 at station no.60 which is lower than that in the rainy season. In the summer season, all groundwater samples do not show high alkaline (pH>7) (see Figure 4.4).

The pH of the surface water samples in the rainy season ranged from 7.3 to 9.46. The maximum pH was 9.46 at station no.09, while pH in the summer season is in a range from 6.83 to 7.9 with the maximum pH was 7.9 at station no.66. All of surface

water samples measured in the summer have pH lower than those in the rainy season, which showed a similar results as found in the groundwater (see Figure 4.5).
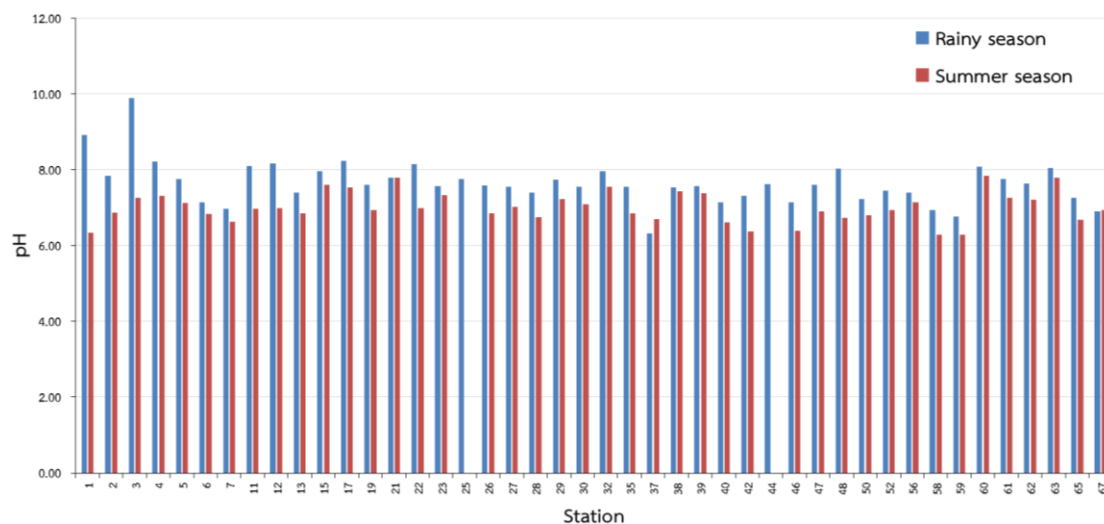
Figure 4.4 The pH of groundwater in the summer and rainy seasons
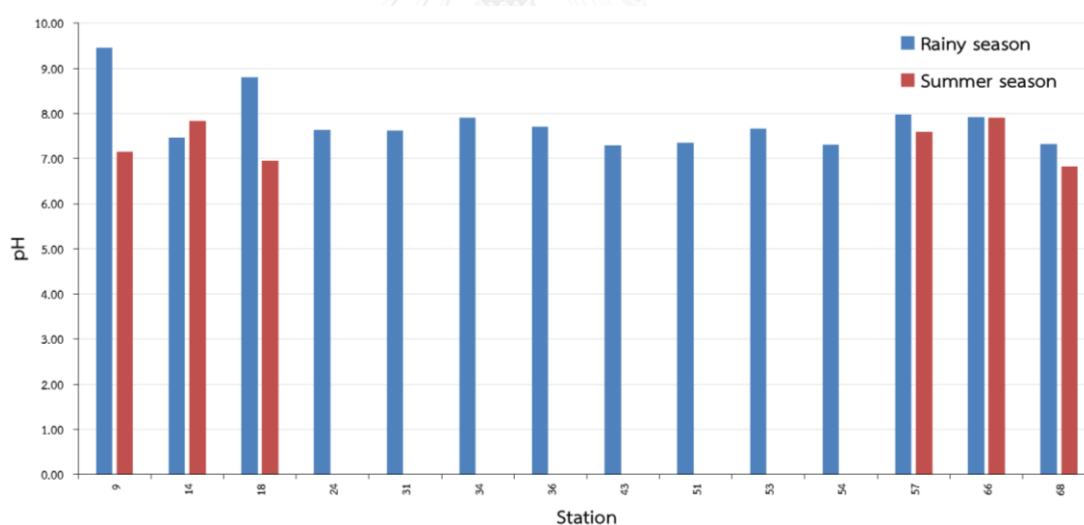
Figure 4.5 The pH of surface water in the summer and rainy seasons

4.3.2 Temperature

The temperature of groundwater in two seasons is rather similar with a range from 27°C to 37°C. The average temperature in rainy season and summer were 29.82°C and 31.97°C, respectively, which is relatively high in the summer season. The maximum temperature in the rainy and summer seasons were 35°C and 36.7°C at

station nos.19 and 35, respectively (see Figure 4.6). However, at station nos. 06, 15, 19, 21, 26, 47, 48, 52 and 65, the temperature in the summer are less than those in the rainy season. However, based on a statistical analysis, it is found that the average temperature of two seasons were not significantly different at 0.05 level.

The temperature of surface water was in a range from 27°C to 38°C. The average temperature in the rainy and summer seasons were 29.6°C and 32.5°C, respectively. The temperature in the summer of station no. 18 was less than that in the rainy season about 0.5°C. The maximum of temperature in the rainy and summer season were 37.6°C and 34.7°C at station nos. 24 and 57, respectively (see Figure 4.7).
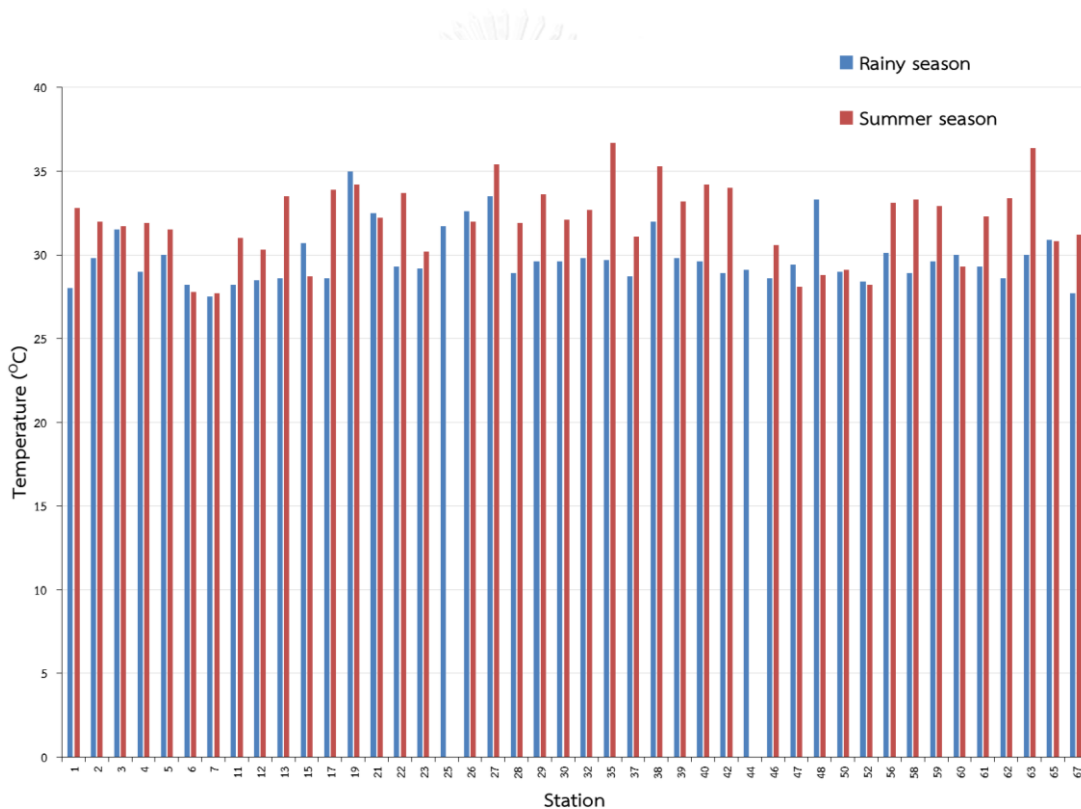
Figure 4.6 The temperature of groundwater in the summer and rainy seasons
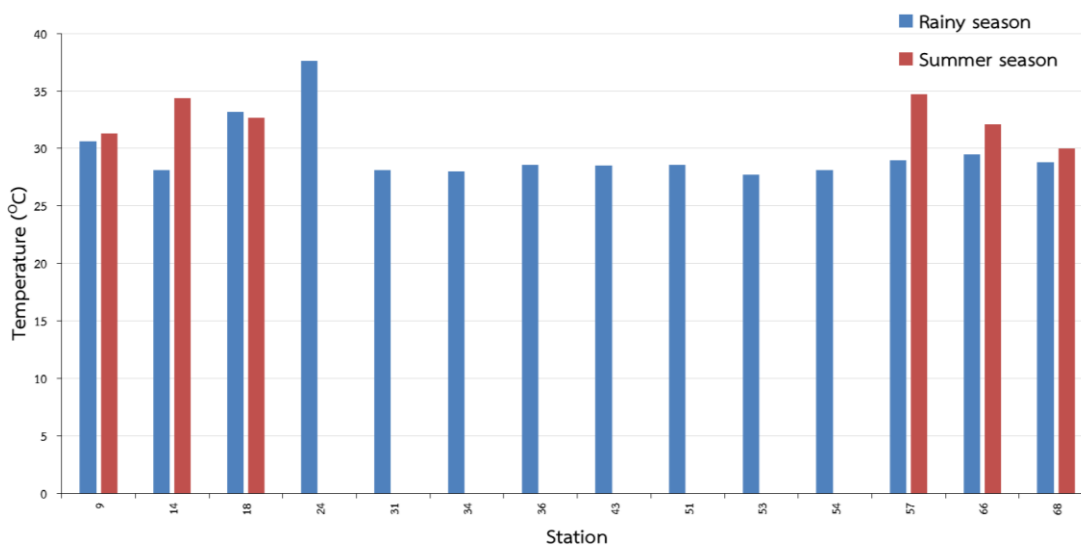
Figure 4.7 The temperature of surface water in the summer and rainy seasons

4.3.3 Electrical Conductivity

The EC of groundwater samples in the summer season varied from 116 µS/cm to 1,893 µS/cm, and the rainy season varied from 128 µS/cm to 1145 µS/cm. The average EC in the summer and rainy seasons were 821 µS/cm and 644 µS/cm. The summer has EC higher than the rainy season, except for station nos. 29, 42 and 65. The maximum EC in the rainy and summer seasons were 1,145 µS/cm and 1,893 µS/cm at station nos.21 and 67, respectively (see Figure 4.8).

The EC of surface water in the rainy season ranged from 40 to 244 µS/cm with an average of 106 µS/cm, whereas those in the summer season were in a range from 58 to 185 µS/cm with an average of 146 µS/cm. The maximum EC in the rainy season and summer seasons were 244 µS/cm and 185.2 µS/cm at station nos.24 and 57, respectively (Figure 4.9).
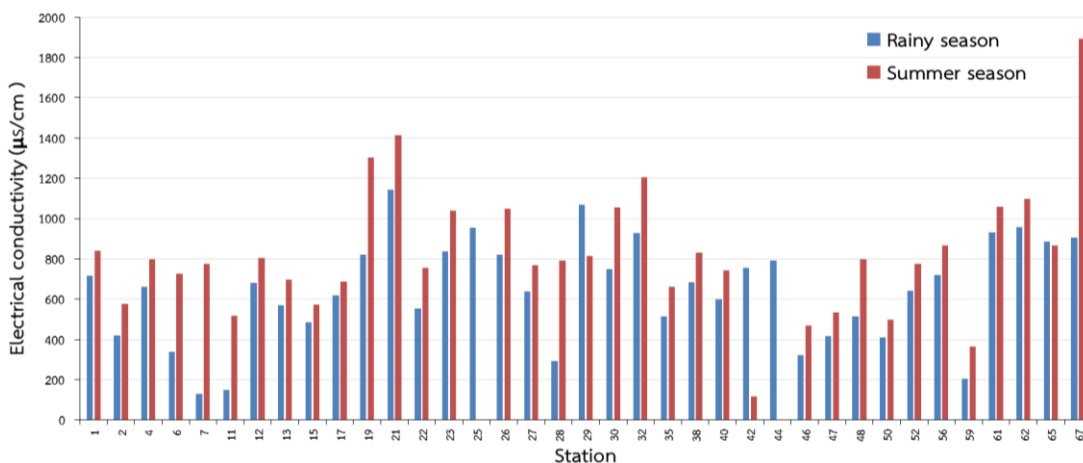
Figure 4.8 The EC of groundwater in the summer and rainy seasons
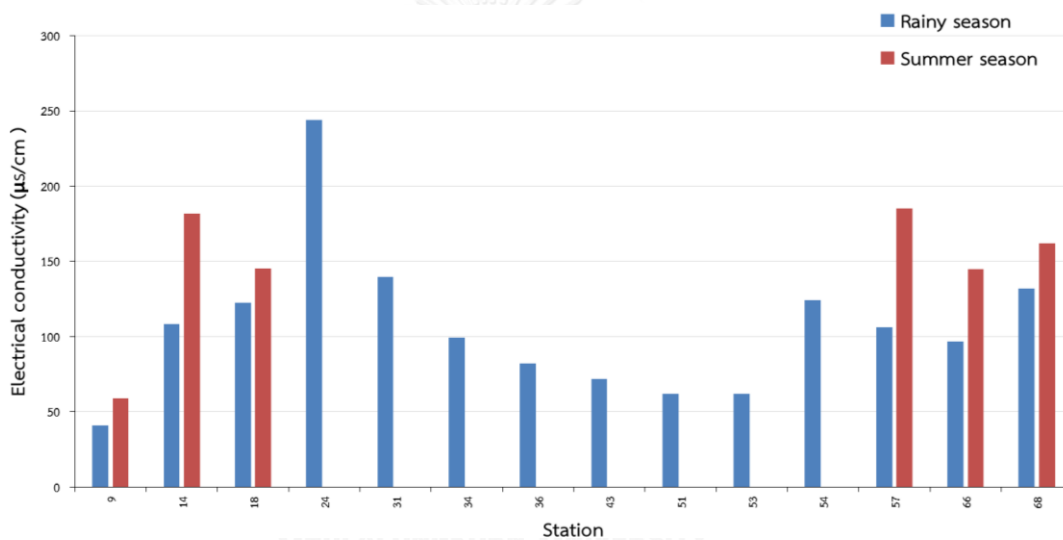
Figure 4.9 The EC of surface water in the summer and rainy seasons

4.3.4 Total Dissolved Solid (TDS)

The TDS of groundwater in the rainy season ranged from 64.2 mg/l to 572.5 mg/l with an average TDS of 315.53 mg/l, while those in the summer were in a range from 58.2 mg/l to 946.5 mg/l with an average of 410.91 mg/l. The maximum TDS in rainy and summer seasons were 572.5 mg/l and 946.5 mg/l at station nos. 21 and 67, respectively (see Figure 4.10).

The TDS of surface water in the rainy season ranged from 20.35 to 122 mg/l with an average of 53.23 mg/l, while those in the summer were in a range from 29.49 to 92.6 mg/l with an average of 73.18 mg/l (Figure 4.11). These values in summer were

high as well as the EC. The maximum TDS in the rainy and summer seasons were 122 mg/l and 92.6 mg/l at station nos.24 and 57, respectively.
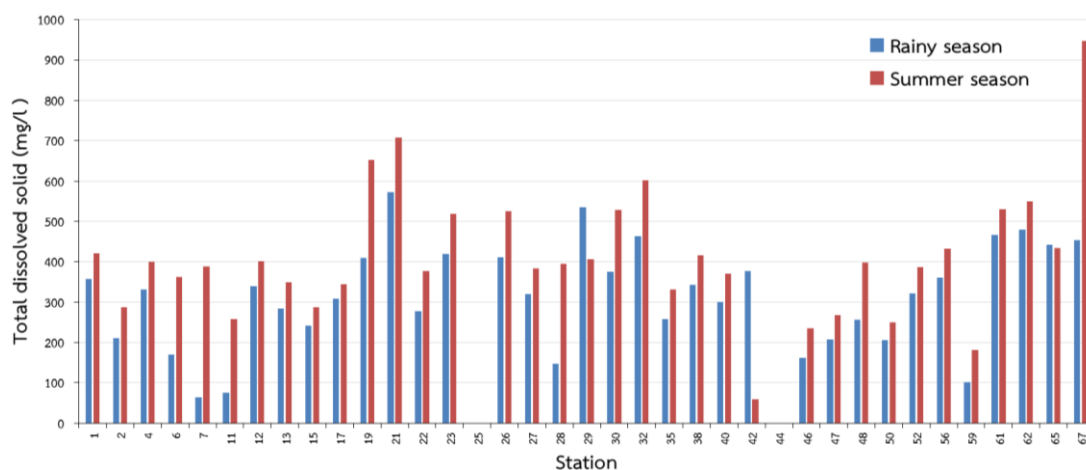
Figure 4.10 The TDS of groundwater in the summer and rainy seasons.
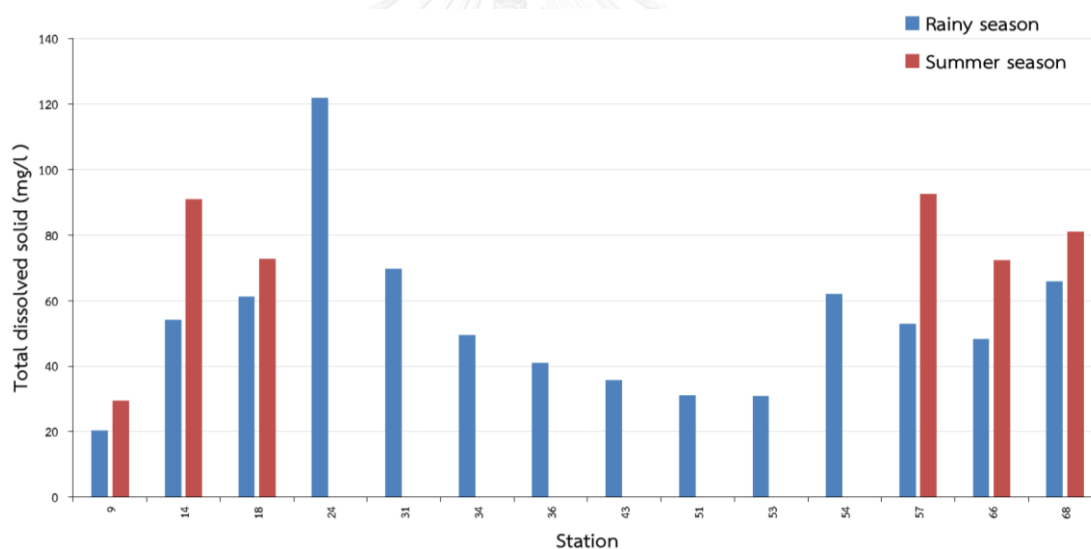
Figure 4.11 The TDS of surface water in the summer and rainy seasons

4.3.5 Oxidation Reduction Potential (ORP)

The ORP values in the rainy and summer seasons mostly were positive, indicating that the oxidation reaction mainly presents in groundwater. However, except for station nos. 02, 06, 11, 19, 38, 46, 52 and 67 in rainy season and station nos. 06, 07 and 11 in the summer season that occur the reduction reaction since they showed negative ORP values in groundwater. The ORP of groundwater in the rainy season

ranged from -164.2 to 221 mV. A station no.50 showed the highest positive ORP and station no.67 showed a highest negative ORP. The ORP in the summer season ranged from -152.5 to 263 mV. A station no.59 showed the highest positive ORP and station no.11 showed the highest negative ORP.

The ORP values of surface water in the rainy season ranged from 95.1 to 230.5 mV, and the values in the summer ranged from 198.9 to 264.1 mV. The highest ORP value was found at station nos. 54 and 18 in the rainy and summer seasons, respectively.

4.3.6 Dissolved Oxygen

A concentration of DO could be measured only in the summer season because the DO meter was out of order during the rainy period. The DO of groundwater showed a range from 0.7 to 8 mg/l with an average of 4.25 mg/l. The maximum of DO was found at station no.60.

The DO of surface water in summer ranged from 3.2 to 7.4 with an average of 5.48 mg/l. The maximum of DO was found at station no.14.

4.3.7 Concentrations of metals, cations and anions

The hydrogeochemical properties of groundwater and surface water are express in form of concentration of all ions, which the concentrations of cations and anions are summarized in Table 4.1-4.8. Moreover, Table 4.1 and 4.5 show isotope composition of groundwater and surface water in the summer season.

Table 4.1 The analyzed hydrogeochemical (cations) and isotopic of groundwater samples in the rainy season.

Station	Hydrogeochemistry (mg/L)						Isotope (%0)	
	Na^+	K^+	Ca^{2+}	Mg^{2+}	NH_4^+	Fe	$\delta^{18}O$	δD
1	41.50	1.01	66.91	11.01	n.a.	n.a.	-6.62	-43.54
2	15.10	2.39	47.38	2.47	0.05	6.93	-6.75	-45.88
3	38.16	1.49	35.54	0.04	n.a.	n.a.	-6.51	-43.40
4	39.38	2.88	65.70	2.34	n.a.	n.a.	-6.88	-45.70
5	41.39	1.18	38.52	2.00	n.a.	3.25	-6.69	-43.95
6	16.86	1.31	26.70	2.85	0.15	13.36	-6.77	-45.17
7	8.20	3.68	15.29	n.a.	n.a.	0.67	-7.15	-47.02

Station	Hydrogeochemistry (mg/L)						Isotope (%0)	
	Na⁺	K⁺	Ca²⁺	Mg²⁺	NH₄⁺	Fe	$\delta^{18}O$	δD
11	10.63	6.21	14.37	n.a.	n.a.	2.53	-6.97	-46.67
12	33.41	2.01	66.09	4.18	n.a.	n.a.	-6.83	-45.25
13	33.64	4.29	49.36	12.15	n.a.	0.43	-7.24	-47.89
15	40.02	0.68	32.94	0.67	n.a.	0.05	-6.48	-43.18
17	50.45	1.71	32.77	7.51	n.a.	n.a.	-6.32	-43.42
19	72.81	1.96	44.56	7.64	n.a.	0.12	-6.02	-41.02
21	n.a.	0.29	30.35	4.39	n.a.	n.a.	-6.05	-41.65
22	42.29	1.40	47.74	7.69	n.a.	n.a.	-6.00	-42.53
23	48.91	0.47	85.71	6.22	n.a.	n.a.	-5.30	-37.55
25	124.40	0.90	43.63	1.24	n.a.	0.11	-7.05	-47.32
26	100.80	0.33	39.65	2.87	n.a.	1.22	-6.40	-43.28
27	36.20	0.60	57.78	5.53	n.a.	n.a.	-5.91	-40.99
28	26.09	0.56	27.46	0.43	n.a.	n.a.	-6.08	-42.17
29	124.91	1.41	44.31	7.72	n.a.	n.a.	-7.01	-47.25
30	54.25	0.72	66.49	2.53	n.a.	n.a.	-6.62	-44.09
32	53.37	1.95	71.87	15.01	n.a.	0.06	-5.99	-41.61
35	41.99	2.08	48.05	4.53	n.a.	n.a.	-6.41	-42.79
37	26.61	2.59	3.57	n.a.	n.a.	12.12	-7.08	-47.99
38	40.90	2.87	81.39	4.73	n.a.	0.09	-6.84	-45.54
39	32.67	2.66	67.02	3.00	n.a.	0.48	-6.90	-47.08
40	37.46	3.22	70.90	3.29	n.a.	n.a.	-6.90	-45.44
42	39.03	2.88	76.13	5.96	n.a.	0.38	-6.85	-45.07
44	30.18	0.72	62.22	40.84	n.a.	0.09	-5.83	-39.86
46	25.69	0.44	25.19	8.91	n.a.	1.63	-6.90	-45.67
47	17.55	2.51	57.31	2.00	0.07	0.26	-7.03	-45.44
48	19.18	2.07	63.72	5.59	0.03	n.a.	-7.34	-48.04
50	39.34	2.15	47.92	0.05	n.a.	n.a.	-7.11	-46.19
52	36.26	3.69	60.92	7.74	n.a.	0.85	-7.09	-46.29
56	47.57	1.77	72.03	4.11	n.a.	n.a.	-6.92	-46.22
58	43.49	1.28	46.36	1.51	n.a.	2.73	-6.68	-44.34
59	22.87	1.75	12.94	0.75	n.a.	n.a.	-6.25	-43.17
60	130.13	2.24	11.47	4.82	n.a.	0.16	-6.74	-45.16
61	69.83	2.13	68.05	6.10	n.a.	0.49	-6.75	-45.34
62	52.18	2.76	82.92	10.93	n.a.	0.44	-6.64	-43.87
63	50.13	0.72	18.35	1.30	n.a.	n.a.	-6.24	-42.25
65	39.52	1.35	58.44	19.74	n.a.	0.04	-6.04	-40.52
67	45.28	6.45	74.97	38.36	0.24	n.a.	-6.69	-43.77

n.a. = not applicable

Table 4.2 The analyzed hydrogeochemical (anions) of groundwater samples in the rainy season.

Station	Hydrogeochemistry (mg/L)							
	Cl⁻	F⁻	Br⁻	NO₂⁻	NO₃⁻	SO₄²⁻	PO₄³⁻	HCO₃⁻
1	9.01	0.23	0.02	0.09	2.99	7.58	n.a.	311.2
2	12.02	0.45	0.02	0.45	7.11	4.31	n.a.	213.4
3	28.76	0.14	0.05	0.05	n.a.	12.44	n.a.	229.6
4	13.96	0.35	0.04	0.04	0.17	26.74	n.a.	327.2
5	24.94	0.19	0.05	0.05	n.a.	9.85	n.a.	289.4
6	2.98	0.14	0.01	0.10	0.30	2.70	n.a.	164.2
7	9.14	0.10	0.03	0.04	0.15	9.29	15.22	51.8
11	7.27	0.09	0.02	0.09	0.25	1.33	n.a.	74.6
12	5.86	1.13	0.01	0.02	0.20	1.88	n.a.	358.4
13	15.31	1.26	0.05	0.37	n.a.	23.48	13.88	291.6
15	26.98	0.30	0.04	0.04	1.62	8.99	n.a.	197.0
17	4.90	0.67	0.01	0.03	0.23	2.41	n.a.	307.2
19	33.33	0.26	0.14	0.06	0.34	6.52	13.90	238.8
21	27.32	0.15	0.03	0.04	3.02	20.98	n.a.	62.0
22	4.73	0.13	0.01	0.05	0.22	3.69	n.a.	241.8
23	33.34	0.40	0.16	0.01	n.a.	96.64	n.a.	335.0
25	22.05	2.84	n.a.	0.05	n.a.	166.51	n.a.	316.8
26	33.89	0.12	0.04	0.07	3.55	26.72	n.a.	397.0
27	15.59	0.15	0.02	0.03	0.66	5.41	n.a.	329.4
28	13.76	0.18	0.02	0.04	0.98	9.22	n.a.	143.6
29	22.57	0.86	n.a.	0.02	n.a.	247.47	n.a.	227.2
30	27.88	0.70	0.02	0.04	1.73	82.17	n.a.	279.0
32	44.28	0.22	0.10	0.06	2.37	59.86	n.a.	331.2
35	25.93	0.21	0.04	0.03	2.46	20.85	n.a.	247.0
37	25.18	0.36	0.07	0.04	n.a.	31.17	n.a.	0.0
38	25.22	0.13	0.02	0.04	n.a.	33.84	n.a.	296.0
39	19.23	0.14	0.01	0.02	n.a.	59.86	n.a.	250.0
40	27.95	0.61	0.04	0.03	n.a.	16.44	n.a.	231.6
42	37.26	0.24	0.06	0.05	n.a.	44.82	n.a.	307.6
44	13.66	0.88	0.02	0.05	1.36	21.51	n.a.	473.6
46	7.16	1.05	0.01	0.25	0.09	7.79	13.85	171.6
47	4.19	0.51	0.01	0.05	0.02	2.40	n.a.	192.8
48	6.22	0.36	0.02	0.05	3.12	7.80	n.a.	284.0
50	3.40	0.42	n.a.	0.06	0.64	1.60	n.a.	240.4
52	6.11	0.38	0.01	0.06	0.06	7.03	n.a.	317.8
56	5.97	0.79	0.02	0.31	n.a.	40.79	13.85	329.8
58	27.62	0.17	0.25	0.05	n.a.	12.93	n.a.	219.6

Station	Hydrogeochemistry (mg/L)							
	Cl^-	F^-	Br^-	NO_2^-	NO_3^-	SO_4^{2-}	PO_4^{3-}	HCO_3^-
59	13.98	59	13.98	59	13.98	59	13.98	59
60	14.28	60	14.28	60	14.28	60	14.28	60
61	19.86	61	19.86	61	19.86	61	19.86	61
62	46.87	62	46.87	62	46.87	62	46.87	62
63	15.39	63	15.39	63	15.39	63	15.39	63
65	54.54	65	54.54	65	54.54	65	54.54	65
67	188.15	67	188.15	67	188.15	67	188.15	67

n.a. = not applicable

Table 4.3 The analyzed hydrogeochemical (cations) and isotopic of groundwater samples in the summer season.

Station	Hydrogeochemistry (mg/L)					
	Na^+	K^+	Ca^{2+}	Mg^{2+}	NH_4^+	Fe
1	48.29	1.27	26.11	25.10	0.19	n.a.
2	18.41	2.67	66.84	15.64	0.05	18.26
3	72.31	1.65	21.51	6.62	n.a.	0.08
4	74.01	3.01	26.86	10.64	0.10	0.03
5	95.89	1.64	33.09	11.41	3.16	13.87
6	30.82	0.92	31.71	26.84	0.14	15.32
7	19.15	3.07	86.35	5.58	0.19	0.60
11	23.66	14.39	41.55	5.42	11.77	25.70
12	68.03	2.73	20.49	12.92	0.13	n.a.
13	32.52	7.87	33.57	11.42	0.10	1.94
15	75.70	0.80	18.58	3.74	n.a.	0.10
17	100.87	0.79	15.72	12.83	n.a.	n.a.
19	158.34	0.76	25.01	17.82	n.a.	n.a.
21	254.13	0.57	12.56	13.31	n.a.	n.a.
22	63.80	1.25	29.66	17.82	0.05	0.05
23	202.90	0.64	54.91	14.77	0.31	n.a.
25						
26	158.59	0.32	39.72	9.73	n.a.	2.44
27	68.48	0.86	30.91	14.72	n.a.	n.a.
28	70.94	2.53	23.79	9.84	0.08	n.a.
29	91.67	1.53	28.99	11.66	0.97	0.29
30	113.07	1.21	50.97	10.30	0.26	0.03
32	106.55	2.05	34.77	27.58	0.17	n.a.
35	52.95	2.84	49.17	12.67	n.a.	0.04
37	29.00	4.58	10.57	0.95	0.52	22.29
38	48.07	3.72	41.25	13.44	0.08	1.44

Station	Hydrogeochemistry (mg/L)					
	Na$^+$	K$^+$	Ca^{2+}	Mg^{2+}	NH$_4^+$	Fe
39	96.72	3.09	47.23	11.26	n.a.	3.95
40	46.78	4.03	59.19	9.95	n.a.	n.a.
42	11.65	4.57	4.35	0.93	0.43	2.22
44						
46	20.64	0.79	41.18	19.96	0.11	4.81
47	21.88	2.66	51.10	8.54	n.a.	0.02
48	36.73	3.05	32.96	17.92	n.a.	n.a.
50	42.20	2.69	52.39	1.88	n.a.	n.a.
52	45.58	4.95	37.75	18.26	0.06	0.48
56	73.08	2.60	31.28	10.77	n.a.	n.a.
58	50.30	1.67	54.15	5.42	n.a.	1.34
59	39.24	2.67	26.40	4.67	0.10	n.a.
60	179.59	2.26	8.39	9.48	n.a.	0.02
61	119.95	2.70	38.58	13.19	n.a.	0.40
62	83.28	3.80	49.66	19.72	0.83	1.73
63	96.59	0.83	15.45	2.03	n.a.	0.05
65	67.41	1.80	45.02	24.99	0.10	0.18
67	83.55	6.66	147.18	93.69	1.57	10.29

n.a. = not applicable

Table 4.4 The analyzed hydrogeochemical (anions) of groundwater samples in the summer season.

Station	Hydrogeochemistry (mg/L)							
	Cl$^-$	F$^-$	Br$^-$	NO$_2^-$	NO$_3^-$	SO$_4^{2-}$	PO$_4^{3-}$	HCO$_3^-$
1	8.47	0.35	0.87	n.a.	3.53	7.58	0.013	347.4
2	10.59	0.30	0.90	0.116	5.59	5.12	n.a.	291.8
3	30.95	0.29	0.66	0.016	0.87	13.02	n.a.	269.0
4	11.99	0.24	0.87	0.007	0.88	30.59	n.a.	335.8
5	37.39	0.29	0.71	0.030	2.08	2.89	0.057	399.4
6	4.00	0.34	0.96	0.013	0.97	2.64	0.015	324.8
7	15.21	0.04	0.82	n.a.	0.86	15.39	0.024	359.6
11	38.38	0.03	0.67	0.016	1.22	0.98	n.a.	194.4
12	6.41	0.99	0.88	0.016	1.09	2.84	n.a.	347.0
13	6.42	0.32	0.73	0.005	0.78	29.98	0.040	241.2
15	26.08	0.32	0.77	0.024	2.39	10.60	0.010	254.4
17	3.65	0.42	1.11	0.009	0.88	1.99	0.014	376.0
19	48.84	0.24	1.32	0.010	2.76	10.81	0.041	617.0
21	28.45	0.32	1.52	0.043	n.a.	21.79	0.011	628.6
22	2.09	0.23	1.08	n.a.	0.80	1.95	0.017	421.4

Station	Hydrogeochemistry (mg/L)							
	Cl^-	F^-	Br^-	NO_2^-	NO_3^-	SO_4^{2-}	PO_4^{3-}	HCO_3^-
23	30.44	0.36	1.13	0.019	0.20	297.86	0.036	376.0
25								
26	13.19	0.18	1.33	0.012	2.71	14.74	n.a.	535.8
27	15.52	0.25	0.79	0.011	1.97	6.66	n.a.	392.2
28	34.75	0.14	0.70	0.015	4.55	17.05	n.a.	264.6
29	17.51	1.40	1.94	n.a.	1.55	47.15	n.a.	370.0
30	29.74	0.73	1.02	0.020	0.88	193.51	0.069	295.0
32	76.47	0.55	1.13	0.021	2.44	67.10	n.a.	414.0
35	26.38	0.17	0.69	0.018	4.21	29.06	n.a.	285.4
37	21.54	0.03	0.35	0.055	1.23	5.31	n.a.	83.2
38	25.51	0.08	0.75	0.010	1.76	33.66	0.010	261.2
39	24.96	0.24	1.02	n.a.	0.18	123.55	0.038	360.0
40	25.23	0.08	0.64	0.008	0.88	17.25	0.012	337.4
42	10.02	0.08	0.04	0.013	0.82	18.51	0.024	19.0
44								
46	6.91	0.33	086	n.a.	1.01	14.76	0.032	231.8
47	3.33	0.44	0.91	n.a.	0.74	3.13	0.011	282.6
48	11.62	0.35	0.76	0.011	1.68	12.76	n.a.	301.6
50	2.86	0.35	0.90	0.012	2.16	2.63	0.051	267.0
52	5.50	0.27	0.95	0.014	1.01	7.90	n.a.	389.8
56	2.79	0.20	0.83	0.007	0.69	44.48	n.a.	337.8
58	27.70	0.37	0.70	n.a.	0.70	13.67	n.a.	252.0
59	13.47	0.28	0.69	0.005	1.97	6.06	n.a.	168.2
60	10.46	0.68	1.31	0.018	0.89	19.94	0.010	514.8
61	23.81	0.34	0.84	0.007	0.62	103.24	0.011	434.6
62	69.77	0.20	0.15	0.017	2.90	33.60	0.066	405.4
63	12.80	0.41	0.95	0.020	0.85	8.04	0.011	259.2
65	47.81	0.49	1.24	0.017	1.57	25.58	n.a.	365.4
67	218.56	0.87	3.41	0.106	1.57	39.86	0.188	527.0

n.a. = not applicable

Table 4.5 The analyzed hydrochemical (cations) and isotopic of surface water samples in the rainy season.

Station	Hydrogeochemistry (mg/L)						Isotope (%0)	
	Na⁺	K⁺	Ca²⁺	Mg²⁺	NH₄⁺	Fe	δ¹⁸O	δD
9	5.16	3.94	3.39	n.a.	0.02	0.67	-6.71	-44.69
14	7.91	2.75	9.26	0.05	n.a.	0.18	-6.78	-45.79
18	7.45	2.91	10.29	0.58	n.a.	n.a.	-4.71	-37.50
24	18.79	9.13	14.52	0.12	2.72	0.93	-5.35	-37.82
31	11.11	5.28	8.56	n.a.	1.29	1.36	-6.00	-40.20
34	9.17	3.36	5.70	0.13	n.a.	0.86	-6.35	-42.18
36	6.70	3.07	6.00	0.23	0.05	0.86	-6.65	-44.35
43	7.65	2.70	5.57	0.13	n.a.	0.88	-6.89	-44.88
51	18.88	1.70	2.62	n.a.	n.a.	0.52	-7.49	-49.13
53	7.84	2.44	4.18	n.a.	n.a.	0.61	-7.39	-48.54
54	9.99	3.86	9.73	0.73	n.a.	0.82	-5.84	-40.05
57	8.53	4.11	7.96	0.29	n.a.	1.17	-5.87	-39.89
66	7.70	2.86	8.50	0.68	n.a.	0.16	-6.78	-45.52
68	18.69	2.41	9.10	0.54	n.a.	0.88	-5.99	-42.37

n.a. = not applicable

Table 4.6 The analyzed hydrochemical (anions) of surface water samples in the rainy season.

Station	Hydrogeochemistry (mg/L)							
	Cl⁻	F⁻	Br⁻	NO₂⁻	NO₃⁻	SO₄²⁻	PO₄³⁻	HCO₃⁻
9	4.49	0.10	n.a.	0.052	0.11	0.72	n.a.	20.2
14	3.71	0.13	0.011	0.062	0.26	2.87	n.a.	51.4
18	3.38	0.27	0.007	0.032	n.a.	2.94	n.a.	60.8
24	18.50	0.28	0.021	0.074	n.a.	10.27	n.a.	71.8
31	11.08	0.18	0.032	0.110	0.53	4.51	n.a.	49.6
34	9.14	0.06	0.116	0.021	0.63	2.85	n.a.	35.2
36	4.19	0.14	0.011	0.044	1.10	2.87	n.a.	38.8
43	4.81	0.15	0.012	0.036	n.a.	6.33	n.a.	33.2
51	7.44	0.10	0.025	0.362	3.70	2.64	13.92	39.4
53	3.03	0.16	0.011	0.078	1.05	2.69	n.a.	26.8
54	5.25	0.22	0.012	0.053	n.a.	4.11	n.a.	61.8
57	5.68	0.11	0.014	0.062	0.33	3.04	n.a.	46.4
66	3.75	0.37	0.009	0.027	n.a.	3.50	n.a.	46
68	7.11	0.79	0.024	0.219	0.25	3.07	13.89	70.76

n.a. = not applicable

Table 4.7 The analyzed hydrochemical (cations) and isotopic of surface water samples in the summer season.

Station	Hydrogeochemistry (mg/L)					
	Na^+	K^+	Ca^{2+}	Mg^{2+}	NH_4^+	Fe
9	6.10	2.63	4.24	0.65	0.61	0.37
14	9.54	4.33	14.23	4.39	0.63	0.25
18	10.11	3.99	11.72	2.50	0.37	0.59
24						
31						
34						
36						
43						
51						
53						
54						
57	14.68	8.76	12.32	2.63	0.36	0.21
66	8.37	3.69	13.69	2.52	0.18	0.07
68	10.42	4.09	14.45	2.68	0.11	0.47

n.a. = not applicable

Table 4.8 The analyzed hydrochemical (anions) of surface water samples in the summer season.

Station	Hydrogeochemistry (mg/L)							
	Cl^-	F^-	Br^-	NO_2^-	NO_3^-	SO_4^{2-}	PO_4^{3-}	HCO_3^-
9	2.58	0.05	0.17	0.013	0.88	2.57	0.055	28.0
14	4.04	0.18	0.44	0.010	0.81	4.02	0.026	83.6
18	4.32	0.09	0.32	0.013	1.53	5.84	n.a.	64.8
24								
31								
34								
36								
43								
51								
53								
54								
57	9.91	0.11	0.37	0.008	1.13	4.80	0.021	77.8
66	3.13	0.08	0.34	n.a.	0.84	4.44	n.a.	69.8
68	4.29	0.10	0.38	0.024	1.25	4.04	0.022	76.8

n.a. = not applicable

4.3.7.1 Iron (Fe)

The concentrations of iron (Fe) were relatively low and variably. Groundwater samples have Fe in a range from 0.04 mg/l to 13.26 mg/l with an average of 1.56 mg/l. The maximum concentration of Fe in rainy season was at station no.06. More than half of all samples in the rainy season were below a detection limit. The concentrations of Fe in summer was also below a detection limit and ranged from 0.02 to 25.70 mg/l with an average of 4.11 mg/l. However, the concentration of Fe of each station in the summer was higher than those in the rainy season, except station nos.07, 19, 32, 47, 52 and 61. The highest concentration of Fe was found at station no.11, followed by station no.02 and 06 (see Figure 4.12).

The concentrations of Fe in surface water in the rainy season ranged from 0.16 to 1.36 mg/l with an average of 0.76 mg/l. All of samples were above a detection limit except station no.18. The maximum concentration of Fe in the rainy season was found at station 31. In summer, it ranged from 0.07 to 0.59 mg/l with an average of 0.32 mg/l. The maximum concentration of iron was found at station no. 18. In addition, in each station, the concentration of Fe in the summer season was lower than that in the rainy season, which is not agree with the results of Fe concentration in groundwater (see Figure 4.13).
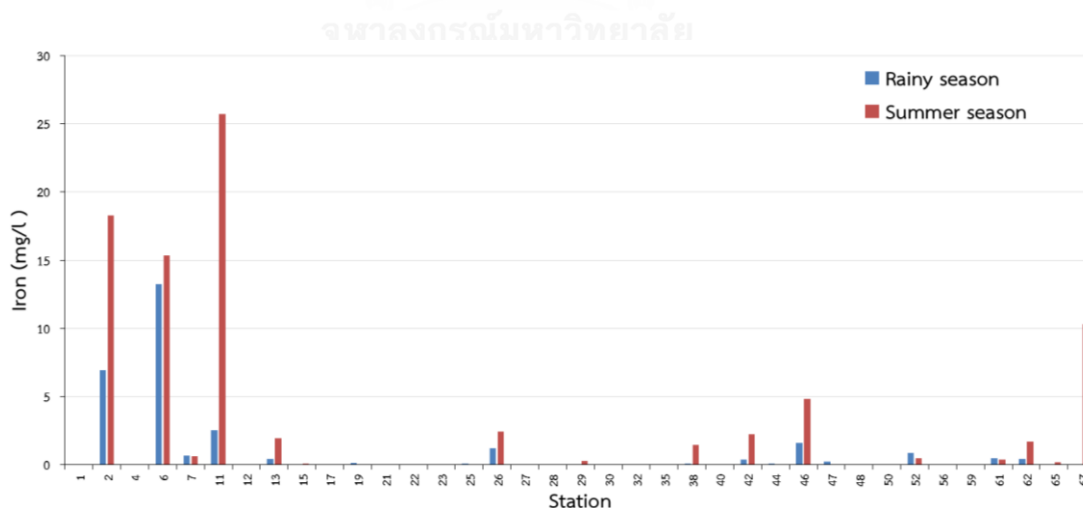
Figure 4.12 The concentrations of Fe in groundwater in the summer and
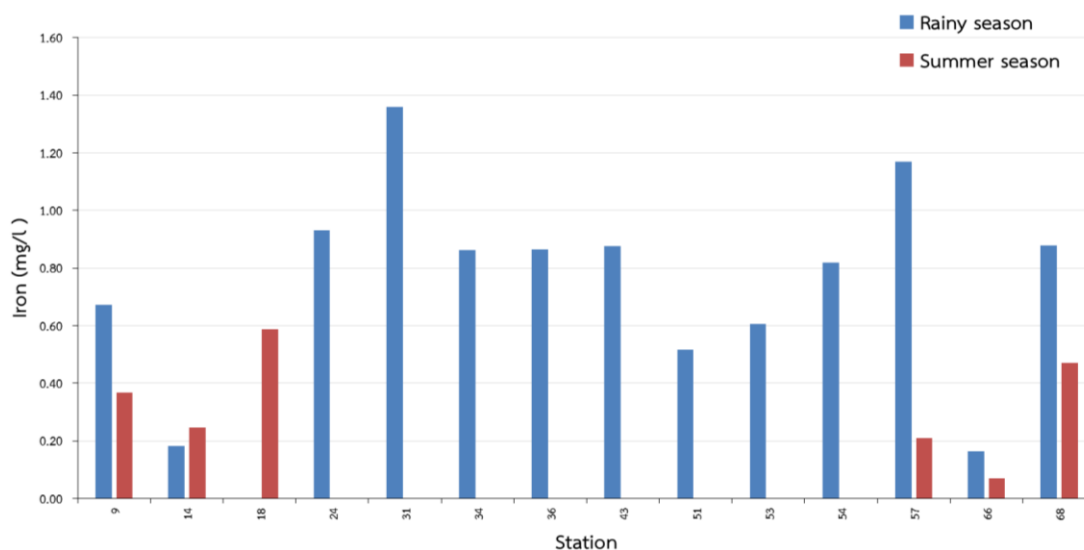
rainy seasons

Figure 4.13 The concentrations of Fe in surface water in summer and rainy seasons

4.3.7.2 Calcium (Ca^{2+})

The concentrations of calcium (Ca^{2+}) in groundwater were in a range from 12.94 mg/l to 85.71 mg/l in the rainy season with an average of 52.44 mg/l. The maximum concentration of Ca^{2+} was found at station no.23. The concentrations of Ca^{2+} in the summer were in a range from 4.35 mg/l to 147.18 mg/l with an average of 40.19 mg/l. The maximum concentration of Ca^{2+} was found at station no.67. The concentration of Ca^{2+} in groundwater samples mostly were less than in those in the rainy season except station no. 02, 06, 07, 11, 26, 35, 46, 50, 59 and 67 (Figure 4.14).

The concentrations of Ca^{2+} in surface water were in a range from 2.62 mg/l to 14.52 mg/l in the rainy season with an average of 7.53 mg/l, while in the summer, the concentrations of Ca^{2+} were in a range from 4.24 to 14.45 mg/l with an average of 11.78 mg/l. The maximum concentration of calcium in the rainy and summer seasons was found at station nos.24 and 68, respectively. All of surface water samples in the summer generally were higher than those in the rainy season (Figure 4.15).
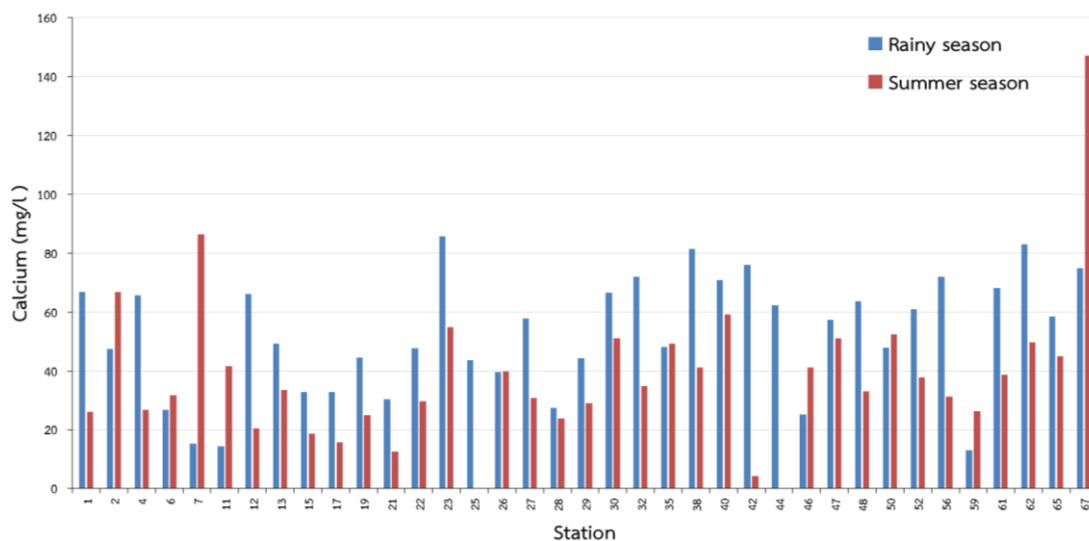
Figure 4.14 The concentrations of Ca^{2+} in groundwater in the summer and
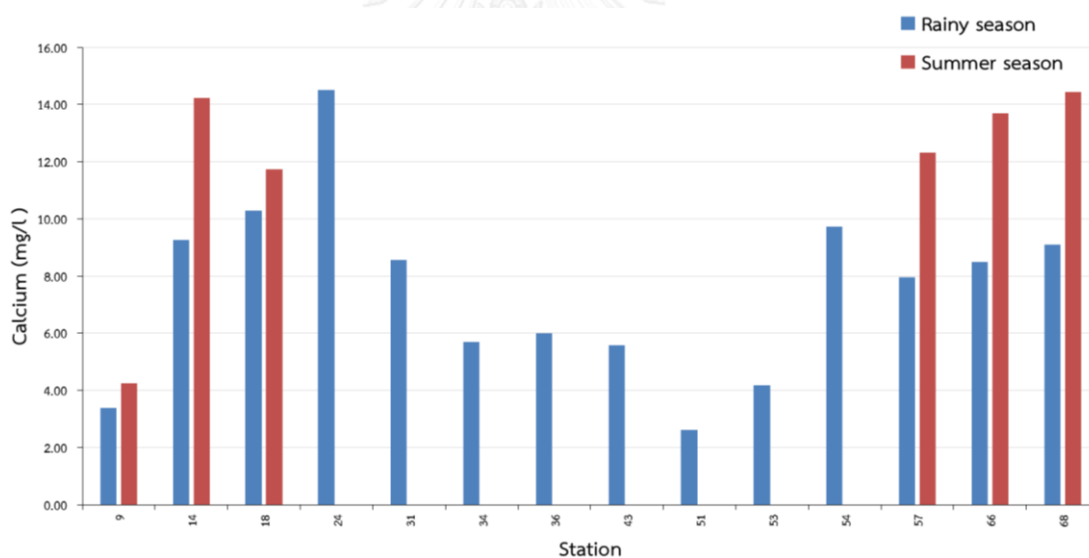
rainy seasons

Figure 4.15 The concentrations of Ca^{2+} in surface water in the summer and

rainy seasons

4.3.7.3 Magnesium (Mg^{2+})

The concentrations of Mg^{2+} in groundwater were in a range from 0.05 mg/l to 40.84 mg/l in the rainy season with an average of 7.66 mg/l. The concentrations of while Mg^{2+} in the summer season were in range from 0.93 mg/l to 93.69 mg/l with an average of 15.66 mg/l. The maximum concentration of Mg^{2+} in the rainy and summer

seasons were found at station nos.44 and 67, respectively. The concentration of Mg^{2+} in groundwater samples mostly were higher than in those in the rainy season except station nos. 13 and 42. Moreover, in the rainy season, concentrations of Mg^{2+} at station nos. 07 and 11 are lower than the detection limit (figure 4.16).

The concentrations of Mg^{2+} in surface water were in a range from 0.05 mg/l to 0.73 mg/l in the rainy season with an average of 0.35 mg/l, while in summer, the concentrations of Mg^{2+} were in a range from 0.65 mg/l to 4.39 mg/l with an average of 2.56 mg/l. The maximum concentrations of Mg^{2+} in the rainy and summer seasons were found at station nos.54 and 14, respectively. All of surface water samples in the summer season were higher than those in the rainy season (Figure 4.17).

Figure 4.16 The concentrations of Mg^{2+} in groundwater in the summer and rainy seasons
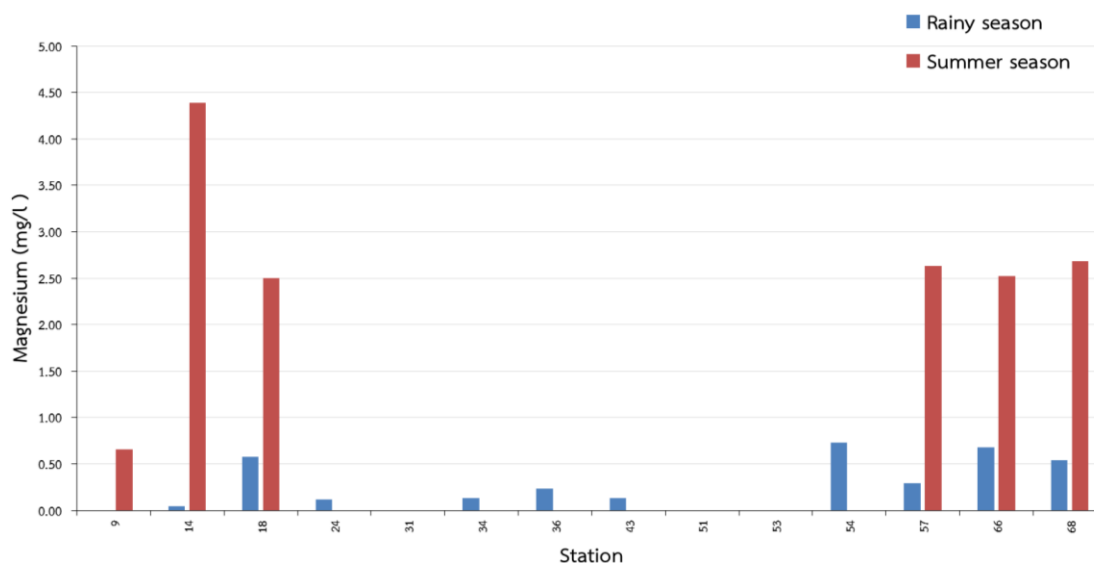
Figure 4.17 The concentrations of Mg^{2+} in surface water in the summer and rainy seasons

4.3.7.4 Sodium (Na$^+$)

The concentrations of Na^+ in groundwater were in a range from 8.2 mg/l to 124.91 mg/l in the rainy season with an average of 43.83 mg/l. Sodium in station no.21 presented a lower detection limit value. The maximum concentration of Na^+ is at station no. 25. While in summer, the concentrations of Na^+ were in a range from 11.65 mg/l to 254.13 mg/l with an average of 73.51 mg/l. The maximum concentration of Na^+ was found at station no.21. The concentration of Na^+ in groundwater samples in the summer season mostly were higher than those in the rainy season except station nos.13, 29, 42 and 46 (Figure 4.18).

The concentrations of Na^+ in surface water were in a range from 5.16 mg/l to 18.88 mg/l in the rainy season with an average of 10.40 mg/l, while in the summer, the concentrations of Na^+ were in a range from 6.10 mg/l to 14.68 mg/l with an average of 9.87 mg/l. The maximum concentrations of Na^+ were found at station no.51 and 57 in rainy and summer seasons, respectively. All of surface water samples in rainy season had higher Na^+ than those in summer season, except at station no.68 (Figure 4.19).
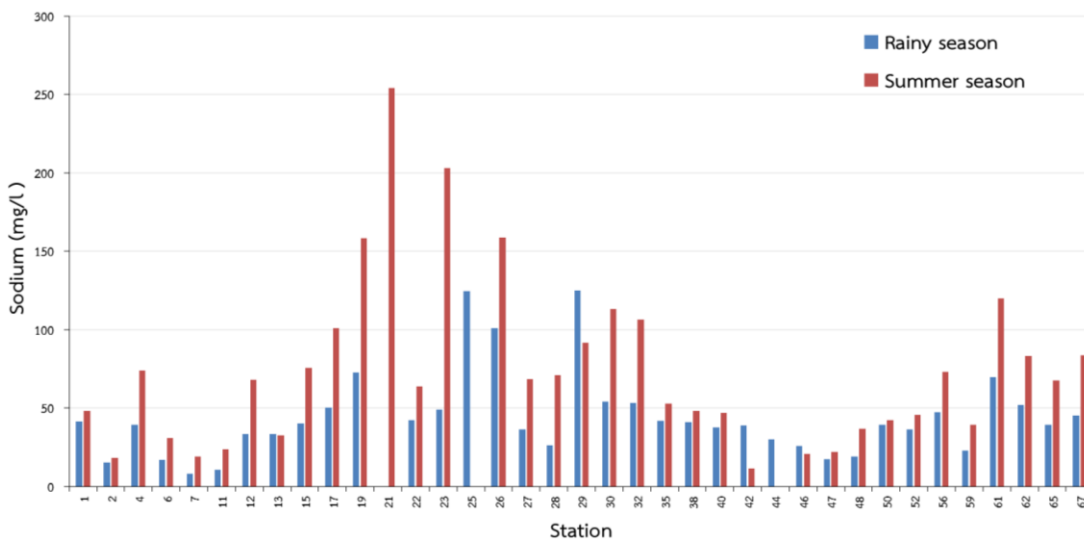
Figure 4.18 The concentrations of Na$^+$ in groundwater in surface water in the summer and rainy seasons
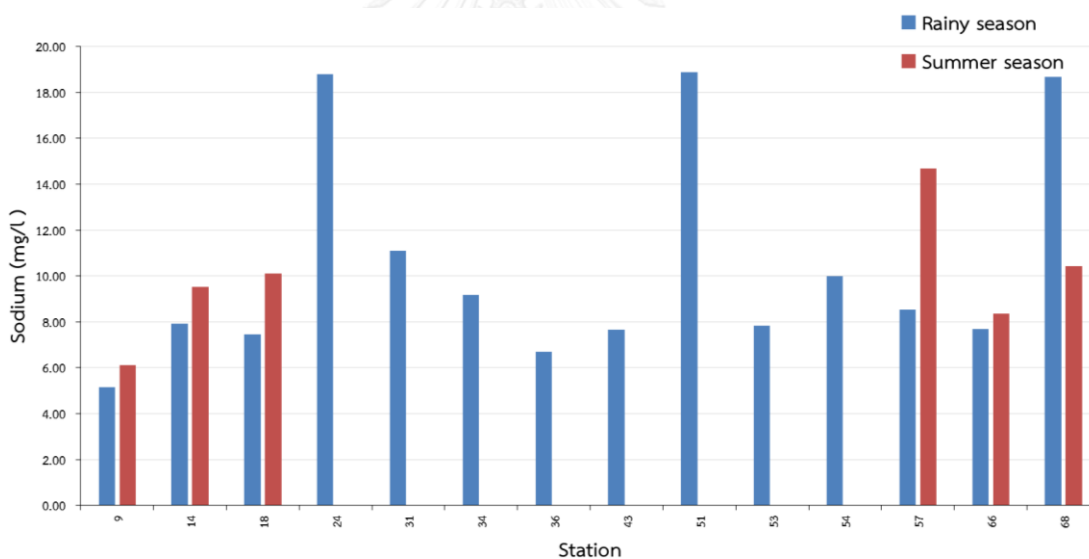
Figure 4.19 The concentrations of Na$^+$ in surface water in the summer and rainy seasons

4.3.7.5 Potassium (K$^+$)

The concentrations of K$^+$ in groundwater were in a range from 0.29 mg/l to 6.45 mg/l in the rainy season with an average of 2.04 mg/l, while in the summer, the concentrations of K$^+$ were in a range from 0.32 to 14.39 mg/l with an average of 2.82 mg/l. The maximum concentrations of K$^+$ were found at station no. 67 and 11 in the rainy and summer seasons, respectively. The concentration of K$^+$ in groundwater

samples in the summer season mostly were higher than those in the rainy season, except station nos. 06, 07, 17, 19, 22 and 26 (Figure 4.20).

The concentrations of K^+ in surface water were in a range from 1.70 mg/l to 9.13 mg/l in rainy season with an average of 3.61 mg/l, while in summer, the concentrations of K^+ were in range from 2.63 to 8.76 mg/l, and the average is 4.58 mg/l. The maximum concentrations of K^+ were at station nos.24 and 57 in the rainy and summer seasons, respectively. All of surface water samples in the summer were higher than those in the rainy season, except at station no. 09 (Figure 4.21).

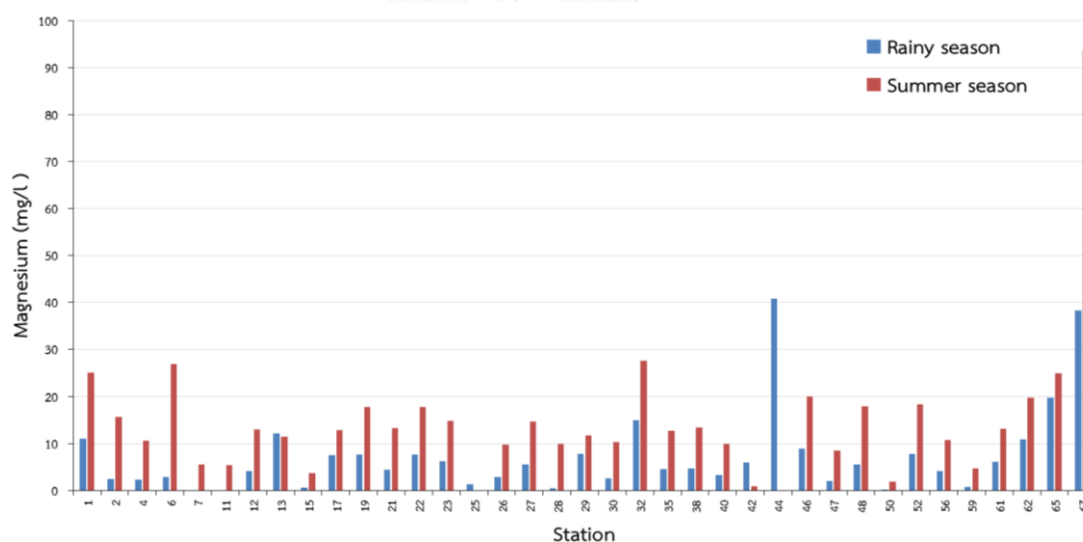**Figure 4.20** The concentrations of K^+ in groundwater in the summer and rainy seasons
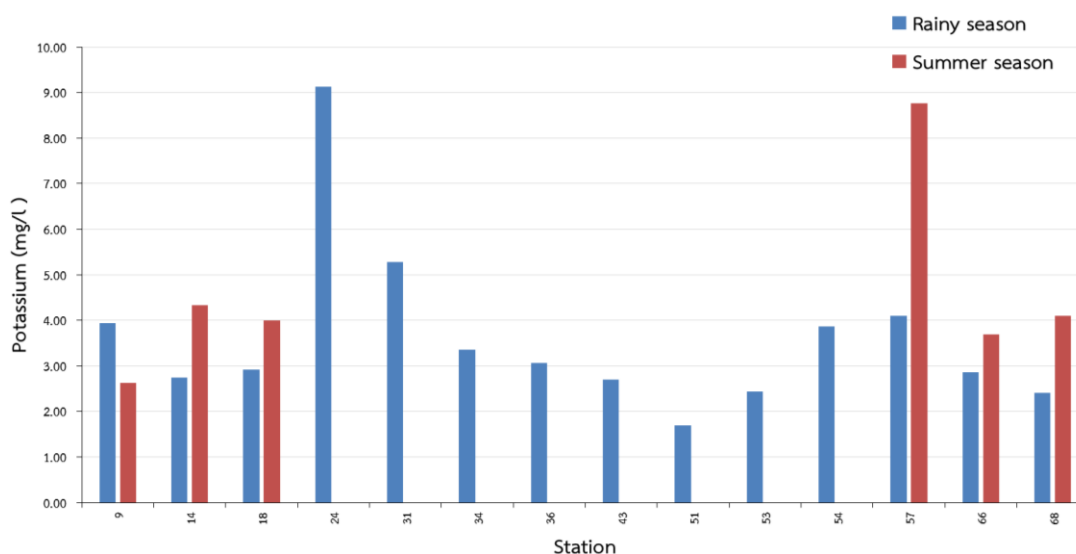
Figure 4.21 The concentrations of K^+ in surface water in the summer and
rainy seasons

4.3.7.6 Ammonium (NH_4^+)

In rainy season, the concentrations of NH_4^+ in groundwater of station nos. 02, 06, 47, 48 and 67 were 0.046 mg/l, 0.151 mg/l, 0.067 mg/l, 0.029 mg/l and 0.239 mg/l, respectively, and the remaining stations were lower than the detection limit. The average concentration of NH_4^+ was 0.106 mg/l and the maximum was found at station no. 67. In the summer season, they were in a range from 0.052 mg/l to 11.774 mg/l with an average of 0.808 mg/l. The concentrations of all samples were mainly less than 1.57 mg/l except a station no. 11 that had a NH_4^+ concentration of 11.77 mg/l. The NH_4^+ concentration of most groundwater samples in summer were more than those in the rainy season except station nos. 06, 47 and 48. The amount of stations having a NH_4^+ value lower than the detection limit in the summer were less than those in the rainy season. Furthermore, station nos.15, 17, 19, 21, 26, 27, 35, 40, 50, 56 and 61 showed values lower than the detection limit in both seasons.

In the rainy season, the NH_4^+ concentrations in surface water of station nos. 09, 24, 31 and 36 were 0.024 mg/l, 2.717 mg/l, 1.287 mg/l and 0.048 mg/l, respectively. The average concentration of NH_4^+ was 1.019 mg/l and the maximum concentration was found at station no.24. The most samples were lower than the detection limit. In the summer, the concentrations of NH_4^+ were in a range from 0.115 mg/l to 0.631 mg/l

with an average of 0.378 mg/l. The maximum concentration of NH_4^+ was found at station no. 14. Most of surface water samples in summer had higher NH_4^+ concentrations than those in rainy season, but the maximum concentration of NH_4^+ in the summer was less than that in the rainy season.

4.3.7.7 Chloride (Cl^-)

The concentrations of Cl^- in groundwater were in a range from 2.98 mg/l to 188.15 mg/l in the rainy season with an average of 23.59 mg/l, while in the summer they were in a range from 2.09 mg/l to 218.56 mg/l with an average of 26.34 mg/l. The maximum concentration of chloride in the both seasons was found at station no.67. More than half of groundwater samples had a higher Cl^- concentrations in the summer season, except station nos. 01, 02, 04, 13, 15, 17, 22, 23, 26, 27, 29, 40, 42, 46, 47, 50, 52, 56 and 59 (Figure 4.22).

The concentration of Cl^- in surface water were in a range from 3.03 mg/l to 18.50 mg/l in the rainy season with an average of 6.54 mg/l, while in the summer, the Cl^- concentrations were in a range from 2.58 mg/l to 9.91 mg/l with an average of 4.71 mg/l. The maximum Cl^- concentration were found at station nos. 24 and 57 in the rainy and summer seasons, respectively. (Figure 4.23).

Figure 4.22 The concentrations of Cl^- in groundwater in the summer and rainy seasons
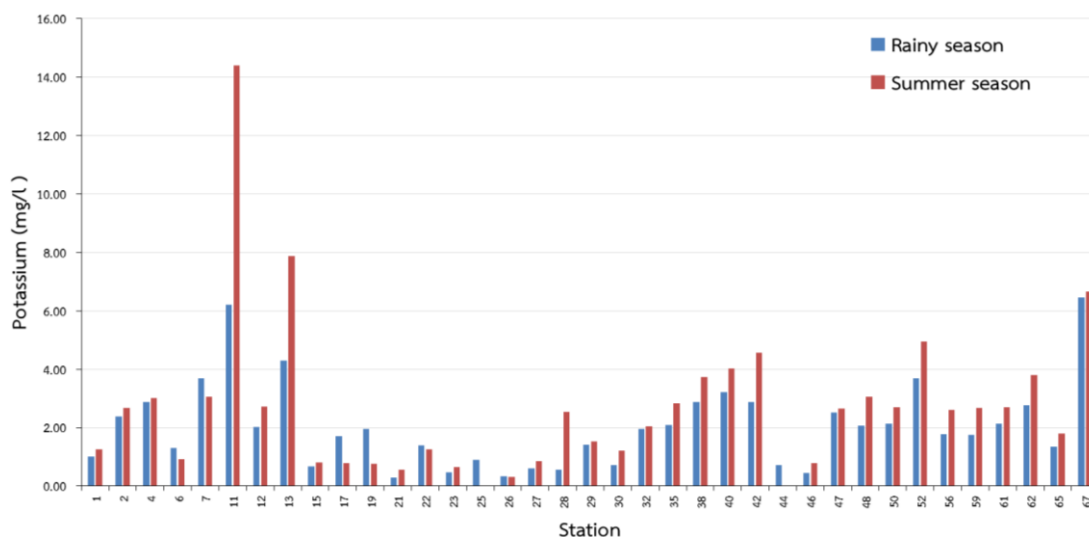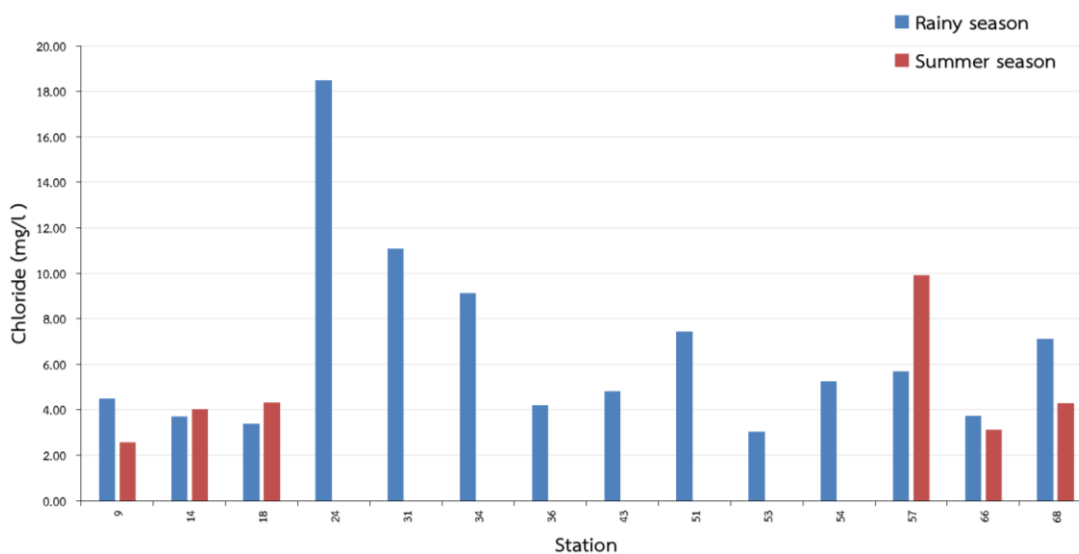
Figure 4.23 The concentrations of Cl⁻ in surface water in the summer and
rainy seasons

4.3.7.8 Sulfate (SO$_4^{2-}$)

The SO$_4^{2-}$ concentrations in groundwater were in a range from 1.33 mg/l to
247.47 mg/l in the rainy season with an average of 32.68 mg/l, while in the summer,
they were in a range from 0.98 mg/l to 297.86 mg/l with an average of 33.68 mg/l. The
maximum concentrations of SO$_4^{2-}$ were found at station nos.29 and 23 in the rainy and
summer seasons, respectively. The SO$_4^{2-}$ concentration of most groundwater samples
in summer were more than those in the rainy season except station nos. 06, 11, 17, 22,
26, 29, 38, 42, 61, 62 and 65 (Figure 4.24).   The SO$_4^{2-}$ concentrations in surface water
were in a range from 0.72 mg/l to 10.27 mg/l in the rainy season with an average of
3.74 mg/l, while in summer, the concentration of sulfate is in range from 2.57 to 5.84
mg/l, and the average is 4.29 mg/l. The maximum SO$_4^{2-}$ concentrations of were at
station nos. 24 and 18 in the rainy and summer seasons, respectively. At each station,
the most surface water samples had a higher SO$_4^{2-}$ concentration in the summer season
except station no.14 (Figure 4.25).
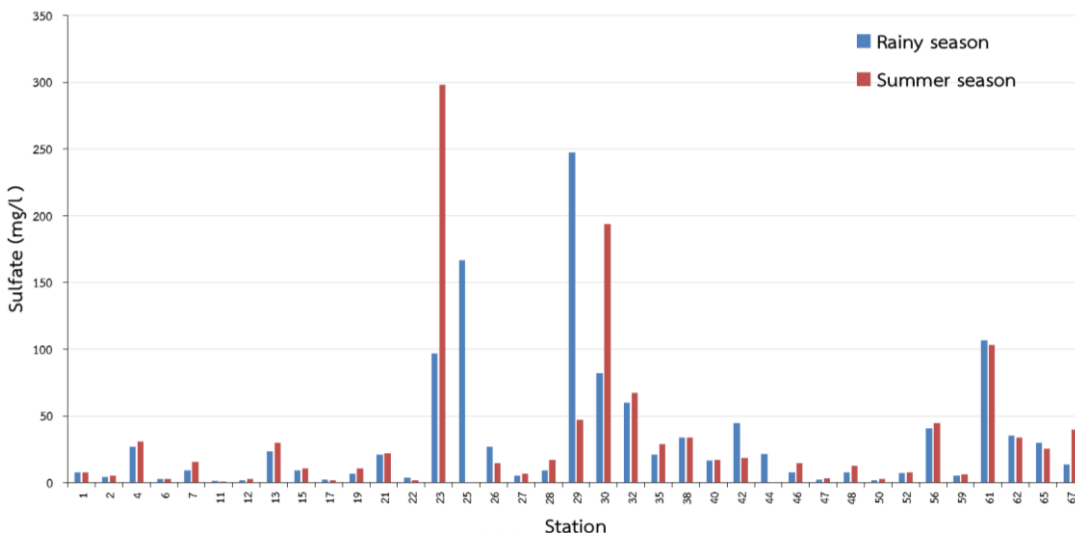
Figure 4.24 The SO_4^{2-} concentrations in groundwater in the summer and
rainy seasons
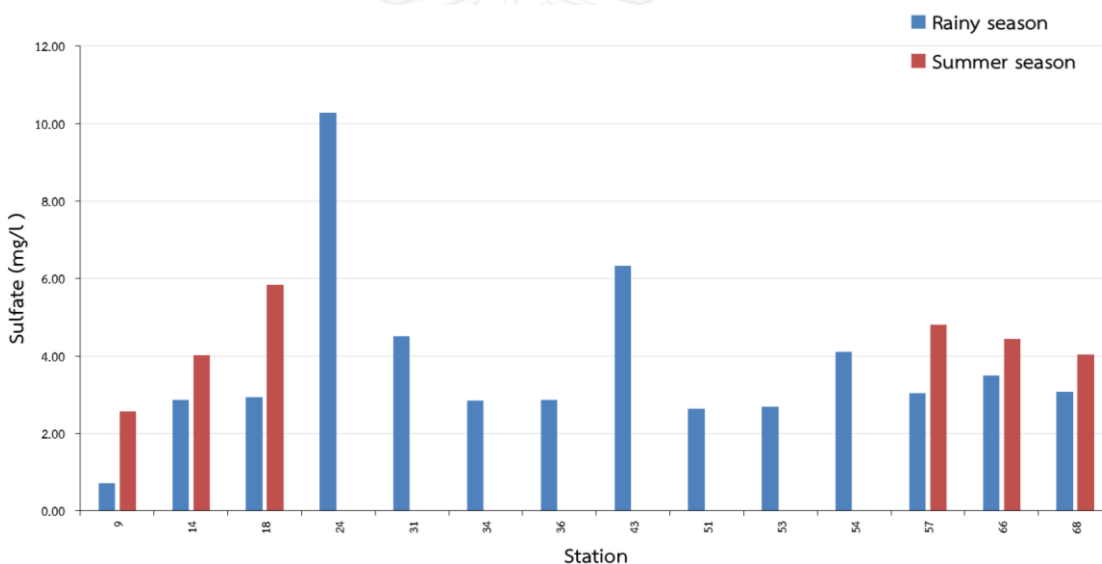
Figure 4.25 The SO_4^{2-} concentrations in surface water in the summer and
rainy seasons

4.3.7.9 Fluoride (F⁻)

The F concentrations in groundwater were in a range from 0.07 mg/l to 2.84 mg/l in the rainy season with an average of 0.50 mg/l, while in the summer, they were in a range from 0.03 mg/l to 1.40 mg/l with an average of 0.35 mg/l. The maximum F⁻ concentration of F⁻ were found at station nos. 25 and 29 in rainy and summer seasons, respectively. The F⁻ concentration of most groundwater samples in summer were less

than those in the rainy season except station nos. 01, 06, 15, 21, 22, 26, 27, 29, 30, 32, 65 and 67 (Figure 4.26).

The F⁻ concentrations in surface water were in a range from 0.06 mg/l to 0.79 mg/l in the rainy season with an average of 0.22 mg/l, while in summer, the F⁻ concentrations were in a range from 0.05 mg/l to 0.18 mg/l with an average of 0.10 mg/l. The maximum F⁻ concentrations were found at station nos. 68 and 14 in the rainy and summer seasons. The F⁻ concentrations of most surface water samples in summer were less than those in the rainy season except station no.14 (Figure 4.27).
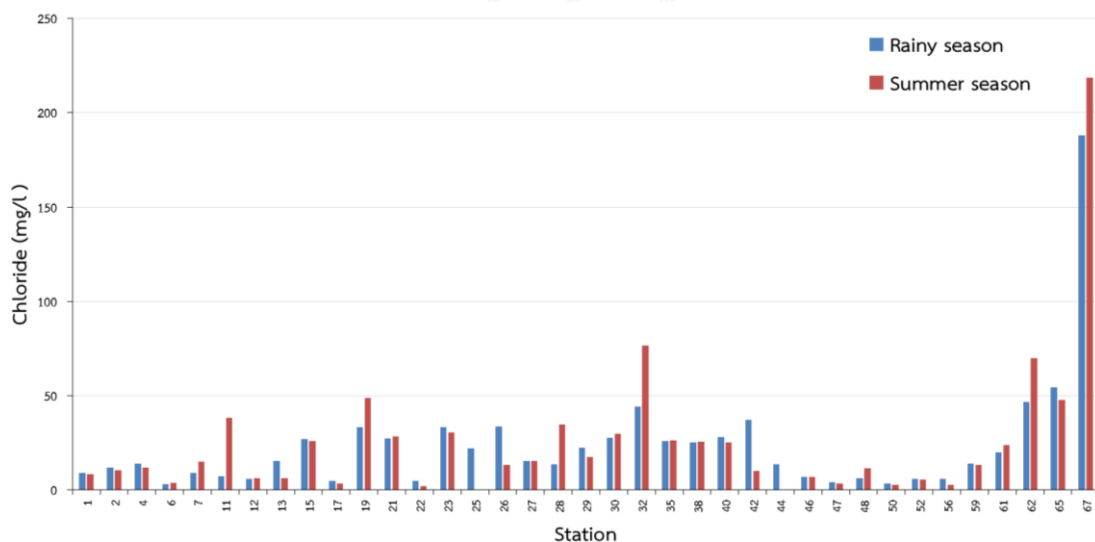

Figure 4.26 The F⁻ concentrations in groundwater in the summer and rainy seasons
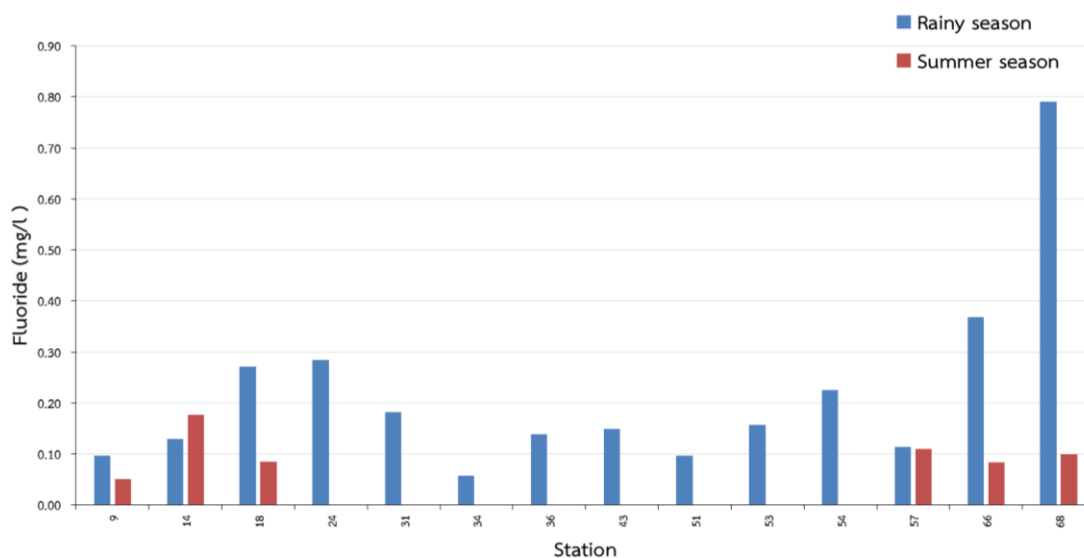
Figure 4.27 The F⁻ concentrations in surface water in the summer and rainy seasons

4.3.7.10 Phosphate (PO_4^{3-})

In the rainy season, the PO_4^{3-} concentrations at station nos. 07, 13, 19, 46, 56 and 62 are 15.22 mg/l, 13.88 mg/l, 13.90 mg/l, 13.85 mg/l, 13.85 mg/l, 13.87 mg/l and 13.96 mg/l, respectively, with an average of 14.08 mg/l. The maximum PO_4^{3-} concentration was found at station no. 07. In summer the PO_4^{3-} concentrations were in a range from 0.01 mg/l to 0.19 mg/l with an average of 0.03 mg/l. The maximum PO_4^{3-} concentration was found at station no.67. The remaining groundwater samples were lower than the detection limit. When comparing PO_4^{3-} concentration of each station during two seasons, it was found that the PO_4^{3-} concentration in the summer season was much less than that in the rainy season.

In the rainy season, the PO_4^{3-} concentration in surface water found at station 51 and 68 were approx. 13.92 mg/l and 13.89 mg/l, respectively, with an average concentration of 13.91 mg/l, while the PO_4^{3-} concentration in the summer was found only at station nos. 09, 14, 57 and 68 of about 0.0551 mg/l, 0.0255 mg/l, 0.0212 mg/l and 0.0215 mg/l, respectively. The average PO_4^{3-} concentration was about 0.03 mg/l. The remaining stations had PO_4^{3-} concentration lower than the detection limit. The maximum PO_4^{3-} concentration was found at station no. 09.

4.3.7.11 Nitrite (NO_2^-)

The NO_2^- concentrations in groundwater were in a range from 0.009 mg/l to 0.453 mg/l in the rainy season with an average of 0.087 mg/l, while in summer they were in a range from 0.005 mg/l to 0.116 mg/l with an average of 0.021 mg/l. The maximum NO_2^- concentration in both seasons was found at station no. 02. The NO_2^- concentration of most of groundwater samples in summer were less than those in the rainy season, except station nos.21, 23, and 67. Especially at station nos.01, 07, 22, 29, 46 and 47 had NO_2^- values, which were decreased to be lower than the detection limit (Figure 4.28).

The NO_2^- concentrations in surface water is in a range from 0.021 mg/l to 0.362 mg/l in the rainy season with an average of 0.088 mg/l while in summer, they were in a range from 0.008 to 0.024 mg/l with an average of 0.014 mg/l. The maximum NO_2^- concentrations were at station nos. 51 and 68 in the rainy and summer seasons, respectively. The NO_2^- concentration of most surface water samples in the summer were less than those in the rainy season. Especially at station no.66 had a NO_2^- value, which was decreased to be lower than the detection limit (Figure 4.29).

Figure 4.28 The concentrations of NO_2^- in groundwater in the summer and rainy seasons
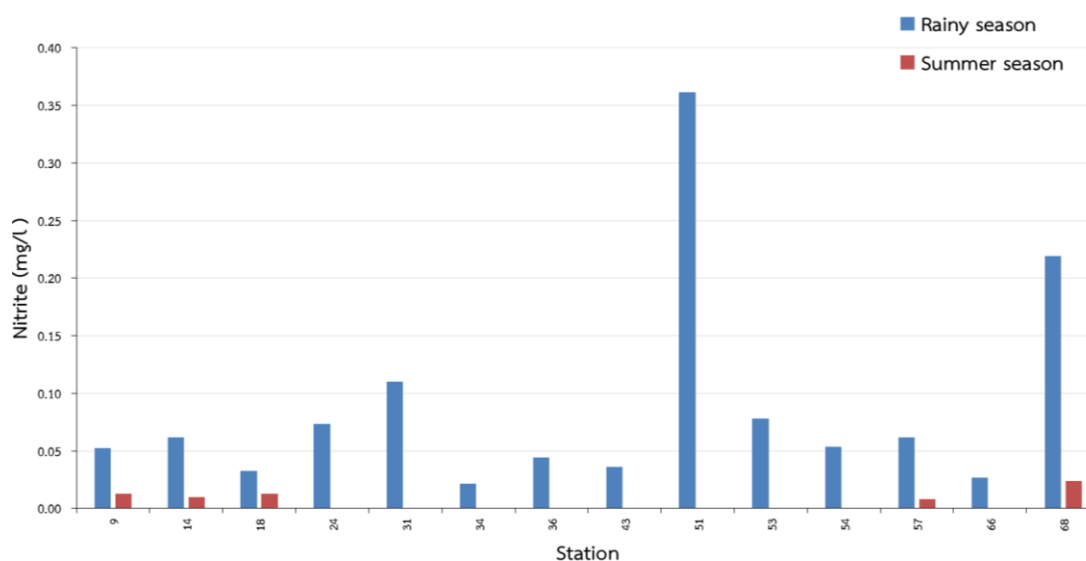
Figure 4.29 The concentrations of NO_2^- in surface water in the summer and rainy seasons

4.3.7.12 Nitrate (NO_3^-)

The NO_3^- concentrations in groundwater is in a range from 0.018 mg/l to 7.106 mg/l in the rainy season with an average of 1.409 mg/l, while in the summer they were in a range from 0.203 mg/l to 5.590 mg/l with an average of 1.754 mg/l. The maximum NO_3^- concentration in both seasons was found at station no.02, which is same as the NO_2^- concentration. The NO_3^- concentration of groundwater samples in summer were more than those in the rainy season, especially at station nos.13, 23, 29, 38, 40, 42, 56, 61 and 62, which increased from values lower than the detection limit. Except for station nos.02, 21, 26, 30, 48 and 59, especially at station no.21 that was lower than the detection limit (Figure 4.30).

The NO_3^- concentrations in surface water were in a range from 0.114 mg/l to 3.695 mg/l in the rainy season with an average of 0.883 mg/l while in summer, the NO_3^- concentrations were in a range from 0.810 mg/l to 1.533 mg/l with an average of 1.073 mg/l. The maximum NO_3^- concentration were found at station nos.51 and 18 in rainy and summer seasons, respectively. All of surface water samples in the summer were higher than those in the rainy season, especially at station nos. 18 and 66. (Figure 4.31).
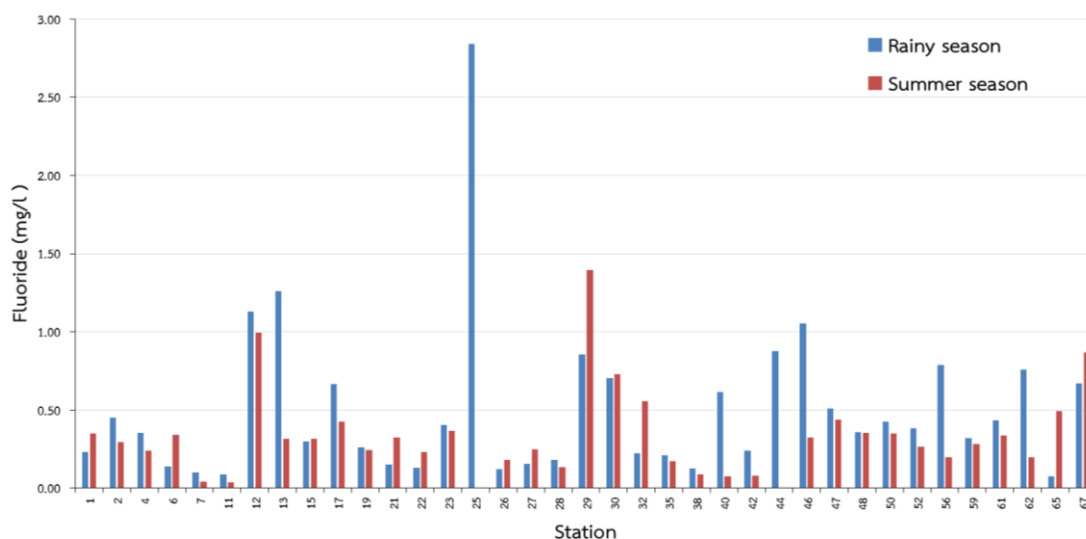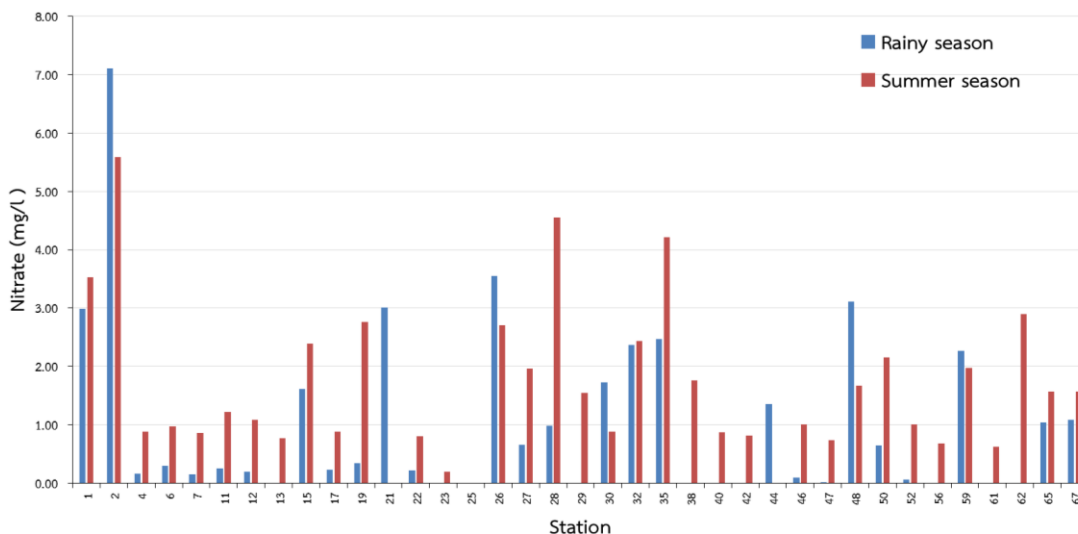
Figure 4.30 The NO_3^- concentrations in groundwater in the summer and rainy seasons
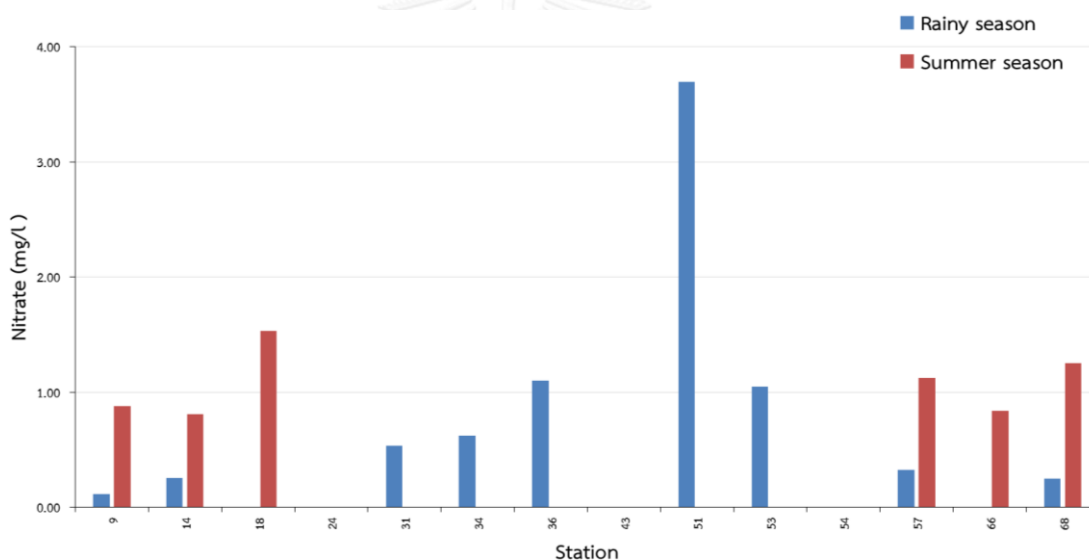
Figure 4.31 The NO_3^- concentrations in surface water in the summer and

rainy seasons

4.3.7.13 Bromide (Br⁻)

The Br⁻ concentrations in groundwater were in a range from 0.01 mg/l to 0.411 mg/l in the rainy season with an average of 0.057 mg/l, while in summer they were in a range from 0.04 mg/l to 3.41 mg/l with an average of 0.978 mg/l. The maximum Br⁻ concentration in both seasons was at station no.67. The Br⁻ concentration in most groundwater samples in summer had a value over than that in rainy season, especially at station nos.29 and 50 which increase from a value lower than the detection limit.

However, except for station nos.42 and 62 which had Br⁻ values in the summer less than those in the rainy season (Figure 4.32).

The Br⁻ concentrations in surface water were in a range from 0.007 mg/l to 0.116 mg/l in the rainy season with an average of 0.024 mg/l while in summer, the Br⁻ concentrations were in a range from 0.168 mg/l to 0.440 mg/l with an average of 0.337 mg/l. The maximum Br⁻ concentration were found at station nos. 34and 14 in the rainy and summer seasons. All of surface water samples in the summer were higher than those in the rainy season, especially at station no.09 (Figure 4.33).
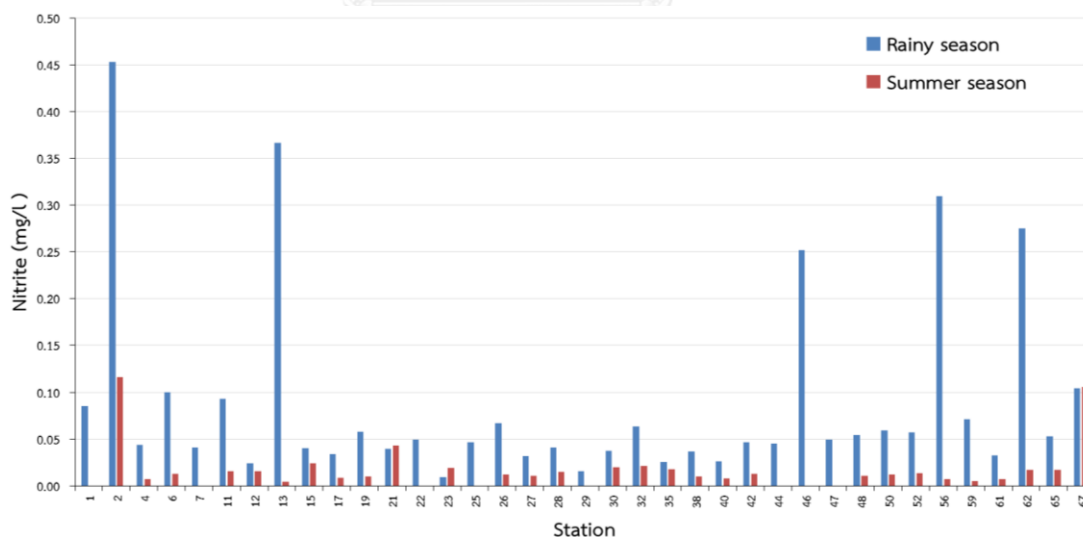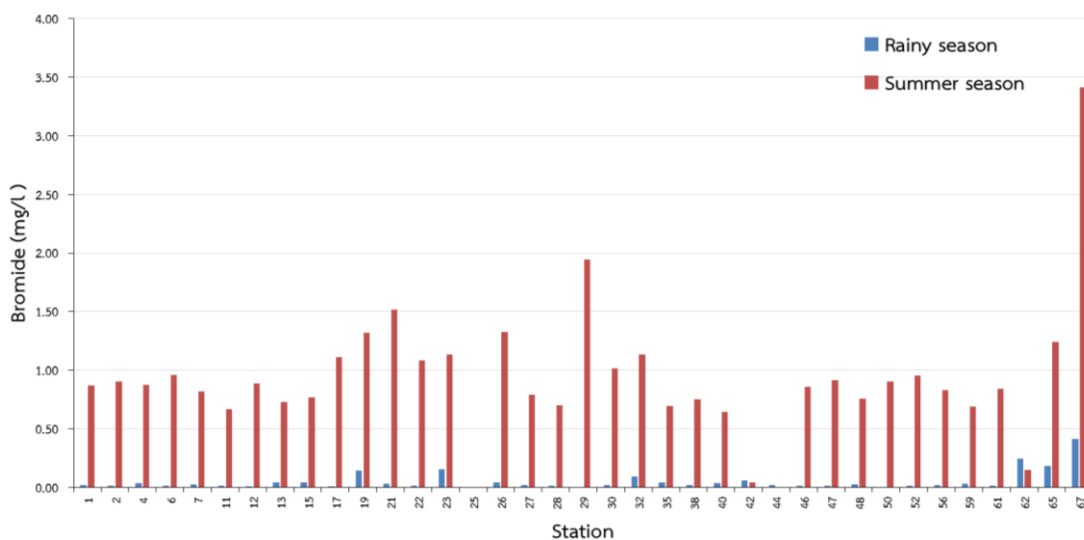

Figure 4.32 The Br⁻ concentrations in groundwater in the summer and rainy seasons
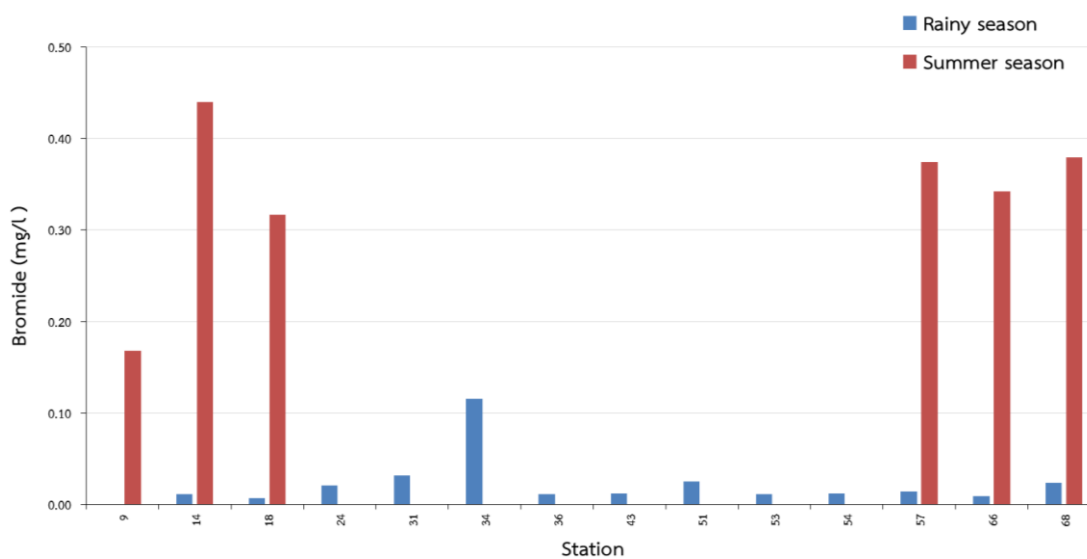
Figure 4.33 The Br⁻ concentrations in surface water in the summer and rainy seasons

4.3.7.14 Total Alkalinity

The concentrations of total alkalinity in groundwater were in a range from 51.80 mg/l to 473.6 mg/l in the rainy season with an average of 267.30 mg/l while the summer is in range from 19 to 628.6 mg/l and the average is 342.89 mg/l. The maximum concentrations of total alkalinity were found at station nos.44 and 21 in the rainy and summer seasons, respectively. The concentrations of total alkalinity of most groundwater samples in the summer were higher than those in the rainy season, except station nos.12, 13, 38, 42 and 62. (Figure 4.34).

The concentrations of total alkalinity in surface water were in a range from 20.2 mg/l to 71.8 mg/l in the rainy season with an average of 46.58 mg/l while in summer, the concentrations of total alkalinity were in a range from 28 mg/l to 83.6 mg/l with an average of 66.8 mg/l. The maximum concentrations of total alkalinity were found at station nos.24 and 14 in the rainy and summer seasons, respectively. The maximum concentration of total alkalinity is at station no.14. All of surface water samples in summer were higher than those in the rainy season (Figure 4.35).
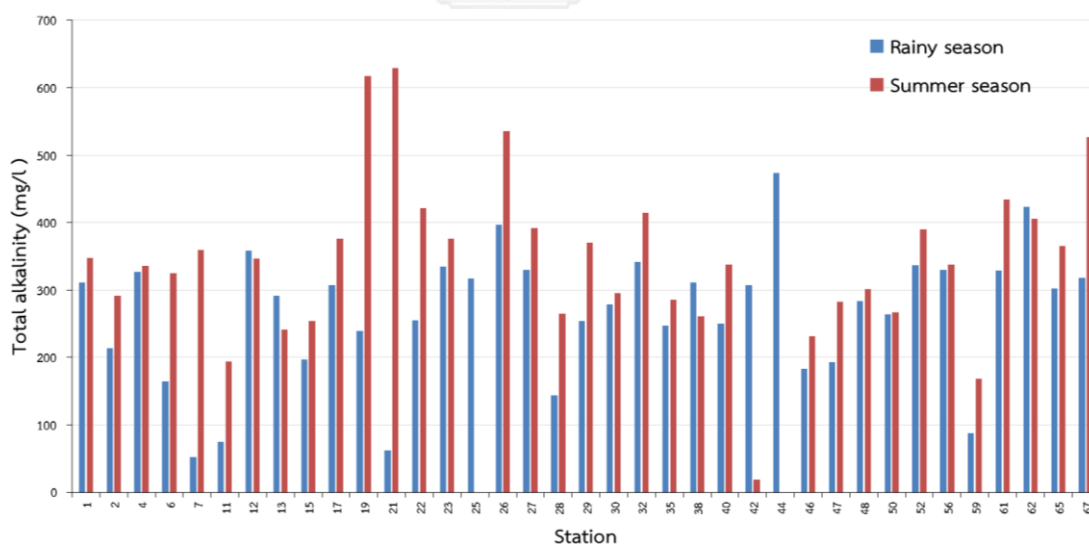
Figure 4.34 The concentrations of total alkalinity in groundwater in the summer and rainy seasons
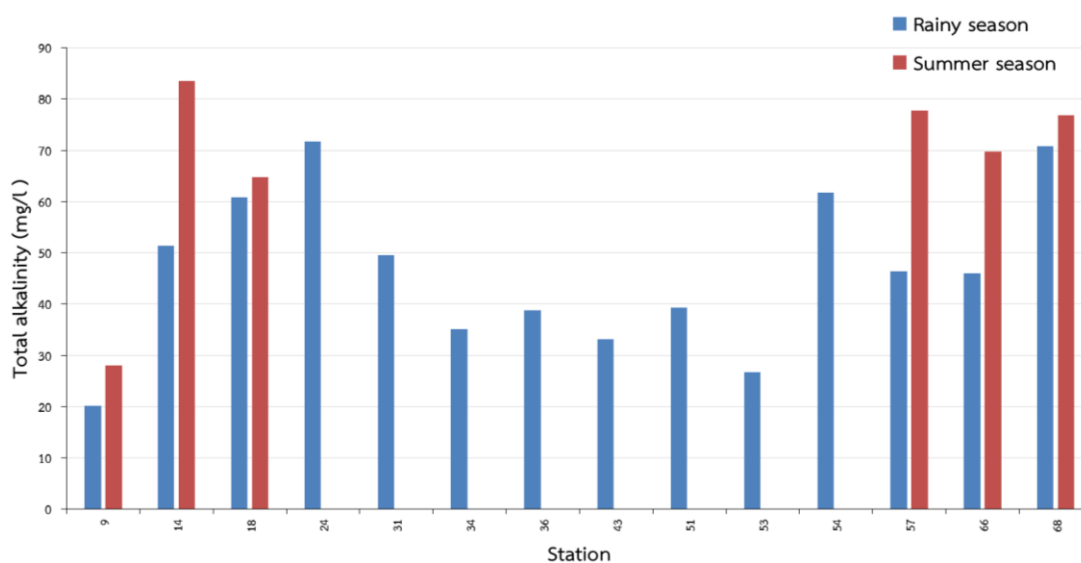
Figure 4.35 The concentrations of total alkalinity in surface water in the summer and rainy seasons

The average concentrations of all cations in groundwater were compared and found that the concentration of most cations in the rainy season was less than those in the summer, except Ca^{2+}. An average concentration of each ion was arranged in a descending trend as followings: $Ca^{2+} > Na^+ > Mg^{2+} > K^+ > Fe > NH_4^+$ in the rainy season and $Na^+ > Ca^{2+} > Mg^{2+} > Fe > K^+ > NH_4^+$ in the summer season (Figure 4.36).

The average concentrations of cations in surface water were compared and found that average Fe, Na and NH_4^+ concentrations had higher concentrations in the rainy season than those in the summer, while Ca^{2+}, Mg^{2+} and K^+ have a concentration in the rainy season less than those in the summer. A concentration of each ion was arranged in a descending trend as followings: $Na^+ > Ca^{2+} > K^+ > NH_4^+ > Fe > Mg^{2+}$ in the rainy season and $Ca^{2+} > Na^+ > K^+ > Mg^{2+} > NH_4^+ > Fe$ in the summer season (Figure 4.37).

The average concentrations of all anions in groundwater were compared and found that the average concentrations of most anions in the rainy season were less than those in the summer season, except F^-, NO_2^- and PO_4^{3-}. A concentration of each ion in the rainy season was arranged in a descending trend as followings: total alkalinity > $SO_4^{2-} > Cl^- > PO_4^{3-} > NO_3^- > F^- > NO_2^- > Br^-$ in the rainy season and total alkalinity >

$SO_4^{2-} > Cl^- > NO_3^- > Br^- > F^- > PO_4^{3-} > NO_2^-$ in the summer (Figure 4.38). The average concentrations of anions in surface water were compared and found that Cl^-, F^-, NO_2^- and PO_4^{3-} have a higher concentration in the rainy season than those in the summer, while SO_4^{2-}, NO_3^-, Br^- and total alkalinity have a lower concentration in the rainy season than those in the summer. A concentration of each ion was arranged in a descending trend as followings: total alkalinity $> PO_4^{3-} > Cl^- > SO_4^{2-} > NO_3^- > F^- > NO_2^- > Br^-$ in the rainy season and total alkalinity $> Cl^- > SO_4^{2-} > NO_3^- > Br^- > F^- > PO_4^{3-} > NO_2^-$ in the summer season (Figure 4.39).

The average concentrations of all anions in groundwater were compared and found that the average concentration of each anion were arranged in a descending trend as followings: total alkalinity $> Ca^{2+} > Na^+ > SO_4^{2-} > Cl^- > PO_4^{3-} > Mg^{2+} > K^+ > Fe > NO_3^- > F^- > NH_4^+ > NO_2^- > Br^-$ in the rainy season and total alkalinity $> Na^+ > Ca^{2+} > SO_4^{2-} > Cl^- > Mg^{2+} > Fe > K^+ > NO_3^- > Br^- > NH_4^+ > F^- > PO_4^{3-} > NO_2^-$ in the summer season (Figure 4.40). The average concentrations of anions in surface water were compared and found that a concentration of each ion was arranged in a descending trend as followings: total alkalinity $> PO_4^{3-} > Na^+ > Ca^{2+} > Cl^- > SO_4^{2-} > K^+ > NH_4^+ > NO_3^- > Fe > Mg^{2+} > F^- > NO_2^- > Br^-$ in the rainy season and total alkalinity $> Ca^{2+} > Na^+ > Cl^- > K^+ > SO_4^{2-} > Mg^{2+} > NO_3^- > NH_4^+ > Br^- > Fe > F^- > PO_4^{3-} > NO_2^-$ in the summer season (Figure 4.41).
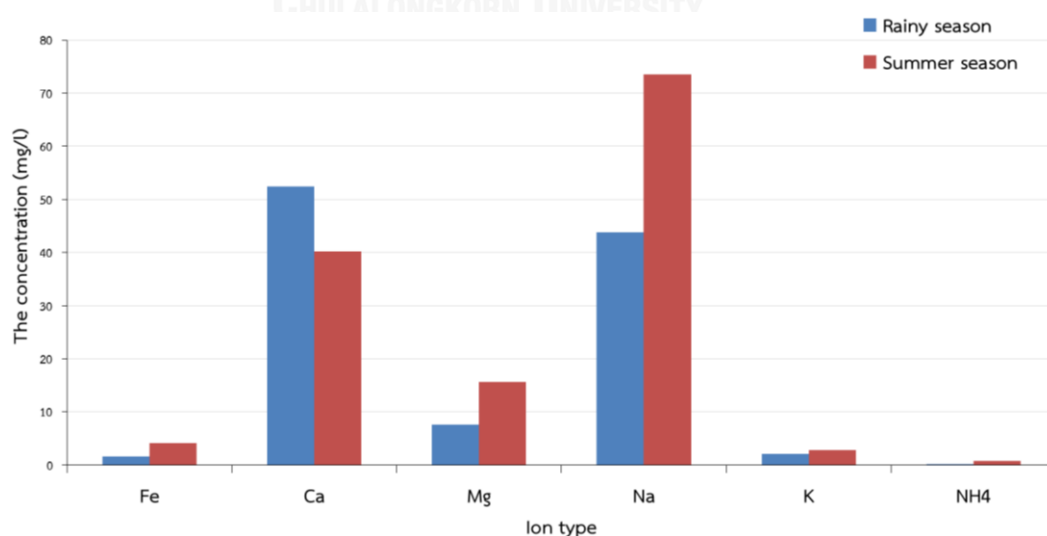
Figure 4.36 A comparison of concentration of each cation in groundwater in the summer and rainy seasons
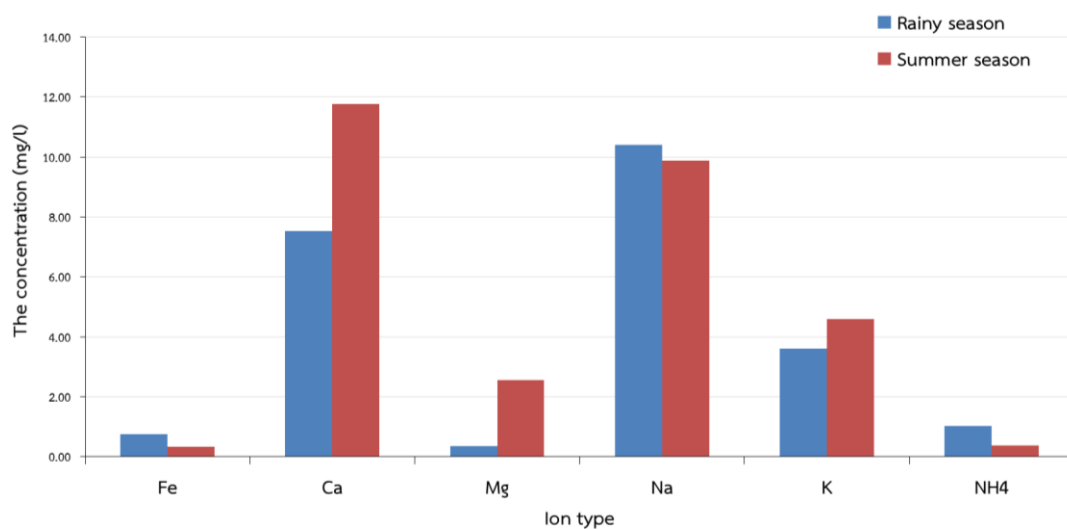
Figure 4.37 A comparison concentration of each cation in surface water in the summer and rainy seasons
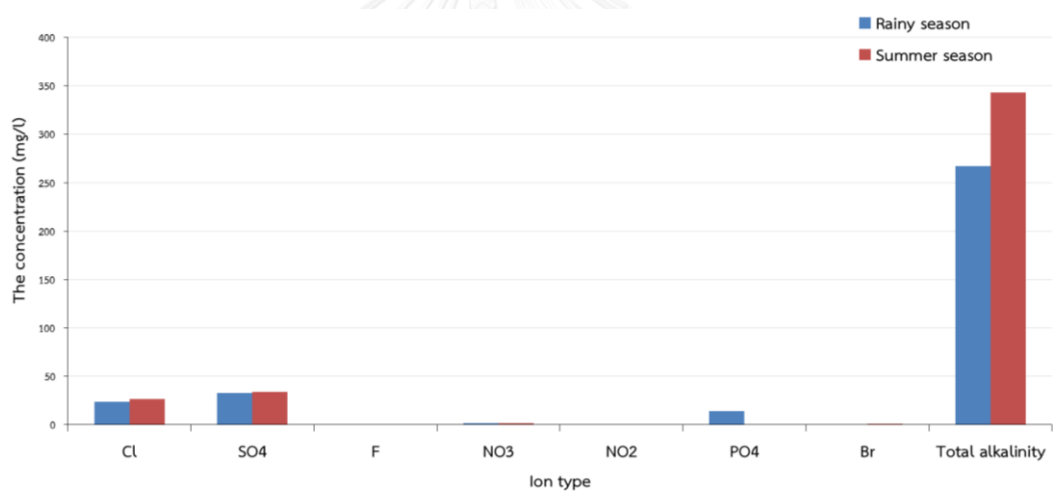
Figure 4.38 A comparison concentration of anions in groundwater in the summer and rainy seasons
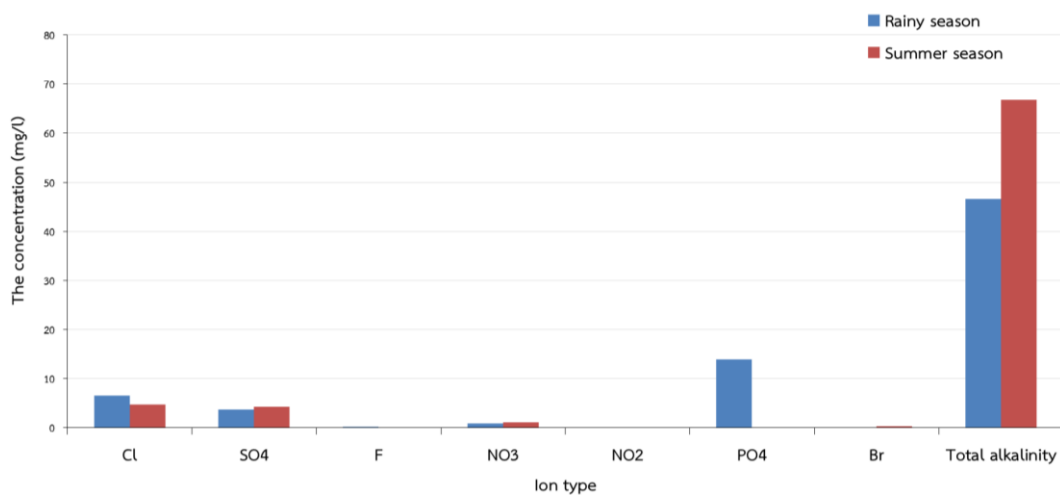
Figure 4.39 A comparison of concentrations of anions in surface water in the summer and rainy seasons
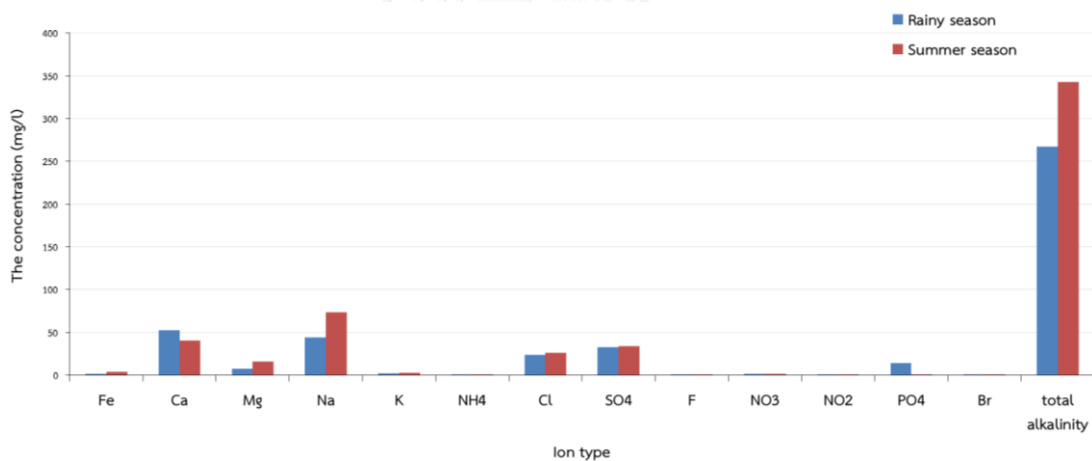
Figure 4.40 A comparison of concentrations of ions in groundwater in the summer and rainy seasons
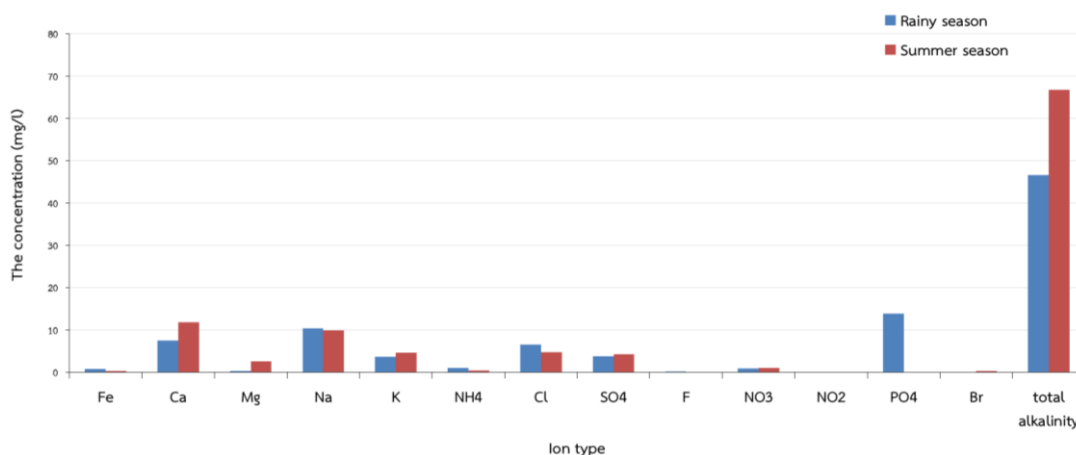
Figure 4.41 A comparison of concentrations of ions in surface water in the summer and rainy seasons

4.4 The water types

Hydrochemical facies classification of groundwater samples can be classified by the piper diagram (Galloway & Kaiser, 1980), which plots between the percentage of cations and anions. The cations consists of calcium (Ca^{2+}), magnesium (Mg^{2+}), sodium (Na^+), potassium (K^+), and the anions consists of chloride (Cl^-), sulfate (SO_4^{2-}) and the sum between carbonate (CO_3^{2-}) and bicarbonate (HCO_3^-). The water types in study of Galloway and Kaiser (1980) are divided into 10 classes as follows: Ca-HCO_3, Ca-Na-HCO_3, Ca-HCO_3-Cl, Ca-Cl, Ca-Na-Cl, Na-HCO_3, Na-HCO_3-Cl, Ca-Na-HCO_3-Cl, SO_4 and Na-Cl. A hydrochemical facies of groundwater in both seasons are shown in Table 4.9. In the rainy season, the water types of the groundwater in the study area include Ca-Na-HCO_3, Ca-HCO_3, (Ca-Na-HCO_3) + (Ca-HCO_3), Na-HCO_3, Ca-HCO_3-Cl, Na-HCO_3-Cl, Na-HCO_3-Cl, SO_4 and (Ca-Na-HCO_3) + (Na-HCO_3) (Figure 4.42). The main hydrochemical facies are follows: Ca-Na-HCO_3 (~ 56.75 % of whole samples), Ca-HCO_3 (~ 13.51 %), Ca-Na-HCO_3 + Ca-HCO_3 (~5.40%) and Ca-HCO_3-Cl (~5.40%). The water types could be used to preliminarily evaluate about their sources. If the hydrochemical facies of water are different, it indicates that the cations and anions appearing in the groundwater may come from the different sources. For example, water types in station nos.21 and 67, 25 and 29 were Ca-HCO_3-Cl, Na-HCO_3-Cl and Na-HCO_3-Cl, SO_4 respectively, Which these are different from the other stations because they has a high concentration of chloride in the groundwater samples,

indicating that water may be contaminated from the human activities (Figure 4.42). In the summer season, the water types of the groundwater in the study area include 7 types as follows: Ca-Na-HCO_3, Ca-HCO_3, (Ca-Na-HCO_3) + (Na-HCO_3), Na-HCO_3, Ca-HCO_3-Cl, Na-HCO_3-Cl, SO_4 and (Na-HCO_3-Cl, SO_4), (Ca-Na-HCO_3)-Cl, SO_4 (Figure 4.43). The main hydrochemical facies are follows: Ca-Na-HCO_3 (~ 42.85 %), Na-HCO_3 (~ 30.95 %) and Ca-HCO_3 (~11.90 %), However, water types at station nos. 23 and 42 are Na-HCO_3-Cl, SO_4. At station no.30 is (Na-HCO_3-Cl, SO_4), (Ca-Na-HCO_3)-Cl, SO_4 and station no.67 is Ca-HCO_3-Cl. These 4 stations (nos. 23, 42, 30 and 60) demonstrated different water types from the main hydrochemical facies in other wells, probably contaminating from human activities. When comparing hydrochemical facies during two seasons, there were not found these two water types: (Na-HCO_3-Cl, SO_4) and (Ca-Na-HCO_3)-Cl, SO_4 in the rainy season, whereas these two water types: (Ca-Na-HCO_3) + (Ca-HCO_3) and Na-HCO_3-Cl were not found in the summer season. Moreover, the principal ion is Ca ion in the rainy season, but in the summer season, the principal ion is Na ion instead, which is not surprisingly because Ca ion in groundwater may be replaced by Na ion, resulting in increasing the bicarbonate concentration and pH as shown in the following reaction (Baba & Olowoyeye, 2011) (Figure 4.44).

$$CaCO_3 + CO_2 (g) + H_2O = Ca^{2+} + 2HCO_3^-$$
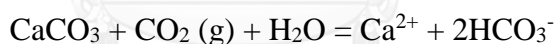
Table 4.9 Details of hydrochemical facies of groundwater and surface water

Station	Ion Charge Balance (%)		Hydrochemical facies		Water Types
	Rainy	Summer	Rainy	Summer	
ST01	4.72	-5.25	(Ca-Na-HCO_3) + (Ca-HCO_3)	Ca-Na-HCO_3	Groundwater
ST02	-9.20	2.66	Ca-HCO_3	Ca-HCO_3	Groundwater
ST03	-25.08	-7.36	Ca-Na-HCO_3	Ca-HCO_3	Groundwater
ST04	-9.28	-8.17	Ca-Na-HCO_3	(Ca-Na-HCO_3) + (Na-HCO_3)	Groundwater
ST05	-24.33	-6.05	Ca-Na-HCO_3	Ca-HCO_3	Groundwater
ST06	-9.78	-3.34	Ca-Na-HCO_3	Ca-HCO_3	Groundwater
ST07	-3.64	-7.86	Ca-Na-HCO_3	Ca-HCO_3	Groundwater
ST08					Precipitation
ST09	1.72	0.86	Na-HCO_3	Ca-Na-HCO_3	Surface water

Station	Ion Charge Balance (%)		Hydrochemical facies		Water Types
	Rainy	**Summer**	**Rainy**	**Summer**	
ST10					Precipitation
ST11	-4.36	-4.57	$Ca-Na-HCO_3$	$Ca-Na-HCO_3$	Groundwater
ST12	-8.80	-7.81	$(Ca-Na-HCO_3)$ + $(Ca-HCO_3)$	$(Ca-Na-HCO_3)$ + $(Na-HCO_3)$	Groundwater
ST13	-6.77	-6.06	$Ca-Na-HCO_3$	$Ca-Na-HCO_3$	Groundwater
ST14	-7.05	0.59	$Ca-Na-HCO_3$	$Ca-Na-HCO_3$	Surface water
ST15	-9.63	-6.26	$Ca-Na-HCO_3$	$Na-HCO_3$	Groundwater
ST16					Precipitation
ST17	-7.89	-0.67	$Ca-Na-HCO_3$	$Na-HCO_3$	Groundwater
ST18	-9.78	0.83	$Ca-Na-HCO_3$	$Ca-Na-HCO_3$	Surface water
ST19	9.60	-9.88	$Ca-Na-HCO_3$	$Na-HCO_3$	Groundwater
ST20					Precipitation
ST21	-8.45	4.96	$Ca-HCO_3-Cl$	$Na-HCO_3$	Groundwater
ST22	2.82	-9.92	$Ca-Na-HCO_3$	$Ca-Na-HCO_3$	Groundwater
ST23	-9.98	-1.69	$Ca-Na-HCO_3$	$Na-HCO_3-Cl,SO_4$	Groundwater
ST24	-3.83		$Ca-Na-HCO_3$		Surface water
ST25	-10.0		$Na-HCO_3-Cl$		Groundwater
ST26	-9.70	1.12	$Na-HCO_3$	$Na-HCO_3$	Groundwater
ST27	-9.48	-9.91	$Ca-Na-HCO_3$	$Ca-Na-HCO_3$	Groundwater
ST28	-7.08	-4.92	$Ca-Na-HCO_3$	$Na-HCO_3$	Groundwater
ST29	-6.93	-8.42	$Na-HCO_3-Cl,SO_4$	$Na-HCO_3$	Groundwater
ST30	-9.25	-7.74	$Ca-Na-HCO_3$	$(Na-HCO_3-Cl,SO_4)$, $(Ca-Na-HCO_3-Cl,SO_4)$	Groundwater
ST31	-8.08		$(Ca-Na-HCO_3)$ + $(Na-HCO_3)$		Surface water
ST32	-7.04	-8.80	$Ca-Na-HCO_3$	$Ca-Na-HCO_3$	Groundwater
ST33					Precipitation
ST34	-6.95		$Na-HCO_3$		Surface water
ST35	-5.83	-1.38	$Ca-Na-HCO_3$	$Ca-Na-HCO_3$	Groundwater
ST36	-8.80		$Ca-Na-HCO_3$		Surface water
ST37	-22.24	-2.44	$Na-HCO_3-Cl$	$Na-HCO_3$	Groundwater
ST38	-3.65	-3.22	$(Ca-Na-HCO_3)$ + $(Ca-HCO_3)$	$Ca-Na-HCO_3$	Groundwater
ST39	-15.24	-9.66	$(Ca-Na-HCO_3)$ + $(Ca-HCO_3)$	$Ca-Na-HCO_3$	Groundwater
ST40	-0.47	-5.56	$(Ca-Na-HCO_3)$ + $(Ca-HCO_3)$	$Ca-Na-HCO_3$	Groundwater
ST41					Precipitation

Station	Ion Charge Balance (%)		Hydrochemical facies		Water Types
	Rainy	Summer	Rainy	Summer	
ST42	-7.47	-3.48	(Ca-Na-HCO$_3$) + (Ca-HCO$_3$)	Na-HCO$_3$-Cl,SO$_4$	Groundwater
ST43	-8.53		Ca-Na-HCO$_3$		Surface water
ST44	-5.15		Ca-HCO$_3$		Groundwater
ST45					Precipitation
ST46	-7.61	3.29	Ca-Na-HCO$_3$	Ca-HCO$_3$	Groundwater
ST47	6.86	-5.98	Ca-HCO$_3$	Ca-HCO$_3$	Groundwater
ST48	-5.10	-7.36	Ca-HCO$_3$	Ca-Na-HCO$_3$	Groundwater
ST49					Precipitation
ST50	-7.80	1.52	Ca-Na-HCO$_3$	Ca-Na-HCO$_3$	Groundwater
ST51	4.14		Na-HCO$_3$		Surface water
ST52	-7.29	-10.06	Ca-Na-HCO$_3$	Ca-Na-HCO$_3$	Groundwater
ST53	1.92		Na-HCO$_3$		Surface water
ST54	-7.70		Ca-Na-HCO$_3$		Surface water
ST55					Precipitation
ST56	-3.35	-7.03	Ca-Na-HCO$_3$	Ca-Na-HCO$_3$	Groundwater
ST57	-4.90	1.51	Ca-Na-HCO$_3$	Ca-Na-HCO$_3$	Surface water
ST58	-10.55	0.99	Ca-Na-HCO$_3$	Ca-Na-HCO$_3$	Groundwater
ST59	-5.73	2.92	(Ca-Na-HCO$_3$) + (Na-HCO$_3$)	Ca-Na-HCO$_3$	Groundwater
ST60	-14.53	-0.65	Na-HCO$_3$	Na-HCO$_3$	Groundwater
ST61	-7.95	-9.12	Ca-Na-HCO$_3$	Na-HCO$_3$	Groundwater
ST62	-10.08	-8.77	Ca-Na-HCO$_3$	Ca-Na-HCO$_3$	Groundwater
ST63	-24.09	3.61	Na-HCO$_3$	Na-HCO$_3$	Groundwater
ST64					Precipitation
ST65	-10.52	-4.06	Ca-HCO$_3$	Ca-Na-HCO$_3$	Groundwater
ST66	-3.47	0.73	Ca-Na-HCO$_3$	Ca-Na-HCO$_3$	Surface water
ST67	-9.09	9.20	Ca-HCO$_3$-Cl	Ca-HCO$_3$-Cl	Groundwater
ST68	-3.27	1.00	Na-HCO$_3$	Ca-Na-HCO$_3$	Surface water
ST68	-3.27	1.00	Na-HCO$_3$	Ca-Na-HCO$_3$	Surface water
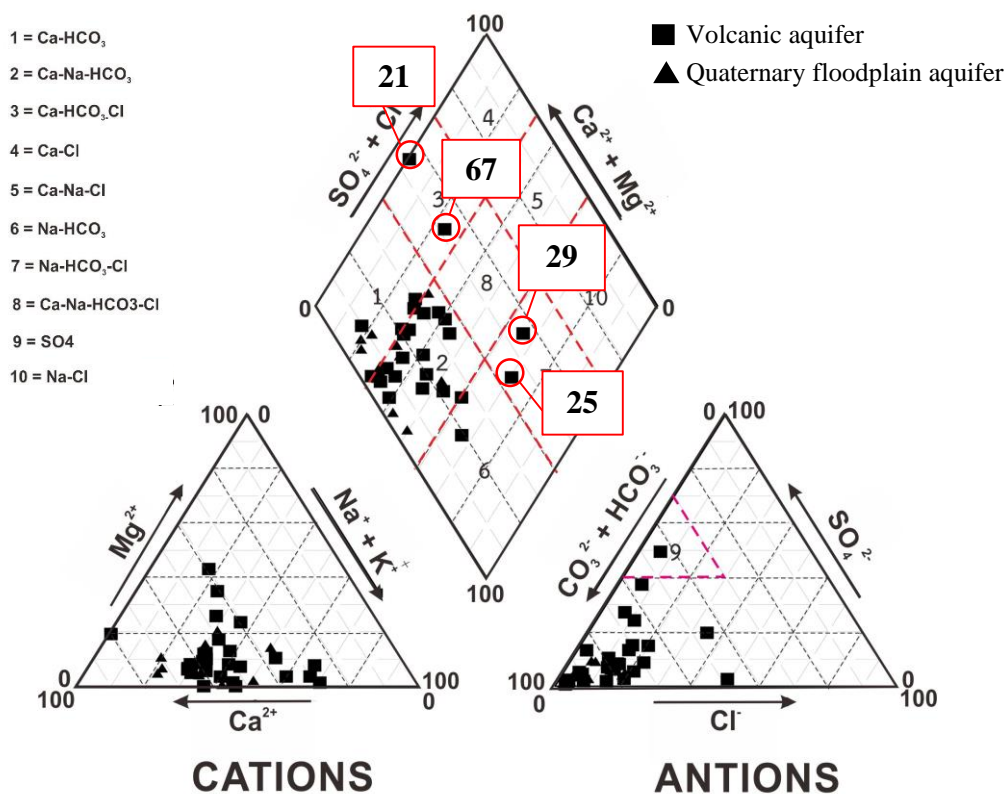
Figure 4.42 Piper diagram of groundwater in the rainy season
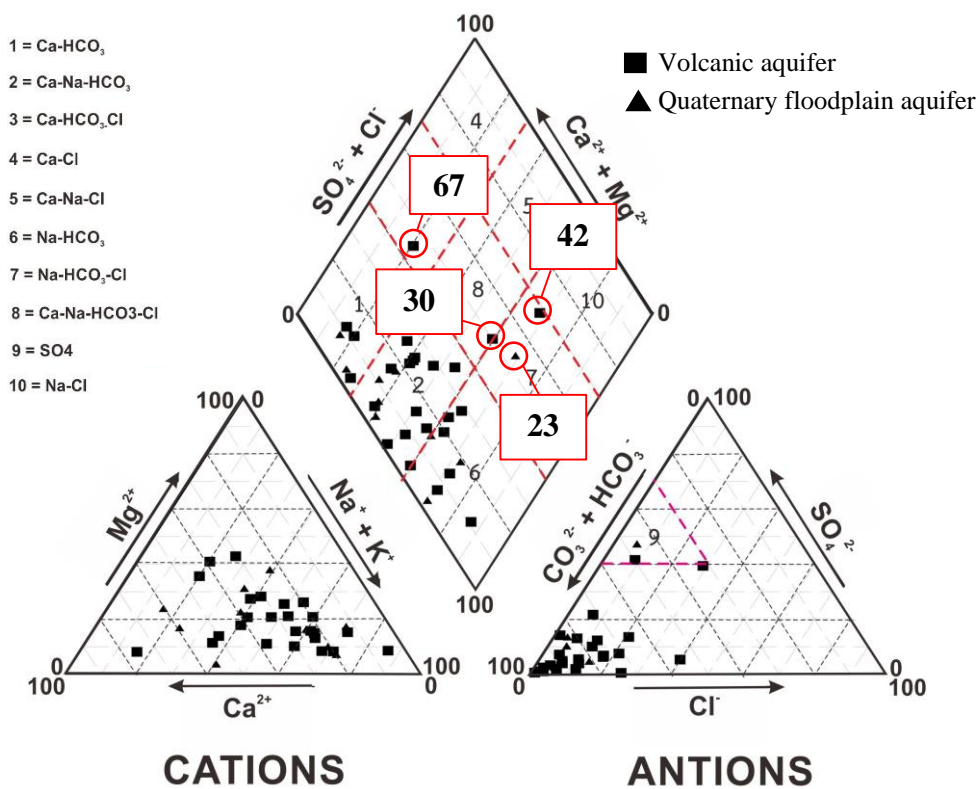
Figure 4.43 Piper diagram of groundwater in the summer season

Moreover, figure 4.42-4.43 show the relationships between the water types of samples that are in Quaternary floodplain aquifer and volcanic aquifer are not different. Thus, the sediments in floodplain aquifer are weathering from the rock in area and affect to hydrochemical facies of groundwater. However, position of anomaly point in both figures are the volcanic aquifer (except station 23), so the concentration of SO_4^{2-} and Cl^- that are high, there are possibility result from the ages of groundwater as shown in the following reaction (Chebotarev, 1955).

Travel along flow path $\longrightarrow$

$HCO_3^- \longrightarrow HCO_3^- + SO_4^{2-} \longrightarrow SO_4^{2-} + HCO_3^- \longrightarrow$

$\hspace{8cm} SO_4^{2-} + Cl^- \longrightarrow Cl^- + SO_4^{2-} \longrightarrow Cl^-$

Incresing age $\longrightarrow$
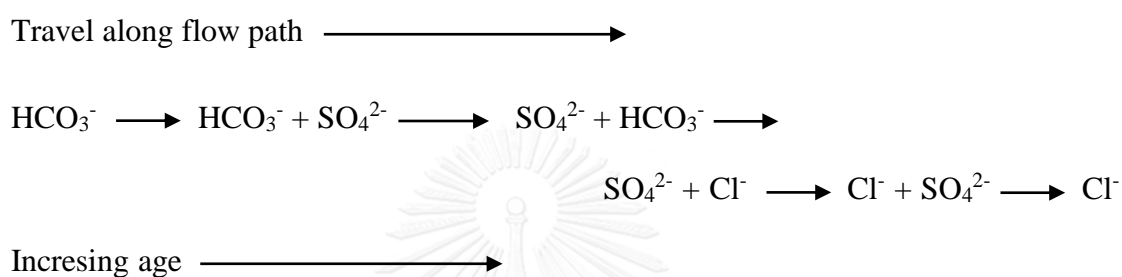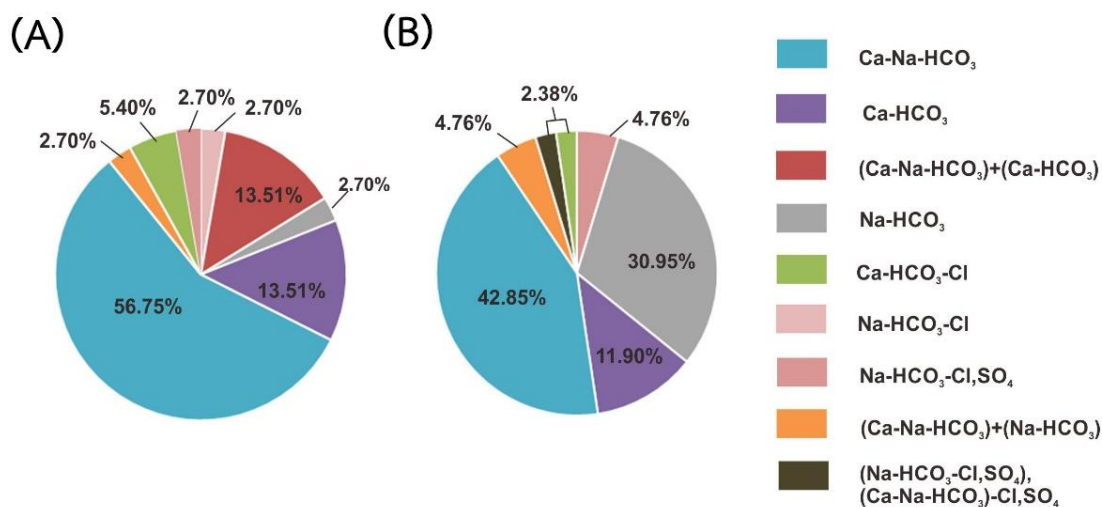
Figure 4.44 The proportion of each hydrochemical facies of groundwater (A) The water types in the rainy season (B) The water types in the summer season

The water types of surface water in the rainy season included Ca-Na-HCO$_3$, Na-HCO$_3$ and (Ca-Na-HCO$_3$) + (Na-HCO$_3$). The main hydrochemical facies are follows: Ca-Na-HCO$_3$ (~ 57.14 %), Na-HCO$_3$ (~ 35.71)and (Ca-Na-HCO$_3$) + (Na-HCO$_3$) (~7.14), whereas all surface water samples in the summer season are Ca-Na-HCO$_3$; however, many stations (i.e., nos. 24, 31, 34, 36, 43, 51, 53 and 54) could not be collected the samples because of no surface runoff during the summer season. Furthermore, the rainwater samples did not analyze to the hydrochemical facies because the samples were kept in a water tank for a long period of time, causing contamination from surrounding environments, such as wall of water tank, and finally leading to the ion balance error. (Figures 4.45-4.47)
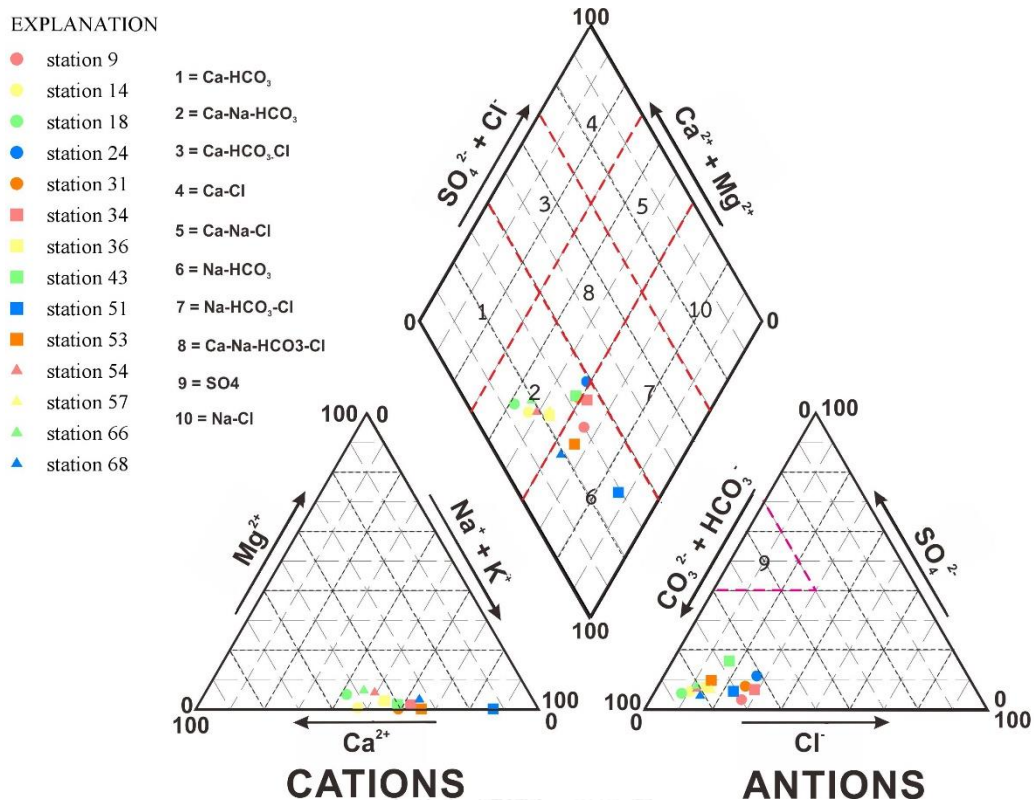
Figure 4.45 Piper diagram of surface water in the rainy season
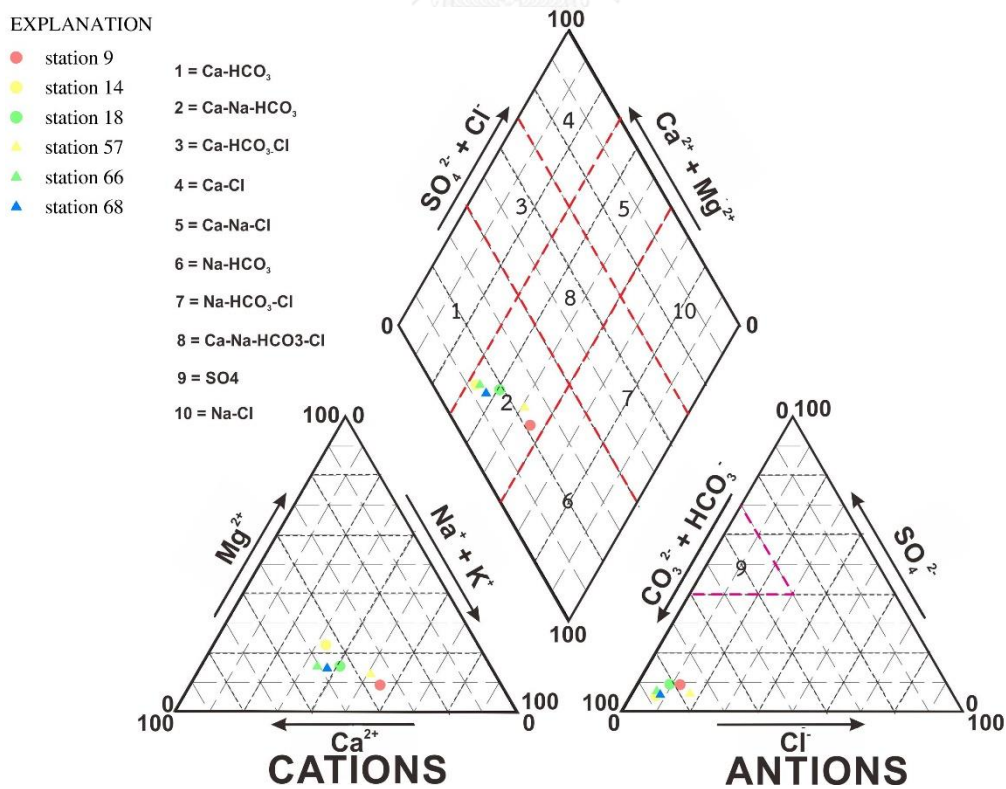
Figure 4.46 Piper diagram of surface water in the summer season
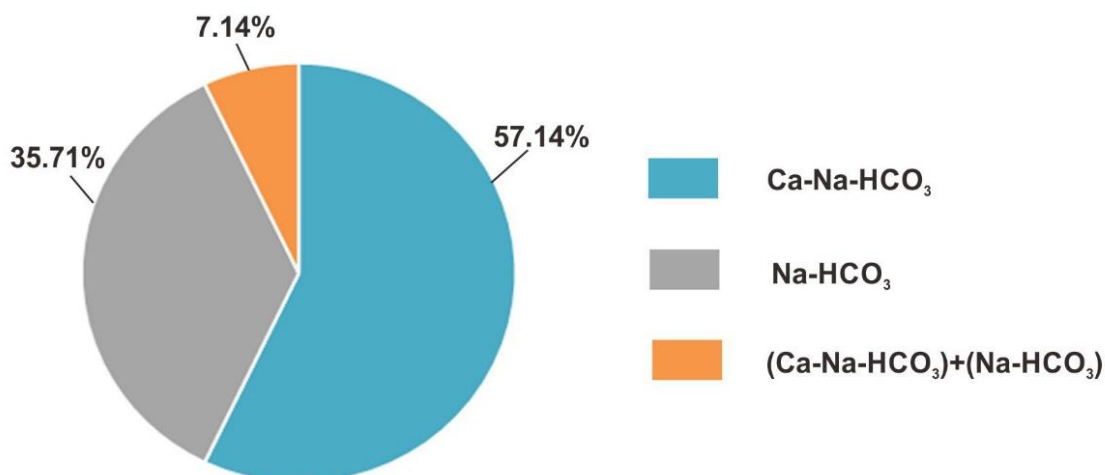
Figure 4.47 The proportion of hydrochemical facies in surface water in the rainy season

4.5 The distribution of NO_3^- concentration in groundwater

The NO_3^- concentration contaminated in groundwater and surface water during rainy and summer seasons were lower than the maximum contamination level for drinking water. Moreover, the NO_3^- concentration of groundwater is higher than that in surface water in both seasons and in the rainy season the NO_3^- concentration was less than those in the summer season. (Macler, 2007; WHO, 1998; Woolverton, 2015), which is not harmful to human health and ecosystem. However, although levels of NO_3^- is not over the standard, the NO_3^- concentration may not only come from the nature, i.e., rock and water interaction, but it may come from other sources, causing from anthropogenic activities, such as irrigation, livestock and industrial activities, etc. NO_3. The NO_3^- concentration of groundwater in rainy season ranged from lower than the detection limit to 7.105 mg/l with an average NO_3^- concentration of approx. 1.41 mg/l. A NO_3^- concentration in groundwater appears to be high concentration in the northwest part of the area (see Figure 4.48). NO_3^- concentrations were related to the groundwater along the hydrogeological cross-section, for example, the southeast part of the area, it seems to be found high NO_3^- concentration at station no. 48 (see Figure 4.48), which is related to groundwater flow and located in a recharge area from isotope results . In fact, the concentration of NO_3^- should be less, but it is not so the area has been affected by human activities. In addition, the NO_3^- distribution in both seasons is similar pattern, when comparing during both seasons, areas with a higher NO_3^- concentration in the

summer season was greater than in the rainy season (see Figure 4.49). The NO_3^- concentration in summer season was in a range from 0.20 mh/l to 5.59 mg/l with an average NO_3^- concentration of 1.75 mg/l. The most NO_3^- concentrations of nitrate in groundwater in the summer were higher than those in the rainy season, suggesting that the influence of rain helps to dilute the NO_3^- concentration of nitrate in groundwater during the rainy season. However, there were some wells showing a lower NO_3^- concentration in the summer season, which they are in a proper condition for biodegradation, resulting in a decrease of NO_3^- levels in groundwater.

In surface water, according to the watershed classification, this areas can be separated into 3 sub-watersheds. The watershed 1 is located in the northern part of area which the main river is Huay Lee (see Figure 4.50), where is delivered water by the small river consisting of Huay Wa and Huay The watershed 2 is located in the central part of area, where the main river is Khong Phriao or known as Khong Khok Krung. The last watershed is located in the southern part of the area where the main river is Huay Haeng or so-called, Huay Takhe. The flow direction of surface water conforms to the groundwater flow, which flows from east to west direction. All rivers flows into the Khong Phriao reservoir. According to results of NO_3^- concentration in surface water, it found that the NO_3^- concentration was relatively high in downstream areas, especially in Huay Haeng watershed. Most NO_3^- concentration appeared to be decreased along the flow direction of surface water, except station no. 36. The maximum concentration was found at station no.51, adjacent with station no.48, which is the groundwater well located in the recharge area of the Huay Haeng watershed (Figure 4.51). However, in summer season the NO_3^- concentration was found relatively high in the central of area, especially in in the Khong Phriao watershed. Similar in the rainy season, the NO_3^- concentration tended to be was decreased along the flow direction, except station no.18, where presented the maximum NO_3^- concentration. When considering at the same station, the NO_3^- concentration was found in the summer higher than that in the rainy season and the higher NO_3^- concentration were found in the upstream areas (see Figure 4.52).
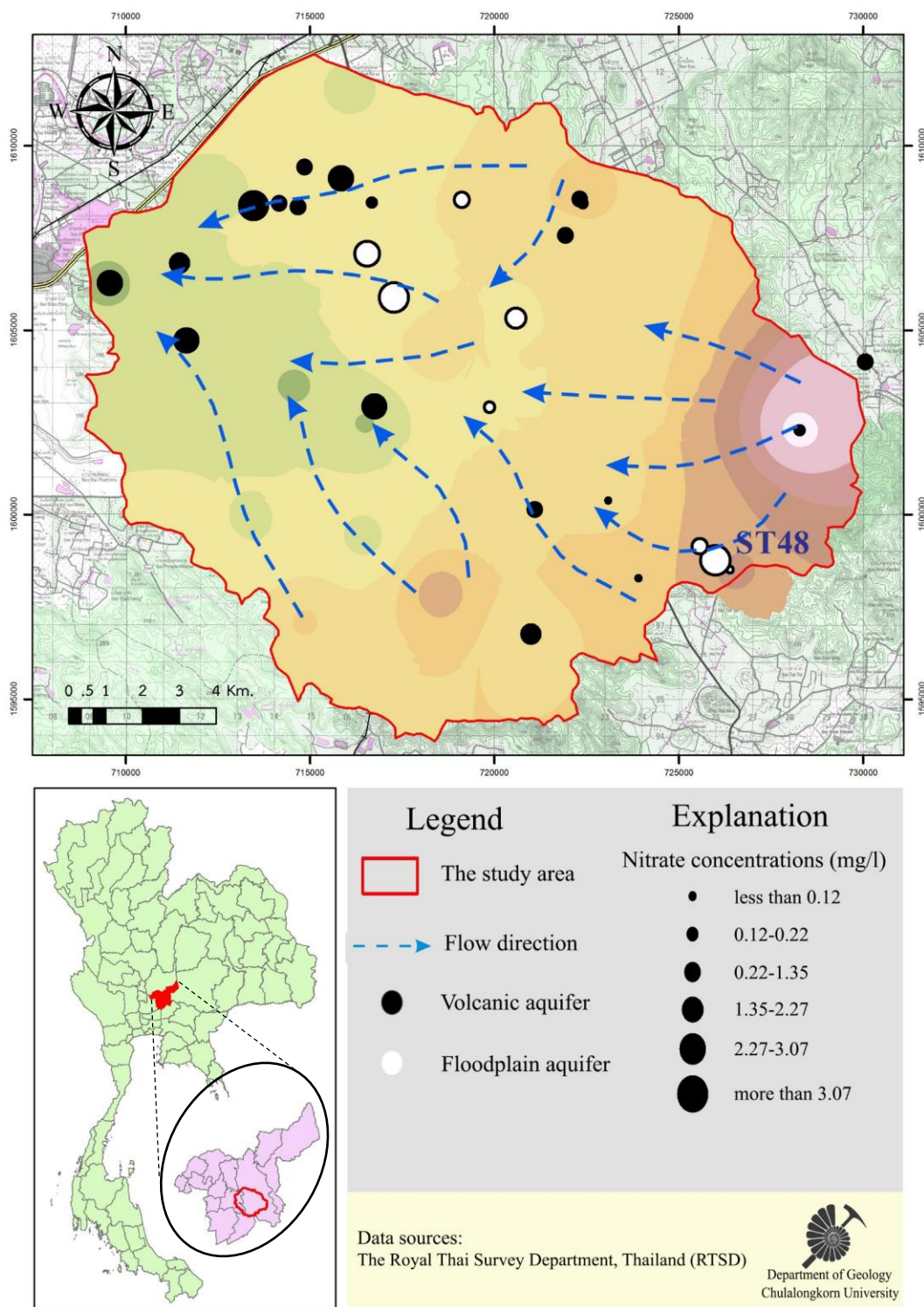
Figure 4.48 The distribution of NO$_3^-$ concentration in groundwater in the rainy season
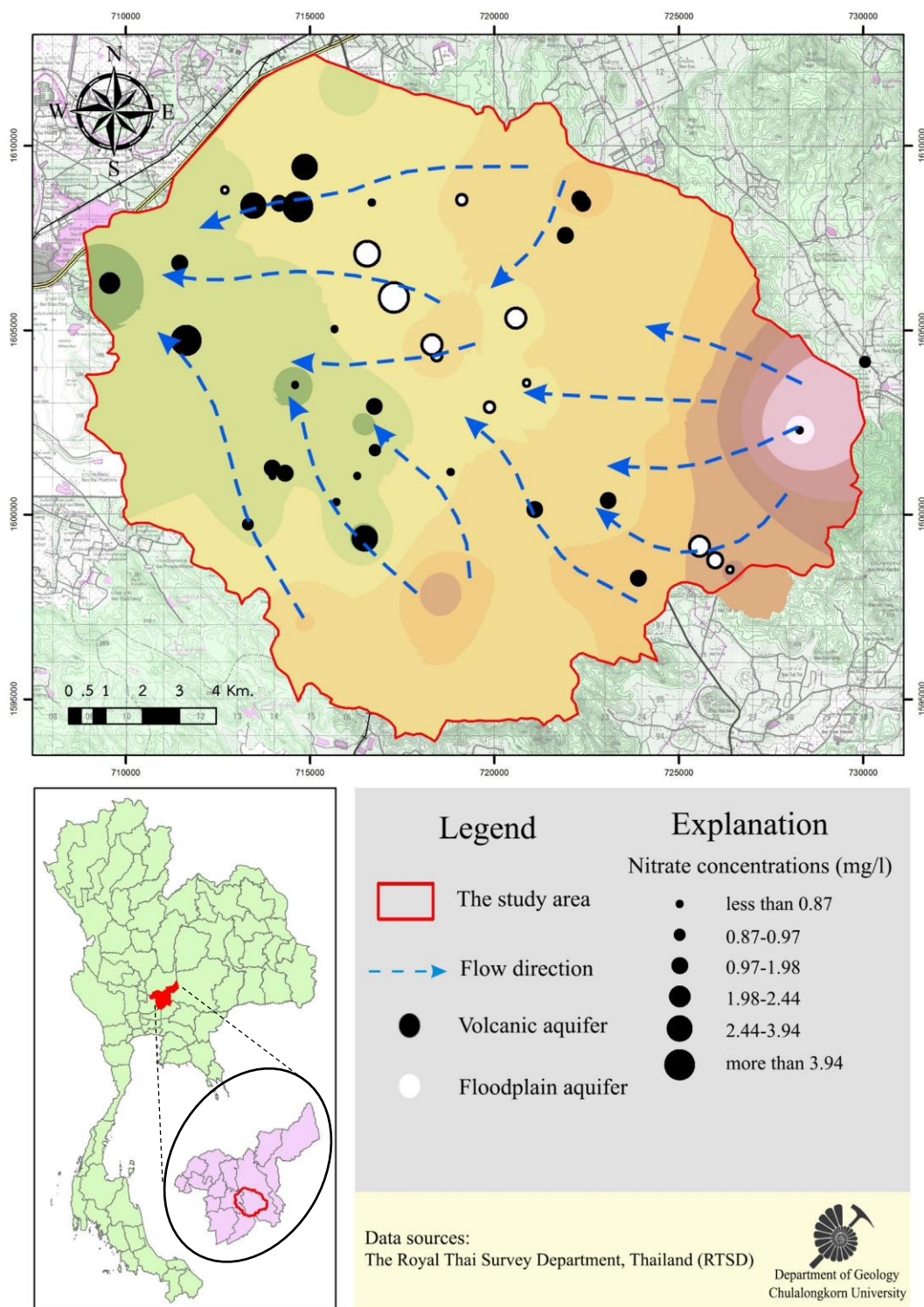
Figure 4.49 The distribution of NO_3^- concentration in groundwater in the summer season
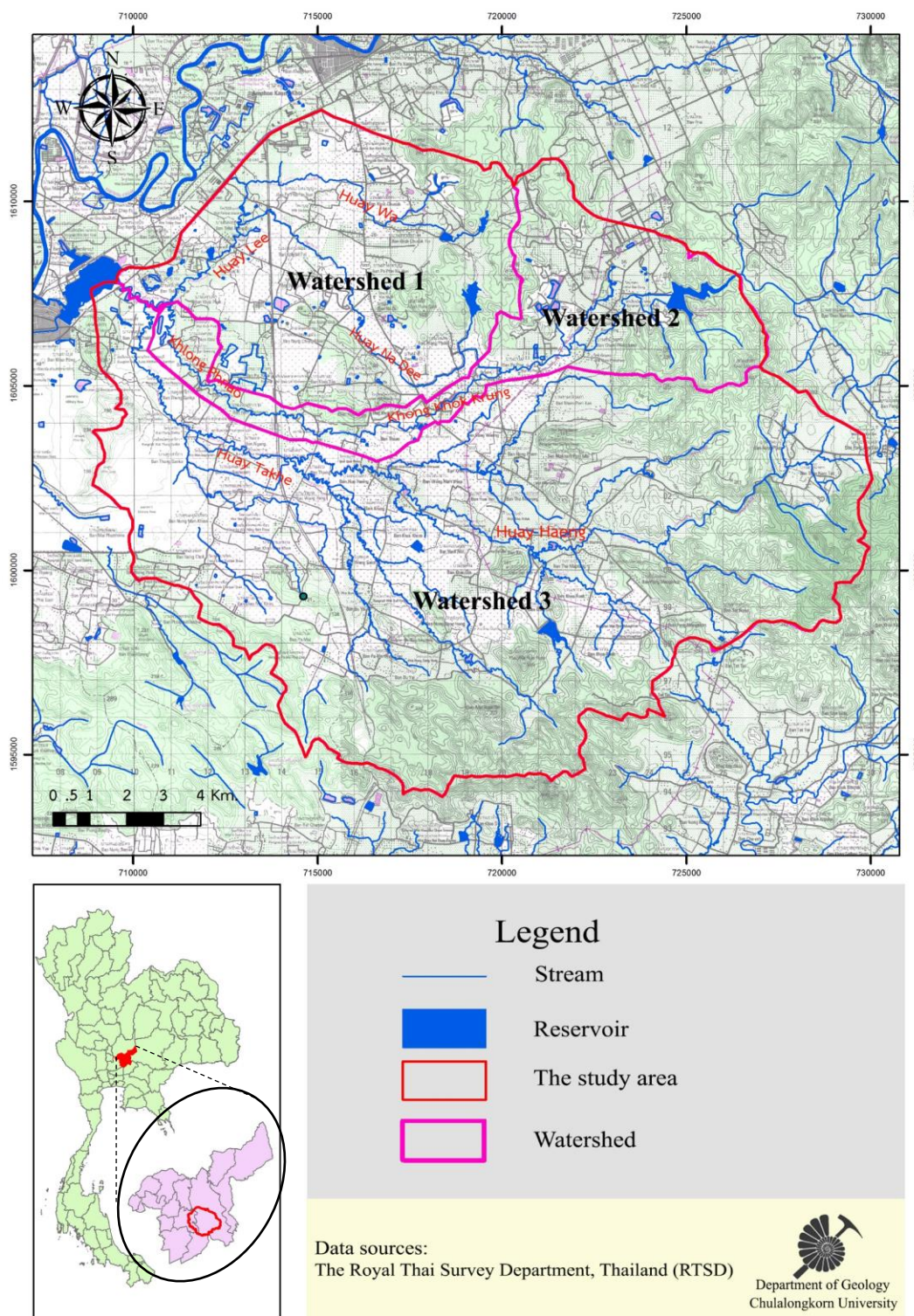
Figure 4.50 The boundary of sub-watershed in area
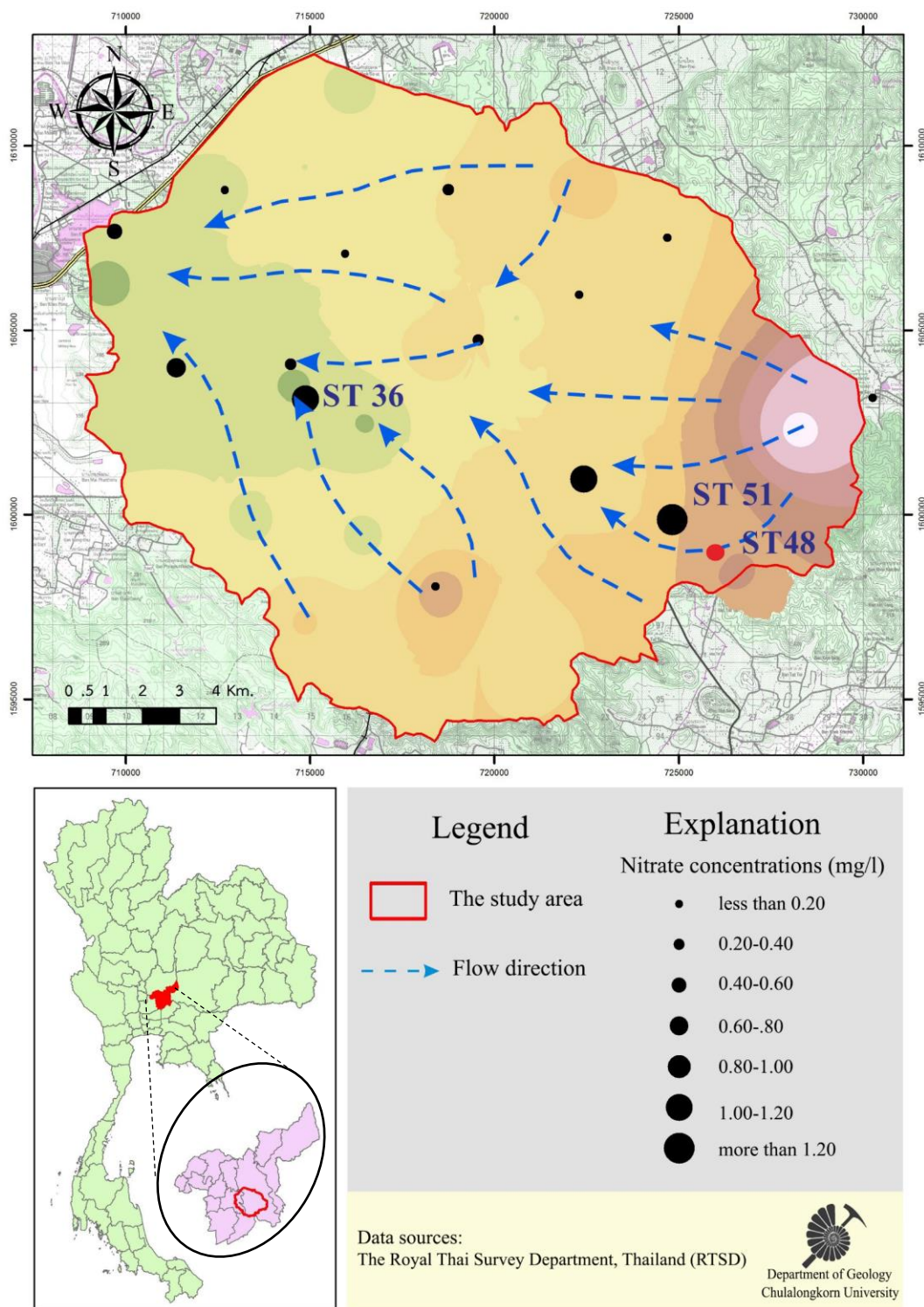
Figure 4.51 The distribution of NO_3^- concentration in surface water in the rainy season
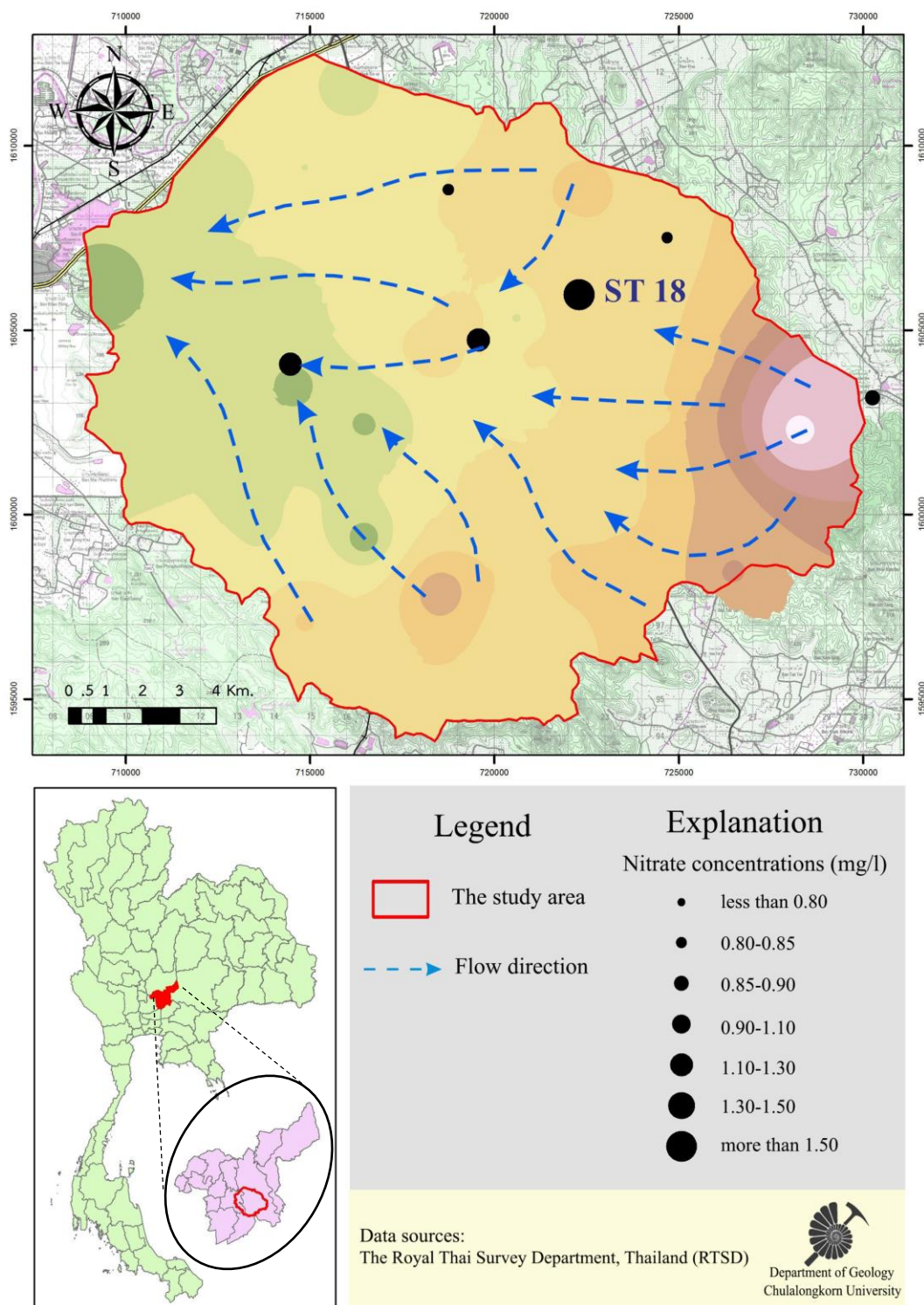
Figure 4.52 The distribution of NO_3^- concentration in surface water in the summer season

4.6 The comparison of NO$_3^-$ concentrations

By using the t-test technique to compare between two seasons, the average NO$_3^-$ concentrations in groundwater selected only from groundwater wells (~25 wells), which could be collected in both seasons and had NO$_3^-$ concentration higher than the detection limit, the results found that the NO$_3^-$ concentration in rainy season was not significantly different from that in the summer ($p>0.05$).

Studies of Guo and Jiang (2009), Gao, Yu, Luo, and Zhou (2012) and Mo, Chen, Zhou, Chen, and Duan (2016), they found that NO$_3^-$ concentrations in November was lower than those in in May. Which is similar trend to NO$_3^-$ concentrations in this study area (see Figures 4.53-4.54).
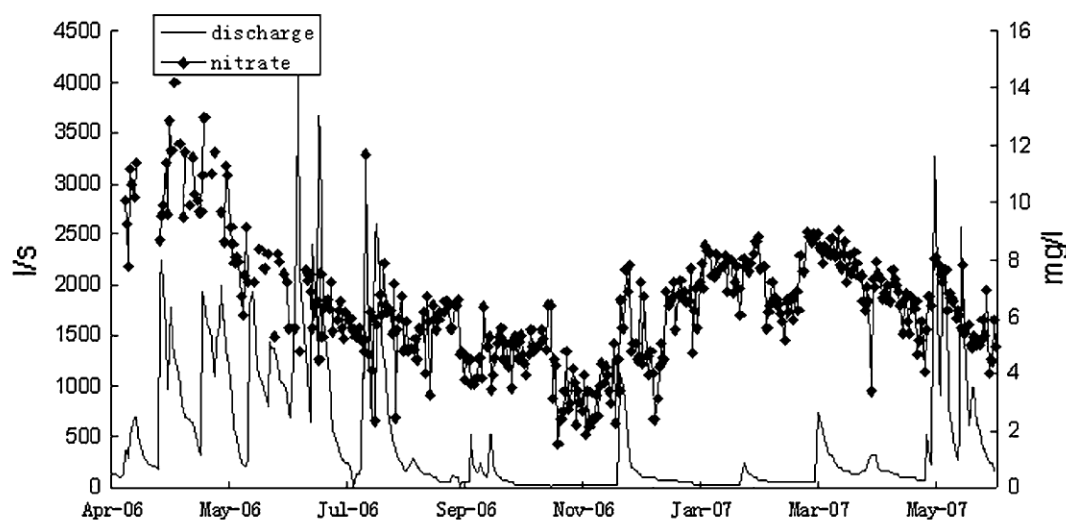
Figure 4.53 The NO$_3^-$ concentration from April 2006 to May 2007
(Guo & Jiang, 2009)

In Figure 4.54, at station nos. 02, 26, 30, 48 and 59, they had higher NO$_3^-$ concentration in November than of those in May. By applying t-test method to, the results showed that two groups are not significantly different ($p>0.05$). And the study of Silva, Souza, and Abreu (2015), they explained that NO$_3^-$ concentration was rather high in the summer as a result of nitrification process, which is the process of bacteriological oxidation of nitrogenous materials in soil.
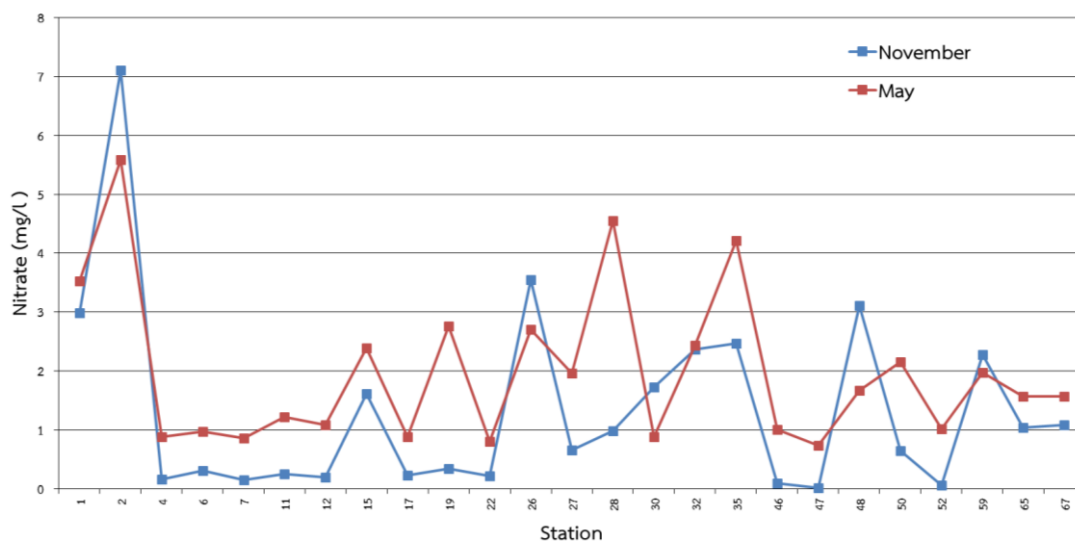
Figure 4.54 The NO_3^- concentration in November 2014 and May 2015 in the study area

Furthermore, we create the box plot to distinguish the difference of data more clearly because it shows the median, fluctuation and anomaly of data. The box plot is used to compare groups of data, which can be presented the data into 3 main parts. Part 1, so-called, 1st quartile or 25th percentile shows data ranging from 10 percent to 25 percent of all data. Part 2, namely, 2nd quartile or 50th percentile shows data ranging from 25 percent to 75 percent. This part presents a middle value of data (median) or inter quartile as well as the width of this section represents the fluctuation of data. The last part is known as 3rd quartile or 75th percentile shows data ranging from > 75 percent to 90 percent (Sabseree, 2010). The box plots of NO_3^- concentration during two seasons are shown in Figure 4.55. It represents a 25th percentile, median and 75th percentile of NO_3^- concentrations in the summer were higher than those in the rainy season. However, the high fluctuation of NO_3^- concentrations was presented in the rainy season than in the summer season.

In Figure 4.56, NO_3^- concentrations at 90th percentile were 3.07 and 3.94 mg/l in rainy and summer seasons, respectively. If a concentration is beyond either the upper outer or lower outer $(Q3\pm3(Q3-Q1))$, that concentration appears to be an anomaly point.In Figure 4.53, The box plot revealed that 3 stations had the NO_3^- anomaly in the rainy season include station no.02, 26 and 48 with NO_3^- concentrations of 7.11 mg/l,

3.55 mg/l and 3.11 mg/l , respectively. Likewise, in summer season, it showed 3 stations had NO_3^- anomaly anomaly include station nos. 02, 28 and 35 with NO_3^- concentrations of 5.59 mg/l, 4.55 mg/l and 4.21 mg/l respectively. These anomaly stations should be carefully considered where the sources of NO_3^- come from.
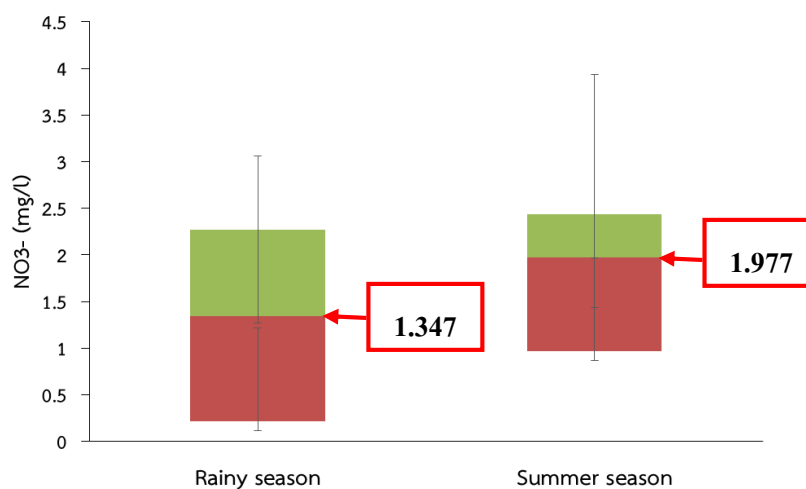
Figure 4.55 The box plot showing the median of NO_3^- concentration during two seasons
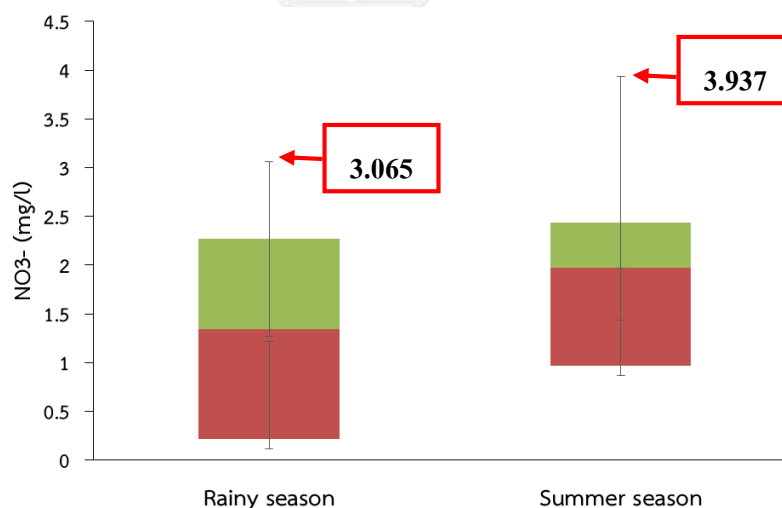
Figure 4.56 The box plot showing the 90th-percentile NO_3^- concentration during two seasons

According to the study of Kolpin, Burkart, and Goolsby (1999), they suggested the NO_3^- concentration is lower than 2 mg/l, indicating the area may not be contaminated from human activities. Moreover, the study of Choi et al. (2007a) found that if NO_3^- concentration exceeds 3 mg/l, suggesting that the NO_3^- contamination

results from anthropogenic sources. As mentioned about the criteria from previous studies, the stations having NO_3^- concentration over 2 mg/l were selected to further find out sources of NO_3^- contamination in groundwater. There were 7 stations (nos. 01, 02, 26, 32, 35, 48 and 59) and 9 stations (nos. 01, 02, 15, 19, 26, 28, 32, 35 and 50) in the rainy and summer seasons, respectively. When considering the stations mentioned in both seasons, we selected station nos. 01, 02, 26, 32 and 35 because these stations had concentrations exceeding 2 mg/l in both seasons. Apart from above criteria, based on land use types, we found the 5 interesting stations since they are located in the specific land use types, as follows: station no. 28 (paddy area), station no.48 (cultivated palm area), station no.59 (residential area), station no.65 (chicken farms), and station no.67 (cultivated corn and tapioca areas). Although NO_3^- concentrations in these 5 stations did not exceed over 2 mg/l in both seasons, for examples, NO_3^- concentration of station no.28 was 0.98 mg/l in the rainy, but these stations were included to identify whether NO_3^- concentrations measured in the wells related to land use types or not. We discussed more about such effects further in the next section. Due to aforementioned land use may be lead to sources of NO_3^- in those area. Based on the criteria of NO_3^- exceeding 2 mg/l, only one station, station no.51, in the rainy season was selected.

By plotting Cl^- concentration and specific conductance of 2 groups of groundwater derived from a pristine aquifer and road salt affected water, S. V. Panno et al. (2006) suggested that background concentration of chloride in groundwater ranges from 1 mg/l to15 mg/l and specific conductance not exceeding 750 μS/cm. According to the criteria suggested by S. V. Panno et al. (2006), when the groundwater sample having Cl^- concentration and specific conductance beyond the threshold, suggesting that such groundwater is anthropogenically affected. Thus, we used the criteria to further select the stations, which were affected anthropogenic sources. Finally, according to the criteria, accounting for NO_3^- concentration exceeding 2 mg/l, only station nos. 21 and 30 were selected (Figures 4.57-4.58). In summary, all stations selected totally were 13 stations consisting of 12 groundwater wells and 1 surface water sampling point as shown the details in Table 4.1 and locations of each station is shown in Figure 4.59.
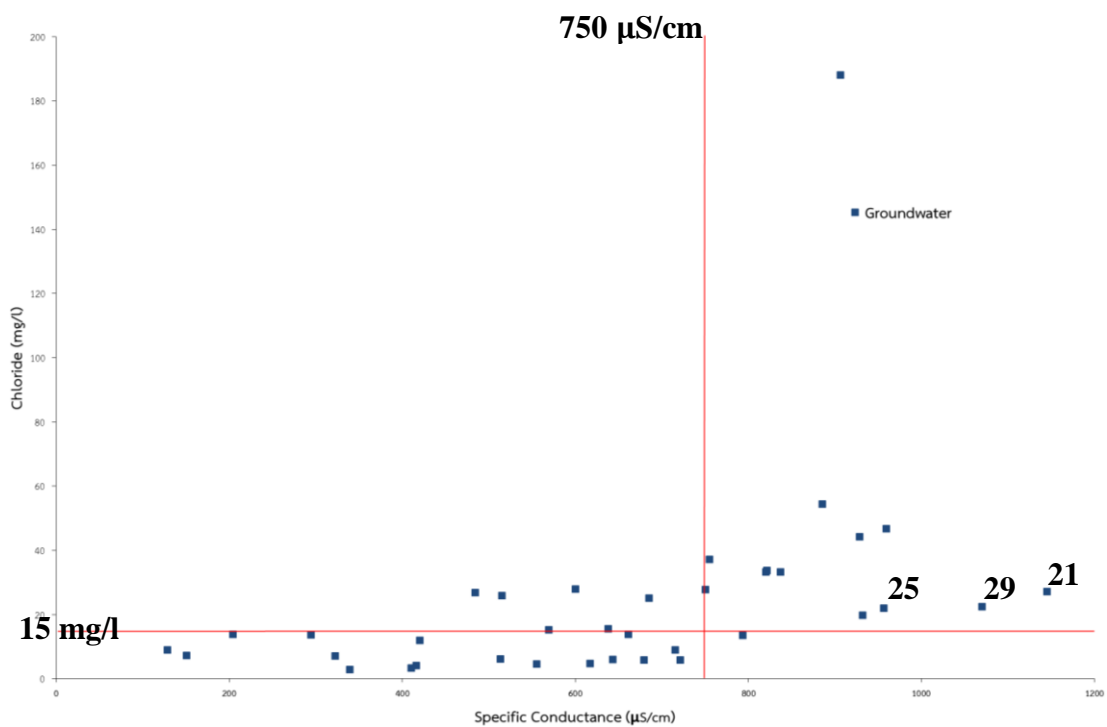
Figure 4.57 The graph plotting between specific conductance and Cl⁻ in groundwater in the rainy season (modified from Panno et al., 2006)
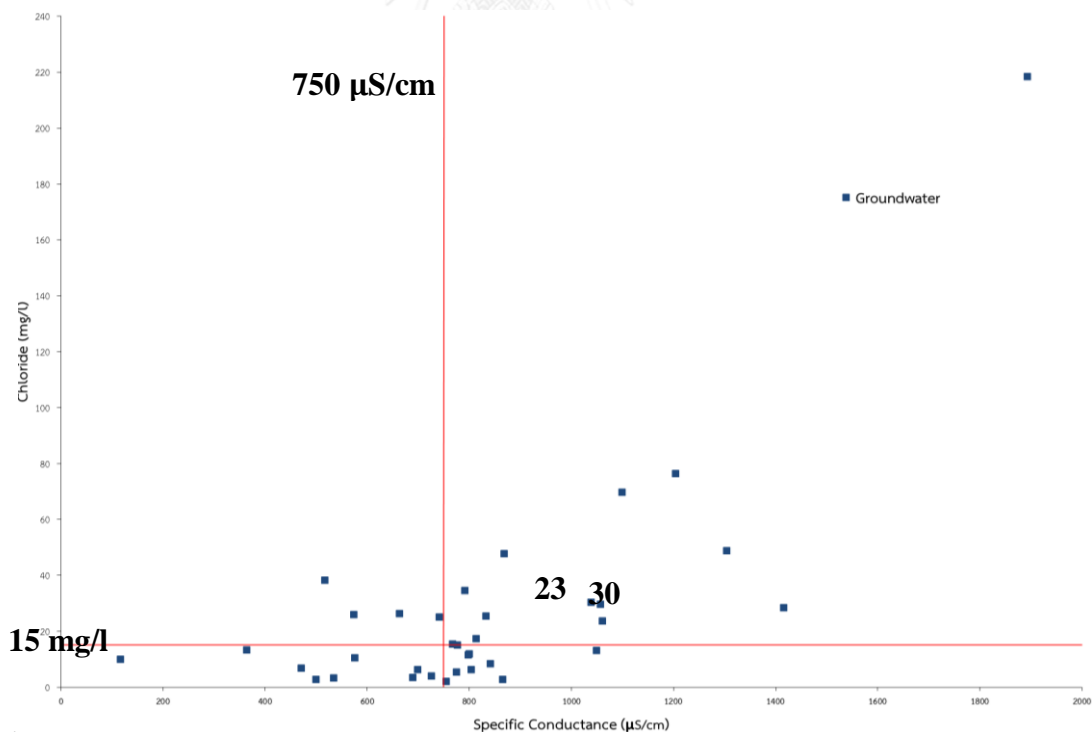
Figure 4.58 The graph plotting between specific conductance and Cl⁻in groundwater in the summer season (modified from Panno et al., 2006)

Table 4.10 NO_3^- concentrations of stations selected to identify sources of NO_3^-

Station	East	North	Nitrate concentration (mg/l)	
			Rainy season	Summer season
ST01	716539	1607076	2.99	3.52
ST02	717275	1605897	7.10	5.58
ST21	715830	1609126	3.01	LOD
ST26	713464	1608383	3.54	2.70
ST28	714671	1608348	0.98	4.55
ST30	711461	1606825	1.72	0.87
ST32	709563	1606287	2.37	2.43
ST35	711636	1604727	2.46	4.20
ST48	725990	1598761	3.11	1.67
ST51*	724824	1599866	3.69	-
ST59	716739	1602934	2.27	1.97
ST65	721091	1600142	1.04	1.57
ST67	721925	1607575	1.08	1.56

LOD : Lower limit of detection limit

* Surface water

- No sample
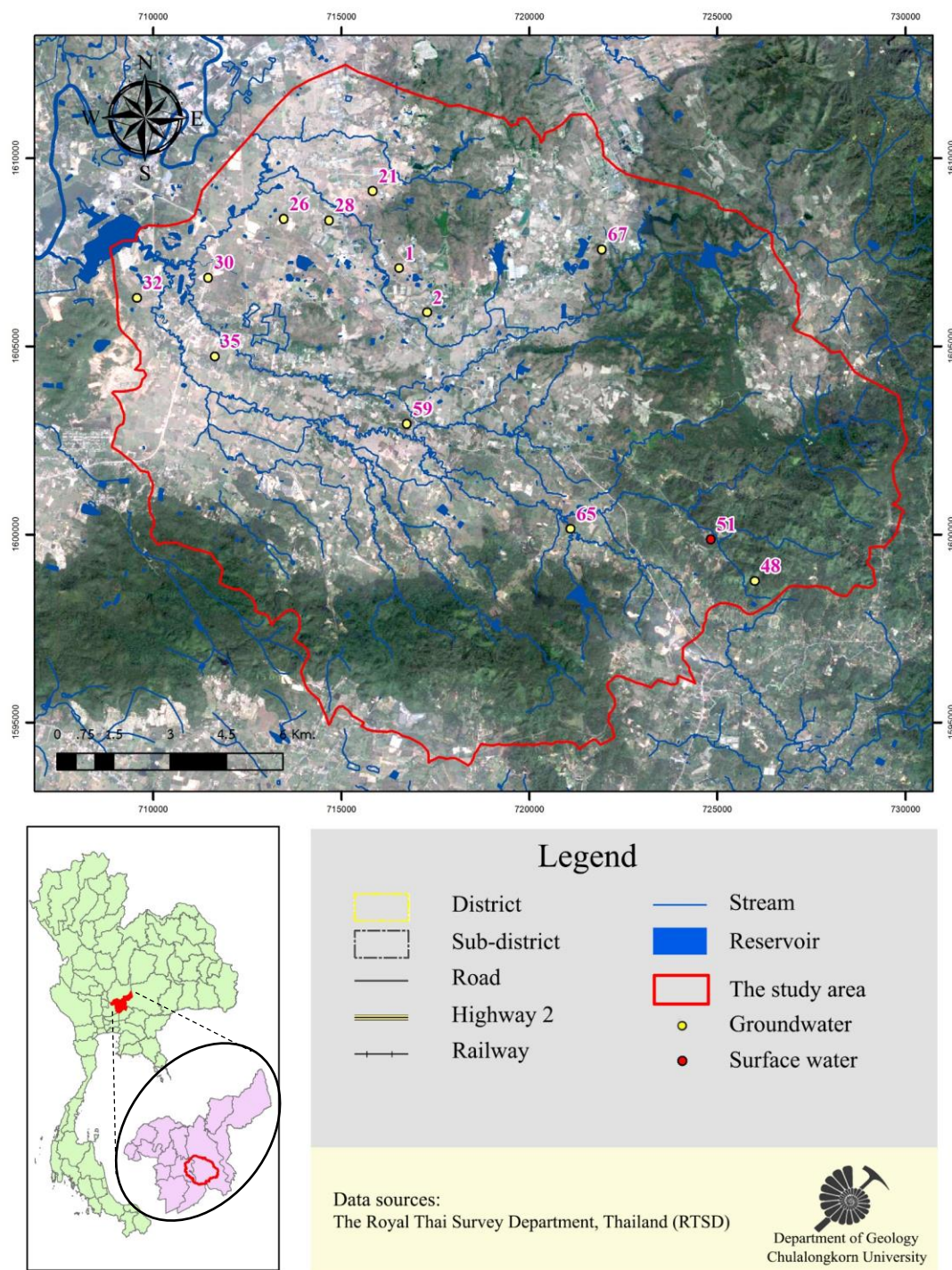
Figure 4.59 The locations of each station chosen to identify sources of NO_3^-

4.7 The sources of NO$_3^-$ concentration

The method is used to classify sources of NO$_3^-$ in stations as shown in Table 4.1, we applied the mixing curves, which plots cations and/or anions from geochemical analysis along with curves, containing endpoints of each contaminated sources, for examples, brine, road salt, septic waste, animal waste, fertilizer, fresh water, from previous researchers to identify sources of NO$_3^-$. These methods has been developed and used to indirectly indicate sources of NO$_3^-$ contamination in groundwater (Heston, 2015). The details of these relationship as mentioned displayed in the following section below moreover the sources of NO$_3^-$ in each station is summarized in Table 4.10

4.7.1 Relationship between Cl$^-$/Br- ratios and total nitrogen

Chloride (Cl$^-$) and Br$^-$ ions are conservative anions, so they have minimal interactions with the surrounding substrate in sites (HEM, 1985), that why the Cl$^-$/Br$^-$ mass ratio is an useful inexpensive tool, which can indicate whether water resources are contaminated by Na$^+$ and Cl$^-$ and it can be used to assess the origin of the saline groundwater, atmospheric precipitation, domestic sewage as well as groundwater movement (Devis, Whittemore, & Fabryka-Martin, 1998; Richter & Kreitler, 1993). However, this technique is not definitive because of the similarities of range Cl$^-$/Br$^-$ ratios; so many hydrochemical parameters are used to conjunction with Cl$^-$/Br$^-$ ratios to clearly discriminate sources of NO$_3^-$ (S. V. Panno et al., 2006).

Marie and Vengosh (2001) using NO$_3^-$ concentration as an indicator of the affected groundwater by sewage effluent, so it can be used as a potential tools for delineating the possible contaminant sources, while S. V. Panno et al. (2006) using total nitrogen (TKN) concentration instead NO$_3^-$ concentration. This relationship can separate groundwater samples affected by landfill leachate, septic effluent and animal waste from another affected by road salt. In this study, in the rainy season all of groundwater and surface water samples were fallen in the boundary of affected water, Likewise, in the summer, all of samples were falled down in the boundary of affected water. As mentioned above, the results could preliminarily let us know that groundwater in most wells and surface water were affected (Figures 4.60 and 4.61).
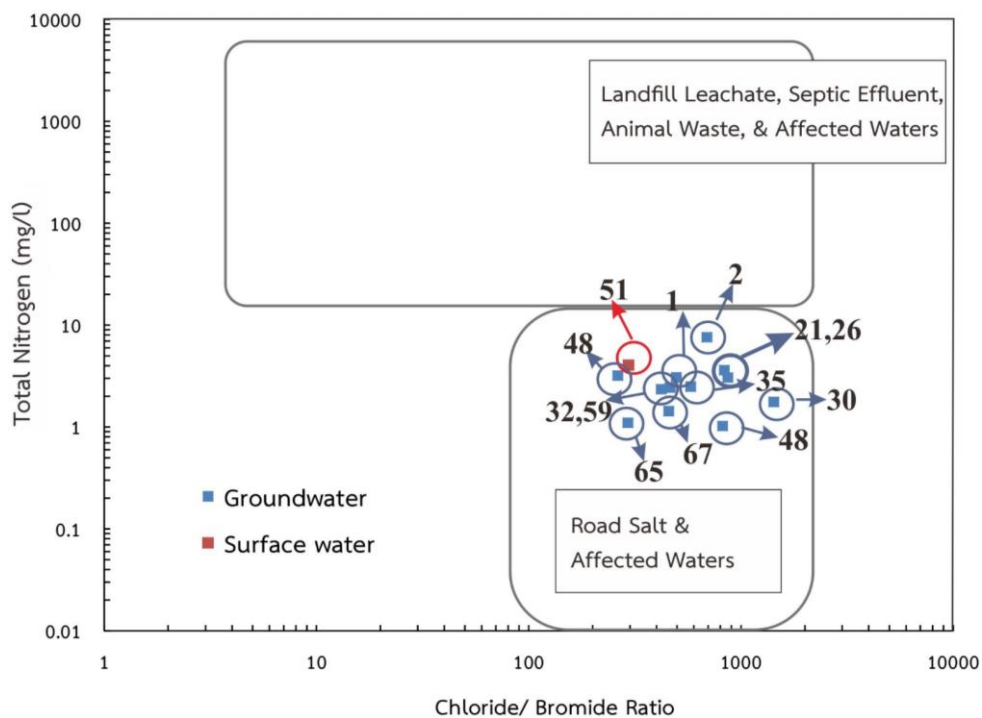
Figure 4.60 Total nitrogen and Cl⁻/Br⁻ ratios of groundwater and surface water in the rainy season (modified from Marie and Vengosh, 2001)
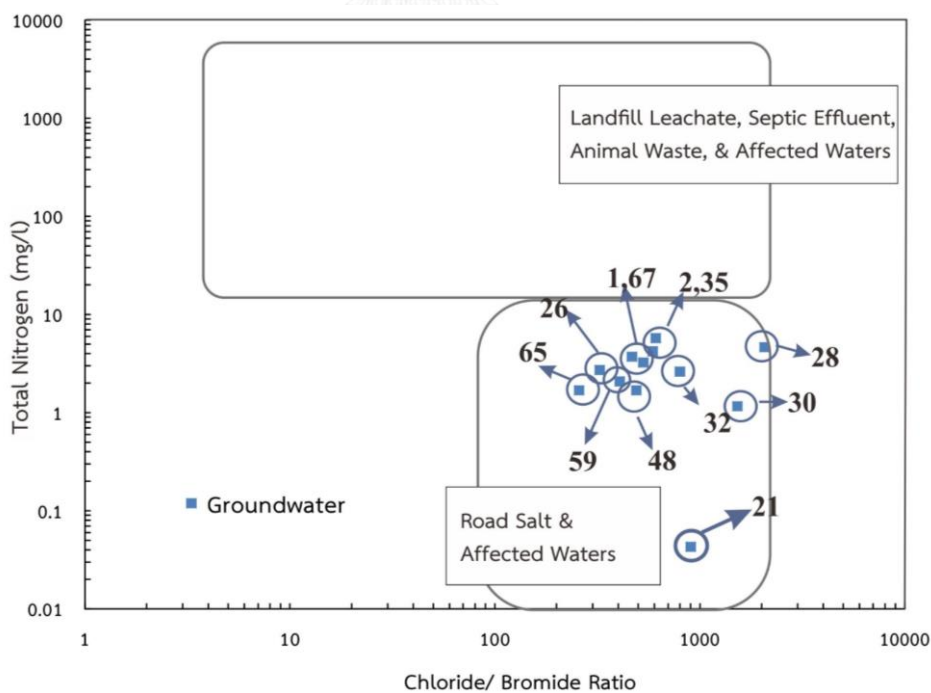
Figure 4.61 Total nitrogen and Cl⁻/Br⁻ ratios of groundwater in the summer season (modified from Marie and Vengosh, 2001)

4.7.2 Relationship between Cl⁻/Br⁻ ratios and Cl⁻ concentration

S. V. Panno et al. (2006) proposed the relationship between Cl^-/Br^- ratios and Cl^- concentration to identify sources of NO_3^- in groundwater. According to this relationship, they can classify approximate regions of sources of NO_3^- contamination as follows: background precipitation, unsaturated zone or soil water, pristine aquifer, artificial fertilizer (KCl), road salt, septic effluent, animal waste, landfill leachate, seawater and basin brines & saline springs. Therefore, we refers to this relationship to delineate NO_3^- sources in the study area. After plotting our data following this relationship, we found that in rainy season, station nos. 01, 02, 28, 30, 48 and 59 may be contaminated from fertilizer, while station nos. 26, 32 and 35 were fallen in the boundary of road salt and septic effluent, as well as station nos. 65 and 67 were in the boundary of basin brines and animal waste. Moreover, we found only station no.21 where was contaminated from mix sources between fertilizer, road salt and septic effluent. For surface water, it was affected from a fertilizer.

In the summer season, the Cl^-/Br^- ratios were lower than that in the rainy season. These can be concluded as follows: the station nos. 01, 02, 21, 26, 30, 48, 59 and 65 were in the boundary of pristine aquifer; station no.48 was in the boundary of precipitation; station no.35 was affected between precipitation and pristine aquifer; station no.32 was affected from precipitation and landfill leachate and station no.67 was affected from precipitation, pristine aquifer and landfill leachate. It would be noticed that in the summer may have some processes causing NO_3^- concentrations in groundwater (Figures 4.62-4.63).

Figure 4.62 Cl$^-$/Br$^-$ ratios and Cl$^-$ concentration of groundwater and surface water in the rainy season (modified from Panno et al., 2006)

Figure 4.63 Cl$^-$/Br$^-$ ratios and Cl$^-$ concentration of groundwater in the summer season (modified from Panno et al., 2006)

Furthermore, Pasten-Zapata et al. (2014) investigated the relationship between Cl^-/Br^- ratios and Cl^- concentration as similar to the previous study mentioned earlier. In their study, they separated the NO_3^- sources into 3 groups, including agrochemical, animal affected and landfill leachate. In addition, they also indicated the trend of urine and biodegradation in their relationship as well. According to this relationship, in the rainy season, most groundwater and surface water were in the boundary of agrochemicals, except station nos. 32 and 65, where were in the boundary of animal-affected. Besides, only station no.67 was fallen in the mixed zone between animal-affected and landfill leachate. Nevertheless, we discerned the biodegradation process occurring in the summer season, suggesting that most groundwater samples did not fall in the extent of NO_3^- sources, but all samples were affected from biodegradation mechanism (Figures 4.64-4.65).

Figure 4.64 Cl^-/Br^- ratios and Cl^- concentration of groundwater and surface water in rainy season (modified from Pasten-Zapata et al., 2014)
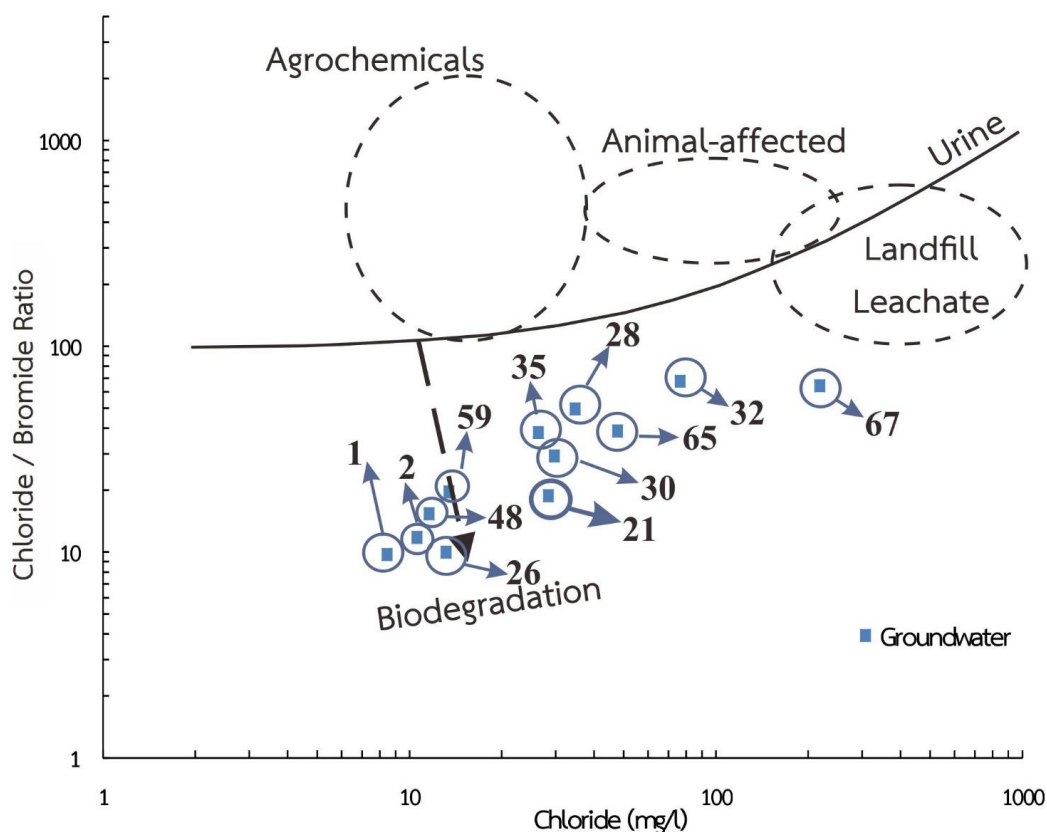
Figure 4.65 Cl⁻/Br⁻ ratios and Cl⁻ concentration of groundwater in the summer season (modified from Pasten-Zapata et al., 2014)

4.7.3 Relationship between NO_3^-/Cl^- ratio and Cl^- concentration

Yanpeng Zhang et al. (2015) studied the sources of NO_3^- in groundwater by applying the relationship between NO_3^-/Cl^- ratio and Cl^- concentration (mol/l). They suggested that difference of NO_3^- sources can be classified from this relationship, which can classify into 3 NO_3^- sources as follows: agriculture, wastewater and natural sources. Agricultural inputs show high NO_3^-/Cl^- ratios and low Cl^- concentration, whereas wastewater shows low NO_3^-/Cl^- ratios and high Cl^- concentration. The last one, natural sources primarily mention about precipitation and soil organic nitrogen, which commonly show low NO_3^-/Cl^- ratios with Cl^- concentration. So, based on this concept, we created the mixed triangle to indicate where they come from. For a point referring to natural sources, we use the hydrogeochemical data of this study at upstream Bandong reservoir. For other two points referring to the wastewater and agricultural sources, we

calculated the ratio with Cl⁻ concentration derived the hydrochemical data from the Thailand Institute of Nuclear Technology (TINT).

In the rainy season, there are 6 stations that are fallen outside the mixed triangle and all stations were not clearly delineated the sources, except station no.67, which was separated out of the others and may be affected from wastewater which is in lined with the both previous relationships as mentioned before. Station nos.01, 02, 48 and 51 were affected from agriculture and natural sources. Station nos.32 and 65 were affected from natural sources and wastewater. The last group included station nos.21, 26, 28, 30, 35 and 59 were fallen in the mixed triangle, suggesting that various sources can jointly exaggerate the pollution in groundwater (Yanpeng Zhang et al., 2015). In the summer season, herein we neglected station no. 21 and looked only 11 stations because NO_3^- concentration of station no. 21 was lower than the detection limit. There is 5 stations outside the mixed triangle, consisting of station nos.01 and 02 were affected from agriculture and natural sources as well as station nos.30, 32 and 65 were affected from natural sources and wastewater. Besides, station nos.26, 28, 35, 48 and 59 were affected from these three sources because they were inside the mixed triangle, except station no.67 was clearly separated from other stations as found in the rainy season, indicating this station are affected from wastewater (Figures 4.66-4.67).
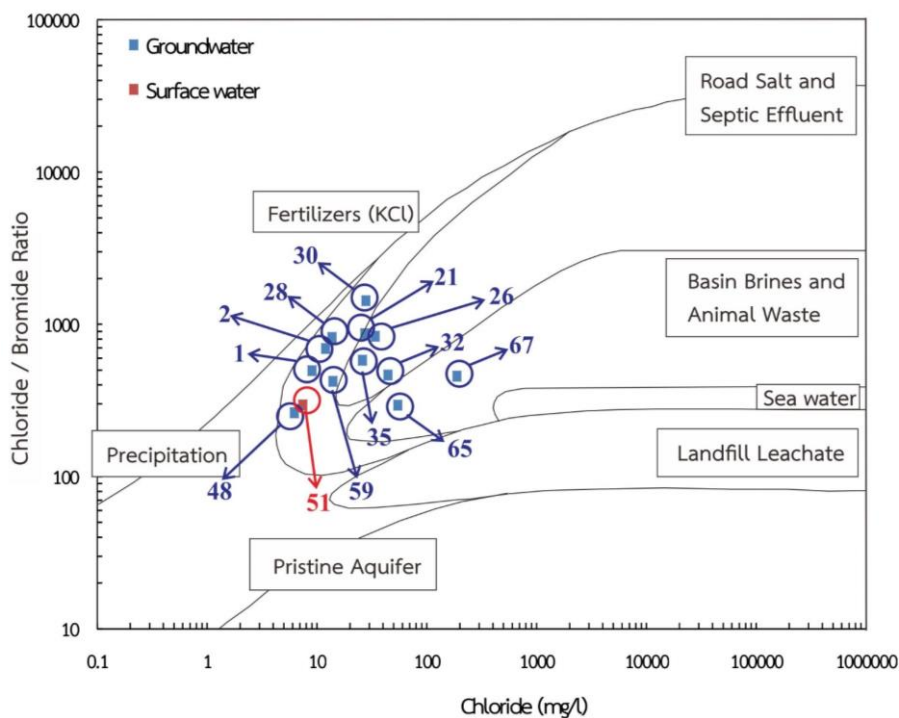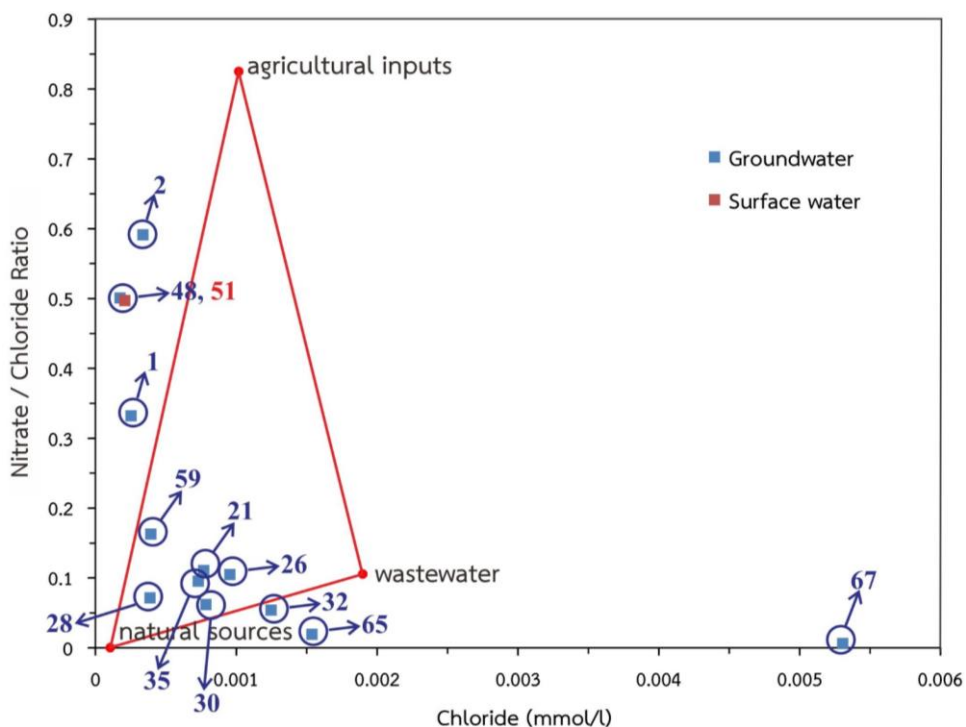
Figure 4.66 NO₃⁻/Cl⁻ ratios and Cl⁻ concentration of groundwater and surface water in the rainy season (modified from Zhang et al., 2015)
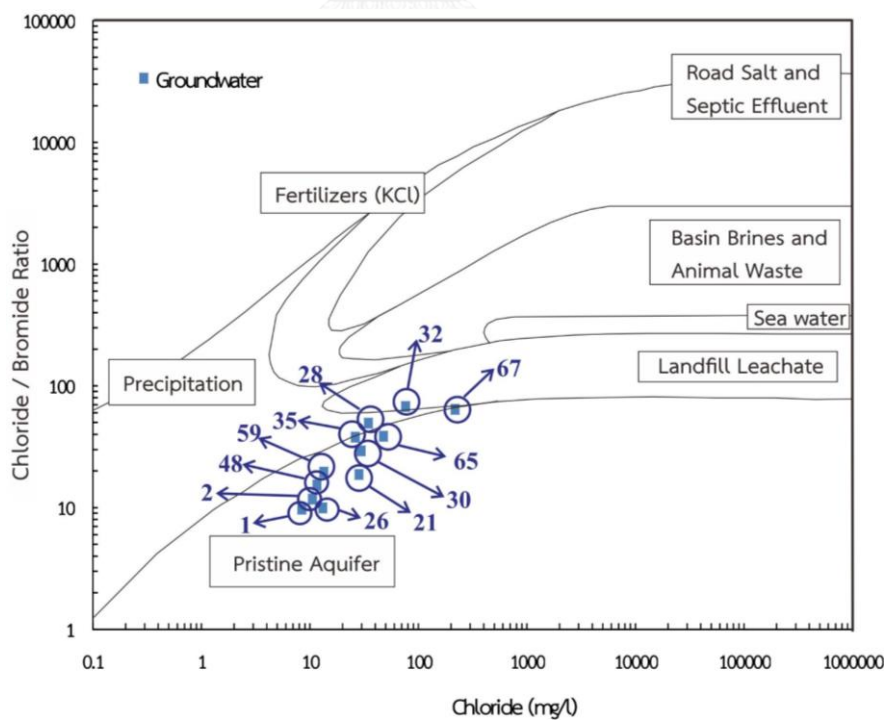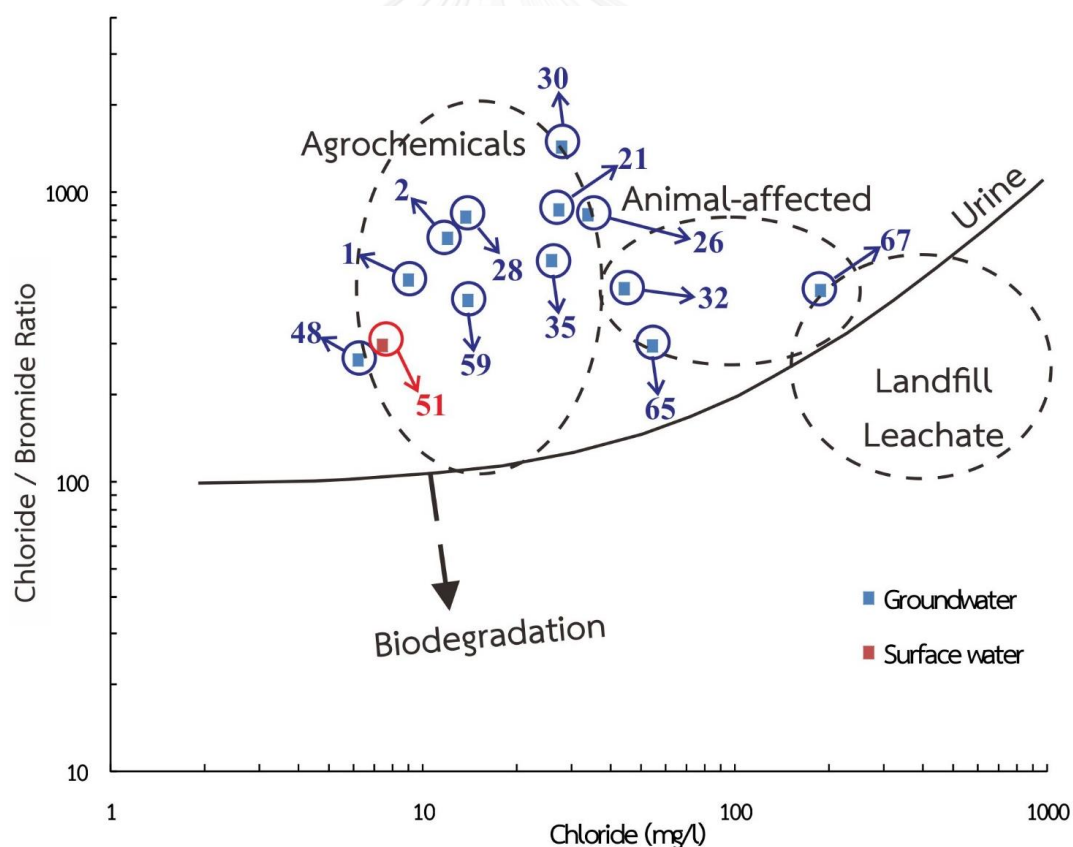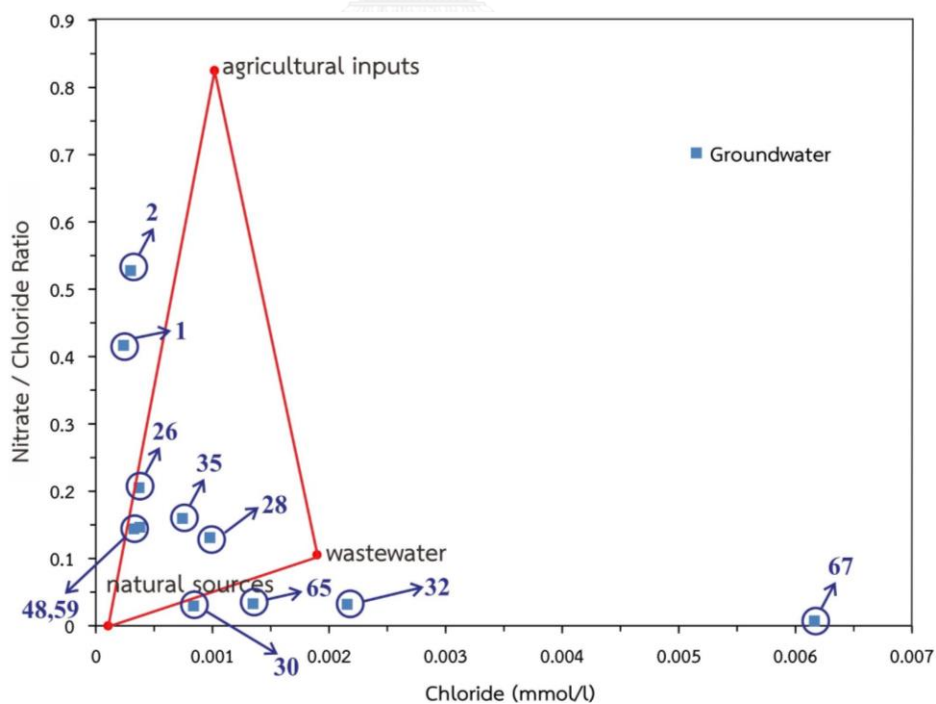

Figure 4.67 NO₃⁻/Cl⁻ ratios and Cl⁻ concentration of groundwater in the summer season (modified from Zhang et al., 2015)

4 .7.4 Causes of different land use types onto NO$_3^-$ contaminated in groundwater

In this part, we would use the geochemical results from the previous section, accounting for information of land use types to help in clearly indicating NO$_3^-$ sources in groundwater. The details in each station were presented as follows:

1) **Station no.01**

From the Gibbs diagram, it can indicate that the groundwater is affected from rock-water interaction in both seasons. According to relationships between Cl$^-$/Br$^-$ ratios and Cl$^-$ concentration of studies of S. V. Panno et al. (2006) and Pasten-Zapata et al. (2014), it could indicate that the groundwater affected from fertilizers or agrochemicals in the rainy season, but in the summer it was affected from the pristine aquifer. Similarly, the relationship between NO$_3^-$/Cl$^-$ ratios and Cl$^-$ concentration modified from Yanpeng Zhang et al. (2015), it indicated that the groundwater was affected from both agriculture and natural sources in both seasons. When considering the location of this station in land use map and from the field survey, this station is in the boundary of deciduous forest and locate near the mountainous areas. So, water may be affected from both natural and anthropogenic sources (see Figure 4.68).

Figure 4.68 A picture showing land use type of station no. 01

2) Station no.02

From the Gibbs diagram, it can indicate that the groundwater is affected from rock-water interaction in both seasons. According to relationships between Cl^-/Br^- ratios and Cl^- concentration of studies of S. V. Panno et al. (2006) and Pasten-Zapata et al. (2014), it could indicate that the groundwater affected from fertilizers or agrochemicals in the rainy season, but in the summer it was affected from the pristine aquifer. Moreover, from the relationship between NO_3^-/Cl^- ratios and Cl- concentration modified from Yanpeng Zhang et al. (2015), it indicated that the groundwater was affected from both agriculture and natural sources in both seasons. When considering the location of this station in land use map and from the field survey, this station is in the boundary of village and locate near paddy field. So, water may be affected from both natural and anthropogenic sources (see Figure 4.69).

Figure 4.69 A picture showing land use type of station no.02

3) Station no.21

From the Gibbs diagram, it can indicate that the groundwater is affected from rock-water interaction in the rainy season and affected from precipitation in the summer season. According to relationships between Cl^-/Br^- ratios and Cl^- concentration of studies of S. V. Panno et al. (2006) and Pasten-Zapata et al. (2014), it could indicate that the groundwater affected from fertilizers or agrochemicals and septic effluent in the rainy season, but in the summer it was affected from the pristine aquifer. Moreover, from the relationship between NO_3^-/Cl^- ratios and Cl^- concentration modified from Yanpeng Zhang et al. (2015), it indicated that the groundwater was affected from both agriculture, wastewater and natural sources in the rainy season. When considering the location of this station in land use map and from the field survey, this station is in the boundary of village and locate in grass of school. So, water may be affected from both natural and anthropogenic sources (see Figure 4.70).

Figure 4.70 A picture showing land use type of station no.21

4) Station no.26

From the Gibbs diagram, it can indicate that the groundwater is affected from rock-water interaction in both seasons. According to relationships between Cl^-/Br^- ratios and Cl^- concentration of studies of S. V. Panno et al. (2006) and Pasten-Zapata et al. (2014), it could indicate that the groundwater affected from septic effluent and agrochemicals in the rainy season, but in the summer it was affected from the pristine aquifer. Moreover, from the relationship between NO_3^-/Cl^- ratios and Cl^- concentration modified from Yanpeng Zhang et al. (2015), it indicated that the groundwater was affected from both agriculture, wastewater and natural sources in both seasons. When considering the location of this station in land use map and from the field survey, this station is in the boundary of village and locate near the house. It is hand pump wells and a condition around the wells not good so a chance that precipitation easy to reach the groundwater So, water may be affected from both natural and anthropogenic sources (see Figure 4.71).

Figure 4.71 A picture showing land use type of station no.26

5) Station no.28

From the Gibbs diagram, it can indicate that the groundwater is affected from rock-water interaction in both seasons. According to relationships between Cl^-/Br^- ratios and Cl^- concentration of studies of S. V. Panno et al. (2006) and Pasten-Zapata et al. (2014),it could indicate that the groundwater affected from fertilizers or agrochemicals in the rainy season, but in the summer it was affected from the precipitation. Moreover, from the relationship between NO_3^-/Cl^- ratios and Cl^- concentration modified from Yanpeng Zhang et al. (2015), it indicated that the groundwater was affected from both agriculture, wastewater and natural sources in both seasons. When considering the location of this station in land use map and from the field survey, this station is in the boundary of village and locate near paddy field. So, water may be affected from both natural and anthropogenic sources (see Figure 4.72).
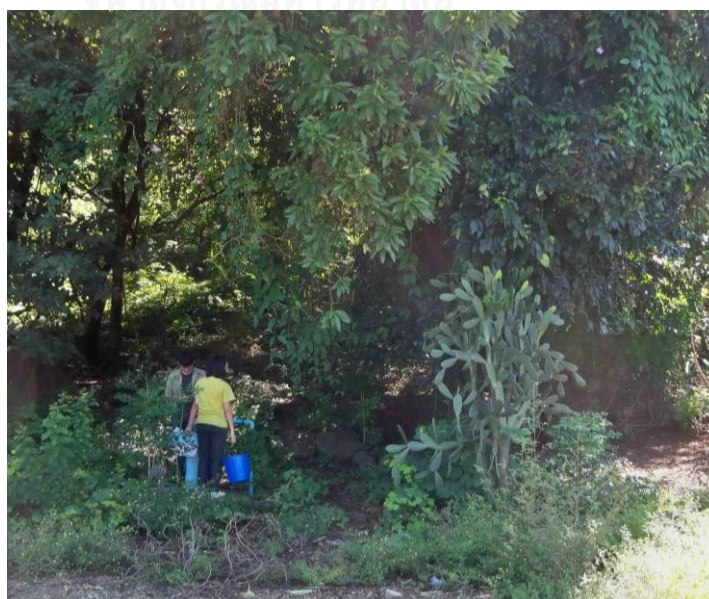

Figure 4.72 A picture showing land use of station no.28

6) Station no.30

From the Gibbs diagram, it can indicate that the groundwater is affected from rock-water interaction in both seasons. According to relationships between Cl^-/Br^- ratios and Cl^- concentration of studies of S. V. Panno et al. (2006) and Pasten-Zapata et al. (2014), it could indicate that the groundwater affected from fertilizers or agrochemicals in the rainy season, but in the summer it was affected from the pristine aquifer. Moreover, from the relationship between NO_3^-/Cl^- ratios and Cl^- concentration modified from Yanpeng Zhang et al. (2015), it indicated that the groundwater was affected from both agriculture, wastewater and natural sources in both seasons. When considering the location of this station in land use map and from the field survey, this station is in the boundary of paddy field and locate in grass of temple. So, water may be affected from both natural and anthropogenic sources (see Figure 4.73).

Figure 4.73 A picture showing land use type of station no.30

7) Station no.32

From the Gibbs diagram, it can indicate that the groundwater is affected from rock-water interaction in both seasons. According to relationships between Cl^-/Br^- ratios and Cl^- concentration of studies of S. V. Panno et al. (2006) and Pasten-Zapata et al. (2014), it could indicate that the groundwater affected from septic effluent and animal affected in the rainy season, but in the summer it was affected from the precipitation and landfill leachate. Moreover, from the relationship between NO_3^-/Cl^- ratios and Cl^- concentration modified from Yanpeng Zhang et al. (2015), it indicated that the groundwater was affected from both wastewater and natural sources in both seasons. When considering the location of this station in land use map and from the field survey, this station is in the boundary of institutional land and locate in the school and near the toilet. So, water may be affected from both natural and anthropogenic sources (see Figure 4.74).

Figure 4.74 A picture showing land use type of station no.32

8) Station no.35

From the Gibbs diagram, it can indicate that the groundwater is affected from rock-water interaction in both seasons. According to relationships between Cl^-/Br^- ratios and Cl^- concentration of studies of S. V. Panno et al. (2006) and Pasten-Zapata et al. (2014), it could indicate that the groundwater affected from septic effluent and agrochemicals in the rainy season, but in the summer it was affected from the precipitation and pristine aquifer. Moreover, from the relationship between NO_3^-/Cl^- ratios and Cl^- concentration modified from Yanpeng Zhang et al. (2015), it indicated that the groundwater was affected from both agriculture, wastewater and natural sources in both seasons. When considering the location of this station in land use map and from the field survey, this station is in the boundary of village and locate in the house. So, water may be affected from both natural and anthropogenic sources (see Figure 4.75).

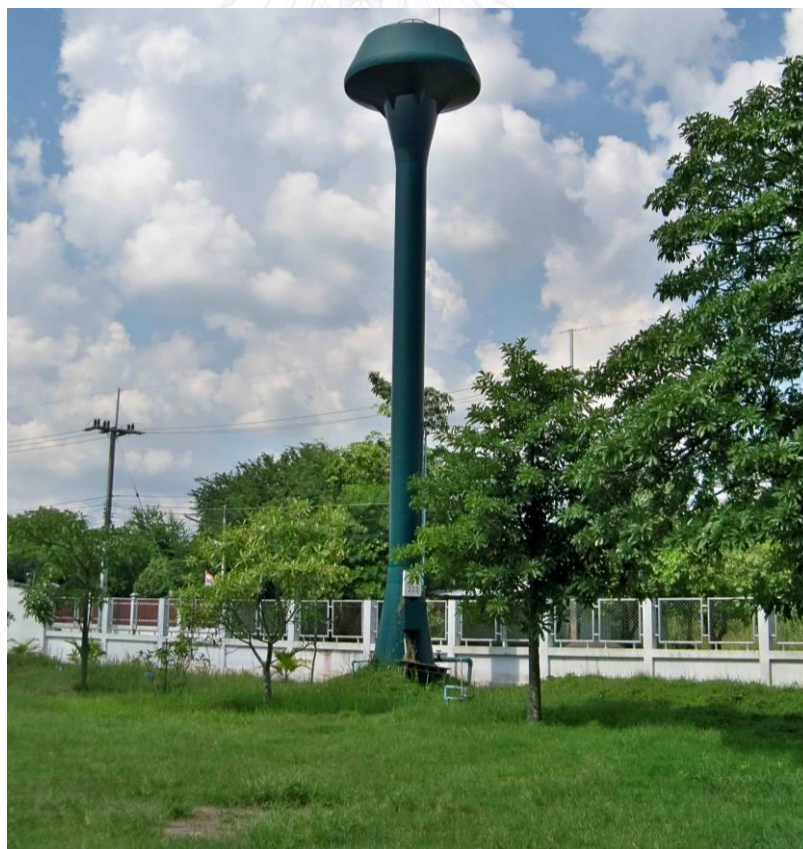**Figure 4.75** A picture showing land use of station 35

9) Station no.48

From the Gibbs diagram, it can indicate that the groundwater is affected from rock-water interaction in both seasons. According to relationships between Cl^-/Br^- ratios and Cl^- concentration of studies of S. V. Panno et al. (2006) and Pasten-Zapata et al. (2014), it could indicate that the groundwater affected from fertilizers or agrochemicals in the rainy season, but in the summer it was affected from the pristine aquifer. Moreover, from the relationship between NO_3^-/Cl^- ratios and Cl^- concentration modified from Yanpeng Zhang et al. (2015), it indicated that the groundwater was affected from both agriculture and natural sources in the rainy season, but in the summer it was affected from agriculture, wastewater and natural sources. When considering the location of this station in land use map and from the field survey, this station is in the boundary of village and locate in the palm area. So, water may be affected from both natural and anthropogenic sources (see Figure 4.76).

Figure 4.76 A picture showing land use of station 48

10) Station no.59

From the Gibbs diagram, it can indicate that the groundwater is affected from rock-water interaction in both seasons. According to relationships between Cl^-/Br^- ratios and Cl^- concentration of studies of S. V. Panno et al. (2006) and Pasten-Zapata et al. (2014), it could indicate that the groundwater affected from fertilizers or agrochemicals in the rainy season, but in the summer it was affected from the pristine aquifer. Moreover, from the relationship between NO_3^-/Cl^- ratios and Cl^- concentration modified from Yanpeng Zhang et al. (2015), it indicated that the groundwater was affected from both agriculture, wastewater and natural sources in both seasons. When considering the location of this station in land use map and from the field survey, this station is in the boundary of village and locate in the house. So, water may be affected from both natural and anthropogenic sources (see Figure 4.77).

Figure 4.77 A picture showing land use of station 59

11) Station no.65

From the Gibbs diagram, it can indicate that the groundwater is affected from rock-water interaction in both seasons. According to relationships between Cl^-/Br^- ratios and Cl^- concentration of studies of S. V. Panno et al. (2006) and Pasten-Zapata et al. (2014), it could indicate that the groundwater affected from animal waste in the rainy season, but in the summer it was affected from the pristine aquifer. Moreover, from the relationship between NO_3^-/Cl^- ratios and Cl^- concentration modified from Yanpeng Zhang et al. (2015), it indicated that the groundwater was affected from both wastewater and natural sources in both seasons. When considering the location of this station in land use map and from the field survey, this station is in the boundary of factory and locate in the chicken farm. So, water may be affected from both natural and anthropogenic sources (see Figure 4.78).

Figure 4.78 A picture showing land use of station 65

12) Station no.67

From the Gibbs diagram, it can indicate that the groundwater is affected from rock-water interaction in both seasons. According to relationships between Cl^-/Br^- ratios and Cl^- concentration of studies of S. V. Panno et al. (2006) and Pasten-Zapata et al. (2014), it could indicate that the groundwater affected from animal waste and landfill leachate in the rainy season, but in the summer it was affected from the precipitation, landfill leachate and pristine aquifer. Moreover, from the relationship between NO_3^-/Cl^- ratios and Cl^- concentration modified from Yanpeng Zhang et al. (2015), it indicated that the groundwater was affected from both agriculture, wastewater and natural sources in both seasons. When considering the location of this station in land use map and from the field survey, this station is in the boundary of mixed orchard and locate in the house. So, water may be affected from both natural and anthropogenic sources (see Figure 4.79).

Figure 4.79 A picture showing land use of station 67

13) Station no.51

From the Gibbs diagram, it can indicate that the surface water is affected from rock-water interaction in the rainy season. According to relationships between Cl^-/Br^- ratios and Cl^- concentration of studies of S. V. Panno et al. (2006) and Pasten-Zapata et al. (2014),it could indicate that the surface water affected from fertilizers or agrochemicals in the rainy season. Moreover, from the relationship between NO_3^-/Cl^- ratios and Cl^- concentration modified from Yanpeng Zhang et al. (2015), it indicated that the surface water was affected from both agriculture and natural sources in both seasons. When considering the location of this station in land use map and from the field survey, this station is in the boundary of scrub and locate near upstream area. So, water may be affected from both natural and anthropogenic sources (see Figure 4.80).

Figure 4.80 A picture showing land use of station 51

Table 4.11 The summary NO_3^- sources in groundwater.

Station	Sources			
	rock-water interaction	**precipitation**	**fertilizer**	**wastewater**
1	✓			
2	✓	✓	✓	
21	✓		✓	✓
26	✓	✓		✓
28	✓		✓	✓
30	✓		✓	✓
32	✓			✓
35	✓			✓
48	✓		✓	
59	✓			✓
65	✓			✓
67	✓	✓		✓
51	✓	✓	✓	

4.8 The mechanism changes NO_3^- concentration

In this research we studied the mechanism that effect to a changes in NO_3^- concentration. We necessary to using NO_3^- concentration together with groundwater flow direction to explain the process that occur in our area.

4.8.1 The deuterium and oxygen isotope

From the chapter 2, we mentioned about the oxygen isotope which it was used to study the hydrologic system, by often in combination with deuterium isotope. In this research we used these isotope for study about interaction between surface water and groundwater moreover it used to study evaporation process. As a molecule of water consists of oxygen and hydrogen, the isotope ratio of oxygen ($\delta^{18}O$) and hydrogen (δD) can be used to trace a source of groundwater, since the ratios of $\delta^{18}O$ and δD in sea

water, glaciers, water vapor, precipitation and run-off are different, depending on vapor pressure, humidity, altitude, temperature and evaporation (Gonfiantini, Roche, Olivry, Fontes, & Zuppi, 2001; IAEA, 2006; Kamdee et al., 2011; Kamdee et al., 2013; Katsuyama, Yoshioka, & Konohira, 2015; J.-E. Lee & Fung, 2008; Noipow, 2015; Nunak & Suesut, 2012; Peng, Mayer, Harris, & Krouse, 2004; Tang et al., 2015). This information can help characterize a groundwater system and estimate the long-term usage of groundwater consumption so it will not exceed groundwater inflow and can protect the recharge areas from potential sources of contamination (Wisittammasri & Chotpanrat, 2015). The analysis results of water samples were compared with the mean stable isotope compositions (δD, $\delta^{18}O$) in rainfall of the Bangkok station, known as "Bangkok Local Meteoric Water Line (BKK LMWL)", which was created from a long-term dataset and collected by The Global Network for Isotopes in Precipitation (GNIP, 4845500) (data from the International Atomic Energy Agency (IAEA, 2006) and are shown in Figure 4.81.

As a result, the linear relationship between δD and $\delta^{18}O$ could be analyzed using the following equation: $\delta D = 7.329 \, \delta^{18}O + 5.1652$, for comparison of isotope characteristics of water samples in this study. According to the stable isotope data of rainfall in the study area, it was found that the local meteoric water line (LMWL) relatively resembled the BKK LMWL and could be expressed by the following equation: $\delta D = 7.1755 \, \delta^{18}O + 3.4789$ as shown in Figure 4.82. Since the study area is located in central Thailand, approx. 107 km away from Bangkok, climatic conditions are relatively similar. However, the slope of LMWL was slightly lower, showing that rainfall came from a vapor source with a slightly high humidity (Breitenbach et al., 2010; Peng et al., 2004). Moreover, the isotope characteristics mainly showed an increase in delta values, reflecting warmer weather and lower altitude as a result of the initial period of rainfall or pre-monsoon period (Kamdee et al., 2011). The $\delta^{18}O$ and δD ranged from -7.83‰ to -4.59‰ and -54.18‰ to -30.00‰ with average values of -6.50+1.12‰ and -43.17+8.19‰, respectively.
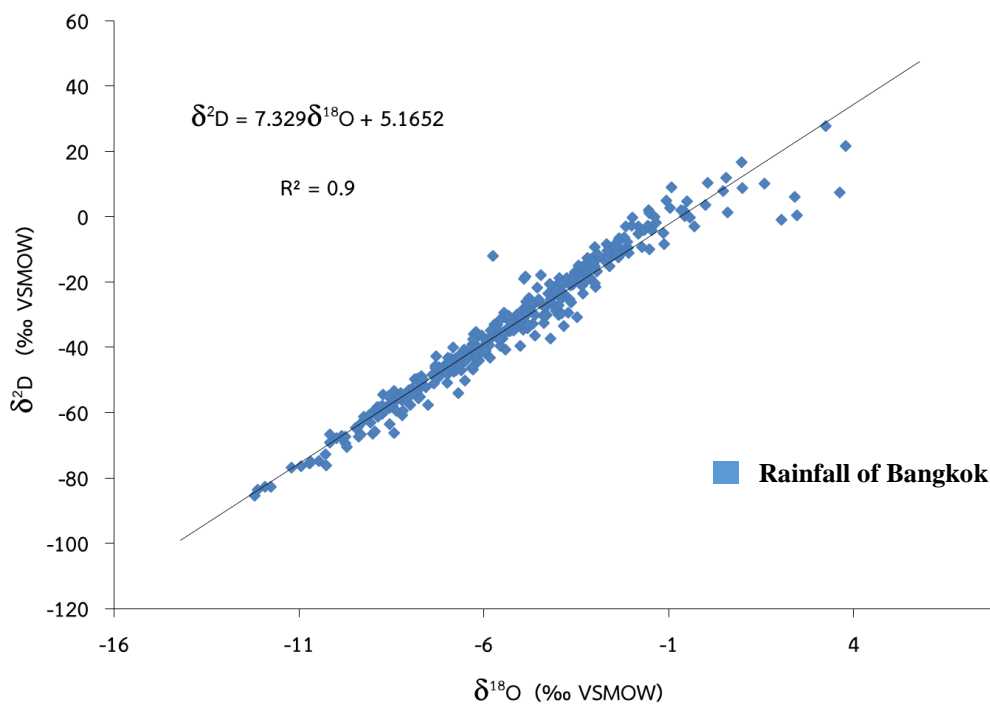
Figure 4.81 Plots of δD and δ^{18}O of rainfall of BKK LMWL during 1968-2009.

(IAEA, 2006)
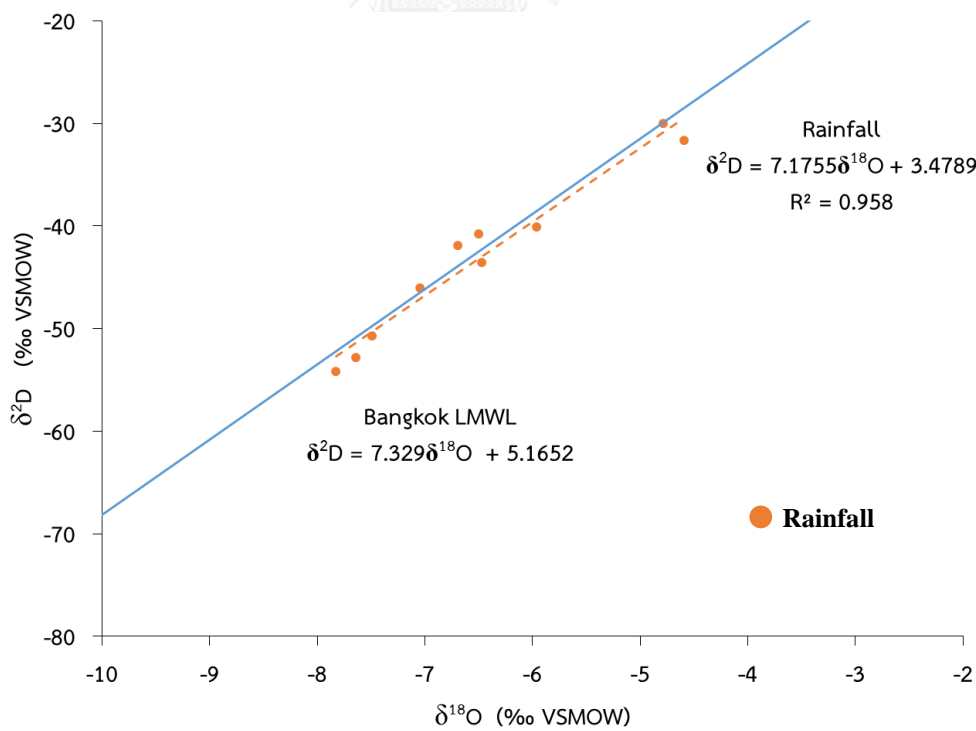
Figure 4.82 Plots of δD and δ^{18}O of rainfall of LMWL in 2014 compared with BKK

LMWL

The $\delta^{18}O$ and δD of the surface water samples ranged from -7.49‰ to -4.71‰ and -49.13‰ to -37.50‰ with average values of -6.34+0.77‰ and -43.07+3.67‰, respectively. When comparing the stable isotope data of surface water with the BKK LMWL, it was found that the relationship between δD and $\delta^{18}O$ of surface water in the area was relatively different from that of BKK LMWL. The regression line of surface water deviated from the BKK LMWL and intercepted with the BKK LMWL at δD of -46‰. Since the surface water is directly exposed to the atmosphere, when rain falls onto surface water with low relative humidity and high temperature, it will evaporate quickly, resulting in a different fractionation of isotope composition from the BKK LMWL. A linear regression analysis of surface water as shown in the following equation: $\delta D = 4.2485\, \delta^{18}O - 15.935$ had a slope of evaporation line that ranged between 4 and 5, expressing moderate relative humidity (25%-75%) (Clark & Fritz, 1997). Furthermore, the samples from ST43, ST51 and ST53 were plotted on the slope of BKK LMWL, indicating that these samples were in a high altitude area where the water did not evaporate.

The intercept point (see Fig.4.83) could specify the approximate position of average annual rainfall, which could preliminarily be separated between high and low altitude (USGS, 2004). The $\delta^{18}O$ and δD of the groundwater samples ranged from -7.34‰ to -5.30‰ and -48.04‰ to -37.55‰ with average values of -6.61+0.45‰ and -44.33+2.37‰, respectively. According to the isotopic compositions of groundwater, the hydrogen and oxygen isotope compositions in some groundwater samples corresponded well to those of the BKK LMWL (Group 1), accounting for 63.63% of all groundwater samples. This could be possible because the stations are located in recharge areas that receive rainfall directly. However, most groundwater samples were agglomerated, while only 4 stations, ST01, ST05, ST62 and ST67, presented low delta values, indicating that these stations were probably located at low altitude or where there was mixing with rainfall in the summer season, when weather is warmer (Figure 4.85) (SAHRA, 2005). The remaining 11 groundwater samples (Group 2) were distributed along the evaporation line. These samples could have been recharged from surface water or interacted with surface water (Clark & Fritz, 1997). In other words, these areas did not receive recharge water directly from rainfall (Figure 4.83).

The groundwater wells (Group 1) received rainfall directly that was distributed over the study area. It was found that the eastern area, a high plain where most groundwater wells are located, could be recharge areas for a confined aquifer while the central area, a floodplain, is where most groundwater wells are located in a shallow aquifer. The groundwater wells (Group 2), which interact with surface water, are mainly distributed in the central and western plains. Thus, it should be a vital concern as to whether the area is used properly because contaminated surface water can be infiltrate and contaminate groundwater resources. The recharge area is delineated by isotope data of Group 1 along with fault zones. When considering with the fault and fracture zones, they generally increases secondary porosity and permeability in hard rock, resulting in rainfall can infiltrate quickly into aquifers underneath. (Figure 4.85)
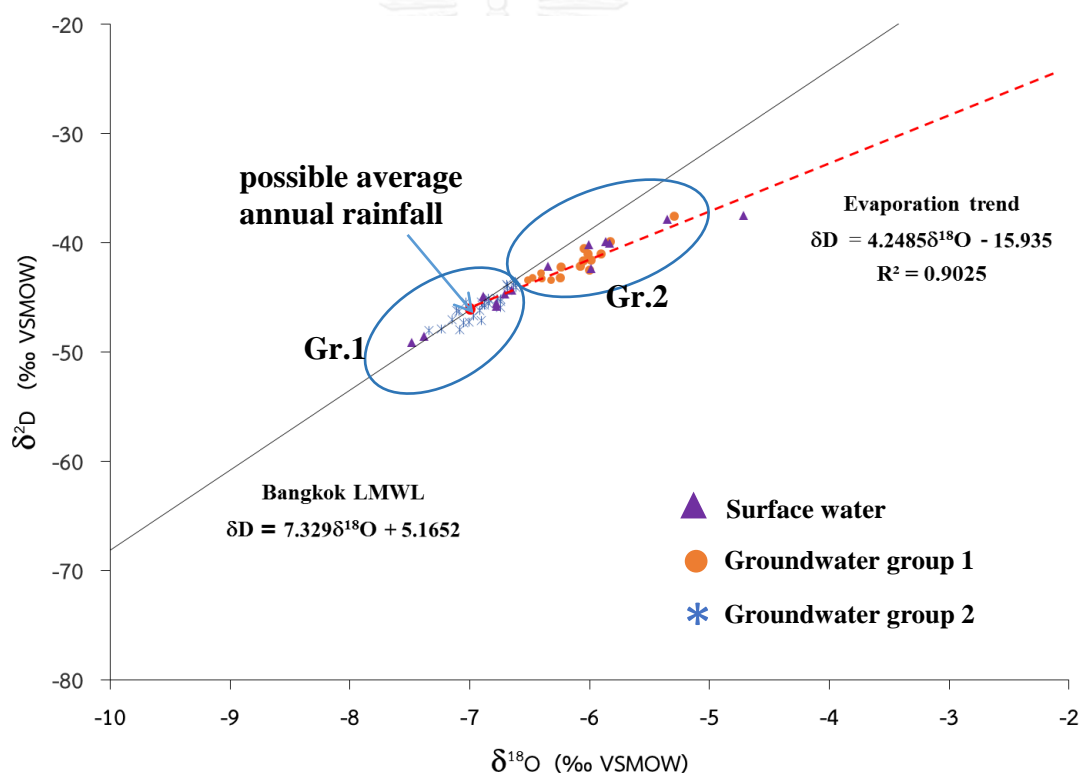
Figure 4.83 Plot of δD and δ^{18}O of surface water and groundwater compared with BKK LMWL
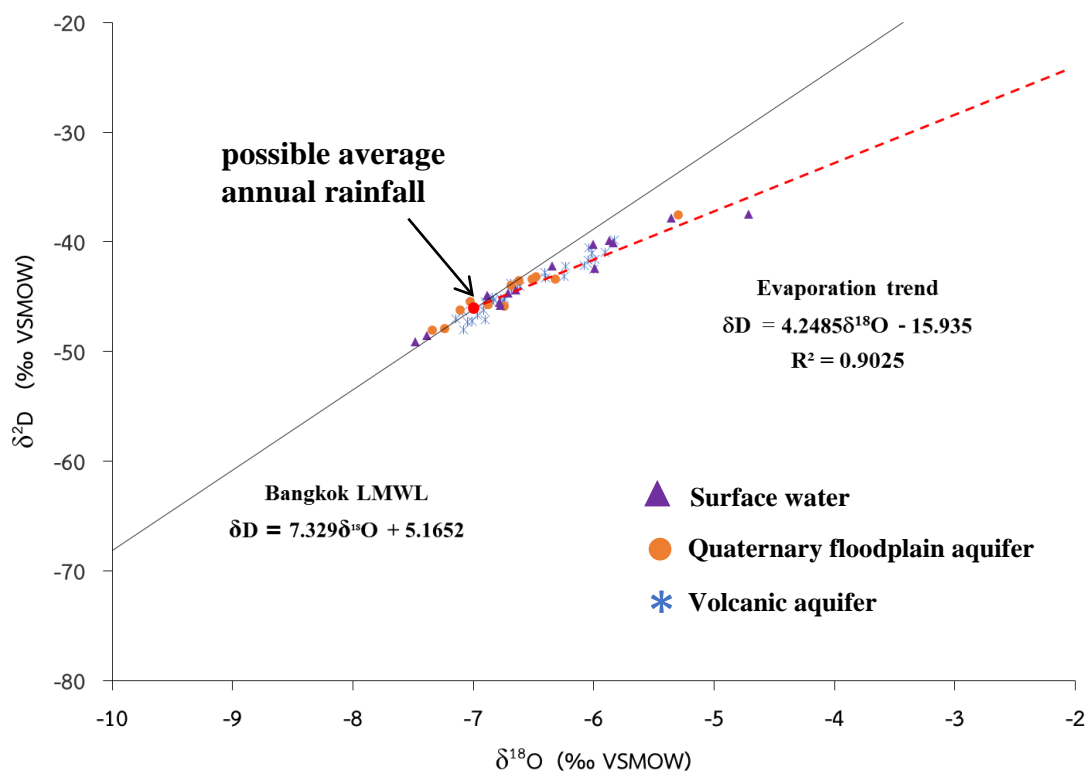
Figure 4.84 Plot of δD and δ^{18}O of groundwater in Quaternary flood plain aquifer and volcanic aquifer compared with BKK LMWL

In figure 4.84, show the groundwater in Quaternary flood plain aquifer and volcanic aquifer were plotted compare with BKK LMWL and evaporation trend. It found that 22 stations of groundwater in volcanic aquifer that are in line of BKK LMWL, accounted for 50% of all data and 10 stations are along evaporation trend, accounted for 22.72% of all data. It means the groundwater in these aquifer has been filled by rainfall which in some area are a deep aquifer so the groundwater was added slowly and cause evaporation occur. In other words, the groundwater is old. In addition, a 11 stations of groundwater in floodplain aquifer are along line of BKK LMWL, accounted for 25% of all data except station no 23 was along evaporation trend, accounted for 2.27 % of all data. Which the depth of wells is shallow, these are lead to easily contamination in groundwater.

Aforementioned, it was found that the station affected from evaporation process are 11 stations consist of station 19, 21, 22, 23, 27, 28, 32, 44, 59, 63 and 65. In other words, these stations may have an interaction with surface water. This information is

an additional choice to help explanation about mechanism. In addition, it has 5 stations including station 03, 15, 17, 26 and 35. This does not clearly separate from Bangkok Local Meteoric Water Line (BKK LMWL) and evaporation trend. So this groundwater may be recharged from rainfall in lower altitude or it may be interacted with surface water. The amount of samples received rainfall directly are 63.64 percent of all samples. The samples which interacted with surface water or corresponded evaporation trend account for 25 percent of all samples and the samples which interacted with surface water or received rainfall in low altitude account for 11.36 percent of all samples. In Figure 4.85, a positions of station scatter around the river. Thus this is not a surprise if it interacts with the surface water, especially at station 23, the same place to station 24. Distances of station 44, 59, 63 and 65 to river are shorter than other station. Furthermore, we separated preliminary aquifer types in a case of non-measured depth.
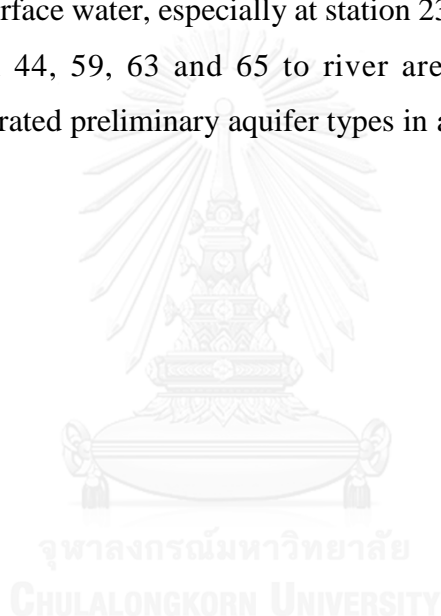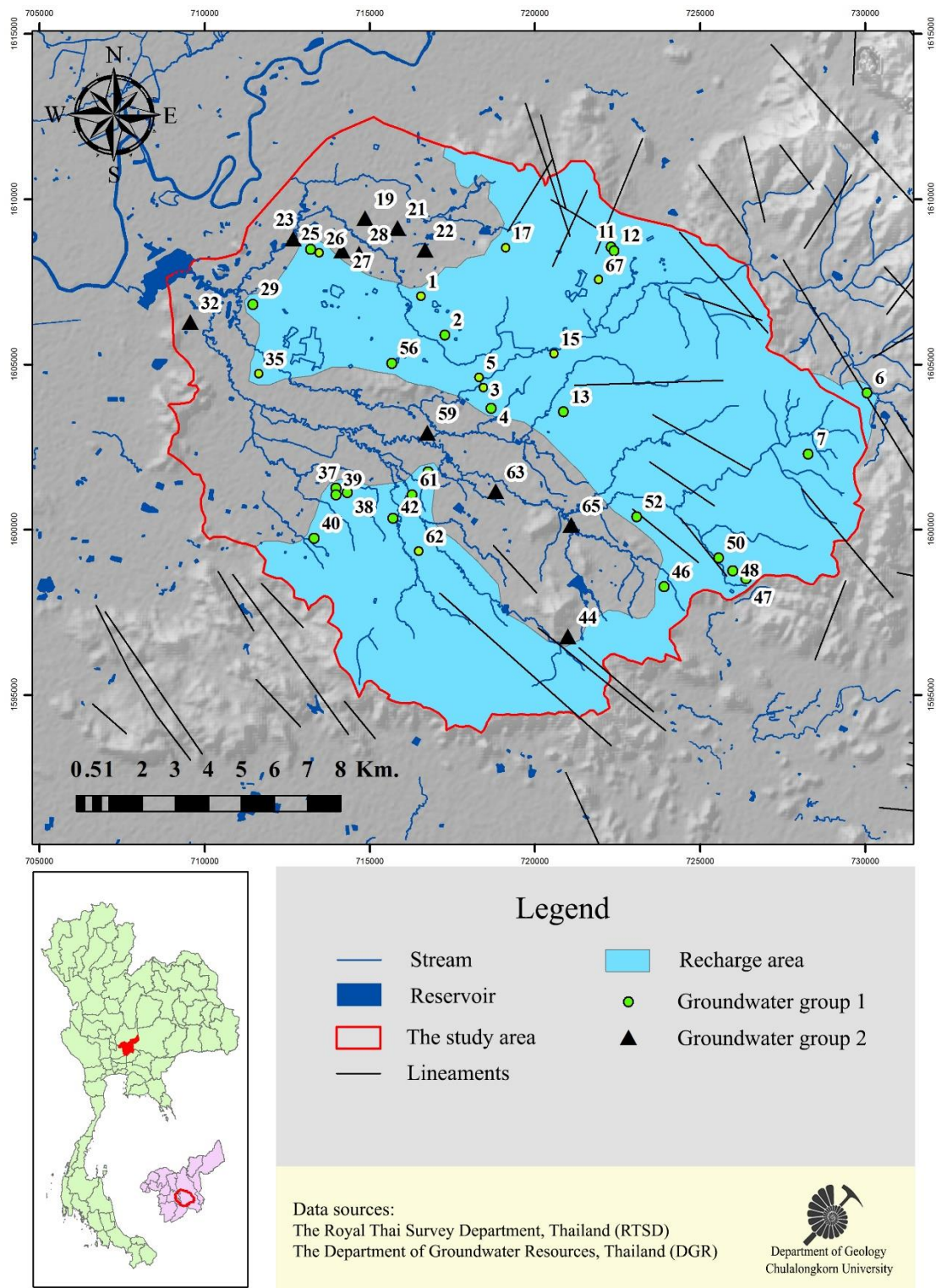
Figure 4.85 Map of recharge area

4.8.2 High NO₃⁻ concentration zone

A subtitle 4.5 mentions the distribution of NO_3^- concentration and the distribution of concentration map in rainy season and summer, as shown in figure 4.48-4.49. After that, two maps were compared and found that the northwest area is interesting for studying mechanism in the study area. (Figure 4.86)
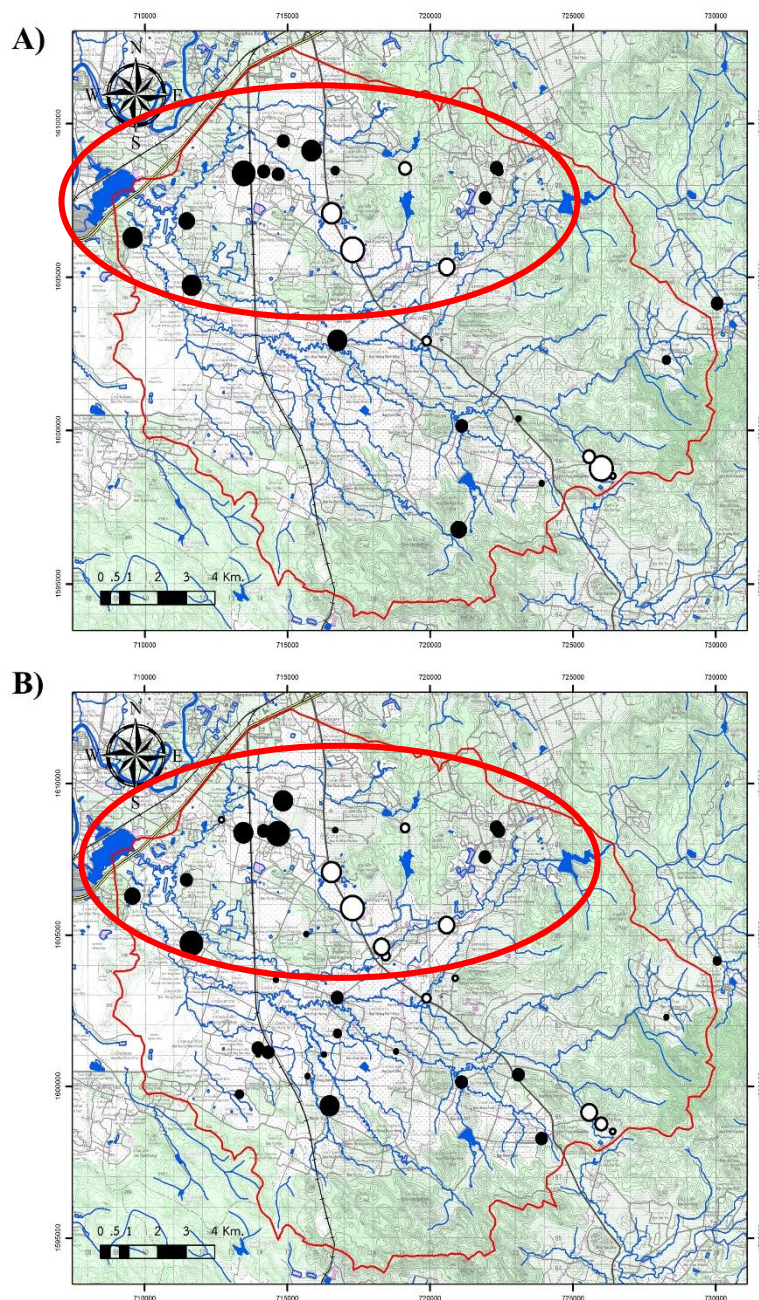
Figure 4.86 The pictures compare NO_3^- concentration map in both seasons. (A) The NO_3^- concentration in rainy season. (B) The NO_3^- concentration in summer

From the chapter 2, ammonification and nitrification are important processes which make the NO_3^- concentration increases and denitrification process reduces NO_3^- concentration. Ammonification and nitrification occur in aerobic condition while denitrification occurs in anaerobic condition. So DO is important to investigate these process. Tan, Ma, Li, Qiu, and Li (2013) offered DO to be a critical factor in nitrification process while denitrification is inhibited under the same conditions. The nitrogen removal was achieved at the DO of 0.5 to 1.0 mg/l because denitrification occurs by anaerobic bacteria. So the presence of oxygen may lead to microorganisms shock and their activities decrease. Pasten-Zapata et al. (2014), their chemical data indicated that denitrification is not a presence when he DO >1 mg/l. Nitrification process rapidly decreased when the concentration of oxygen is about 0.3 mg/l. Y. Zhang et al. (2014) indicated a strong denitrification signal in June and DO concentrations are low that supports the occurrence of denitrification. Lambert, Nwaokoro, and Russo (2004) said that oxygen in liquid is less than 0.5 to 2 mg/l. Which indicates that the anaerobic situation and denitrification would occur after NO_3^- is converted to NO_2^- and finally to gaseous nitrogen. Redox potential or Oxidation-Reduction Potential (ORP) was measured for forecasting the electron activity in environment that comprises of two parts, oxidation potential and reduction potential. If a value shows the negative, it represents reduction reaction. And if a value shows the positive, it represents oxidation reaction. Biological processes are affected by this value so the ORP is a useful tool for indicating of biological processes. P. G. Lee et al. (2000) indicated that the denitrification redound to oxidation-reduction potential is a negative range, approximately -50 to -300 mV. Yoon (2016) noted that, at DO lower than 1 mg/l, nitrification slows down, and at below 0.5 mg/l, nitrification nearly stops and denitrification starts to occur. Dissolved oxygen was used as electron acceptor of microorganism until ORP decreases to +50 mV. Nitrate is replaced the molecular of oxygen. When ORP decreased about -50mV, sulfate was used as electron acceptor. So denitrification can occur at ORP between +50 to -50 mV, but in some a situation may be between -100 to 100 mV. Moreover, denitrification varies depending on water chemistry especially pH and dissolved oxygen. Ammonification, nitrification and denitrification occur by biological activity. The ammonification and nitrification are

about oxidation reaction because they occur in aerobic condition, while denitrification are about reduction reaction and it occurs in anaerobic condition.

For a studying of mechanism which affects to NO_3^- concentration, summer was only be considered because DO was not measured in rainy season due to the problem about instruments. As mentioned in topic 4.2 Ion Charge Balance, seven stations including 03, 05, 37, 39, 58, 60 and 63 have error of ion balance more than 10 percent and this cause may be a result of alkalinity (Anderson & Wedborg, 1983). In this case, many parameters for observing the mechanism are changeable. Only parameters derived from reliable tools in the field were used. Two parameters consist of dissolved oxygen and redox potential (ORP) were chosen to discuss about the processes that possibly occur in the area. Referred from above criteria, denitrification has DO in range from 0.5 to 2 mg/l. If the area has a concentration more than 2 mg/l, nitrification may occur. Oxidation-reduction potential is in range from +50 to -300 mV which encourage an occurrence of denitrification. There are seven stations that DO is in range from 0.5 to 2 mg/l, and five stations which redox potential is in range from +50 to -300 mV. When considered together, it was found that four stations may be affected from denitrification. An each station relatively spread in the area so we cannot consider all station together with the flow direction. Therefore, Eh-pH diagram was used for identifying species of nitrogen in groundwater (Figure 4.87). Eh-pH diagram are also known as Pourbaix Diagrams. These diagrams show stability areas of several species of element in an aqueous solution. Stability areas are function of redox potential and pH. Dot lines appeared in diagram both upper and lower show stability limits of water. A diagram for nitrogen is separated to 4 groups including nitrate (NO_3^-), molecule of nitrogen (N_2), ammonium (NH_4^+) and ammonia (NH_3) (Roine & Anttila, 2006). After four points were plotted into Eh-pH diagram, it was found that station 06 and 37 fall in zone of molecule of nitrogen, and station 07 and 11 fall in a zone of NH_4^+. Denitrification and ammonification were predicted to occur in these stations because molecule of nitrogen is produced during the reduction reaction of NO_3^-, and NH_4^+ is produced during the degradation of amino acid or protein in carcass becoming to ammonia. The redox potential of station 07 and 11 are -145.3 and -152.5 mV

respectively and denitrification is not in these stations. So, redox potential is less than -100 mV. Nitrate is not an electron acceptor (Yoon, 2016).
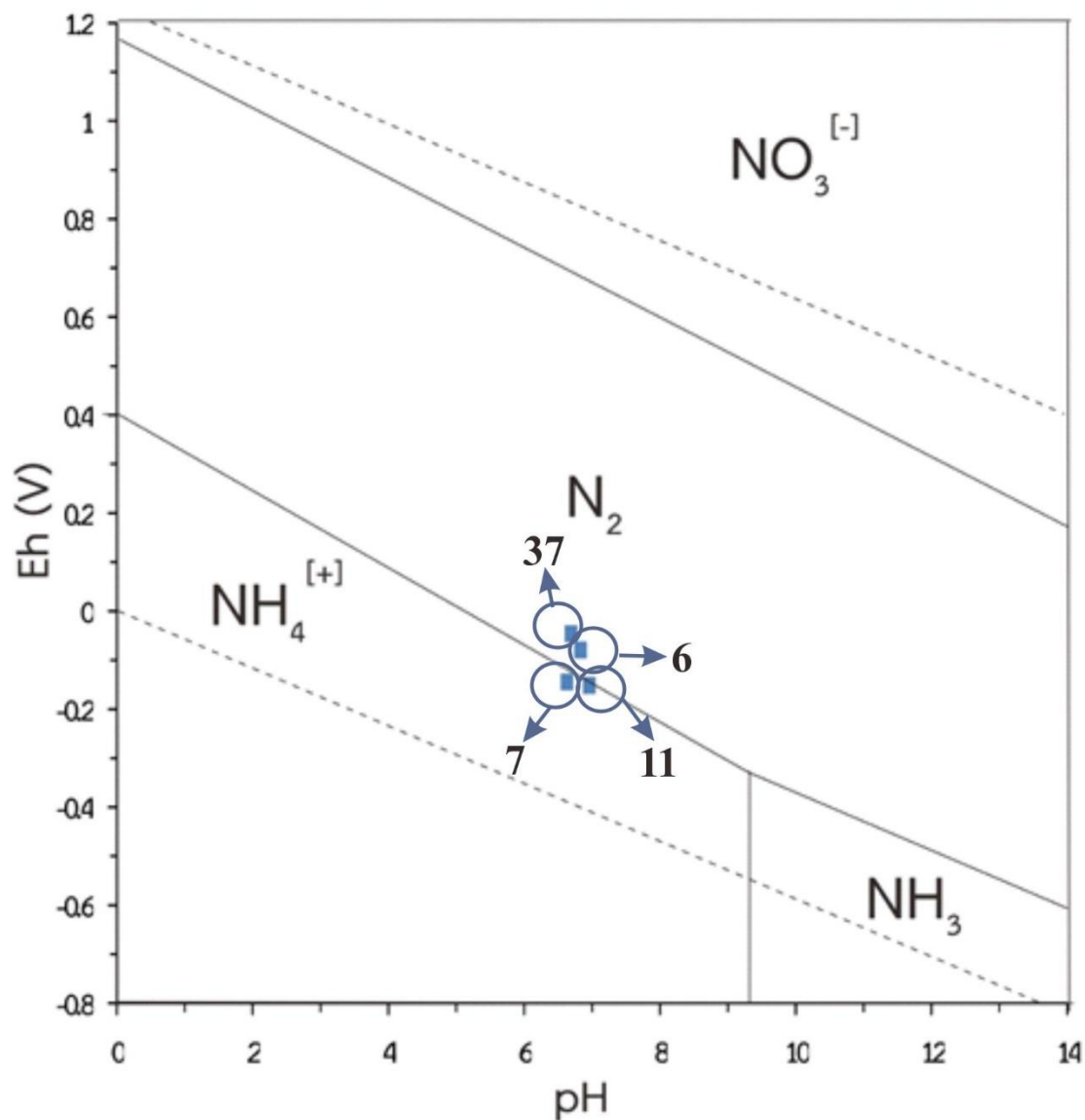
Figure 4.87 The Eh-pH diagram of station 06, 07, 11 and 37
(modified from Takeno, 2005)

Cross section lines were draw in this zone including, A-A', B-B' and C-C'. A length of A-A' is approximately 10 to 11 kilometers. Stations in a cross section line have nine stations including station 32, 29, 23, 25, 26, 27, 28, 22 and 17 (sorting from west to east). Station 25 is ignored because NO_3^- concentration is lower than detection limit in rainy season and the sample in summer season was lost. Moreover, position of station 19 and 21 were projected in cross section line. These data was added to explain

mechanism appear in the area. Section B-B' has a length approximately 14 to 15 kilometers. Seven stations in cross-section line are station 32, 35, 56, 59, 3, 15 and 67 (sorting from west to east). Section C-C' has a length approximately 13 to 14 kilometers. Ten stations including station 32, 35, 58, 37, 38, 59, 60, 62, 63 and 65 (sorting from west to east) were projected in cross section line. A hill was found on the east of cross section line and a plain is on the west of cross section line. Referred to the water level of groundwater, it indicates that flow direction from east to west corresponds to topography (Figure 4.88).
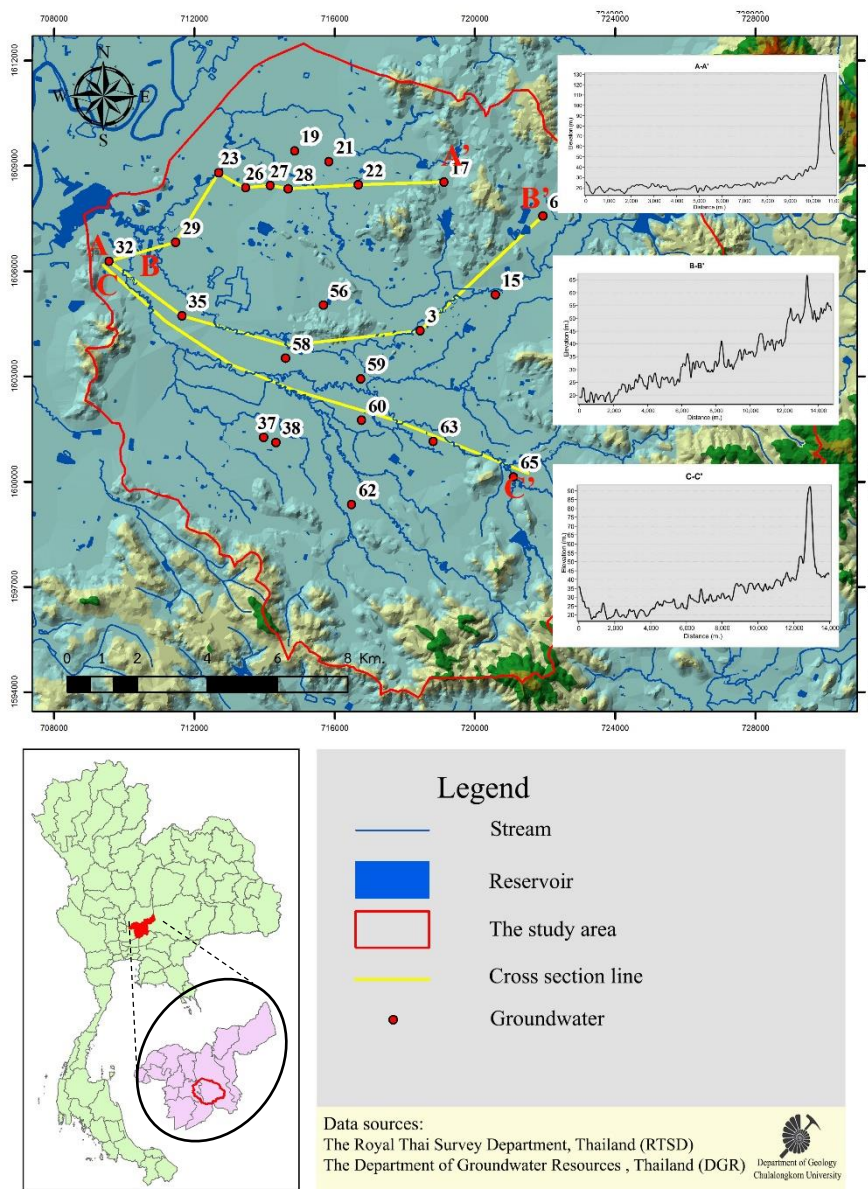
Figure 4.88 Cross section lines in the area

As mentioned above, the mechanism was only determined in a point. So, cross-section line was created to understand mechanism in a local scale. Parameters used for analyzing consist of DO and pH. Aquifer types have to be classified before analysis. Hosono et al. (2013) compared NO_3^- concentration and DO and indicated that if DO rapidly decreases while NO_3^- concentration rapidly increase, i.e. a signal of denitrification. Mohamed et al. (2003) observed a changeable of NO_3^- and pH along the flow direction and identified that the pH increase associated with decrease of NO_3^-, i.e. a signal of denitrification. This is same as a study of Ndegwa, Wang, and Vaddella (2007). They showed that pH is a good indication of biological processes from a decreasing of pH in nitrification. It is an indicative of nitrification processes.

Figure 4.89 shows, a comparison between DO and NO_3^- concentration in all cross section line which interpret referred to a study of Hosono et al. (2013). Mentioned that if Do rapidly decreases while NO_3^- concentration rapidly increases, denitrification must occur, and on the other hand if DO rapidly increases while NO_3^- concentration rapidly decreases, nitrification must occur. At a range of station 29-32 and station 67-15, nitrification must occur in these zones. Highlight in graph is a range that NO_3^- concentration decreases and corresponds with DO increasing which does not mention about denitrification, i.e. about dilution process. In addition, when stable isotope was considered, stations with more than half of sample using in cross-section line are interacted with surface water, i.e. an evidence of dilution. At station 37, DO rapidly decreased. This supports to the idea that NO_3^- concentration was affected from denitrification.
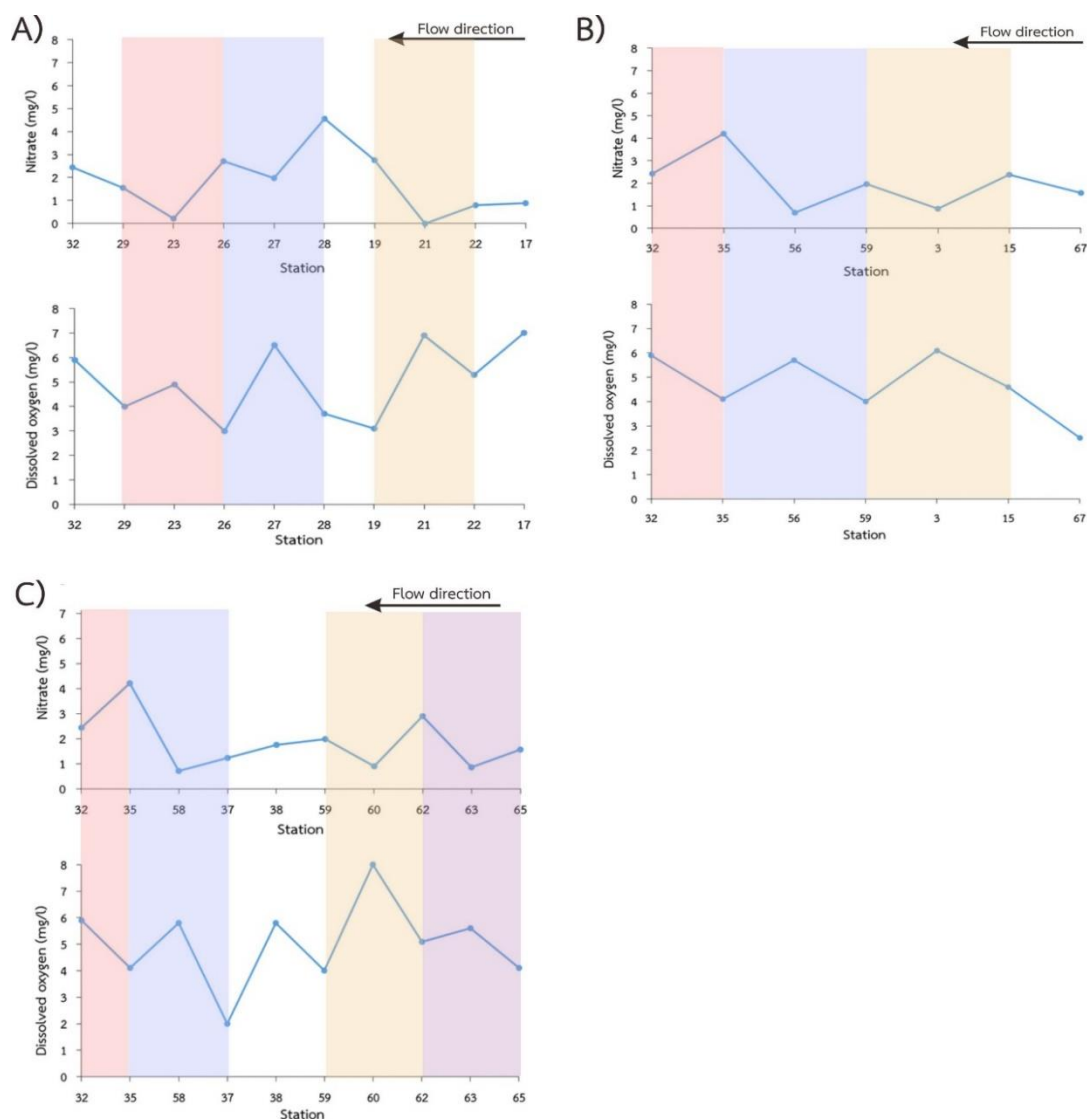
Figure 4.89 Comparison between NO$_3^-$ and DO with cross section line of (A) A-A',
(B) B-B', (C) C-C'

In figure 4.90, a decreasing of pH indicates the nitrification process. Because pH is a positive potential of the hydrogen ion, so it shows the concentration of hydrogen ion. The nitrification process release hydrogen ion during the reaction while the denitrification release hydroxide ion during the reaction (a carbon is electron donor) (Robertson & Groffman, 2007).

The pH in A-A' section is relatively constant than B-B' section and C-C' section respectively. When all of cross–section line was considered, it was found that nitrification process in this area is confirmed by the water analysis result which appears

inorganic form of nitrogen such as NO_3^-, NO_2^- and NH_4^+ which it means that ammonification occurs in this area. However, some range of cross section line was found that pH and NO_3^- increase together and a fluctuation of pH was affected from the other ions. In section C-C', NO_3^- concentration of station 35 is high and pH does not appear trend of nitrification so NO_3^- may come from the sources. And station 37 does not appear nitrification trend. These help to confirm the denitrification.
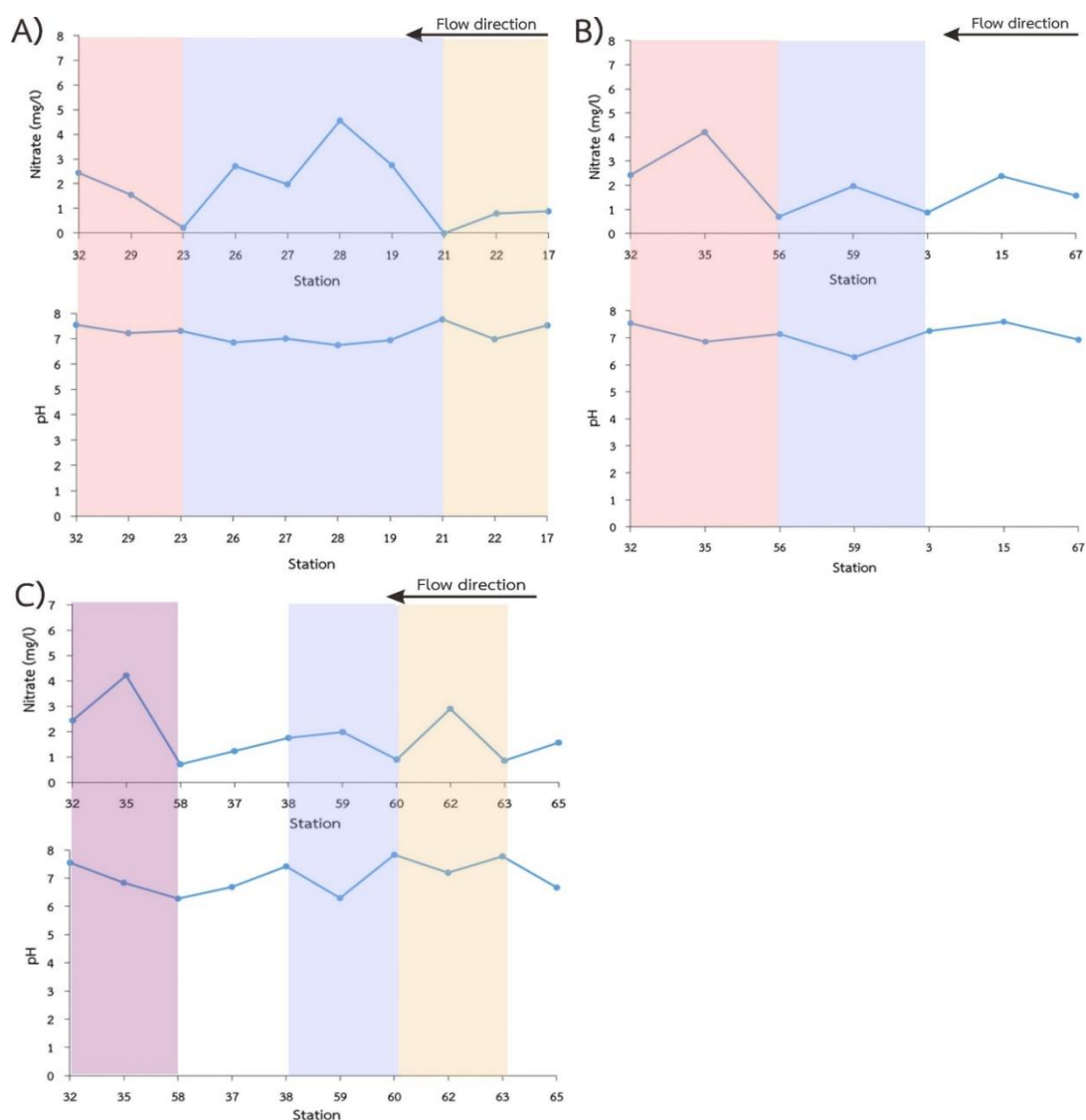
Figure 4.90 Comparison between NO_3^- and pH with cross section line of (A) A-A',
(B) B-B', (C) C-C'

CHAPTER V
CONCLUSIONS AND RECOMMENDATIONS

5.1 Conclusions

5.1.1 General information from field investigation

Topography of the study area is mountainous areas in the east and plains in the west with elevation ranging about 50 to 400 m (amsl). Geology is separated into two main groups including volcanic rock with two subgroups, which are Khao Yai 1 (PTrkr) and Khao Yai 2 (PTrkr) in Permo-Triassic period, and sediments in Quaternary period. The thickness of unconsolidated aquifer is in a range from 50 to 60 m. In some areas, the thickness is higher than 120 m to 130 m. A consolidated aquifer, i.e. the volcanic aquifer, consists of andesite and rhyolite. The capacity of water generating from this aquifer is less than an unconsolidated aquifer. A recharge is in eastern area and a direction of groundwater flow is from east to west corresponding to the topography. Groundwater level in May, 2015 dropped lower than that in November, 2014 about 0.64 m. A large surface water area is in the northeast part at the Ban Dong reservoir and in the northwest part at the Khong Phriao reservoir. Land use can be classified into various types as follows: residence, paddy field, cultivation of tapioca, corn, palm, eucalyptus, cattle farm and chicken farm.

5.1.2 Stable Isotope

A relationship between oxygen isotope and hydrogen isotope as known as the local meteoric water line (LMWL) of surface water is shown in the following equation: $\delta D = 4.2485\delta^{18}O - 15.935$. The 11 stations were in this evaporation trend which interact with surface water. And 33 stations were in the BKK LMWL which recharge directly from the rainfall.

5.1.3 Hydrogeochemical facies

The hydrogeochemical characteristics in groundwater such as pH, temperature, electrical conductivity (EC) and total dissolved solid (TDS) are higher in the summer

than those in the rainy season. A redox potential (Eh) in both seasons showed oxidation reactions. An average of DO in the summer is 4.25 mg/l with the highest at station no.60. The most of groundwater are in aerobic conditions. The concentration of NO_2^-, Br^-, NH_4^+, F^-, NO_3^-, PO_4^{3-}, Fe and K^+ are little in the area while the concentrations of Mg^{2+}, Cl^-, SO_4^{2-}, Ca^{2+}, Na^+ and alkalinity are high in the area. Most types of groundwater consists of $Ca-Na-HCO_3$, $Ca-HCO_3$ and $(Ca-Na-HCO_3) + (Ca-HCO_3)$ in the rainy season and $Ca-Na-HCO3$, $Na-HCO3$ and $Ca-HCO3$ in the summer.

5.1.4 Nitrate sources

The NO_3^- concentration in the summer is greater than in that in the rainy season because temperature is a main factor, contributing bacteria activity. The high NO_3^- zone is located in the northwestern part of the area. However, NO_3^- concentration is less than 45 mg/l NO_3^--N. Nitrate concentration in 5 stations are higher than 2 mg/l. About five stations have an interesting aspect of land use and two stations showed anomaly NO_3^- in water type. These are chosen to find out the NO_3^- sources. The sources of NO_3^- are both natural and anthropogenic activities such as soil-water interaction (dilution of minerals), wastewater, fertilizer.

5.1.5 Nitrate mechanism

The dilution process affect to a NO_3^- decrease that occurs during dissolved oxygen increased, whereas NO_3^- concentration decreased. A relationship between NO_3^- concentration increasing and decreasing of pH occurs that are the evidence of nitrification process which support a raise of NO_3^- in groundwater. While decreasing of NO_3^- concentration together with DO are the foundation of the denitrification process that is found at station nos. 06 and 37. Moreover, a presence of NH_4^+ implies an occurrence of ammonification process.

5.2 Recommendations

A hydrogeochemical is a tool for finding out the preliminary sources of NO_3^-. When it was used together with stable isotope, these help to tracing process occurred in the area. So if analysis DO in both seasons and analysis about bacteria communities, including NH_3 in groundwater as well as nitrogen and oxygen isotope in molecule of

nitrate. If complying these data together, it may be an efficient tool which helps to clearly separate different sources and various mechanisms of NO_3^- in groundwater. These are a benefit for groundwater resources management in the future. This method may be applied with the other place or jointly using the other stable isotope to find out the sources of other contaminants. This research shows the conditions of wells which are not perfect, such as, leakage surrounding of well base and improper well location. Therefore, the initial step is to use water from such wells and then plugs wells by concrete along with considering the new position for drilling wells in the hygienic place.

REFERENCES

Anderson, L., & Wedborg, M. (1983). Determination of alkalinity and total carbonate in seawater by photometric titration. *Oceanologica acta, 6*, 357-364.

Baba, A., & Olowoyeye, O. A. (2011). The hydrochemistry of Angwan Mallam and environs (PART OF KEFFI SHEET 208NE). *Appl. Sci. Environ. Manage., 15*(4), 675-680.

Beaudet, N., Otter, A., Karr, C., Sathyanarayana, S., & Perkins, A. (2014). Nitrates, Methemoglobinemia, and drinking water: A factsheet for clinicians. *Pediatric Environmental Health Specialty Units*.

Boonkaewwan, S. (2013). *An assessment of nitrate and phosphate in lower yom river using swat.* (Master of science program in environment science), Chulalongkorn University.

BoQiang, Q., Guang, G., GuangWei, Z., YunLin, Z., YuZhi, S., XiangMing, T., . . . JianMing, D. (2012). Lake eutrophication and its ecosystem response. *Chinese Science Bulletin, 58*(9), 961-970. doi:10.1007/s11434-012-5560-x

Boyd, C. E. (2002). Anion-Cation Balance. *THE ADVOCATE*, 74-75.

Breitenbach, S. F. M., Adkins, J. F., Meyer, H., Marwan, N., Kumar, K. K., & Haug, G. H. (2010). Strong influence of water vapor source dynamics on stable isotopes in precipitation observed in Southern Meghalaya, NE India. *Earth and Planetary Science Letters, 292*(1-2), 212-220. doi:10.1016/j.epsl.2010.01.038

Chebotarev, I. I. (1955). Metamorphism of natural waters in the crust of weathering. *Geochim. Cos-mochim, 8*, 22-48.

Chen, J., Tang, C., & Yu, J. (2006). Use of 18O, 2H and 15N to identify nitrate contamination of groundwater in a wastewater irrigated field near the city of Shijiazhuang, China. *Journal of Hydrology, 326*(1-4), 367-378. doi:10.1016/j.jhydrol.2005.11.007

Chen, J., Taniguchi, M., Liu, G., Miyaoka, K., Onodera, S.-i., Tokunaga, T., & Fukushima, Y. (2007). Nitrate pollution of groundwater in the Yellow River delta, China. *Hydrogeology Journal, 15*(8), 1605-1614. doi:10.1007/s10040-007-0196-7

Choi, W.-J., Han, G.-H., Lee, S.-M., Lee, G.-T., Yoon, K.-S., Choi, S.-M., & Ro, H.-M. (2007a). Impact of land-use types on nitrate concentration and 15N in unconfined groundwater in rural areas of Korea. *Agriculture, Ecosystems & Environment, 120*, 259-268.

Choi, W.-J., Han, G.-H., Lee, S.-M., Lee, G.-T., Yoon, K.-S., Choi, S.-M., & Ro, H.-M. (2007b). Impact of land-use types on nitrate concentration and δ15N in unconfined groundwater in rural areas of

Korea. *Agriculture, Ecosystems & Environment, 120*(2-4), 259-268. doi:10.1016/j.agee.2006.10.002

Clark, I. D., & Fritz, P. (1997). *Environmental Isotopes in Hydrogeology.* Boca Raton: Lewis.

Damrongsri, M., & Pruksanan, S. (2007). *Study of nitrate removal from industrial wastewater treatment effluent by anoxic digester.* Paper presented at the Proceedings of 45th Kasetsart University Annual Conference, Bangkok.

Devis, S. N., Whittemore, D. O., & Fabryka-Martin, J. (1998). Uses of Chloride/Bromide Ratios in Studies of Potable Water. *Ground Water, 36*(2), 338-350.

Duncan, E., Kleinman, P. J., & Sharpley, A. N. (2012). Eutrophication of Lakes and Rivers. doi:10.1002/9780470015902.a0003249.pub2

Environmental Research Institute, C. U. (2014). The development of understanding on the quality of environment for sustainable management: Case study in the project of the land development of Chulalongkorn University, Amphoe Kaeng Khoi , Saraburi.

Fenech, C., Rock, L., Nolan, K., Tobin, J., & Morrissey, A. (2012). The potential for a suite of isotope and chemical markers to differentiate sources of nitrate contamination: a review. *Water Res, 46*(7), 2023-2041. doi:10.1016/j.watres.2012.01.044

Galloway, W. E., & Kaiser, W. R. (1980). Catahoula Formation of the Texas coastal plain; origin, geochemical evolution, and characteristics of uranium deposits. *University of Texas at Austin, Bureau of Economic Geology Report of Investigations Number 100.*

Gao, Y., Yu, G., Luo, C., & Zhou, P. (2012). Groundwater Nitrogen Pollution and Assessment of Its Health Risks: A Case Study of a Typical Village in Rural-Urban Continuum, China. *PLoS One, 7*(4), 1-8.

Gonfiantini, R., Roche, M.-A., Olivry, J.-C., Fontes, J.-C., & Zuppi, G. M. (2001). The altitude effect on the isotopic composition of tropical rains. *Chemical Geology, 181*, 147-167.

Gu, B., Ge, Y., Chang, S. X., Luo, W., & Chang, J. (2013). Nitrate in groundwater of China: Sources and driving forces. *Global Environmental Change, 23*(5), 1112-1121. doi:10.1016/j.gloenvcha.2013.05.004

Gu, B., Zhu, Y., Chang, J., Peng, C., Liu, D., Min, Y., . . . Ge, Y. (2011). The role of technology and policy in mitigating regional nitrogen pollution. *Environmental Research Letters, 6*(1), 014011. doi:10.1088/1748-9326/6/1/014011

Guo, F., & Jiang, G. (2009). Nitrogen budget of a typical subterranean river in peak cluster karst area. *Environmental Geology, 58*(8), 1741-1748. doi:10.1007/s00254-008-1673-6

HEM, J. D. (1985). *Study and Interpretation of the Chemical Characteristics of Natural Water* (3 ed.). U.S. Geological Survey Water-Supply Paper 2254.

Hensler, R. F., & Attoe, O. J. (1970). *Rural source of nitrate in water.* Paper presented at the Twelfth Sanitation Engineering Conference Proceeding., Engineering Publication Office,USA.

Heston, D. (2015). Using Chloride and Bromide Mass Ratios and Binary Mixing Curves to Evaluate Anthropogenic Influences on Groundwater in Lycoming and Wayne counties, Pennsylvania. *GEO 546.*

Hoefs, J. (1997). Stable Isotope Geochemiatry. *Springer-Verlag.*

Hosono, T., Tokunaga, T., Kagabu, M., Nakata, H., Orishikida, T., Lin, I. T., & Shimada, J. (2013). The use of delta15N and delta18O tracers with an understanding of groundwater flow dynamics for evaluating the origins and attenuation mechanisms of nitrate pollution. *Water Res, 47*(8), 2661-2675. doi:10.1016/j.watres.2013.02.020

HYDRAULICS, D. C. B. D., & HALCROW, T., CES, ORG & JPS. (1999). Major Ions in Water *Hydrology Project Training Module* (pp. 1-41).

IAEA. (2006). *Isotope Hydrology Information System. The ISOHIS Database.* http://isohis.iaea.org.

Ionic Balance Calculations. (2014). ALS Environmental Limited. www.alsenvironmental.co.uk.

Jin, Z., Pan, Z., Jin, M., Li, F., Wan, Y., & Gu, B. (2012). Determination of nitrate contamination sources using isotopic and chemical indicators in an agricultural region in China. *Agriculture, Ecosystems & Environment, 155*, 78-86. doi:10.1016/j.agee.2012.03.017

Kaff, M. A. (2012). Eutrophication in Shallow Lakes and Water Dams. *Envirocities eMagazine*(2), 32-35.

Kamdee, K., Laoharojanaphand, S., Noipow, N., Jaruratana, A., Detoup, D., & Chantarachot, W. (2011, 6-7 July 2011). *Improvement of Groundwater Modeling by Using of the Environmental Isotopes with Liquid Water Isotope Analyzer.* Paper presented at the The 12th Conference on Nuclear Science and Technology, Shangri-La Hotel, Bangkok, Thailand.

Kamdee, K., Srisuk, K., Lorphensri, O., Chitradon, R., Noipow, N., Laoharojanaphand, S., & Chantarachot, W. (2013). Use of isotope

hydrology for groundwater resources study in Upper Chi river basin. *Journal of Radioanalytical and Nuclear Chemistry, 297*(3), 405-418. doi:10.1007/s10967-012-2401-y

Kaown, D., Koh, D.-C., Mayer, B., & Lee, K.-K. (2009). Identification of nitrate and sulfate sources in groundwater using dual stable isotope approaches for an agricultural area with different land use (Chuncheon, mid-eastern Korea). *Agriculture, Ecosystems & Environment, 132*(3-4), 223-231. doi:10.1016/j.agee.2009.04.004

Katsuyama, M., Yoshioka, T., & Konohira, E. (2015). Spatial distribution of oxygen-18 and deuterium in stream waters across the Japanese archipelago. *Hydrology and Earth System Sciences, 19*(3), 1577-1588. doi:10.5194/hess-19-1577-2015

Kellman, L. M., & Hillaire-Marcel, C. (2003). Evaluation of nitrogen isotopes as indicators of nitrate contamination sources in an agricultural watershed. *Agriculture, Ecosystems & Environment, 95*(1), 87-102. doi:10.1016/s0167-8809(02)00168-8

Kendall, C., & Caldwell, E. A. (1998). Isotope Tracer in Catchment Hydrology. *Elsevier Sciene B.V.*, 51-86.

Kolpin, D., Burkart, M., & Goolsby, D. (1999). Nitrate in groundwater of the midwestern United States: a regional investigation on relations to land use and soil properties. *Impact of Land-Use Change on Nutrient Loads from Diffuse Sources, 257*(111-116).

Lambert, W., Nwaokoro, R., & Russo, S. (2004). Simultaneous Nitrification and Denitrification in a Sequencing Batch Reactor. *Nutrient Removal Project*.

Lee, J.-E., & Fung, I. (2008). "Amount effect" of water isotopes and quantitative analysis of post-condensation processes. *Hydrological Processes, 22*(1), 1-8. doi:10.1002/hyp.6637

Lee, K. S., Bong, Y. S., Lee, D., Kim, Y., & Kim, K. (2008). Tracing the sources of nitrate in the Han River watershed in Korea, using delta15N-NO3- and delta18O-NO3- values. *Sci Total Environ, 395*(2-3), 117-124. doi:10.1016/j.scitotenv.2008.01.058

Lee, P. G., Lea, R. N., Dohmann, E., Prebilsky, W., Turk, P. E., Ying, H., & Whitson, J. L. (2000). Denitrification in aquaculture systems: an example of a fuzzy logic control problem. *Aquacultural Engineering, 23*, 37-59.

Li, J., Li, F., Liu, Q., & Suzuki, Y. (2014). Nitrate pollution and its transfer in surface water and groundwater in irrigated areas: a case study of the Piedmont of South Taihang Mountains, China. *Environ Sci Process Impacts, 16*(12), 2764-2773. doi:10.1039/c4em00200h

Macler, B. (2007). Drinking water standards and health advisories table. *United States Environment Protection Agency*, 29.

Mahler, R. L., colter, A., & Hirnyck, R. (2007). Nitrate and groundwater. *University of Idaho college of agricultural and life sciences*(furtherance of cooperative extension work in agriculture and home economics).

The map of land use, Changwat Saraburi (2011). Retrieved from www.Idd.go.th:

Marie, A., & Vengosh, A. (2001). Sources of Salinity in Ground Water from Jericho Area, Jordan Valley. *Ground Water, 39*(2), 240-248.

Mcquillan, D. (2004, 11/7-10/2004). *Ground-water quality impacts from on-site septic systems.* Paper presented at the National Onsite Wastewater Recycling Association 13, Albuquerque, NM.

Meybeck, M., & Helmer, R. (1996). *Water quality assessments.* (D. Chapman Ed. Second ed.). Published on behalf of UNESCO, WHO and UNEP by E&FN Spon, London.

Min, J.-H., Yun, S.-T., Kim, K., Kim, H.-S., & Kim, D.-J. (2003). Geologic controls on the chemical behaviour of nitrate in riverside alluvial aquifers, Korea. *Hydrological Processes, 17*(6), 1197-1211. doi:10.1002/hyp.1189

Minaudo, C., Meybeck, M., Moatar, F., Gassama, N., & Curie, F. (2015). Eutrophication mitigation in rivers: 30 years of trends in spatial and seasonal patterns of biogeochemistry of the Loire River (1980–2012). *Biogeosciences, 12*(8), 2549-2563. doi:10.5194/bg-12-2549-2015

Mo, Q., Chen, N., Zhou, X., Chen, J., & Duan, S. (2016). Ammonium and phosphate enrichment across the dry-wet transition and their ecological relevance in a subtropical reservoir, China. *Environ Sci Process Impacts, 18*(7), 882-894. doi:10.1039/c6em00225k

Mohamed, M., Terao, H., Suzuki, R., Babiker, I., Ohta, K., Kaori, K., & Kato, K. (2003). Natural denitrification in the Kakamigahara groundwater basin, Gifu prefecture, central Japan. *The Science of The Total Environment, 307*(1-3), 191-201. doi:10.1016/s0048-9697(02)00536-3

Motzer, W. E. (2006). Nitrate Forensic. *Fall 2006 HydroVisiond Newsletter*.

Motzer, W. E. (2006). Nitrate forensics. *Fall 2006 HydroVisions Newsletter*, 1-7.

Munster, J. E. (2008). *Nonpoint sources of nitrate and perchlorate in urban land use to groundwater, Suffolk Country, NY.* (Docter of Philosophy), Stony Brook.

Ndegwa, P. M., Wang, L., & Vaddella, V. K. (2007). Potential strategies for process control and monitoring of stabilization of dairy wastewaters in batch aerobic treatment systems. *Process Biochemistry, 42*(9), 1272-1278. doi:10.1016/j.procbio.2007.06.001

Noipow, N. (2015, July 7-8, 2015). *Seasonal Variation of the Stable Isotope Fingerprints in daily precipitations and Mekong River, the implication on Hydrological Study of Thailand and Lao PDR.* Paper presented at the The 3 rd Lao-Thai Technical Conference.

Nunak, N., & Suesut, T. (2012). *Measurement and Instruments in the Food Industry*. Faculty of Engineering, King Mongkut's Institute of Technology Ladkrabang.

Osthoff, H. D., Brown, S. S., Ryerson, T. B., Fortin, T. J., Lerner, B. M., Williams, E. J., . . . Ravishankara, A. R. (2006). Measurement of atmospheric NO2 by pulsed cavity ring-down spectroscopy. *Journal of Geophysical Research, 111*(D12305), 1-10. doi:10.1029/2005JD006942

Panno, S. V., Hackley, K. C., Hwang, H. H., Greenberg, S. E., Krapac, I. G., Landsberger, S., & O'Kelly, D. J. (2006). Characterization and identification of na-cl sources in ground water. *Ground Water, 44*(2), 176-187. doi:10.1111/j.1745-6584.2005.00127.x

Panno, S. V., Hackley, K. C., Hwang, H. H., & Kelly, W. R. (2001). Determination of the sources of nitrate contamination in karst springs using isotopic and chemical indicators. *Chemical Geology, 179*, 113-128.

Pasten-Zapata, E., Ledesma-Ruiz, R., Harter, T., Ramirez, A. I., & Mahlknecht, J. (2014). Assessment of sources and fate of nitrate in shallow groundwater of an agricultural area by using a multi-tracer approach. *Sci Total Environ, 470-471*, 855-864. doi:10.1016/j.scitotenv.2013.10.043

Peng, H., Mayer, B., Harris, S., & Krouse, H. R. (2004). A 10-yr record of stable isotope ratios of hydrogen and oxygen in precipitation at Calgary, Alberta, Canada. *Tellus B, 56*(2), 147-159.

Pietro, S. (2006). Nitrate in vegetables: toxicity, content, intake and EC regulation. *Journal of the Science of Food and Agriculture, 86*(1), 10-17. doi:10.1002/jsfa.2351

Polishchuk, O. M., Fakeev, A. A., Krasil'shchik, V. Z., & Vendilo, A. G. (2012). Preparation of extrapure potassium nitrate. *Inorganic Materials, 48*(8), 836-840. doi:10.1134/s0020168512070138

The quality standard of the surface water. (1994). *The announcement of the National Environment Committee, 8*, 234-240.

Richter, B. C., & Kreitler, C. W. (1993). *Geochemical Techniques for Identifying Sources of Ground-Water Salinization*. Boca Raton, Florida: C.K. Smoley.

Robertson, G. P., & Groffman, P. M. (2007). Nitrogen transformation. *Biochemistry and Ecology*, 341-364.

Roine, A., & Anttila, K. (2006). Eh - pH - DIAGRAMS (Pourbaix-diagrams). *HSC Chemistry7.0*(17), 1-19.

Sabseree, J. (2010). Box Plot. *for Quality Production, 16*(148), 35-37.

Sahanawin, N. (2012). Euthrophication. *Physical Education Students 15 (special edition)*.

SAHRA. (2005). *Isotope Oxygen.* University of Arizona. http://web.sahra.arizona.edu/programs/isotopes/oxygen.html

Silva, M. A. M., Souza, M. F. L., & Abreu, P. C. (2015). Spatial and Temporal variation of Dissolved Inorganic Nutrients, and Chlorophyll-a in a Tropical Estuary in Northeastern Brazil: Dynamics of Nutrient Removal. *Brazilian Journal of Oceanography, 63*(1), 1-15. doi:10.1590/s1679-87592015064506301

Sindelar, J. J., & Milkowski, A. L. (2012). Human safety controversies surrounding nitrate and nitrite in the diet. *Nitric Oxide, 26*(4), 259-266. doi:10.1016/j.niox.2012.03.011

Sprague, M. K. (2012). *CAVITY RINGDOWN SPECTROSCOPY, KINETICS, AND QUANTUM CHEMISTRY OF ATMOSPHERICALLY RELEVANT REACTIONS.* (Doctor of Philosophy), California Institue of Technology.

Stewart, M. K., Stevens, G., Thomas, J. T., Raaij, R. v. d., & Trompetter, V. (2011). Nitrate sources and residence times of groundwater in the Waimea Plains, Nelson. *Journal of Hydrology, 50*(2), 313-338.

Tan, C., Ma, F., Li, A., Qiu, S., & Li, J. (2013). Evaluating the effect of dissolved oxygen on simultaneous nitrification and denitrification in polyurethane foam contact oxidation reactors. *Water Environ Res, 85*(3), 195-202.

Tang, Y., Pang, H., Zhang, W., Li, Y., Wu, S., & Hou, S. (2015). Effects of changes in moisture source and the upstream rainout on stable isotopes in precipitation – a case study in Nanjing, eastern China. *Hydrology and Earth System Sciences, 19*(10), 4293-4306. doi:10.5194/hess-19-4293-2015

Tantanasarit, S. (2006). Introduction to water quality. *P10-water resource*, 239.

Tirado, R. (2007). Nitrates in drinking water in the Philippines and Thailand. *Greenpeace Research Laboratories*(GRL-TN-10-2007), 9-13.

Townsend, M. A., & Whittemore, D. O. (2005). Identification of nitrate and chloride sources affecting municipal well waters of the city of Mcpherson, Kansas.

The types of land use Thailand map 2010-2013. (2014). Retrieved from http://www.ldd.go.th/web_OLP/result/luse_result53-56.htm:

USGS. (2004). *Resources on Isotopes*. http://wwwrcamnl.wr.usgs.gov/isoig/period/h_iig.html

Vityakorn, P. (2014). *Soil fertility and plant nutrition*. lecture. Land resources and environment. Khonkaen University.

Vonlathen, P., Bittner, D., & Hudson, A. G. (2012). Eutrophication led to fish extinctions in Alps. *Science for Environment Policy*(290). doi:10.1038/nature0824

Ward, M. H., deKok, T. M., Levallois, P., Brender, J., Gulis, G., Nolan, B. T., & VanDerslice, J. (2005). Workgroup Report: Drinking-Water Nitrate and Health—Recent Findings and Research Needs. *Environmental Health Perspectives, 113*(11), 1607-1614. doi:10.1289/ehp.8043

WHO. (1998). Guidelines for Drinking-Water quality. *WHO Library Cataloguing in Publication Data Guidelines for drinking-water quality, 1*, 36.

Wieben, C. M., Baker, R. J., & Nicholson, R. S. (2013). Nutrient concentrations in surface water and groundwater, and nitrate source identification using stable isotope analysis, in the Barnegat Bay-Little Egg Harbor watershed, New Jersey, 2010-11. 17-33.

Winkler, R., & Peters, R. (2013). Cavity Ring-Down Spectroscopy (CRDS): High precision measurements suitable for field, mobile and lab-based work. *PICARRO*.

Wisittammasri, W., & Chotpanrat, S. (2015). The survey on surface water condition in the area surrounding land of Chulalongkorn University, Kaeng Khoi district, Saraburi province. *Environmental Journal 19 years*(2), 54-65.

Wongcharlie, P. (1991). *Determination of quantity of nitrate and phosphate in Chonburi, Rayong and Chanthaburi bain*. Bangkok: The Graduate School Kasetsart University.

Woolverton, P. (2015). Nitrate in drinking water. *Water Quality Division Drinking Water Protection Program*.

Yoon, S.-H. (2016). *Effect of ORP*. Denitrification. http://onlinembr.info/nutrient-removal/denitrification/.

Zhang, Y., Li, F., Zhang, Q., Li, J., & Liu, Q. (2014). Tracing nitrate pollution sources and transformation in surface- and ground-waters using environmental isotopes. *Sci Total Environ, 490*, 213-222. doi:10.1016/j.scitotenv.2014.05.004

Zhang, Y., Zhou, A., Zhou, J., Liu, C., Cai, H., Liu, Y., & Xu, W. (2015). Evaluating the Sources and Fate of Nitrate in the Alluvial Aquifers in the Shijiazhuang Rural and Suburban Area, China: Hydrochemical and Multi-Isotopic Approaches. *Water, 7*(4), 1515-1537. doi:10.3390/w7041515

APPENDIX

Station 01 Kaeng Khoi- Ban Na road (จด 0499, depth is 60 m.)

Figure A.1 groundwater station no.01

Station 02 Ban Na Dee (PW6075, depth is 27 m.)

Figure A.2 groundwater station no.02

Station 03 Khok Krung Temple (TV246, depth is 96 m.)

Figure A.3 groundwater station no.03

Station 04 Ban Nong Kla (depth is 120 m.)

Figure A.4 groundwater station no.04

Station 05 Ban Khok Krung (PW2836, depth is 18.2 m.)

Figure A.5 groundwater station no.05

Station 06 Ban Pong Kon Sao (ว 4826, depth 60 m.)

Figure A.6 groundwater station no.06

Station 07 Ban Pong Kon Sao (ง 4824, depth is 60 m.)

Figure A.7 groundwater station no.07

Station 11 Ban Don Jan (ง 4591, depth is 60 m.)

Figure A.11 groundwater station no.11

Station 12 Cattle farm (depth is 160 m.)

Figure A.12 groundwater station no.12

Station 13 Wat Sun Tree Ya Ka Was school (depth is 100 m.)

Figure A.13 groundwater station no.13

Station 15 Pa Phai temple (ง 4589, depth is 80 m.)

Figure A.15 groundwater station no.15

Station 17 Ket Kaeo Mani temple (DE475, depth is 66 m.)

Figure A.17 groundwater station no.17

Station 19 Na Boon temple (MD24, depth is 24 m.)

Figure A.19 groundwater station no.19

Station 21 Ban Wat Na Boon school (ขด 0455 ,depth is 80 m.)

Figure A.21 groundwater station no.21

Station 22 Chuenchom Technology THAI-GERMAN College (depth is 60 m.)

Figure A.22 groundwater station no.22

Station 23 Ban Huay Lee (รท 0107, depth is 40 m.)

Figure A.23 groundwater station no.23

Station 25 Taling Chan

Figure A.25 groundwater station no.25

Station 26 Ban Huay Lee (PW6653, depth is 24 m.)

Figure A.26 groundwater station no.26

Station 27 Ban Khun Jum Pa (รท 0108, depth is 45 m.)

Figure A.27 groundwater station no.27

Station 28 Ban Khun Som Sak (รท 0109, depth is 45.5 m.)

Figure A.28 groundwater station no.28

Station 29 Khok Phek temple (MR14, depth is 39 m.)

Figure A.29 groundwater station no.29

Station 30 Khok Phek temple (TE70, depth is 90 m.)

Figure A.30 groundwater station no.30

Station 32 Wat Suwan Khiri (TW174, depth is 90 m.)

Figure A.32 groundwater station no.32

Station 35 Ban Kut Nok Plao (TE279, depth is 120 m.)

Figure A.35 groundwater station no.35

Station 37 Nong Nam Khiao (DOH20139)

Figure A.37 groundwater station no.37

Station 38 Ban Huay Haeng (depth is 120 m.)

Figure A.38 groundwater station no.38

Station 39 Nong Nam Khiao school (TE404, depth is 210 m.)

Figure A.39 groundwater station no.39

Station 40 Ban Khun Da Ru Nee (depth is 95 m.)

Figure A.40 groundwater station no.40

Station 42 Ban Nong Prue (ง 4801, depth is 60 m.)

Figure A.42 groundwater station no.42

Station 44 Ban Khao Ruak (P721, depth is 13.5 m.)

Figure A.44 groundwater station no.44

Station 46 Pong Mong khon (TE107, depth is 42 m.)

Figure A.46 groundwater station no.46
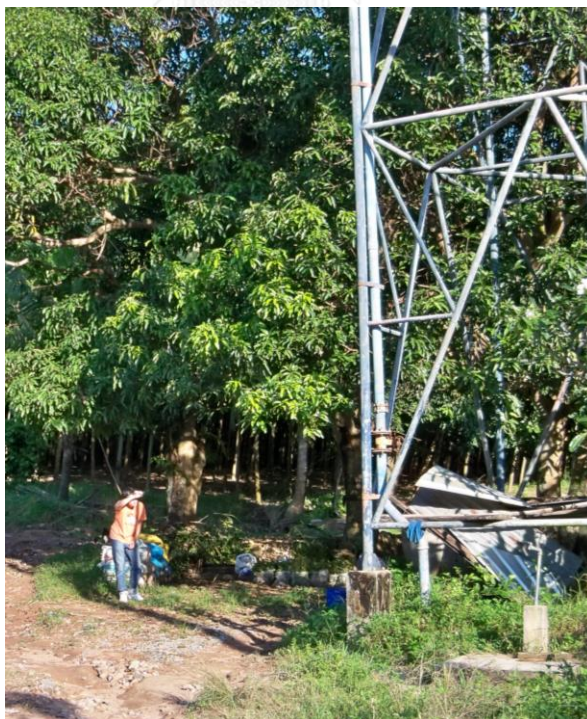
Station 47 Ban Cha-Om (TE238, depth is 156 m.)

Figure A.47 groundwater station no.47

Station 48 Palm area (DOH20015)

Figure A.48 groundwater station no.48

Station 50 Ban Cha-Om (depth is 110 m.)

Figure A.50 groundwater station no.50

Station 52 Ban Tha Maprang (งด0501, depth is 60 m.)

Figure A.52 groundwater station no.52

Station 56 (depth is 90 m.)

Figure A.56 groundwater station no.56

Station 58 Ban Khun Sukri (ง 4599, depth is 60 m.)

Figure A.58 groundwater station no.58

Station 59 Ban Sopha (ง 4818, depth is 60 m.)

Figure A.59 groundwater station no.59

Station 60 Ban Huay Haeng (SRB91, depth is 42 m.)

Figure A.60 groundwater station no.60

Station 61 Ban Nong Prue (DOH20130)

Figure A.61 groundwater station no.61

Station 62 Buri Ka Ram temple (SRB90, depth is 74 m.)

Figure A.62 groundwater station no.62

Station 63 Ban Huay Haeng (จ 4820, depth is 60 m.)

Figure A.63 groundwater station no.63

Station 65 PP Kaeng Khoi (depth is 60 m.)

Figure A.65 groundwater station no.65

Station 67 Ban Don Jan public health center (DOH20043, depth is 100 m.)

Figure A.67 groundwater station no.67

VITA

Miss Wanlapa Wisittammasri graduated high school from Srinagarindra The Princess Mother School Kanchanaburi Under Patronage Of Princess Maha Chakri Sirinthorn in 2008. Thereafter, she graduated Bachelor's Degree (B.Sc.) at Geoscience Peogram, Faculty of Science, Mahidol University in 2012 and got Development and Promotion of Science and Technology Talents Project (Royal Government of Thailand scholarship) during to the studying. A project report title in Bachelor's Degree is "A Study of Relationship between Atterberg's Limits Test, Unconfined Compression Test and Field Vane Shear Test to estimate the Test Results in Electrical Conduit Manhole Construction with Mass Rapid Transit Authority of Thailand (MRTA) Purple Line Contract 1 Bang Yai-Bang Sue, Bangkok" and study in Master's Degree Program at Department of Geology, Faculty of Science, Chulalongkorn University in 2012. Her research is supported by 90th year Chulalongkorn Scholarship. Some part of research in name "Isotope evidence of rainfall and groundwater for tracing recharge areas in Kaeng Khoi district, Saraburi" was published in Applied Environmental Research. Moreover, an article name "The survey of surface water in the area of Chulalongkorn University, Kaeng Khoi. Saraburi (in Thai)" was published in Environmental Journal in 2015.